Molecular Aspects of Hepatitis C Virus Infection and Associated Mitochondrial DNA Damage

Thesis

Molecular Aspects of Hepatitis C Virus Infection and Associated Mitochondrial DNA Damage

A thesis submitted to the Open University for the degree of Doctor of Philosophy

By Kathryn Jane Rolfe (BSc. Hons, MSc. Dist)

1st July 2008

Date of submission. 2 July 2008
Date of award: 13 October 2008

Affiliated Research Centre: Health Protection Agency, Centre for Infections

For Mum & Dad

"Learn from yesterday, live for today, hope for tomorrow. The important thing is not to stop questioning."

Albert Einstein

ACKNOWLEDGEMENTS

I would like to take this opportunity to thank each of my supervisors. To Dr Martin Curran for his help, guidance and 'open-door' policy. I couldn't have done this without your positive attitude and patience. To Dr Graeme Alexander, for clinical advice and guidance. To Dr Tim Wreghitt, my training supervisor, for his energy, enthusiasm and constant support.

I would also like to express my thanks and appreciation to the following people:
To Surendra Parmar for his advice and technical guidance and to Dr Hamid Jalal for the use of his β-globin assay.

To Dr Helen Harris for her tremendous help with the HCV clearance study and for securing the funding for the study and to Dr Nick Andrews for his input into the statistical analysis.

To Tracy Woodall, Clinical Nurse Specialist, for obtaining clinical data for the HCV clearance study and to Dr Mike Allison for obtaining ethical approval for the clinical study on mitochondrial DNA damage in liver disease.

To the Health Protection Agency for providing the opportunity and funding which enabled me to carry out this PhD and to all the staff (past and present) at the Cambridge Microbiology and Public Health Laboratory, Addenbrooke's Hospital. Special thanks to Janet Burton, a colleague and friend.

To my parents for their last minute proof-reading of chapters and 'gentle' reminders to save everything, everywhere.

Final thanks goes to my family, to Mum, Dad, Suzanne, Stan, Kaitlyn and baby Ella who have endured me and encouraged me through the difficult times during this PhD and to Mr Iain Todd, who has seen me through the darkest days to the light at the end of the tunnel. Your never-ending support and encouragement gave me the strength to keep going. For this I am eternally grateful.

ABSTRACT

Hepatitis C virus (HCV) is the main cause of viral hepatitis in the UK and leads to chronic liver disease in many infected individuals. There is a substantial burden on diagnostic laboratories to provide rapid, cost-effective tests for monitoring HCV infection. Commercial assays are expensive and so the development of validated in-house methods is beneficial. This thesis describes the development and implementation of rapid and inexpensive real-time PCR assays for HCV quantitation and genotyping to support clinical practice. Additionally, the development of methods for defining HCV isolates at the subtype level, important in epidemiological and transmission studies, is described. These assays were utilised in a study on spontaneous HCV clearance, the results of which suggest that HCV type 1 infection and younger age at infection are factors which are associated with spontaneous viral clearance.

Chronic HCV infection is linked to oxidative stress with numerous deleterious cellular effects. Mitochondrial DNA (mtDNA) is more susceptible to oxidative damage than nuclear DNA making it an ideal marker to assess the overall level of cellular DNA damage – including deletions and mutations. This thesis illustrates the development of real-time PCR assays to detect and quantify two major mtDNA deletions. The D-loop region of mtDNA is particularly prone to damage – with two well recognised 'hotspots of mutation'. The creation of an RSCA (heteroduplex-based) method using capillary electrophoresis, to detect and quantify damage in this region, is described.

To evaluate the clinical utility of these assays, a study of mtDNA damage in patients with liver disease was undertaken. The aim of this study was to identify whether chronic HCV infection results in increased levels of mtDNA damage compared to other liver pathologies. Low levels of mtDNA deletions were detected in the majority of liver biopsy specimens and there was no correlation between liver aetiology and quantity of deletions. The RSCA method identified numerous D-loop mtDNA species within the liver tissue of several individuals. There was no correlation between liver aetiology and the presence of multiple D-loop species.

ABBREVIATIONS

8-OHdG	8-hydroxydeoxyguanosine
A	Adenine
ABI	Applied Biosystems
Acc no	Accession number
Acetyl-CoA	Acetyl co-enzyme A
ADP	Adenosine diphosphate
ALT	Alanine aminotransferase
ATM	Ataxia-telangiectasia mutated
ASH	Alcoholic steatohepatitis
ATP	Adenosine triphosphate
BER	Base excision repair
BHQ-2	Black Hole Quencher-2
BLAST	Basic Local Alignment Search Tool
bp	Base pair
C	Cytosine
Ca^{2+}	Calcium ion
cDNA	copy DNA
CI	Confidence intervals
CCD	Charged coupled device
CSB	Conserved sequence block
Ct	Threshold Cycle
CV	Co-efficient of variation
ddH_20	Distilled and deionised water
D-loop	Displacement loop
DGGE	Denaturing gradient gel electrophoresis
DNA	Deoxyribonucleic acid
DoH	Department of Health
dsDNA	Double stranded DNA
EIA	Enzyme immunoassay
EPP	Exposure prone procedure
ER	Endoplasmic reticulum
ETC	Electron transport chain
EVR	Early virologic response
FAD	Flavin adenine nucleotide
FLR	Fluorescent labelled reference
HLA	Human leucocyte antigen
ISS	Internal size standard
LFT	Liver function test
G	Guanine
GSH	Glutathione
GSSG	Glutathione disulphide
H_2O_2	Hydrogen peroxide
HBV	Hepatitis B virus
HCC	Hepatocellular carcinoma
HCV	Hepatitis C virus
HCW	Health care worker
HIV	Human immunodeficiency virus
HNH	Hepatocellular nodular hyperplasia

HPA	Health Protection Agency
H-strand	Heavy strand
HVR	Hypervariable region (HCV)
HVS1	Hypervariable segment 1 (mtDNA)
HVS2	Hypervariable segment 2 (mtDNA)
IC	Internal control
IDU	Injecting drug use
iNOS	Inducible nitric oxide synthase
IRES	Internal ribosome entry site
ISDR	Interferon sensitivity determining region
IU	International units
KSS	Kearns-Sayre syndrome
LB	Luria-Bertani
LFT	Liver function test
LNA	Locked nucleic acid
LREC	Local Research Ethics Committee
L-strand	Light strand
MDA	Malondialdehyde
MELAS	Mitochondrial encephalomyopathy with lactic-acidosis and stroke-like episodes
MGB	Minor groove binding
MnSOD	Manganese superoxide dismutase
mtDNA	Mitochondrial DNA
NAD^+	Nicotinamide adenine nucleotide
NAFLD	Non-alcoholic fatty liver disease
NASH	Non-alcoholic steatohepatitis
NAT	Nucleic acid testing
NC	Non-coding
NER	Nucleotide excision repair
NFQ	*Non-fluorescent quencher*
NIBSC	National Institute for Biological Standards and Control
NICE	National Institute of Health and Clinical Excellence
NO	Nitric oxide
NOS	Nitric oxide synthase
nt	Nucleotide
O_2^-	Superoxide anion
$OH^\bullet$	Hydroxyl radical
O_H	Origin of heavy strand replication
O_L	Origin of light strand replication
$ONOO^-$	Peroxynitrite
OR	Odds ratio
ORF	Open reading frame
OXPHOS	Oxidative phosphorylation
PBMC	Peripheral blood mononuclear cell
PCR	Polymerase chain reaction
PSSU	Planned Short Stay Unit
QCMD	Quality Control for Molecular Diagnostics
rCRS	Revised Cambridge Reference Sequence (mitochondria)
RFU	Relative fluorescence unit
RNA	Ribonucleic acid

rRNA	Ribosomal ribonucleic acid
RR	Relative risk
RSCA	Reference Strand Mediated Conformation Analysis
ROS	Reactive oxygen species
RPM	Revolution per minute
RT	Reverse transcription
RVR	Rapid virological response
SD	Standard deviation
SOD	Superoxide dismutase
SVR	Sustained virological response
T	Thymidine
TCA	Tricarboxylic acid cycle
TGGE	Temperature gradient gel electrophoresis
Tm	Melting temperature
TNF-α	Tumour necrosis factor-alpha
TLR	Toll-like receptor
tRNA	Transfer ribosomal nucleic acid
TTGE	Temporal temperature gradient gel electrophoresis
UTR	Untranslated region
WHO	World Health Organisation
χ^2	Chi square

TABLE OF CONTENTS

FIGURES

TABLES

CHAPTER ONE

Part One

Hepatitis C Virus

1.1 Hepatitis C virus

An infectious human hepatitis agent was first identified in 1989 as the main cause of post-transfusion and sporadic non-A, non-B hepatitis and was named the hepatitis C virus (Choo *et al*, 1989; Kuo *et al*, 1989). At the turn of the century, there were an estimated 170 million people worldwide infected chronically with HCV (WHO, 1999) and it is now the most common blood-borne virus in Europe and the USA. The UK is probably a low prevalence country, although there have been very few studies on HCV prevalence to confirm this. Seroprevalence studies on samples collected from the mid-1990s estimated prevalence to be around 0.5% (Balogun *et al*, 2002). In a study of pregnant women in the UK, HCV antibody was detected in 0.4% in London and 0.2% in Yorkshire, demonstrating that HCV is seen, albeit at low rates, even in lower risk populations (Balogun *et al*, 2000). Statistical modelling has suggested that, in 2003, there were an estimated 231,000 HCV-antibody positive individuals between 15-59 years of age living in England and Wales, equating to anti-HCV prevalence in this population of 0.72% (HPA, 2006). However, estimates of HCV prevalence must take into account the fact that injecting drug users (IDUs) are at very high risk of HCV infection and make up the bulk of prevalent HCV infections in the UK. This population group is very difficult to study because they move around frequently and are often homeless; as a result they are under-represented in national data sources.

A cumulative total of 62,726 laboratory-confirmed diagnoses of HCV in England were reported to the Health Protection Agency between 1992 and 2006 (HPA, 2007). There has been a steady increase in the number of reports during this time (Figure 1.1). There is no evidence of an increase in incidence, and the rise in

reports is consistent with an increase in testing and public awareness through campaigns and media coverage. Laboratory reporting is, however, incomplete. Data from sentinel surveillance of Hepatitis C testing, which commenced in 2002 and which extracts test results on all individuals tested for hepatitis in participating sentinel centres suggests that routine laboratory reporting underestimates HCV infections by as much as 60% (Brant *et al*, 2007).

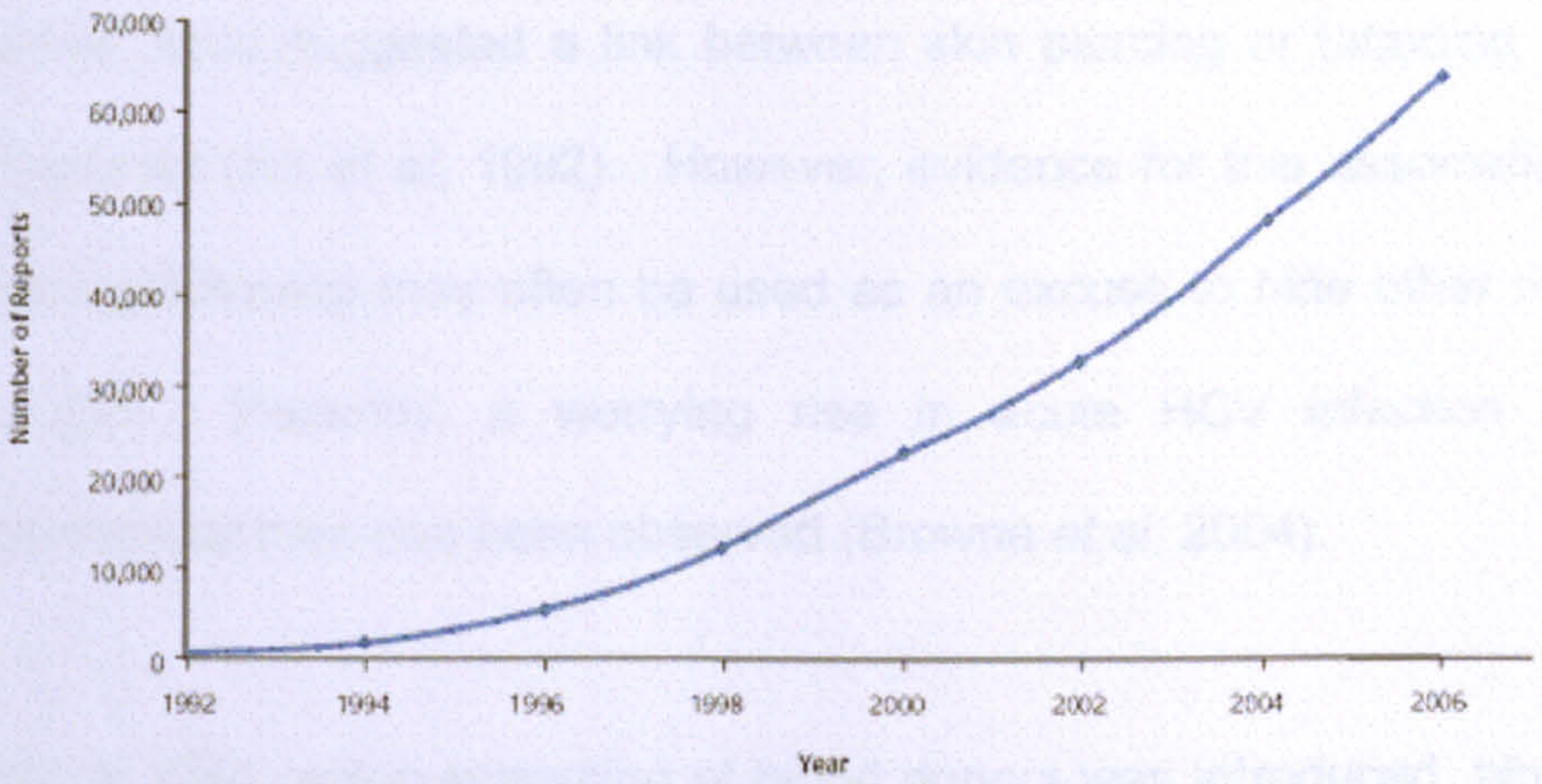

Figure 1.1: Cumulative laboratory reports of confirmed HCV infection in England to the Health Protection Agency: 1992 to 2006 (HPA, 2007). Although this appears to demonstrate a rise in HCV incidence/prevalence, it is actually consistent with an increase in HCV testing.

1.2 HCV transmission

HCV is transmitted through contact with blood and blood products. In the UK, sharing of contaminated equipment whilst injecting recreational drugs is the single most important reported risk factor, with 82% of HCV positive individuals reporting injecting drug use (IDU) as the main risk exposure (Brant *et al*, 2007). In this country, HCV infection is most common in the younger age group and is highest in

25-34 year olds, regardless of whether injecting drug use is reported as a risk factor (HPA, 2006).

Other, less common risk factors include vertical (mother to baby) transmission (Ohto *et al*, 1994). The reported rate of vertical transmission varies between studies, but is around 6%, with increased rates seen when mothers have high HCV viral loads and/or are co-infected with HIV (Thomas *et al*, 1998). Sexual transmission does occur (Alter, 1993) but is very rare (Balogun *et al*, 2003). Some studies have suggested a link between skin piercing or tattooing with non-sterile equipment (Ko *et al*, 1992). However, evidence for this association is weak and piercing/tattooing may often be used as an excuse to hide other risk factors such as IDU. Recently, a worrying rise in acute HCV infection in HIV-positive homosexual men has been observed (Browne *et al*, 2004).

Prior to 1991, when screening of blood donors was introduced, blood transfusions and receiving blood products were major risk factors for HCV (Alter *et al*, 1992; van der Poel, 1999; Soldan *et al*, 2002). This led to HCV infection in almost all haemophiliacs treated with clotting factors. Each unit of factor VIII received by a haemophiliac consisted of blood plasma from 30-40 donors, vastly increasing the likelihood of HCV transmission to these individuals. Following the introduction of donor screening, and more recently, nucleic acid testing (NAT) of blood donations, infection through these routes is now extremely rare (Soldan *et al*, 2005). For HCV, the frequency of infectious donations was 1 in 520,000 during 1993–1998 and fell to 1 in 30 million during 1999–2001 when all donations were tested for HCV RNA (Soldan *et al*, 2003). In under-developed parts of the world, particularly

in rural areas, blood screening does not occur. Many infections in these areas occur as a result of blood transfusion or, more commonly, re-use of needles and syringes.

1.3 HCV disease and diagnosis

Most people have no signs or symptoms of acute HCV infection and are diagnosed as a result of routine blood tests. Many people are, therefore, unaware of their infected status, increasing the risk of transmission. When symptoms do occur, these include flu-like illness, nausea, fatigue, depression, jaundice and abdominal pain. Blood samples may reveal abnormal liver function tests (LFTs) within 4-12 weeks including raised alanine aminotransferase (ALT) which is a crude indicator of liver injury.

Diagnosis of HCV is via serological detection of HCV antibodies with enzyme immunoassays (EIAs) which have antigens derived from the core and/or non-structural proteins. Initial positive anti-HCV results are confirmed using either a second EIA, or a line assay which has antigens impregnated onto strips. Antibody detection is less useful to diagnose infection in the immunocompromised patient (including those co-infected with HIV) (Chamot *et al*, 1990) and those receiving haemodialysis (Schneeberger *et al*, 1998) as they may not have a detectable HCV antibody response. Antibody detection is not useful to detect mother-to-baby transmission as neonates will have maternal antibody for several months after birth.

Serological techniques are limited as it can take up to three months for antibodies to HCV to become detectable following infection. Combined assays which detect both HCV antigen (Ag) and antibody (Ab) are invaluable to detect infections prior to seroconversion and are often used as confirmatory tests. The Bio-Rad MONOLISA HCV Ag-Ab ultra kit consists of a microplate coated with a mixture of recombinant proteins (from the NS3 region), antigen (from the NS4 region), mutated peptide (from the capsid) as well as monoclonal antibodies (against the capsid protein). This allows simultaneous detection of anti-HCV via an indirect test and HCV core antigen via a sandwich test. This shortens the pre-seroconversion window period over conventional HCV Ab screening assays. The detection of HCV RNA by PCR can also be used to confirm HCV diagnosis in individuals pre-seroconversion and in those for whom serological test results are weakly reactive (indeterminate). HCV RNA is seen in the blood 1-3 weeks after initial exposure.

1.4 HCV progression

The clinical progression of HCV varies considerably. HCV persists in 70-80% of primary infections, causing chronic hepatitis. Around 20% of people with chronic infection will develop serious liver disease, such as cirrhosis and fibrosis; 1-4% of those with cirrhosis will develop hepatocellular carcinoma (HCC) each year (DoH, 2002). Figure 1.2 indicates the estimated overall progression of HCV infection, according to Department of Health data. However, recent analysis has demonstrated that event-biased recruitment in studies of HCV progression which often use liver clinic cohorts may produce upwardly biased estimations of progression rates (Freeman *et al*, 2001; Fu *et al*, 2007). Sweeting and colleagues (2006) demonstrated that disease progression varied according to cohort, with the estimated 20-year probability of progression to cirrhosis being 12% in a hospital-

based cohort, 6% in a post-transfusion cohort and 23% in a cohort recruited from a tertiary referral centre (Sweeting *et al*, 2006).

Chronic infection is usually asymptomatic for many years, with symptoms of liver disease usually occurring long after initial infection. However, certain independent host factors are linked to rapid progression to liver disease including being over 40 years old at infection, male gender and high alcohol consumption (Poynard *et al*, 1997). Accelerated development of liver disease appears to be independent of HCV genotype or viral load (Poynard *et al*, 2001). Once chronic HCV has progressed to cirrhosis, symptoms include ascites (accumulation of fluid in the abdomen), bruising/bleeding tendency and varices (enlarged veins, especially in the stomach and oesophagus). Chronic HCV also has many extrahepatic manifestations affecting the joints, muscles, neural and gastrointestinal tissues and skin (Sterling and Bralow, 2006).

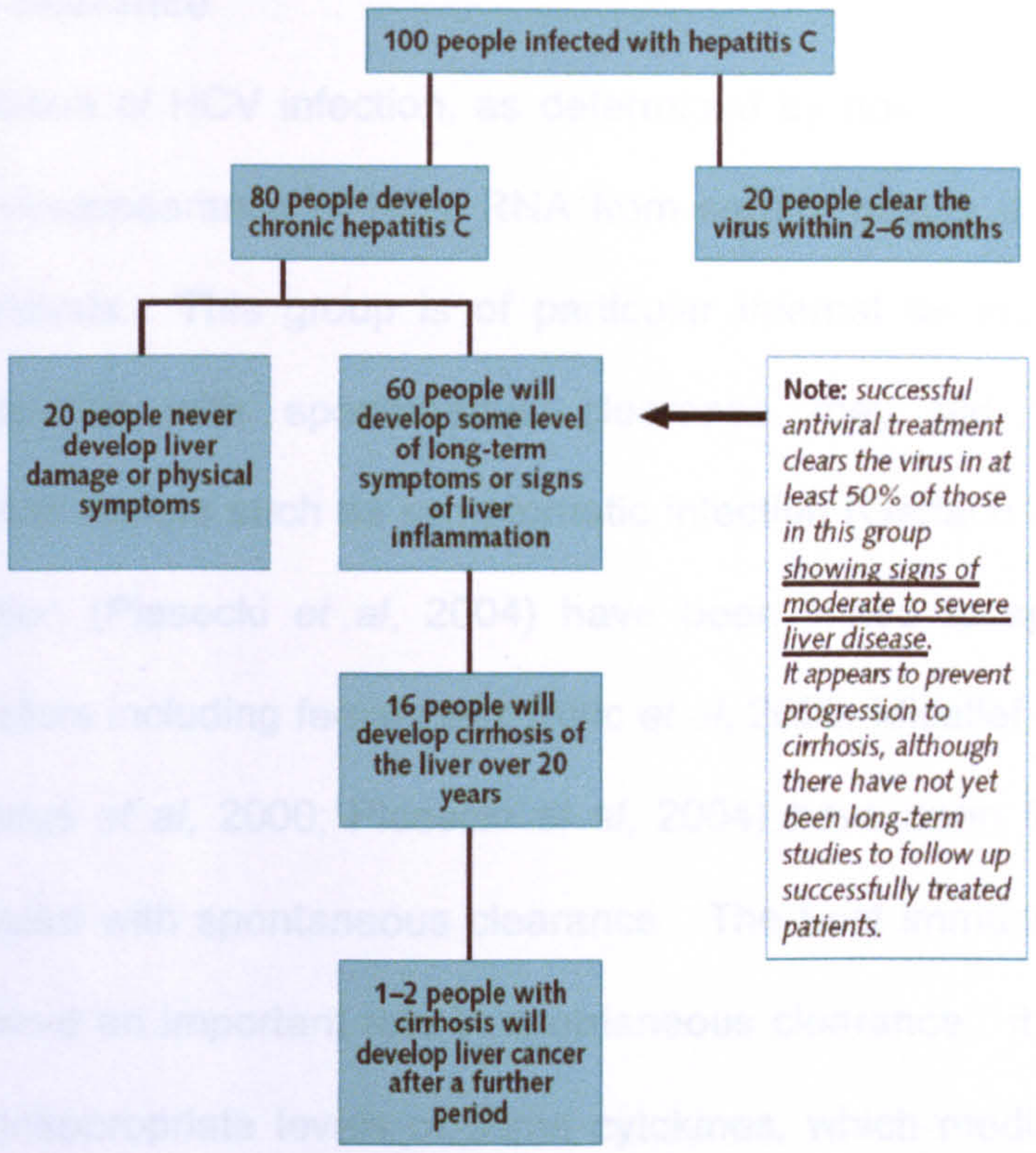

Figure 1.2: Clinical progression of HCV infection. Taken from 'Hepatitis C Strategy for England', DoH 2002.

HCV infection places a substantial burden on health care. Hospital admissions and liver transplants for HCV end stage liver disease continue to rise. Statistical modelling has demonstrated that HCV-related cirrhosis and deaths from hepatocellular carcinoma (HCC) are likely to increase dramatically in the next decade (Sweeting *et al*, 2007). The financial burden of HCV will continue to increase, as although new cases are decreasing due to blood screening, many people who experimented with IDU in the 1960-80s are unknowingly infected with HCV and represent an unknown number of asymptomatic infections which may result in clinical disease.

1.5 Spontaneous clearance

Spontaneous resolution of HCV infection, as determined by normalisation of liver function tests and disappearance of HCV RNA from serum, occurs in 20-30% of HCV-infected individuals. This group is of particular interest as identifying the mechanisms associated with spontaneous clearance may aid in vaccine development. Clinical factors such as symptomatic infection (Gerlach *et al*, 2003) and HBV co-infection (Piasecki *et al*, 2004) have been linked to spontaneous clearance. Host factors including female sex (Alric *et al*, 2000; Micallef *et al*, 2006) and ethnicity (Thomas *et al*, 2000; Piasecki *et al*, 2004) have been found to be significantly associated with spontaneous clearance. The host immune response is also thought to have an important role in spontaneous clearance. It is possible that production of inappropriate levels of some cytokines, which mediate hepatic inflammation and fibrosis in HCV infection, can lead to viral persistence and chronic HCV infection. The difference between individuals in their ability to produce IL-10, TNF-α or IFN-γ cytokines, attributed to certain gene polymorphisms, have been reported as indicators of likelihood of spontaneous viral clearance (Lio *et al*, 2003; Mangia *et al*, 2004) although these findings remain controversial (Kusomoto *et al*, 2006; Minton *et al*, 2005). Certain polymorphisms in some interferon-induced genes whose protein products have antiviral action have been associated with spontaneous clearance (Knapp *et al*, 2003) as have specific HLA type II alleles, (DQB1*0301 and DRB1*1101) (Yee, 2004).

Viral factors have also been reported to affect viral clearance. A study, in Germany, of anti-HCV positive males with history of IDU demonstrated a significant prevalence of genotype 3 in individuals who spontaneously cleared the virus (86%

of type 3 cleared vs. 7% of type 1, n=92) (Lehmann *et al*, 2004). Infection with genotype 1 and specifically subtype 1b has been linked to chronicity (Amoroso *et al*, 1998; Hwang *et al*, 2001). More recently, in a large study, Harris and colleagues (Harris *et al*, 2007) have suggested that HCV genotype 1 infection is more likely to be associated with spontaneous viral clearance than non-1 genotype infection.

Most of the studies examining spontaneous HCV clearance have been very small, with some contradictory results. A recent systematic review of 31 longitudinal studies with 675 study subjects, concluded that the only factors significantly associated with viral clearance were sex, with men being less likely to clear the virus (0.20 *vs.* 0.42, RR 0.43, 95% 0.36–0.53), and acute symptomatic HCV (0.31, 95% CI 0.26–0.36) (Micallef *et al*, 2006).

True spontaneous clearance is, however, difficult to determine. It is presently unclear whether spontaneous clearance is associated with complete eradication of the virus, or whether low-level viral replication persists but is controlled by the cellular and humoral immune responses. Several small studies suggest that HCV RNA can be repeatedly undetectable in serum or plasma by laboratory assays, but are identifiable in serum and peripheral blood mononuclear cells (PBMCs) by molecular tests of enhanced sensitivity in patients thought to have spontaneously resolved HCV infection. Pham and colleagues (Pham *et al*, 2004) detected HCV RNA in serum and/or PBMCs from all tested patients thought to have spontaneously resolved HCV infection (n=5). Similarly, Radkowski *et al* (2005) studied 11 spontaneous clearers and detected HCV RNA in serum samples from 2

(18.2%), in PBMCs from 3 (27.3%) and in both serum and PBMCs from 4 of them. Following stimulation by mitogens which is thought to enhance HCV replication, HCV RNA was detected from all eleven spontaneous clearers.

1.6 HCV structure

Hepatitis C virus (HCV) is the sole member of the genus hepacivirus of the *Flaviviridae* family. It is a small, enveloped virus which is covered in projections which are complexes of the envelope glycoproteins E1 and E2 (Figure 1.3).

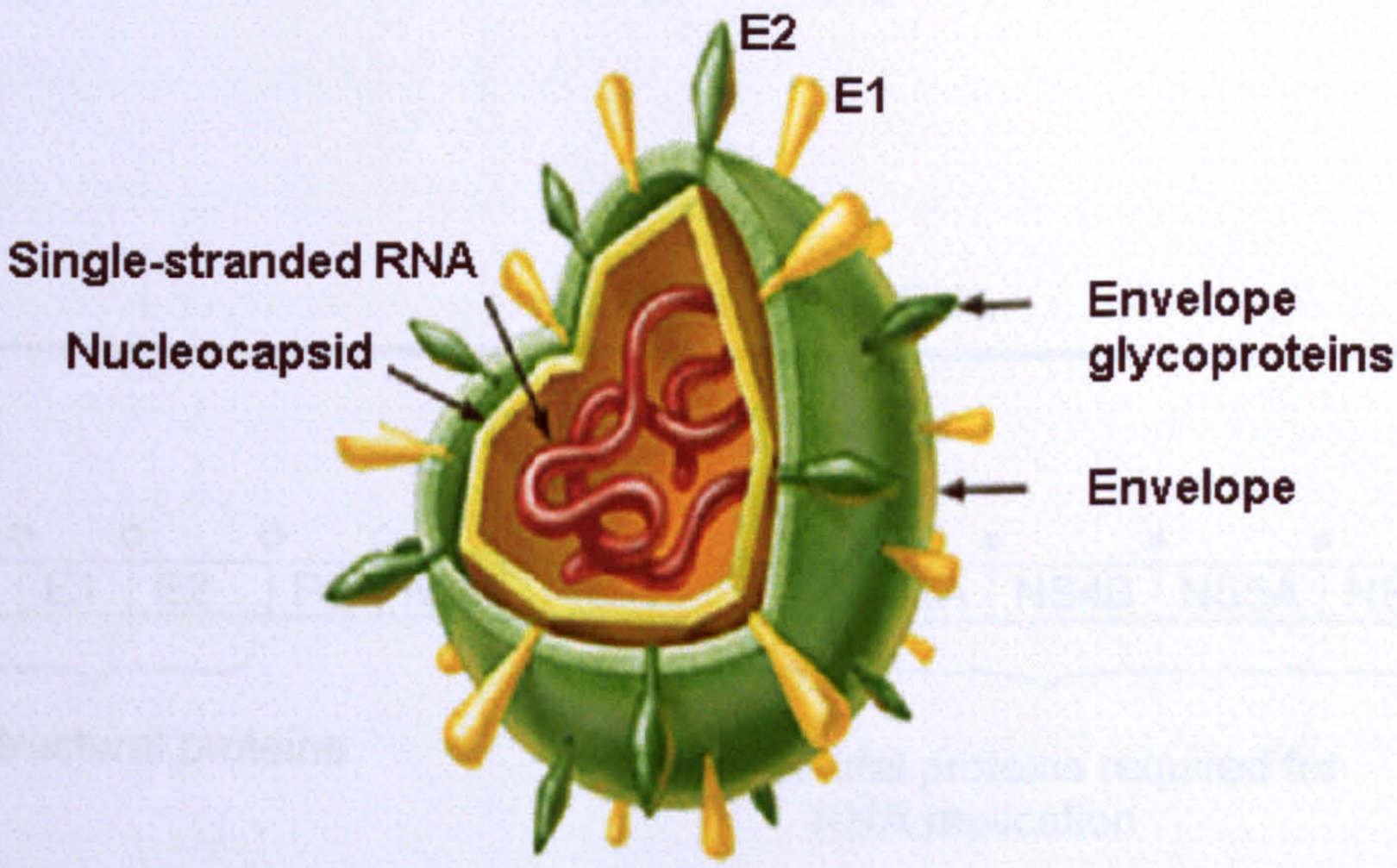

Figure 1.3: The structure of the hepatitis C virus illustrating the RNA genome, nucleocapsid and envelope glycoproteins E1 and E2. Adapted from http://www.viralgenomix.com/vgx_410_HCV.html.

The nucleotide sequence and genetic organisation of HCV was reported in 1991 (Choo *et al*, 1991) and the molecular virology has now been described extensively (Major and Feinstone, 1997; De Francesco, 1999; Lemon *et al*, 2007). The HCV genome is single-strand positive-sense RNA of approximately 9,600 nucleotides in

length and carries a single open reading frame (ORF) which encodes a single polyprotein of around 3000 amino acids. Translation of the ORF is directed via a 5' untranslated region (UTR) which has an internal ribosome entry site (IRES) that functions to bring ribosomes into close contact with the start codon (Lemon *et al*, 2007). The polyprotein is cleaved by viral and cellular proteases into 10 structural and non-structural viral proteins. These consist of 3 structural proteins (core, E1 and E2) located at the N-terminus, p7 and NS2 proteins which probably play essential roles in viral morphogenesis and release and 5 non-structural (NS) proteins which are required for RNA replication (NS3, NS4A, NS4B, NS5A and NS5B) in the remainder of the polyprotein (Figure 1.4).

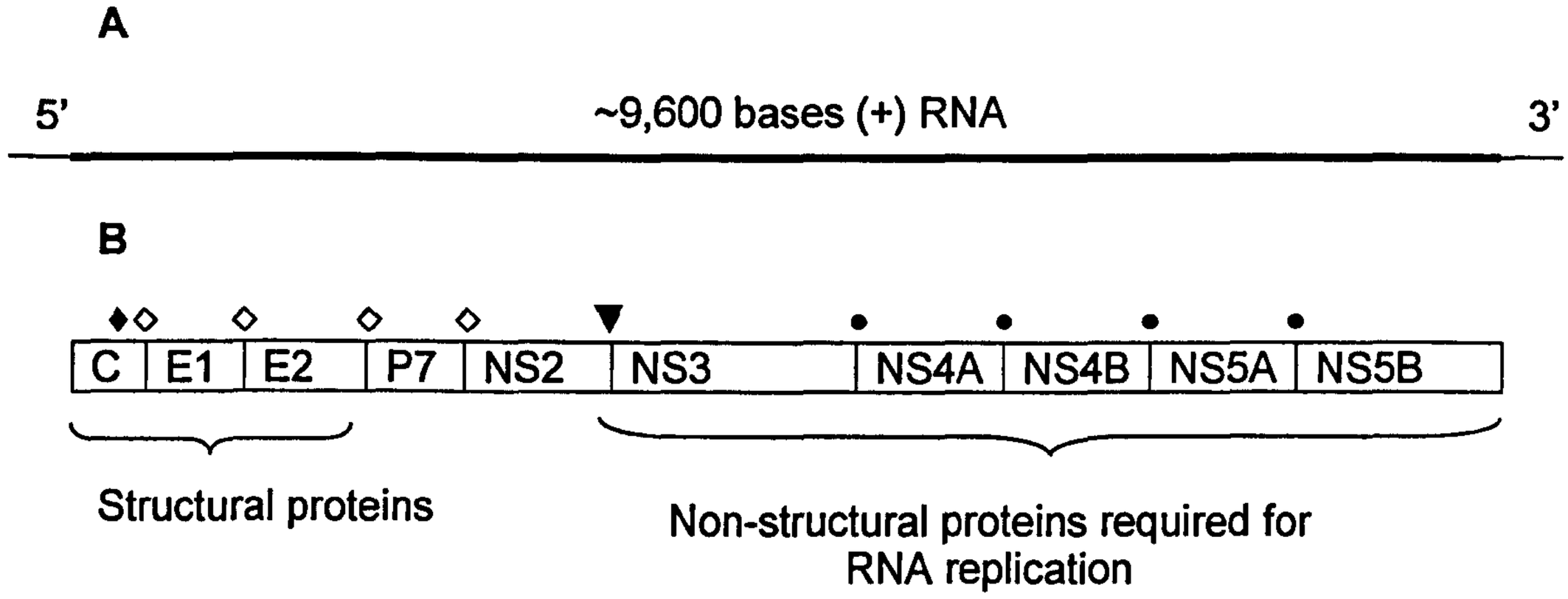

Figure 1.4: A schematic representation of the organisation of the HCV genome and polyprotein. **A**: The HCV genome with non-translated RNA segments shown as thin lines. **B**: Functional organisation and processing of the viral polyprotein. Sites of cleavage by host cell and viral proteases are indicated by symbols. Adapted from Lemon *et al,* 2007, p1256.

The core protein forms the viral nucleocapsid. It can also interact with numerous cellular proteins and affect host cell functions. The envelope glycoproteins E1 and E2 are transmembrane proteins with C-terminal hydrophobic anchors. They are glycosylated in the host cell endoplasmic reticulum (ER). The E1 and E2 glycoproteins are associated in the form of a heterodimer (Deleersnyder *et al*, 1997). The envelope proteins vary considerably among HCV sequences, especially at a hypervariable region (HVR1) located at the amino terminus of E2. HVR1 is also thought to be a critical neutralisation domain for the antibody response to HCV infection (Farci *et al*, 1996). This region mutates rapidly *in-vivo* under the selective pressure of the antibody response, producing many neutralisation escape mutants, a strategy by which the virus can evade the host immune response. p7 may have ion channel activity (Griffin *et al*, 2003), and has been demonstrated to be similar to the M2 ion channel of influenza virus (Griffin *et al*, 2004). It belongs to a group of viral proteins known as 'viroporins' which are hydrophobic proteins which form cation channels. The precise role of p7 in HCV replication is uncertain. NS2 and the N-terminal of NS3 form an autoprotease which cleaves the NS2/NS3 junction. NS3 is a multifunctional protein consisting of a serine proteinase which cleaves all other non-structural protein junctions, an NTPase (nucleotide triphosphatase) and an RNA helicase. The latter protein is involved in the viral replication complex and probably functions to unwind replicative double strand RNA intermediates and to eliminate RNA secondary structures. NS4a is a co-factor for the NS3 serine protease and localises NS3 to the ER. Relatively little is known about the NS4b protein; it localises to the ER and appears to induce the expression of 'membranous webs' which are important in the assembly of the replication complex (Egger *et al*, 2002). NS5a is a zinc

metalloproteinase and is an essential component of the replicase complex. Its phosphorylation status may regulate viral RNA replication (Evans *et al*, 2004). NS5a also contains the interferon sensitivity determining region (ISDR) which can determine response to therapy (Enomoto *et al*, 1996). The NS5b RNA-dependent RNA polymerase is the enzyme for synthesis of new RNA genomes (Oh *et al*, 1999). Table 1.1 shows a summary of each of the HCV proteins and their functions.

Genome Region	Function
5' UTR	Highly conserved. Contains IRES – binds ribosome to *initiation codon*
Core (C)	Nucleocapsid protein
E1	Envelope glycoprotein
E2	Envelope glycoprotein
p7	Potential ion channel activity (viroporin)
NS2	Autoprotease
NS3	Multifunctional protein – serine protease (NH_2 terminal), NTPase and helicase (COOH terminal)
NS4a	Co-factor for full expression of NS3 protease
NS4b	Hydrophobic membrane-associated protein
NS5a	Multifunctional protein – essential component of replicase complex
NS5b	RNA-dependent RNA polymerase activity
3'UTR	Contains a variable region, a U/C rich region and a highly conserved 3' terminal domain

Table 1.1: HCV proteins and their functions. NS; non-structural, UTR; untranslated region.

1.7 HCV replication

The investigation of the HCV life cycle was hampered by the lack of efficient cell culture systems and animal models. However, with *in-vitro* and *in-vivo* model systems now in place, investigation of the life-cycle has intensified and much is

now known about the stages of HCV replication (Bartenschlager and Lohman, 2000; Lemon *et al*, 2007).

1.7.1 Virus attachment and entry

HCV has a predilection for hepatocytes and the liver is the major site of HCV replication. Several groups have suggested the existence of extrahepatic reservoirs of HCV replication, specifically in PBMCs (Wang *et al*, 1992; Muller *et al*, 1993). However, more specific methods for detection of the HCV RNA negative strand, the template for new genomic HCV RNA, failed to detect this in PBMCs, throwing into doubt the possibility of extrahepatic HCV replication (Lanford *et al*, 1995; Laskus *et al*, 1997). This is still subject to controversy as several studies have demonstrated extrahepatic HCV replication occurring in immunosuppressed individuals (Laskus *et al*, 1998; 2007; Radkowski *et al*, 1998).

The first step in replication is the attachment of HCV to specific host cell receptors. It is thought that cell entry requires a set of co-receptors that include the CD81 tetraspanin and the human scavenger receptor class B type 1 (SR-B1) (a high-density lipoprotein internalisation molecule) in addition to other hepatocyte-specific co-factor(s) (Pileri *et al*, 1998; Agnello *et al*, 1999; Bartosch *et al*, 2003). HCV attachment is via the E1-E2 complex, although it remains unclear whether E1 or E2 harbours the fusion peptide. Mutational analysis has indicated that E2 plays a role in refolding of the glycoproteins during fusion (Drummer and Poumbourios, 2004). Cell attachment of HCV leads to clathrin-mediated endocytosis of bound virions (Blanchard *et al*, 2006).

1.7.2 Polyprotein translation and processing

Once inside the cytoplasm, the virus is uncoated and genomic RNA is directly translated. The IRES, comprising almost the entire 5'UTR, directs translation of the polyprotein at the ribosome (Wang *et al*, 1993). The polyprotein is cleaved co- and post-translationally by host signal peptidases and two viral proteinases (see Figure 1.4) to form the 10 protein products. The non-structural proteins form a replication complex which binds to the rough endoplasmic reticulum and coordinates viral replication. Following cleavage from the polyprotein, E1 and E2 enter the lumen of the ER and are glycosylated and joined to form heterodimers.

1.7.3 RNA replication

Following viral protein processing the HCV genome is replicated. The original positive sense RNA strand is used as a template for negative strand synthesis, which is carried out by the RNA-dependent RNA polymerase. The negative strand is then used as a template to produce new genomic HCV RNA. This forms a double-stranded RNA intermediate which must be separated as double-stranded RNA can trigger cellular defences and also takes away the template. The NS3 helicase unwinds the RNA strands using the NTPase. Strand synthesis occurs within a viral replication complex formed by the non-structural proteins which sequesters the process. This complex forms a 'membranous web' on the ER, whose synthesis is thought to involve NS4b (Egger *et al*, 2002).

HCV replication generates virus variants due to the high production rate of viral particles along with the high error rates of the viral RNA-dependent RNA polymerase during RNA replication. A mutation rate of 1.44×10^{-3} base

substitutions per site per year was found over a 13 year period in an HCV-infected patient (Ogata *et al*, 1991). Variability is not spread equally through the genome. E1 and E2 demonstrate the greatest variability, especially in the hypervariable region of E2 (Weiner *et al*, 1991); whilst the core gene and some non-structural genes (such as NS3) are more conserved. The 5' UTR shows the least variability, as specific sequences and RNA secondary structures are required for transcription and translation. Even within an infected individual, HCV exists as a highly heterogeneous viral population. This complex mix of related molecular species, known as quasispecies, consists of a single dominant sequence and a mixture of mutants (Martell *et al*, 1992). In two regions of the E2 protein, termed the hypervariable regions (HVRs), high frequencies of mutations have been identified, which accumulate during chronic infection. The production of quasispecies enables the virus to evade the host immune system and prevents elimination of the virus by the infected host (Weiner *et al*, 1992; Shimizu *et al*, 1994).

Due to this variability, HCV has been classified into six major genotypes of HCV (1-6) which vary by up to 35% in sequence. Within each genotype there are closely related strains, or subtypes (a-k) that differ in sequence by 20-25%. Currently more than 70 subtypes have been identified (Simmonds *et al*, 1993; 1994, Simmonds, 1995). Novel variants from Vietnam, Thailand and Indonesia classified as genotypes 7,8,9,10 and 11 were re-classified into subtypes of type 6 or type 3 (Simmonds *et al*, 1996). International standardisation and nomenclature of HCV genotypes/subtypes is complex and is continually reviewed and updated (Simmonds *et al*, 2005).

1.7.4 Virus assembly and release

Following viral genome replication, viral assembly occurs. The capsid self-assembles from multiple units of the core protein and the genomic RNA is enclosed within the capsid shell. It is thought that, like other flaviviruses, HCV acquires its envelope through budding into the lumen of the ER (where E1 and E2 are attached) and is released from host cells by exocytosis via the Golgi complex (Lemon *et al*, 2007). A schematic representation of the HCV replication cycle is shown in Figure 1.5.

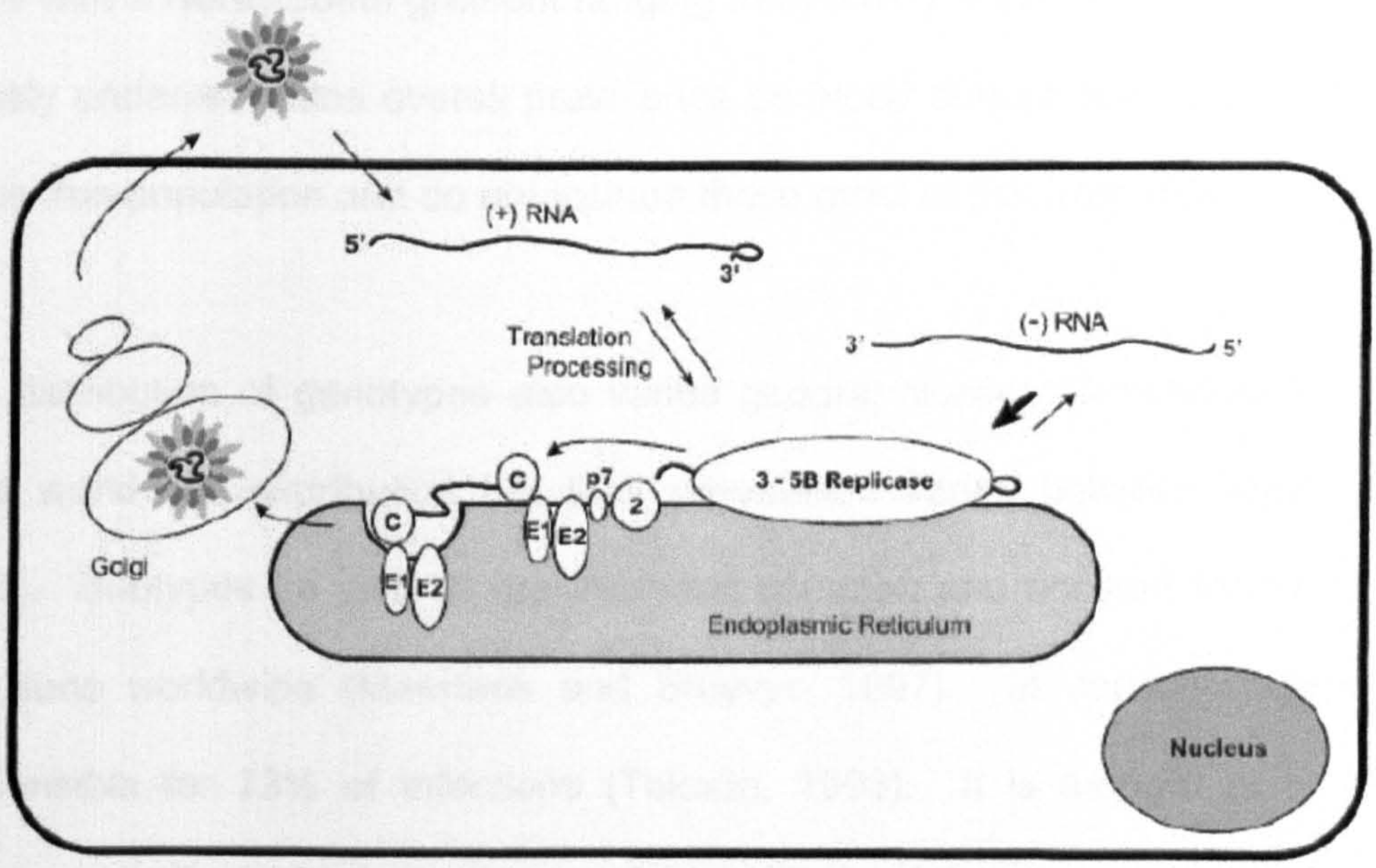

Figure 1.5: An hypothetical model of the HCV replication cycle. The large rectangle represents the host cell. Once inside the cell, the genomic RNA (+RNA) is released into the cytoplasm and translated. The polyprotein is processed and the viral proteins remain tightly associated with the membranes of the ER. The non-structural proteins form a replication complex (3-5B replicase) which binds to the rough endoplasmic reticulum. The original positive sense RNA strand is used as a template for negative strand synthesis which is then used to produce new genomic HCV RNA. The viral particles are enveloped by budding into the lumen of the ER and then exported via transit through the Golgi complex. (Figure adapted from Bartenschlager and Lohmann, 2000).

1.8 HCV epidemiology

HCV is endemic in most parts of the world, with an overall prevalence of around 3%. However, there is great geographical variation in the incidence of HCV, which varies from 1% to greater than 10% (WHO, 2002). The prevalence in some African countries, the Eastern Mediterranean, South East Asia and the Western Pacific are higher than North America and Europe (WHO, 1999). The high number of HCV cases in Egypt is thought to be due to the administration of parenteral anti-schistosomal treatment that requires 10-12 injections, mostly given with reusable needles (Frank *et al*, 2000). The prevalence in blood donors in European countries is 1% with a North-South gradient ranging from 0.04-2% (Touzet *et al*, 2000). This grossly underestimates overall prevalence as blood donors are not representative of the true population and do not include those most at risk from HCV.

The distribution of genotypes also varies geographically. Genotypes 1, 2 and 3 have worldwide distribution but their prevalence varies between regions (Zein, 2000). Subtypes 1a and 1b are the most common and account for over 60% of infections worldwide (Maertens and Stuyver, 1997). In Japan, subtype 1b is responsible for 73% of infections (Takada, 1993). It is thought to be through intravenous drug use that subtypes 1a and 3a have become widely distributed in Western countries (Pawlotsky *et al*, 1995). In Western Africa, genotype 2 causes the majority of infections, whilst in North and Central Africa, genotypes 1 and 4 predominate (Xu *et al*, 1994). Genotype 3 is endemic in South East Asia. In the Middle East (including Egypt) (Chamberlain *et al*, 1997), 4 is the major genotype. Genotypes 5 and 6 are rare and are generally confined to South Africa (genotype 5) and Hong Kong and South East Asia (genotype 6). In Africa and South East

Asia there is far greater diversity of subtypes, supporting the theory that HCV has been endemic in these areas for a long time. The limited diversity of subtypes in the USA and Europe indicates that the occurrence in Western countries is relatively recent, appearing in new risk groups for infection (Simmonds, 2001).

Using age-specific prevalence data, Wasley and Alter (2000) outlined three distinct transmission patterns. In some countries (e.g. Australia and USA), most infections are found in people 30-49 years of age, indicating relatively recent transmission, primarily affecting young adults. In countries such as Japan and Italy, demonstrating the second transmission pattern, most infections are in the older person, indicating infection in the distant past. The third transmission pattern, which is seen in countries such as Egypt, has HCV infection occurring in all age groups indicating ongoing risk of infection. This mirrors the risk factors which are predominantly injecting drug use in countries with the first transmission pattern, and unsafe healthcare procedures seen in countries with the latter two transmission patterns (Wasley and Alter, 2000).

1.9 HCV treatment

There is no effective vaccine available for HCV. Much effort has, therefore, gone into producing a therapeutic regime for its treatment. Interferon (IFN) is the treatment of choice for chronic HCV. The mechanism of action of IFN is not fully understood. It is thought to induce IFN-stimulated genes (ISGs) which establish an antiviral state within the cell (Sen *et al*, 2001). IFN also has an important role in immunomodulation, promoting memory cell proliferation and stimulating natural killer cell activity.

IFN monotherapy has only limited success. A meta-analysis of clinical trials indicated that monotherapy produced an end of treatment virological response in only 29% of treated individuals (Carithers and Emerson, 1997). The addition of ribavirin (a broad-spectrum nucleoside analogue which inhibits a range of DNA and RNA viruses) to IFN treatment, vastly improved the response rate compared to monotherapy for both initial treatment (McHutchison *et al*, 1998; McHutchison and Poynard, 1999) and relapse (Davis *et al*, 1998). More recently, a pegylated form of interferon (peginterferon) has been developed. Two different peginterferons are available, alpha 2a (α-2a) and alpha 2b (α-2b). These have a large molecule of polyethylene glycol (PEG) covalently attached to the interferon molecule. This slows the rate of elimination from the body and has much higher success rates for viral clearance than conventional interferon (Zeuzem *et al*, 2000; Manns *et al*, 2001; Fried *et al*, 2002). Side effects from therapy can be severe. Interferon treatment can lead to influenza-like symptoms, anorexia, nausea, lethargy, cardiovascular problems, nephrotoxicity, hepatotoxicity and depression (including suicidal behaviour) (Fried *et al*, 2002; Joint Formulary Committee, 2008). In addition, ribavirin has a multitude of multi-systemic and unpleasant side effects including haemolytic anaemia.

The aim of interferon therapy is sustained virological response (SVR) which is defined as undetectable levels of HCV RNA following treatment and 6 months thereafter. Early virological response (EVR), which is defined as a reduction in HCV RNA level by at least 2-log from baseline (pre-treatment) at week 12 of therapy is a good indicator of SVR. Failure to achieve EVR is a strong predictor of non-response to treatment. The percentage of patients who do not achieve EVR

and subsequently do not have a SVR is 97-100% (Lee *et al*, 2002; Davis *et al*, 2003). Rapid virological response (RVR) which is defined as undetectable levels of HCV RNA following four weeks of treatment is frequently an indicator of both EVR and SVR. Patients who become HCV RNA negative after 4 weeks have the best chance of achieving a SVR (Jensen *et al*, 2006; Yu *et al*, 2007). Recent studies have demonstrated that achievement of RVR may be used as an indicator for shortening treatment duration for genotypes 1, 2 and 3 (Poordad *et al*, 2008). A transient treatment response occurs in 10-25% of individuals with optimum regimens. SVR may be achieved in these patients following longer courses or higher doses of treatment (Shiffman *et al*, 2002).

HCV genotype is important in predicting response to therapy. Studies have shown that optimal duration of, and response to, treatment are strongly associated with genotype, with response rates 2 to 3 fold higher in patients infected with genotypes 2 and 3 than with genotype 1 (Martinot-Peignoux *et al*, 1995; Poynard *et al*, 1998; Manns *et al*, 2001; Zeuzem *et al*, 2001; Hadziyannis *et al*, 2004). National Institute of Health and Clinical Excellence (NICE) guidelines recommend that patients should be treated with peginterferon-α and ribavirin, with duration of therapy adjusted according to genotype. Those with genotype 2 and/or 3 infection should be treated for 24 weeks, as maximum rate of SVR is attained in this time period for these individuals. For people infected with other genotypes, it may take longer to achieve SVR. Therefore, those with genotypes 1, 4, 5 or 6 should be treated initially for 12 weeks and then a further 36 weeks only if an EVR has been achieved. If this has not occurred then treatment should be discontinued in these patients as it is unlikely that viral eradication will occur. This treatment regime is

quite successful in patients with HCV genotypes 2 and 3 infection, achieving HCV eradication rates of 76-93% (Zeuzem *et al*, 2004; von Wagner *et al*, 2005). However, it is much less effective in patients with genotype 1 infections, with eradication rates of between 42-47% (Manns *et al*, 2001; Fried *et al*, 2002; Zeuzem *et al*, 2004a; Ferenci *et al*, 2005;). Treatment was initially reserved for patients with moderate to severe chronic HCV (NICE, 2004). However, the NICE guidelines have subsequently been updated and now recommend that all patients with chronic HCV infection can be considered for treatment without deferring treatment until the disease has progressed to moderate or severe (NICE, 2006).

Liver biopsy is the most specific test to assess the nature and severity of liver diseases and is an integral part of assessing the extent of chronic HCV. It is the most reliable method to determine the extent of necroinflammatory activity and fibrosis, especially as liver enzymes do not reflect liver damage reliably (Nutt *et al*, 2000). Liver biopsies are stained and examined for evidence of periportal necrosis, intralobular degeneration, portal inflammation and fibrosis or cirrhosis (Figure 1.6). However, it is not always possible to carry out a biopsy and the stage of liver disease must be assessed by alternate methods such as ultrasound scans.

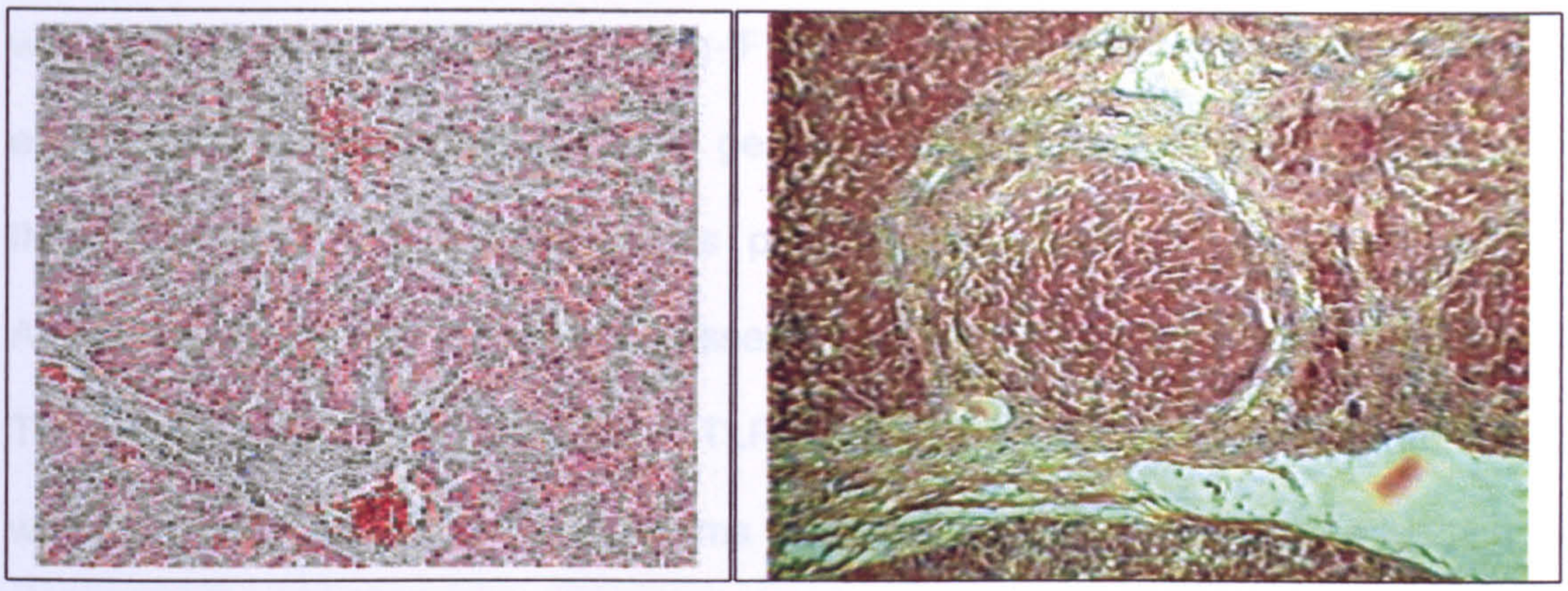

A B

Figure 1.6: Haematoxylin and eosin stained liver biopsies (x1000). (A) Healthy liver. (B) Post hepatic cirrhosis with thickening of Glisson's capsule (outer capsule surrounding the liver) showing severe fibrotic strands with regenerative nodules. Taken from www.tigerpath.com.

1.9.1 New agents for HCV treatment

In the last few years, progress in the understanding of HCV and its life-cycle has lead to a great deal of attention in the field of HCV therapy. In particular, the development of specifically targeted antiviral therapy for HCV (STAT-C) is rapidly advancing. This involves the development of drugs which target specific enzymes important in the replication of HCV. Several effective inhibitors of the viral NS3/NS4a protease and NS5b polymerase have been identified and are now progressing through clinical trials (De Francesco and Carfi, 2007). Telaprevir (Vertex Pharmaceuticals) for example, is an inhibitor of the NS3/NS4a serine protease. Recent large phase II clinical trials have shown that, compared to current treatment, telaprevir, in combination with peg-interferon α-2a and ribavirin resulted in higher rates of RVR and produced greater anti-viral effects within shorter treatment duration (Dusheiko *et al*, 2008; McHutchison *et al*, 2008). R1626 (Roche Pharmaceuticals) is an NS5b polymerase inhibitor. A recent phase IIa study has shown that R1626 in combination with peg-IFN α-2a and ribavirin for four

weeks followed by 44 weeks of peg-IFN α-2a and ribavirin demonstrated higher end of treatment response (84%) in genotype 1-infected individuals compared to those who had received 48 weeks peg-IFN α-2a and ribavirin alone (65%). Additionally, attention is being focussed on immunomodulatory agents such as Toll-like receptor (TLR) agonists. TLRs are key mediators of innate immunity which are activated by microorganisms and induce signalling cascades leading to the production of cytokines and interferons. In phase 1 studies, HCV-infected patients given a TLR-9 agonist, CPG10101, demonstrated increased markers of immune activation and decreased HCV RNA levels (McHutchison *et al*, 2007). Development of new antivirals is a slow process, and many of the potential agents will never be available for the treatment of HCV due to withdrawal from development as a result of issues with toxicity.

1.10 Diagnosis/Monitoring of HCV infection

1.10.1 HCV viral load

Determination of HCV RNA level is an integral part of diagnosis and management of patients with HCV. Routine diagnosis of HCV is based on the detection of HCV-specific antibodies. However, by this means, it is impossible to determine whether the patient has active infection, or has had a past infection which has cleared. Detection of HCV RNA is required as an absolute marker of current infection and can be qualitative. Management of the treatment of HCV is based on quantitative HCV RNA measurements before, during and after interferon therapy. Pre-treatment viral load is thought to be an important predictor of SVR with high pre-treatment viral loads less likely to respond to therapy than low viral loads (Manns *et al*, 2001; Lee *et al*, 2002). HCV viral load measurements also have clinical utility

prior to initiation of therapy and after 12 weeks to determine if EVR has been achieved and the likelihood of SVR (Lee *et al*, 2002; Davis *et al*, 2003).

Quantitation of HCV is problematic as it can circulate in the blood at low copy number and its heterogeneity makes it difficult to ensure sensitivity of detection. Quantitation assays must have linearity over a broad range of viral loads as these cover a wide range from $>10^7$ copies/ml, to below 1000 copies/ml in some chronically infected patients and even lower in patients on interferon therapy (Yasui *et al*, 1998; Zeuzem *et al*, 1998). Initially, comparison of assay performance for quantitative HCV RNA detection was hampered by the lack of standardisation of methods for HCV quantitation. This issue was resolved by the introduction of an HCV World Health Organisation (WHO) first international standard for Nucleic Acid Amplification Technology Assays (96/790). This is a lipophilised genotype 1 sample which was assigned a value of 10^5 IU/ml. This allowed the calibration of all available assays to international units (IU) and standardisation of HCV RNA quantitation (Saldanha *et al*, 1999; Pawlotsky *et al*, 2000). This has recently been replaced by the second international standard (96/798) which was assigned the same unitage as the first standard (Saldanha *et al*, 2005). There is, however, no standard formula for converting the amount of HCV RNA reported in copies/ml to the amount reported in IU. The conversion factor ranges from one to around five HCV RNA copies per IU, depending on the assay used. HCV RNA assays should have a sensitivity of 50 IU/ml to detect low HCV RNA levels after treatment and to distinguish spontaneous viral clearance from low levels of circulating HCV.

1.10.1.1 Commercial HCV quantitation assays

Several qualitative/quantitative HCV viral load kits are commercially available which differ in the lower detection limits and linear ranges of amplification. The branched DNA (bDNA) assay, developed by Chiron relies on signal, rather than target amplification. Viral RNA is captured on microwells by specific synthetic oligonucleotide capture probes. The captured RNA is then hybridised to branched oligonucleotides which are, in turn, hybridised to enzyme-conjugated oligonucleotides which are quantified. A semi-automated bDNA system was introduced (VERSANT HCV RNA 3.0 assay, Bayer Diagnostics, UK) which has a dynamic range of 615-7,700,000 IU/ml and was thought to be equally sensitive across all genotypes (Elbeik *et al*, 2004). However, it has been found recently to underestimate the quantity of genotypes 1 and 3 (Sarrazin *et al*, 2006). The bDNA method is easy and relatively inexpensive for use on a large number of samples and does not have the contamination risk that is associated with molecular methods, but its lower detection limit of ~600 IU/ml means that it lacks sensitivity (Beld *et al*, 2002).

The Cobas Amplicor HCV Monitor 2.0 assay (Roche Diagnostics, UK) is a molecular assay based on conventional RT-PCR in which the amplified products are hybridised, in a separate step, to specific oligonucleotide probes which are detected by colorimetric determination. This assay has a relatively small linear range of 600-<500,000 IU/ml. The test lacks sensitivity as it uses a limited number of amplification cycles so that high target concentrations do not reach saturation (Lee *et al*, 2000; Mellor *et al*, 1999). The low upper end of the linear range means

that sample dilution and re-testing is required for as many as 47.4% of samples (Castelain *et al*, 2004).

Conventional RT-PCR measures the level of product at the end of the amplification which is not ideal as small changes in the amplification efficiency can dramatically affect the amount of final product. Handling of the sample after target amplification causes major problems with contamination. Consequently, real-time PCR has become the preferred method for HCV quantitation with product quantity calculated during the logarithmic phase of the reaction, before the reaction components become limiting and the reaction plateaus. The latest versions of the Roche and Abbott HCV quantitation assays - the Cobas Taqman HCV assay (Roche Diagnostics, West Sussex, UK) and the Abbott RealTime HCV assay (Abbott Diagnostics Division, Berkshire, UK) are both based on automated sample preparation followed by real-time PCR (Kleiber *et al*, 2000). Both assays exhibit a large dynamic range; between 12 - $1x10^8$ IU/ml with the Abbott assay (Halfon *et al*, 2006) and 25 - $5x10^6$ IU/ml with the Roche assay (Germer *et al*, 2005) and are extremely sensitive (Sizmann *et al*, 2007). Some genotypic variability in viral load was reported for both assays (Caliendo *et al*, 2006; Sarrazin *et al*, 2006; Michelin *et al*, 2007). Good correlation has been observed between these two assays which also have the benefit of high throughput, automation and an internal control (Wolff *et al*, 2007).

1.10.1.2 In-house HCV quantitation assays

Although the latest commercial HCV quantitation assays are sensitive, accurate and suitable for high-throughput testing, the major disadvantage is their high cost.

As a result, in-house methods for HCV quantitation based on real-time PCR have been developed. Different methodologies have been described using non-probe based SYBR Green, which rely on melting-curve analysis to determine specificity. SYBR Green binds to all double-stranded DNA and, as a result, non-specific peaks can occur in low positive and HCV negative samples (Komurian-Pradel *et al*, 2001; White *et al*, 2002). Probe-based systems have been designed using either FRET hybridisation probes (Ratge *et al*, 2002), molecular beacons (Yang *et al*, 2002; Morandi *et al*, 2007) or hydrolysis probes (Martell *et al*, 1999; Takeuchi *et al*, 1999; Castelain *et al*, 2004). These are based on calibration to an external standard curve created by modified HCV RNA (Komurian-Pradel *et al*, 2001), commercial RNA standards (Ratge *et al*, 2002; Morandi *et al*, 2007), a dilution of a clinical specimen (Castelain *et al*, 2004) or RNA transcripts produced from plasmid constructs harbouring the HCV template (Takeuchi *et al*, 1999; Yang *et al*, 2002). Modified HCV RNA can be difficult to prepare, commercial RNA standards are expensive and clinical specimens cannot be used long-term as they degrade. Some assays are more prone to contamination as they use a separate reverse transcription step (Komurian-Pradel *et al*, 2001), or require a two-round nested-PCR, which although takes place in a closed capillary, requires a separate centrifugation step to combine first and second round mixtures (Ratge *et al*, 2002).

1.10.1.3 Internal control (IC)

An IC is an important addition to any diagnostic PCR assay. It is included in the preliminary (extraction) step and allows the process to be monitored at all stages. The IC is co-amplified with the target sequence, with a negative IC result being indicative of extraction and/or PCR failure. If both target and IC are negative, then

the sample must be re-extracted and re-tested. ICs can detect false negatives due to inhibition, nucleic acid degradation or user/equipment error. Heparin is a potent inhibitor present in blood specimens that may cause false-negative PCR results (Willems *et al*, 1993). It is used as an anticoagulant for blood collection and can cause problems in HCV quantitation of haemodialysis patients. Other inhibitors found in blood include haemoglobin, haem and urea.

The use of ICs is not a new concept and many types have been developed (reviewed in Hoorfar *et al*, 2004). Non-competitive ICs are amplified using a different primer set to that of the target. This requires two reactions, which may have different kinetics, to proceed concurrently. The use of competitive ICs has been described for use in diagnostic assays (Kim *et al*, 2002). These are amplified with the same primer set as the target; but are modified in some way so as to be differentiated from it. Competition by the IC can lower the sensitivity of target detection and these ICs also require complicated cloning and mutagenesis steps to produce the internal sequence and incorporate it between the primer sites. ICs can be inactivated human or animal viruses spiked into clinical specimens (Castelain *et al*, 2004; Scheltinga *et al*, 2005). These need cultivation in tissue culture systems, which may not be available in laboratories and may also raise issues of safety. ICs for viral RNA assays must be very stable to resist degradation by RNAses. Naked RNA molecules can be used, (Escobar-Herrera *et al*, 2006) but must be pre-treated to ensure stability. 'Armoured RNA', in which the RNA is packaged into bacteriophage proteins to protect it from degradation solves this problem (Beld *et al*, 2004). This technology has been used to produce both RNA ICs and standards (Pasloske, 1998), but is expensive.

Although several in-house real-time RT-PCR assays for HCV quantitation have been developed; only those of Castelain (2004) and Morandi (2007) include an IC. The former assay utilises an inactivated virus, whilst the latter incorporates armoured RNA. All other assays, therefore, risk false negative results due to extraction failure, user error or PCR inhibition. The consequences of releasing an erroneous 'undetectable' HCV RNA result are dire in terms of the likelihood of onward transmission of the virus and of progression of the disease. It is, therefore, imperative that all HCV RNA quantitation assays include an IC to prevent this.

1.10.2 HCV Genotyping

1.10.2.1 Sequencing – the gold standard

The 'gold-standard' for HCV genotyping is nucleotide sequencing of the entire genome followed by phylogenetic analysis. However, this approach is impractical for routine use. Consequently, defined regions of the genome can be amplified, sequenced and analysed as a representative of the entire genome. There is controversy over which region to sequence, with the core, envelope, NS5b and 5' UTR each being used. The HCV genotype classification system is based on NS5b sequencing (Simmonds *et al*, 1993). However, the high variability in this region reduces primer specificity and thus assay sensitivity and is, therefore, not suitable for routine genotyping. The 5' UTR is highly conserved yet displays a number of genotype-specific motifs, and is usually selected for sequencing. The TRUGENE HCV 5'NC genotyping kit (Siemens Medical Solutions Diagnostics, formerly Bayer Diagnostics) utilises PCR fragments produced from the Roche Amplicor HCV test which are subsequently subjected to simultaneous PCR amplification and direct

sequencing (CLIP sequencing) of the 5'UTR (Ross *et al*, 2000). This is a very accurate method for genotype assignation and its sequence databank can be continually updated for improved phylogenetic analysis (Halfon *et al*, 2001; Germer *et al*, 2003). However, it does have the disadvantage of being a time-consuming, labour-intensive methodology.

1.10.2.2 Molecular HCV genotyping methods

Several molecular methods for HCV genotyping have been published. One of the first described utilised amplification of HCV RNA from clinical specimens, followed by amplification with a common 5' primer and a set of type-specific primers, which produced different-sized amplicons on agarose gel electrophoresis (Okamoto *et al*, 1992). This early method was based only on genotypes 1a, 1b and 2a and lacked sensitivity and specificity. It was improved with modifications to include 3a (Okamato *et al*, 1993, 1996), and adapted by others to extend the genotype range (Ohno *et al*, 1997). This method has relatively low specificity/sensitivity (Furione *et al*, 1999) and has the contamination issues involved with nested-PCR assays.

The line-probe assay (LiPA) manufactured by Innogenetics (Belgium) and distributed as the VERSANT™ HCV Genotype Assay (LiPA), version 1 (Siemens Medical Solutions Diagnostics) has historically been the most frequently used protocol for HCV genotyping in clinical laboratories. This is a two stage process which requires PCR amplification of the 5'UTR with biotinylated primers followed by hybridisation with 21 genotype/subtype specific probes which are immobilised on a nitrocellulose membrane. This gives different reactivity patterns used to differentiate the 6 genotypes and many of the subtypes (Stuyver *et al*, 1993, 1996).

This assay shows good specificity of genotype identification but lacks sensitivity (Haushofer *et al*, 2003; Zheng *et al*, 2003). The DNA enzyme immunoassay (DEIA) kit (Gen-Eti-K DeIA; Sorin Biomedica, Saluggia, Italy) also utilises genotype-specific probes but these are adsorbed onto microwell plates which are hybridised with amplicons from the HCV core fragment rather than the 5'UTR. This method compares very favourably against other HCV genotyping methods (Ross *et al*, 2000).

Restriction fragment length polymorphism (RFLP) analysis has also been tested and predicted patterns suggested for each genotype (Nakao *et al*, 1991; McOmish *et al*, 1994). This labour-intensive process involves PCR amplification and digestion with specific restriction endonucleases, followed by gel electrophoresis. Since restriction sites can be created or abolished with a single base mutation, there may be many combinations of RFLP patterns within a genotype and samples often do not match the published patterns (Khan *et al*, 1997).

1.10.2.3 HCV serotyping

Serotyping, uses genotype-specific antibodies as indirect markers for HCV genotypes. However, studies of patients with a defined exposure, such as transfusion, have shown that antibodies are not generally detectable for at least six weeks and may not appear for several months (Alter *et al*, 1989). Serotyping is not clinically useful for those who are immunocompromised, who may lack an immune response. Also, although simple to perform, serotyping often lacks sensitivity compared to other methods (Pawlotsky *et al*, 1997). It is also a costly assay, limiting its usefulness for routine genotyping (Beld *et al*, 1998). HCV serotyping

has, however, found a use in assigning genotype to individuals who have spontaneously cleared HCV infection (Harris *et al*, 2007).

1.10.2.4 Real-time PCR genotyping methods

Real-time PCR is rapidly becoming a platform for HCV genotyping. Two groups (Bullock *et al*, 2002; Schröter *et al*, 2002) have designed a one-step LightCycler method with FRET (hybridisation) probes to detect genotypes 1-4 which can be distinguished by melting point (T_m) curve analysis. Schröter's group relied on two probes with different wavelengths to distinguish genotypes 1, 2 and 4 in one channel and genotype 3 in the other channel. Bullock *et al* optimised their assay so that genotypes 1-4 could be detected with a single set of probes within a single channel. A recent method, the HCV genotyping analyte-specific reagent (ASR) assay (Abbott Molecular Inc, Des Plaines, IL) based on real-time PCR which targets the NS5b region for genotype 1 identification and the 5'UTR for genotypes 2a, 2b, 3, 4, 5 and 6, has been described (Martró *et al*, 2008). This has yet to be fully evaluated but of concern is the high level (4.4%, n=295) of 'indeterminate' results which were not reactive with any genotype/subtype specific probes.

1.10.3 HCV Subtyping

1.10.3.1 Subtyping applications

HCV subtyping is not only of academic interest, it can have applications in the study of HCV evolution, epidemiology and outbreak/transmission investigations. Nosocomial outbreaks of HCV have been reported, especially in settings such as haemodialysis units and haematology wards where vascular access is required for

long periods (Allander *et al*, 1995; Wreghitt, 1999, 2004). Patients who undergo haemodialysis long-term are at increased risk of HCV and prevalence of HCV infection in dialysis patients has been reported to be as high as 14% (Corcoran *et al*, 1994). There have also been several reports of transmission from HCV-infected health care workers (HCWs) to patients during exposure prone procedures (EPPs). Health care workers themselves are also at risk of acquiring HCV from infected patients. Between 1997 and 2005, there were 11 cases of HCV seroconversion in healthcare workers in the UK following significant occupational exposure to HCV (HPA, 2006a). Genotype determination is often not sufficiently discriminatory for outbreak/transmission investigation and knowledge of subtype is required. Most studies of the molecular epidemiology of HCV outbreak/transmission have utilised phylogenetic analysis of variable regions of the HCV genome such as NS5b or E2 (Abacioglu *et al*, 2000; Kondili *et al*, 2006). Other studies have found that only the hypervariable regions show sufficient discriminatory power for outbreak studies (Bracho *et al*, 2005).

Knowledge of HCV subtype may become increasingly important in treatment protocols and predicting HCV progression. An association has been made between infection with subtype 1b and poor response to interferon therapy (Manesis *et al*, 1997) although this is controversial and may depend on other factors, in addition to infecting subtype (Nakano *et al*, 2001). There are also tentative associations between subtype 1b and increased likelihood of chronicity and severity of disease (Amoroso *et al*, 1998; Hwang *et al*, 2001) as well as development of HCC (Silini *et al*, 1996; Bruno *et al*, 1997) but this association has not been confirmed by other studies (Benvegnù *et al*, 1997; Nakano *et al*, 2001a).

Subtype 1b is associated with older age, which may explain, in part, the link with chronicity and HCC (Nousbaum *et al*, 1995).

1.10.3.2 Subtyping using the 5'UTR

Subtyping is problematic as a genomic region must be selected which is sufficiently conserved for maximum sensitivity, but with enough variability to allow discrimination between subtypes. Although the 5'UTR is ideal for genotype assignation, it is of limited use in HCV subtyping. HCV genotyping assays which target the 5'UTR, although highly specific for genotype discrimination, have limited ability to accurately subtype HCV strains (Halfon *et al*, 2001; Germer *et al*, 2003; Nolte *et al*, 2003; Ross *et al*, 2007). The TRUGENE HCV 5'NC genotyping kit, for example, often fails to differentiate subtypes of genotypes 1 and 2 (Ross *et al*, 2000). The discrimination between 1a and 1b subtypes, for example is based on a single nucleotide substitution which may not occur consistently (Chen and Weck 2002).

1.10.3.3 Subtyping using other HCV regions

The NS5b-encoded RNA-dependent RNA polymerase region of the HCV genome shows more variability than the 5' UTR, making it superior for subtyping purposes. A prototype commercial assay, the Trugene HCV NS5b assay, based on sequencing of a 450 bp fragment of the NS5b region, has been developed. A comparison of this assay with the Trugene 5'NC HCV typing kit using a relatively small number of isolates (n=68) demonstrated that whilst both regions were comparable for genotyping of isolates, subtype assignation was superior using the NS5b region, with the 5'NC kit failing to correctly assign subtype or to discriminate

between subtypes in 25.8% of samples. However, the NS5b region was found to be less sensitive, with failure of PCR amplification preventing typing in a small percentage (8.8%) of specimens (Othman *et al*, 2004). An in-house method has also been described (Sandres-Sauné *et al*, 2003) which is based on direct sequencing of a 401 bp amplicon of the NS5b region. In a clinical study of 203 HCV-infected individuals, samples were sequenced following a single-round PCR step and successfully subtyped in 190 (93.6%) samples. If cDNA failed to be amplified then a hemi-nested PCR was used which enabled subtyping of a further 10 (4.9%) samples. Three (1.5%) samples could not be subtyped. This method was found to be superior for HCV subtyping when compared to the Trugene 5'NC genotyping kit which, in this study, could not identify at the subtype level in 67 (33%) of isolates.

There has been recent renewed vigour in the development of HCV subtyping assays, due in part perhaps to the fact that new antiviral compounds are likely to show distinct activities against HCV isolates belonging to certain subtypes (Hinrichsen *et al*, 2004). Transfer of the target of CLIP™ sequencing from the 5'UTR to the core region has expanded its utility for HCV subtyping. CLIP™ sequencing of the core fragment led to an adequate subtype assignment in 97% (n=110) of isolates compared to 81% with the TRUEGENE 5'NC genotyping kit (Ross *et al*, 2008). A new version of the line probe assay (Versant HCV Genotype Assay (LiPA), version 2) has recently been developed. The principle format remains unchanged, but the assay now targets part of the HCV core region in addition to the 5'UTR. This has enhanced its subtype discrimination when compared to the original line probe assay, especially with regard to subtype 1a/1b

and the recognition of certain genotype 6 variants (Ross *et al*, 2007). However, the improvements to this assay have not enabled it to achieve better subtyping with regards to genotypes 2 and 4.

1.11 Real-time PCR

Real-time PCR is becoming increasingly important in diagnostic laboratories and is becoming the preferred platform for HCV diagnosis/monitoring. This technique combines the amplification of nucleic acid with the detection of amplified products during each reaction cycle – in real time. This is less labour-intensive than conventional PCR as there is no analysis of end products by gel electrophoresis. It also prevents contamination by amplicons as the reaction tubes remain closed during the analysis process. Real-time PCR relies on the detection and quantification of a fluorescent reporter, the signal of which increases in direct proportion to the amount of PCR product in the reaction. The initial copy number can be calculated from the cycle number at which a detection threshold is crossed; the threshold cycle (C_T). The higher the starting copy number, the earlier the amplified product is detected. The fluorescent signal is detected on a thermal cycler attached to computer software for data analysis.

1.11.1 Hydrolysis (Taqman) probes

The research described herein uses real-time technology and hydrolysis (Taqman) probes. These are dual labeled hydrolysis probes which utilise the 5' exonuclease of the *Taq* polymerase enzyme for measuring the amount of target sequence in a sample. If the target of interest is present, the probe, which is complementary to an internal sequence between forward and reverse primer sites, anneals. Taqman probes have a fluorescent reporter dye attached to the 5' end (FAM, JOE/VIC,

ROX or Cy5) and a non-fluorescent quencher at the 3' end (NFQ, TAMRA or BHQ-2). In this state, when irradiated, the excited fluorescent dye transfers energy to the nearby quencher rather than fluorescing. During PCR, when the polymerase replicates a template on which a Taqman probe is bound, its 5'-3' exonuclease activity cleaves the probe during the displacement stage. The reporter becomes released from the quencher and fluoresces (Figure 1.7). The intensity of the reporter dye fluorescence increases exponentially as PCR products accumulate. Because cleavage occurs only if the probe hybridises to the target, the fluorescence detected originates from specific amplification.

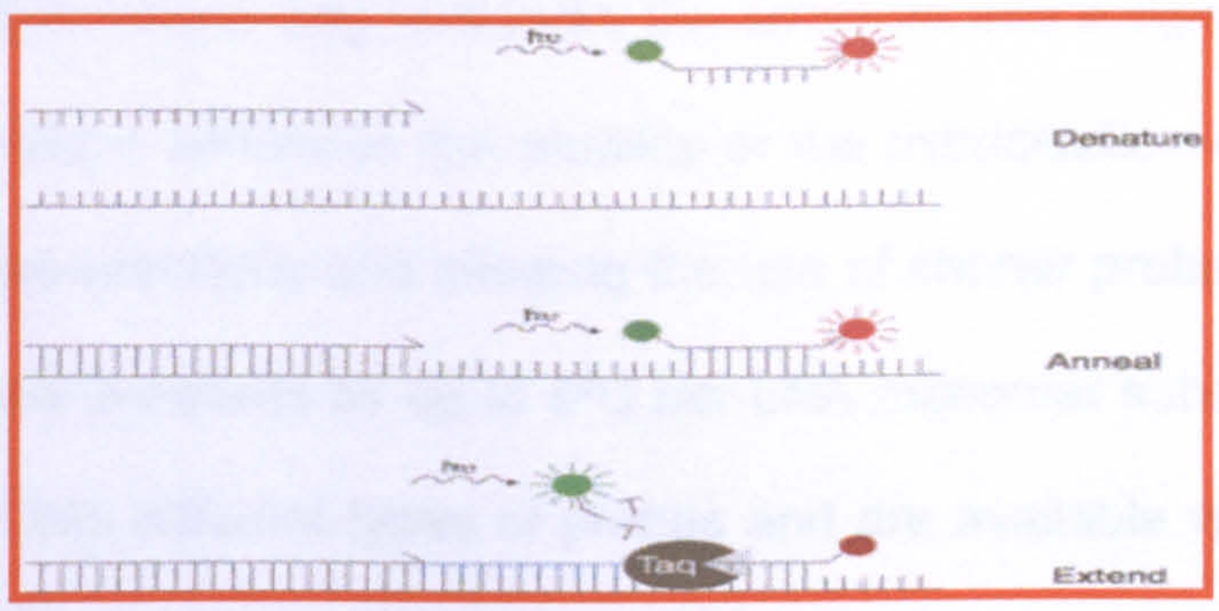

Figure 1.7: Taqman probe technology. (Taken from www.probes.com/handbook/figures/0710.html).

1.11.1.1 Modification of Taqman probes

Taqman probes can be modified to increase their melting temperature (Tm) which allows the use of shorter probes. Two types of modified Taqman probes were used:

1.11.1.2 Taqman® MGB probes

Minor Groove Binding (MGB) probes have a small crescent-shaped molecule that fits into the minor groove of duplex DNA situated at the 3' end of the Taqman probe. This increases the melting temperature by approximately 15°C. Taqman® MGB probes were synthesised by Applied Biosystems (Applied Biosystems, Warrington, UK).

1.11.1.3 Locked Nucleic Acid® probes (LNA®)

LNA is a novel type of nucleic acid analogue that contains a 2'-0, 4'-C methylene bridge (Figure 1.8). This bridge – locked in 3'-endo conformation - restricts the flexibility of the ribofuranose ring and locks the structure into a rigid conformation. This chemical structure enhances the stability of the hybridisation of the probe to its target, improving specificity and allowing the use of shorter probes. The duplex melting temperature increases by up to 8°C per LNA monomer substitution. LNAs can be integrated into different types of probes and are available with FAM, HEX, TET or Cy5 fluorescent labels. LNA probes can be even shorter than MGB probes. These probes also use a different type of quencher molecule, known as Black Hole Quenchers™ which have no native fluorescence, resulting in lower background noise and increased efficiency of quenching. These probes are purchased from Proligo (www.proligo.com).

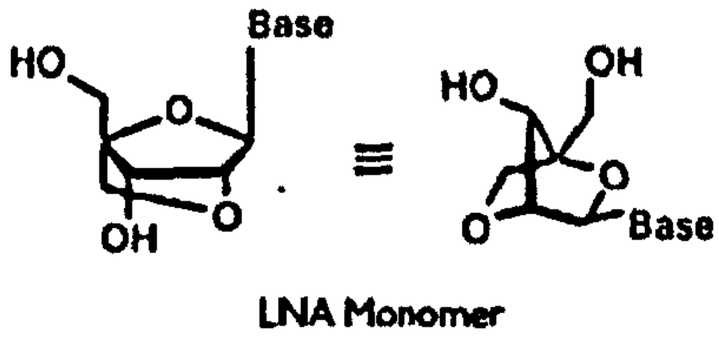

Figure 1.8: Structure of the LNA monomer (taken from www.sigmaaldrich.com).

CHAPTER ONE

Part Two

Mitochondria, Oxidative Stress and HCV

1.11 Mitochondrial structure

Mitochondria are organelles found in all eukaryotic cells except for mature erythrocytes. They consist of a mitochondrial matrix enclosed within two membranes (Figure 1.9). The outer membrane contains numerous porins and is permeable to all molecules of 5000 daltons or less. The inner membrane has no porins and is highly impermeable. This inner membrane divides the mitochondrion into two internal compartments. The first is the intermembrane space, the narrow region between inner and outer membranes. Proteins that function in respiration, such as those which generate adenosine triphosphate (ATP) are built into the inner membrane which has numerous convolutions known as cristae that expand its inner surface (Palade, 1952). The second compartment is the mitochondrial matrix, enclosed by the inner membrane which is rich in enzymes important for metabolic functions. Mitochondria contain their own genome which is separate and distinct from the cell's chromosomal genome.

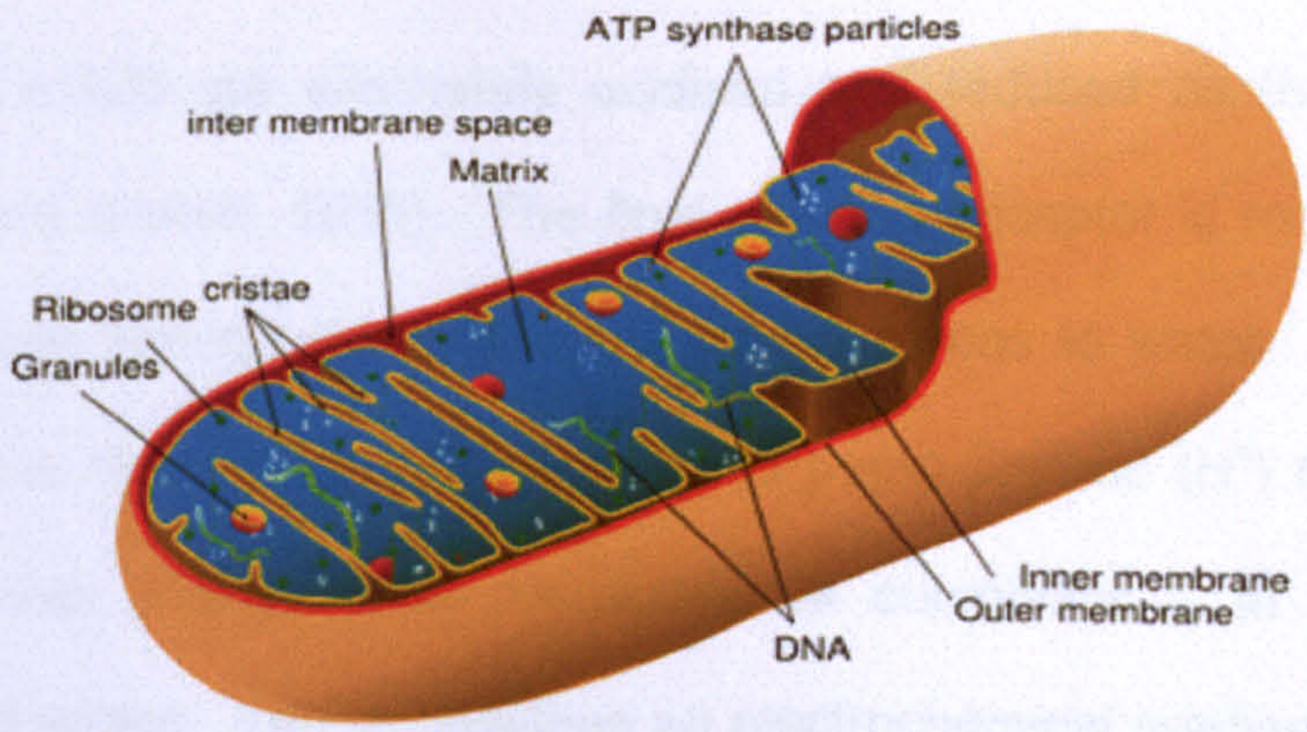

Figure 1.9: A representation of the structure of a mitochondrion showing its major components. Adapted from http://en.citizendium.org/wiki/Mitochondrion.

1.12 Mitochondrial function

Mitochondria are the site of energy production within cells. Tissues that require high amounts of energy such as skeletal and cardiac muscle, brain and liver have the greatest number of mitochondria per cell. Their major role is the generation of ATP through oxidative phosphorylation (OXPHOS). Mitochondria generate over 90% of cellular energy by this process (Chance *et al*, 1979). Pyruvate produced from cellular glycolysis passes into the mitochondrion and enters the matrix. Here it is converted to acetyl co-enzyme A (Acetyl-CoA) and enters the Krebs cycle, also known as the tricarboxylic acid (TCA) cycle. Acetyl-CoA is oxidised in a series of steps and the carbon atoms of the acetyl groups are converted to carbon dioxide (CO_2). The hydrogen atoms are transferred to the carrier molecules flavin adenine nucleotide (FAD) and nicotinamide adenine nucleotide (NAD^+) to produce the reduced forms $FADH_2$ and NADH. These two molecules transfer electrons from the hydrogen atoms to the electron transport chain (ETC), a series of molecules (complexes I-V) built into the inner mitochondrial membrane (Darley-Usmar *et al*, 1994; Lodish *et al*, 2004) (Figure 1.10). The electrons are passed along this series of complexes which are alternately oxidised and reduced as they accept and donate electrons (Hatefi, 1985). The final electron acceptor is molecular oxygen which is reduced through the addition of four electrons to water. The exergonic flow of electrons through the ETC is used to pump protons (H^+) from the matrix through the inner mitochondrial membrane at complexes I, III and IV to the intermembrane space. This establishes an electrochemical gradient known as the 'proton motive force' (expressed as mitochondrial membrane potential). This force drives a flux of protons back into the matrix through ATP synthases (complex V) which are the only parts of the inner membrane that are freely permeable to

protons. As the protons pass through complex V, the ATP synthases harness the exergonic flow to phosphorylate adenosine diphosphate (ADP) to produce ATP, the cellular energy source (Alberts *et al*, 2002) (Figure 1.10). Calcium ions (Ca^{2+}) are an important physiological stimulus for ATP synthesis, and mitochondria have several mechanisms for their uptake.

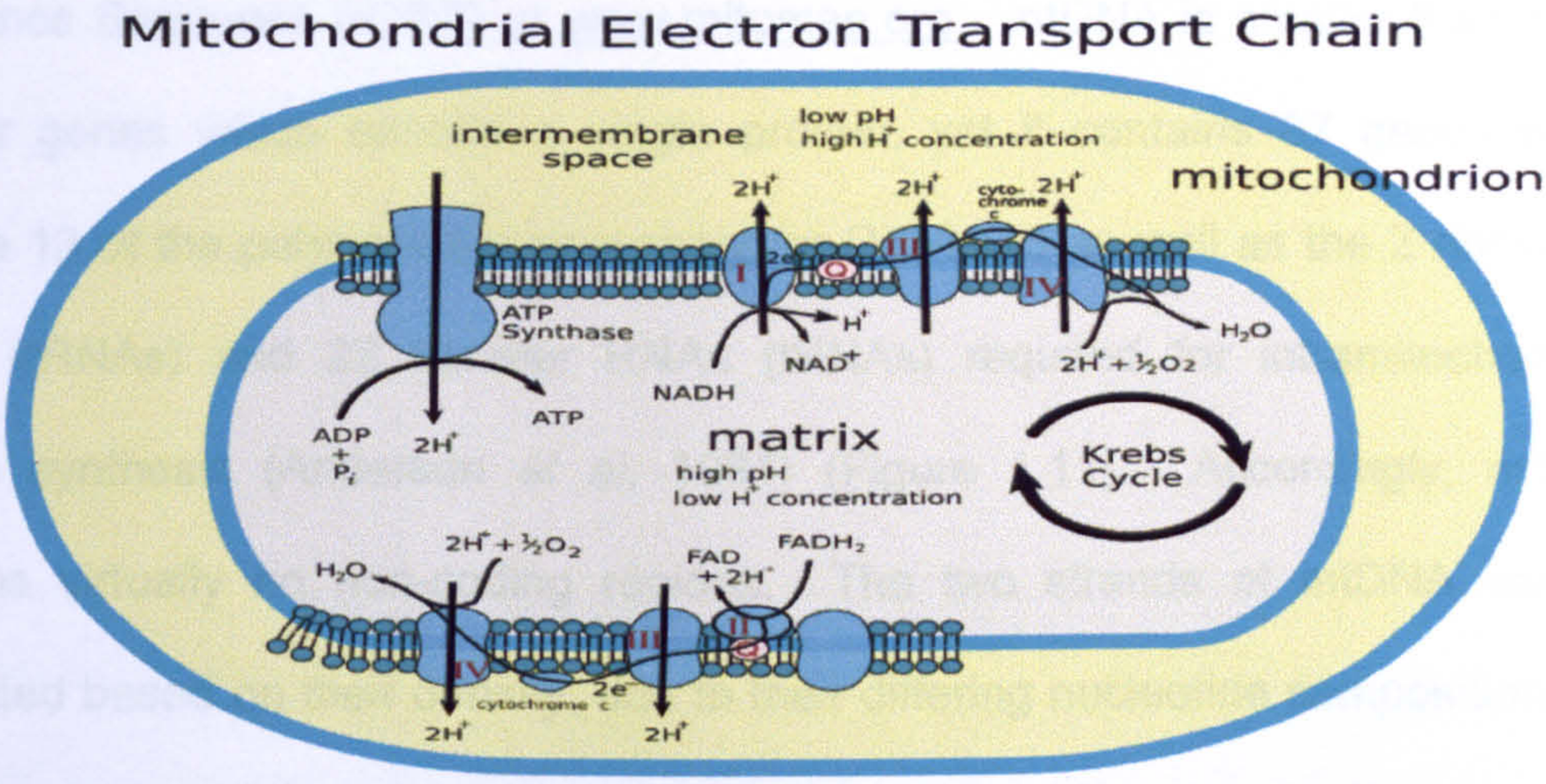

Figure 1.10: A schematic representation of OXPHOS occurring within a mitochondrion. The electron transport chain (ETC) is shown with the efflux of protons (H^+) from the carriers NADH and $FADH_2$ through complexes I, III and IV into the intermembrane space and the influx of protons back into the mitochondrial matrix through the ATP synthase molecule, driving the production of ATP from ADP. Adapted from http://www.answers.com/topic/electron-transport-chain.

1.13 Mitochondrial DNA (mtDNA)

Mitochondria contain the only non-chromosomal DNA in human cells and are able to replicate, transcribe and translate their own genome independently. Mitochondrial DNA (mtDNA) is a maternally inherited, double-stranded, 16,569 bp circular molecule. The human mitochondrial genome was sequenced completely in the early 1980s (Anderson *et al*, 1981). This sequence has recently been re-analysed (Andrews *et al*, 1999) and is available as the revised Cambridge Reference Sequence (rCRS) at www.mitomap.org. mtDNA is smaller than many nuclear genes which encode a single protein, yet it contains 37 genes which encode 13 of the polypeptides necessary for OXPHOS as well as the 2 ribosomal RNAs (rRNAs) and 22 transfer RNAs (tRNAs) required for intramitochondrial protein synthesis (Anderson *et al*, 1981) (Figure 1.11). Accordingly, mtDNA contains virtually no non-coding regions. The two strands of mtDNA can be separated based on their density, due to their differing nucleotide composition and are thus designated as the heavy (H)-strand and light (L)-strand. The H-strand carries 28 genes whilst the L-strand carries only 9 genes. Each cell contains hundreds of mitochondria and each mitochondrion has 2-10 copies of mtDNA; thus there are approximately 10^3 to 10^4 mtDNA copies per human cell (Bogenhagen and Clayton, 1974; Miller *et al*, 2003).

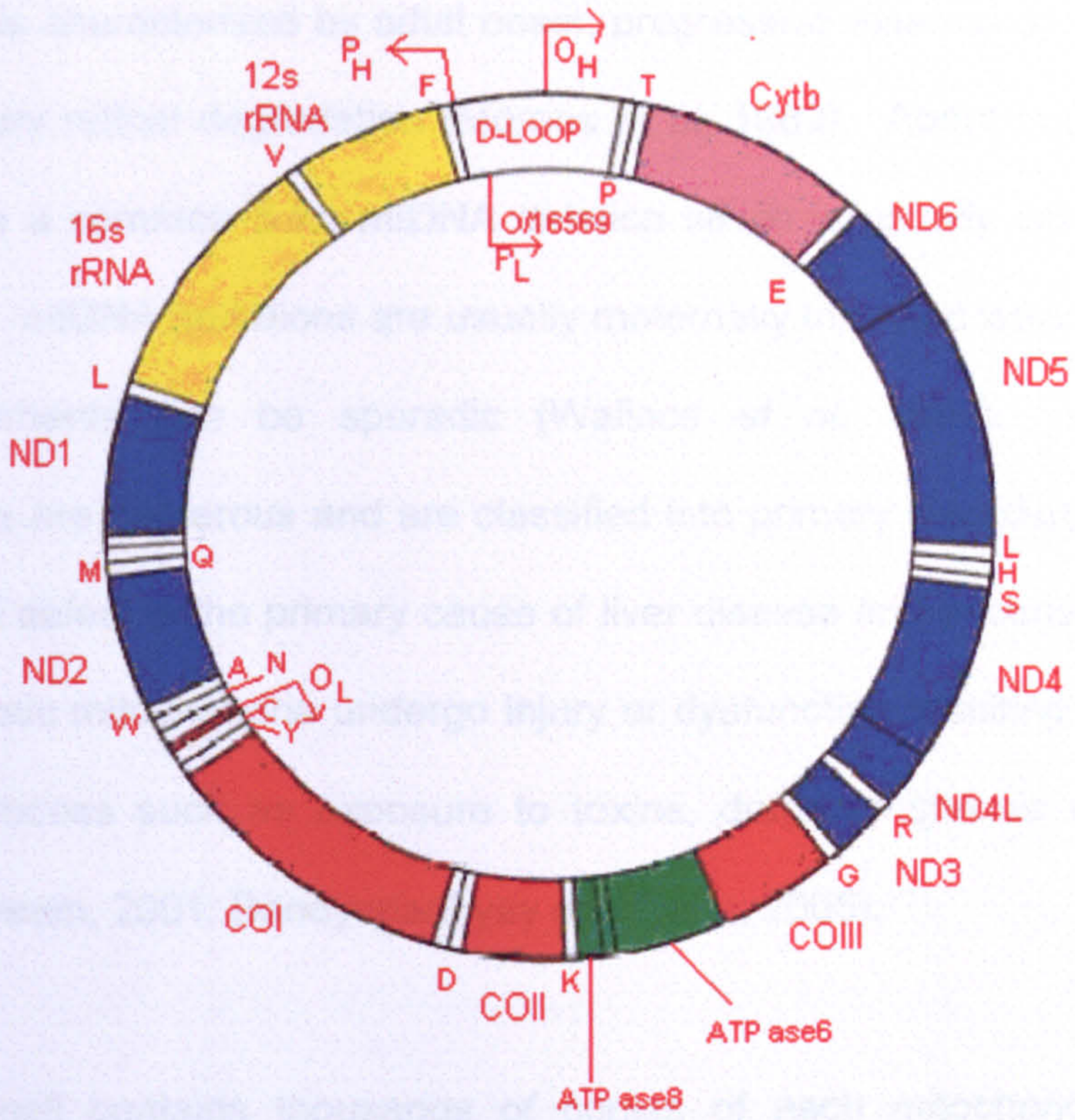

Figure 1.11: A schematic diagram of the 16,569 bp mitochondrial genome (adapted from Van Houten *et al*, 2006). ND1-6; NADH dehydrogenase subunits, COI-III; cytochrome C oxidase subunits, O_H; origin of heavy strand replication, O_L; origin of light strand replication, P_H and P_L; heavy and light-strand promoters respectively, ATP ase6 and 8; ATP synthase F0 subunits. Single capital letters represent the various transfer RNAs (tRNAs).

Normal assembly and operation of the ETC requires an intact and functional mitochondrial genome. This depends on both the copy number and integrity of mtDNA molecules. The importance of the mitochondrial genome is illustrated by the fact that mtDNA defects are a common cause of genetic disease which can have severe manifestations. More than 200 disorders are associated with specific mtDNA point mutations or deletions. Among the most devastating are mitochondrial encephalomyopathy with lactic-acidosis and stroke-like episodes (MELAS) (Goto *et al*, 1990), resulting from an A-to-G transition mutation at nucleotide position 3,243 in the leucine tRNA gene and Kearns-Sayre syndrome

(KSS) which is characterised by adult onset, progressive external ophthalmoplegia and pigmentary retinal degradation (Moraes *et al*, 1989). About one half of KSS patients have a common 5 kb mtDNA deletion which is usually detected only in muscle cells. mtDNA mutations are usually maternally inherited whereas deletions or rearrangements can be sporadic (Wallace *et al*, 1992). Mitochondrial hepatopathies are numerous and are classified into primary disorders in which the mitochondrial defect is the primary cause of liver disease and secondary disorders in which hepatic mitochondria undergo injury or dysfunction resulting from another pathologic process such as exposure to toxins, drugs or chronic viral infection (Sokol and Treem, 2001; Bandyopadhyay and Dutta, 2005).

Since each cell contains thousands of copies of each mitochondrial gene, a mutation/deletion in an mtDNA molecule creates a mixture of wild-type and mutant mtDNAs. Individuals with mitochondrial disease usually harbour a mixture of wild-type and mutant mtDNA, a situation known as heteroplasmy (Lightowlers *et al*, 1997). The percentage of mutant mtDNAs must surpass a critical level to produce a clinical defect – the threshold effect. Studies using cybrid cell lines indicate that the threshold is greater than 90% for mutant tRNA point mutations (Boulet *et al*, 1992; Hanna *et al*, 1995) and must exceed 60% for large scale mtDNA deletions (Bourgeron *et al*, 1993; Sciacco *et al* 1994; He *et al*, 2002). The precise threshold differs from mutation to mutation and between tissue types. Tissues with high requirements for oxidative energy have relatively low thresholds and are particularly vulnerable to mtDNA mutations/deletions.

Mammalian mtDNA is inherited down the maternal line, in a manner which does not conform to Mendel's laws of heredity. If a mother has mitochondrial disease, her offspring may be born without disease or be mildly or severely affected. There may also be variation in severity of disease between siblings. This occurs as a result of the 'mitochondrial genetic bottleneck'. A precursor cell divides early in a woman's development to form a number of oocytes, so the mitochondria from this precursor cell become greatly reduced and randomly distributed between oocytes. In mitochondrial disease, due to this random distribution, females harbouring a mixture of mutant and wild-type mtDNA will form oocytes with a varying proportion of mutant mtDNA. Depending on which one of these oocytes is fertilised, a high proportion of mutant mtDNA may be passed onto the offspring, correlating with increased severity of disease. Alternately an oocyte with a low level of mutant mtDNA may be fertilised, resulting in no or mild mitochondrial disease in the offspring (Cree *et al*, 2008).

1.14 Mitochondrial D-loop and mtDNA replication

The displacement or D-loop encompasses 1122 bp of the mitochondrial genome, between nt 16024 and 576 and is the only major non-coding region (Figure 1.11). It serves as the main site for mitochondrial genomic replication and transcription (Kasamatsu and Vinograd, 1974). It is known as the 'control region' as it contains the signals that control mitochondrial RNA and DNA synthesis (Clayton, 1982; Walberg and Clayton, 1982). It has two major transcription initiation sites – the IT_H which directs transcription of the H-strand and the IT_L which directs transcription of the L-strand. Both initiation sites are encompassed by promoters, which are essential for transcription (Chang *et al*, 1984). The origin of replication of the

heavy strand (O_H) is also contained within the D-loop (Figure 1.12). Despite its important role in both mitochondrial transcription and translation, the D-loop is highly polymorphic in the general population.

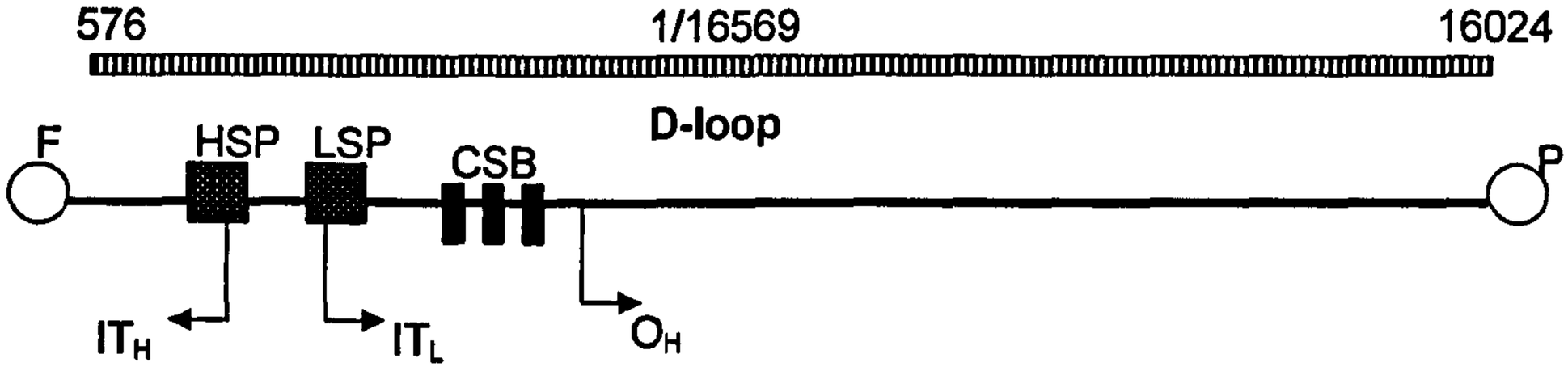

Figure 1.12: Schematic map of the 1.1 Kb mtDNA D-loop region located between nt 16024 and 576 of the circular mitochondrial genome. HSP/LSP; heavy/light strand promoter, IT_H/IT_L; initiation of heavy/light strand transcription, F and P; tRNAs for phenylalanine and proline respectively, CSB; conserved sequence blocks.

mtDNA is replicated from two origins and the replication process is bi-directional and asynchronous (Clayton *et al*, 1982; Brown *et al,* 2005). The H-strand is the leading strand during replication which commences at the O_H and gives rise to a triple-stranded 'loop' structure in which the parental H-strand is displaced as a single-strand segment due to synthesis of a nascent H-strand (Ter Schegget *et al*, 1971). Replication proceeds until two thirds of the genome length at which point the O_L is exposed. mtDNA synthesis from the L-strand then initiates in the opposite direction and elongation continues using the displaced H-strand as a template.

1.15 Oxidative stress

During OXPHOS, some electrons escape from the ETC and combine with oxygen to produce superoxide anions (O_2^-). The electron leakage occurs at two sites in the ETC, complexes I and III. Superoxide anions are converted to hydrogen peroxide (H_2O_2) by superoxide dismutase (SOD). In the presence of iron, both H_2O_2 and O_2^- can be reduced to the highly reactive hydroxyl radical ($OH^\bullet$), through the Fenton reaction in a sequence of events which can be summarised as:

$$H_2O_2 + O_2^- \xrightarrow{Fe^{2+}/\,Fe^{3+}} O_2 + OH^\bullet + OH^-$$

Hydrogen peroxide, superoxide anions and hydroxyl radicals are collectively known as reactive oxygen species (ROS). They are extremely active molecules due to the presence of unpaired electrons. High levels of ROS can result in significant damage to cellular structures, causing lipid peroxidation, oxidation of amino acids in proteins and DNA damage (Yu and Anderson, 1997). Malondialdehyde (MDA) is a lipid peroxidation product and 8-hydroxydeoxyguanosine (8-OHdG) is a product of DNA base modification. Both serve as markers of oxidative stress.

Nitric oxide and calcium are two biological molecules which have important roles in normal cellular function but are also implicated in the cascade of processes leading to oxidative stress. Nitric oxide (NO) is widely used in the body as a signalling molecule. It has roles in vasodilation and regulates the binding and release of oxygen from haemoglobin. It is formed by different isoforms of NO synthase including a constitutively expressed mitochondrial form (mtNOS) (Giulivi *et al*, 1998) and an inducible form (iNOS) which generates NO from L-arginine. NO is,

however, a toxic compound as it reacts with O_2^- to form peroxynitrite anions ($ONOO^-$) which acts as a ROS, destroying cellular constituents (Beckman *et al*, 1990; Wink *et al*, 1991). Peroxynitrite also irreversibly inhibits mitochondrial respiration by blocking the ETC (complexes I, II and V) and disrupting the mitochondrial membrane potential.

Calcium ions (Ca^{2+}) have an important role as second messengers used in cellular signal transduction. They are also an important physiological stimulus for ATP synthesis, and mitochondria have several mechanisms for their uptake. Calcium ions are usually sequestered in the cell's endoplasmic reticulum (ER) but cellular disturbance leads to ER stress and the release of Ca^{2+} into the cytoplasm. The released Ca^{2+} are accumulated by mitochondria which causes depolarisation of the mitochondrial membrane potential, decreasing the OXPHOS capacity of mitochondria. High levels of intramitochondrial Ca^{2+} activate mtNOS generating NO and thus cellular damage (Schild *et al*, 2003).

Around 2% of oxygen consumed by mitochondria is converted to ROS under physiological conditions (Boveris and Chance, 1973). Cells can usually defend themselves against this level of ROS as they have a number of anti-oxidants such as superoxide dismutases (SOD) and catalases. SOD converts superoxide anions to H_2O_2 which is then transformed to water by either catalase or glutathione (GSH), an enzyme which becomes oxidised to glutathione disulphide (GSSG) in the process. Manganese superoxide dismutase (MnSOD) is an important mitochondrial anti-oxidant which is translated in the cytoplasm and transported via a mitochondrion-targeting sequence into the mitochondria (Wispé *et al*, 1989). It is

an inducible enzyme whose expression is enhanced by tumour necrosis factor-α (TNFα), an inflammatory mediator (Larrea *et al*, 1996). In healthy cells, anti-oxidants are plentiful and scavenge for ROS, counteracting their effects. However, during times of cellular stress, the anti-oxidant system may become overwhelmed and ROS accumulate – a state known as oxidative stress.

As OXPHOS occurs within mitochondria, these organelles represent the major source of ROS. They are also its major target as mitochondrial lipid membranes, proteins and DNA lie in close proximity to the ROS. mtDNA is more vulnerable to oxidative damage than nuclear DNA, due in part to its location on the mitochondrial inner membrane. mtDNA damage has been shown to persist longer than nuclear DNA damage (Yakes and Van Houten, 1997). Unlike nuclear DNA, mtDNA lack protective histones which are also required for repair of double-strand DNA breaks (Richter *et al*, 1988; Celeste *et al*, 2003). All components of mtDNA are targets for ROS which can (i) attack deoxyribose causing release of purine and pyrimidine bases, (ii) attack the bases directly, leading to their modification and (iii) cause DNA strand breaks.

Integrity of mtDNA is required for maintenance of OXPHOS; when defects occur they lead to depletion of cellular energy stores. In a vicious cycle, damage to mtDNA impairs the ETC, increasing electron leakage and thus production of ROS causing further damage to the mitochondria. Part of the ageing process is due to a build-up of oxidative damage to various biological molecules within tissue cells (Harman, 1956) with mitochondria being the major target of attack (Harman, 1972, 1981), the so-called 'free-radical theory of ageing'. This theory has gained wide

support and it is now believed that the accumulation of somatic mutations in mtDNA is a significant contributor to human ageing and degenerative disease – the 'mitochondrial theory of ageing' (Linnane *et al*, 1989; Shigenaga *et al*, 1994; Beckman and Ames, 1998).

1.16 mtDNA Damage

1.16.1 mtDNA mutations

ROS induce oxidative damage to mtDNA, including strand breaks and base and nucleotide modifications. Spontaneous mutagenesis results mainly from oxidative events (Rossman and Goncharova, 1998). In mitochondria, oxidative stress causes a vicious cycle, whereby ROS-induced mtDNA mutations interfere with the transcription of mitochondrially-encoded genes including ETC components, inhibiting electron transport, promoting mitochondrial dysfunction and ultimately producing more ROS. Most lesions which persist within DNA result in mutation. mtDNA continues to replicate in post-mitotic cells thus mutations accumulate and erode mitochondrial function. Because of the high mtDNA gene density, any point mutations are likely to affect the expression of mitochondrial genes.

The most documented oxidative stress-associated DNA lesion is the consequence of oxidation of the deoxyguanosine moiety following attack by the hydroxyl molecule forming 8-hydroxydeoxyguanosine (8-OHdG). When DNA becomes single-stranded during replication or transcription, the incorporated 8-OHdG changes conformation and preferentially pairs with adenine rather than cytosine (Shibutani *et al*, 1991). If this is not repaired its presence can result in mutations through G:C-to-T:A transversions. Once incorporated, the 8-OHdG is only very

rarely excised by the proofreading exonuclease of the mitochondrial polymerase (Hanes *et al*, 2006) and the polymerase introduces this mutation at high frequency when replicating past 8-OHdG (Pinz *et al*, 1995). Detection and quantification of 8-OHdG is often used as an indicator of oxidative stress and to compare levels of damage to mtDNA relative to that of nuclear DNA. The usual detection method is via immunohistochemistry, with a monoclonal antibody against 8-OHdG. Richter *et al* (1988) found 8-OHdG to be present at levels of 1 per 130,000 bases in nuclear DNA and 1 per 8000 bases in mtDNA, indicating that the latter was more prone to oxidative damage. Early studies have been criticised as they are thought to have produced erroneously high levels of background oxidation from the methods used for mitochondrial isolation (Helbock *et al*, 1998). Quantitative PCR has been used to compare formation of hydrogen-peroxide induced damage in mitochondrial and nuclear DNA (Yakes and Van Houten, 1997). The technique used was based on the premise that DNA lesions will block the progression of polymerase resulting in a decrease in amplification of the target. Quantitation of a large fragment of mtDNA and of β-globin (a nuclear gene) from transformed cells treated with hydrogen-peroxide demonstrated lower amplification of the mtDNA fragment. This illustrated that mtDNA suffers 3-10 fold more damage than nuclear DNA following oxidative stress. Unlike other studies, the method used did not involve the potentially oxidative mitochondrial isolation steps.

1.16.2 mtDNA deletions

There are 116 mtDNA deletions reported (www.mitomap.org.uk, as of August 27th 2007) which range in length from 4 to 10,987 nucleotides. The most well documented mtDNA deletion removes 4977 bp of the mitochondrial genome and is

known as the 'common deletion' due to the frequency with which it has been reported. This deletion, (identified henceforth as mt^{4977}) spans from nt 8469-13447. The deleted region encodes seven polypeptides which are essential for the OXPHOS pathway; four for complex I (ND3, ND4, ND4L and ND5), one for complex IV (COIII) and two for complex V (ATP6 and ATP8) as well as five tRNA genes (Porteus *et al*, 1998) (Figure 1.13). Another well documented deletion is that of 7436 bp (identified henceforth as mt^{7436}), spanning from nt 8648-16085. This eliminates many of the same genes as mt^{4977} as well as a further subunit of complex 1 (ND6), three additional tRNAs and the complex III cytochrome b gene (Figure 1.13). This deletion has been reported to accumulate in heart tissue during ageing (Hattori *et al*, 1991; Hayakawa *et al*, 1992) and in cirrhotic liver surrounding hepatic tumours (Yamamoto *et al*, 1992).

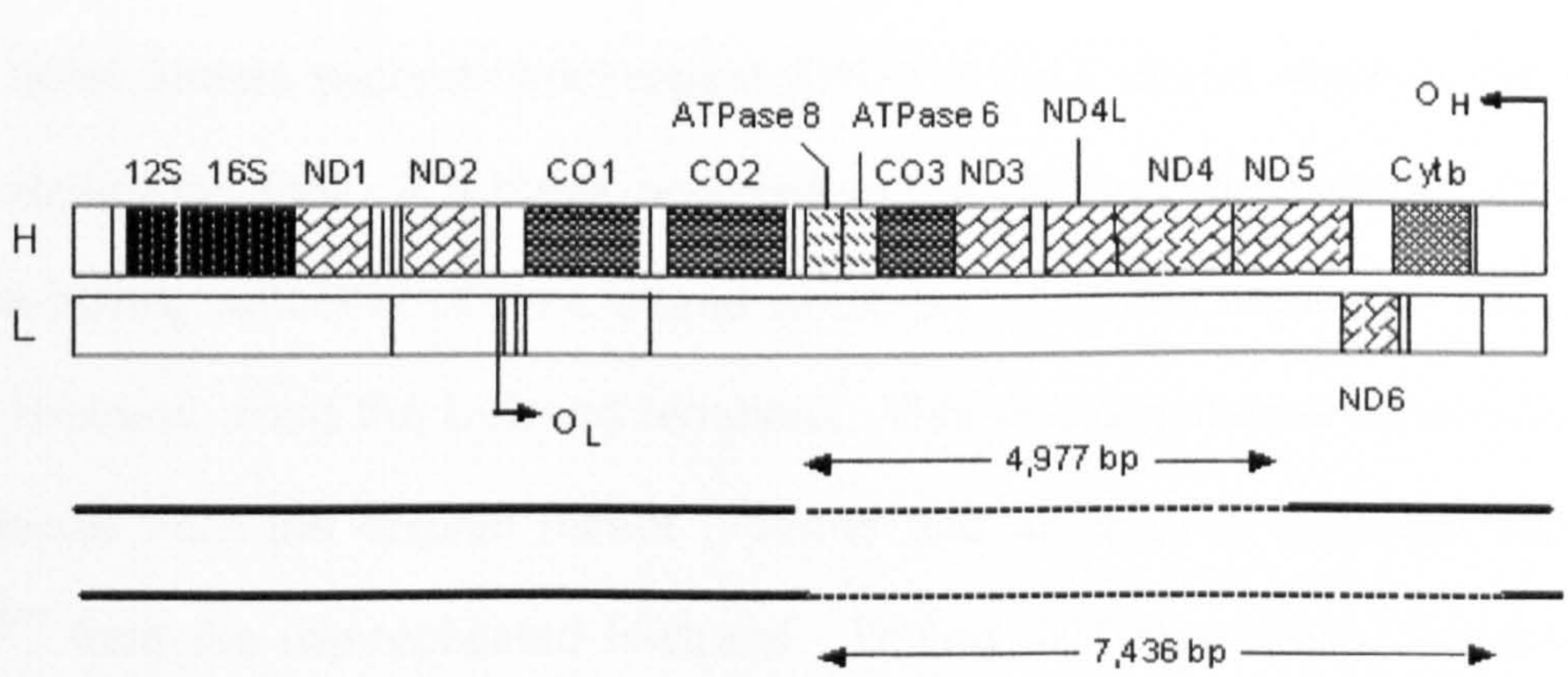

Figure 1.13: A schematic figure of the coding region of mitochondrial genome showing the positions of the mt^{4977} and mt^{7436} deletions. From this Figure, the genes that are truncated or removed by each deletion can be visualised. H; heavy strand, L; light strand, 12S and 16S; 12S rRNA and 16S rRNA respectively, ND; NADH dehydrogenase, CO; cytochrome oxidase, Cyt b; cytochrome b, O_H and O_L; origins of replication of heavy and light strands of mtDNA respectively. Figure adapted from Wei *et al*, (1996).

Recombination via flanking direct repeats is a major cause of large scale deletions in human mtDNA (Mita *et al*, 1990; Johns *et al*, 1989). Most mtDNA deletions (~60%) are flanked by two short homologous direct repeat sequences, one being removed by the deletion process. These are known as class I deletions. Around 30% of mtDNA deletions, known as class II deletions, are flanked by imperfect repeats. Around 10% of mtDNA deletions have no repeats involved. mt^{4977} is found between two 13 bp repeats at nucleotide positions 8470-8482 and 13447-13459. This is the largest perfect direct repeat sequence in the mitochondrial genome and it is thought that this direct repeat creates a hotspot for deletion and may be the principal factor behind the formation of most deletions (Samuels *et al*, 2004). Shoffner *et al* (1989) suggested that mt^{4977} occurs as a result of a slip-replication mechanism. They hypothesise that whilst the H-strand is displaced during replication, the first direct repeat (DR1) from the H-strand can base pair with the down stream second direct repeat (DR2) of the L-strand which is exposed by the replicating fork. If a break occurred in the H-strand downstream from DR1, base-pairing with DR2 of the L-strand would permit further replicative extension of the H-strand along the L-strand template. This would generate a normal mtDNA molecule from the original parent L-strand and an mtDNA molecule harbouring mt^{4977} from the slip-replicated H-strand. During oxidative stress, the deletion is thought to occur as a result of intragenomic recombination between the direct repeats after a single-strand break caused by ROS (Schon *et al*, 1989; Mita *et al*, 1990). mt^{7436} is also flanked by direct repeats of 12 bp located at nt 8637-8648 and 16073-16084. This deletion probably occurs via the same mechanisms as mt^{4977}.

mt^{4977} has been observed in many mitochondrial disease pathologies such as Kearns-Sayres syndrome (KSS) and chronic progressive external ophthalmoplegia (Shanske *et al*, 1990; Holt *et al*, 1989; Moraes *et al*, 1989; Schon *et al*, 1989; Zeviani *et al*, 1988). It has also been detected in some human cancers including oesophageal squamous cell carcinoma (Abnet *et al*, 2004) and oral cancer (Shieh *et al*, 2004). Other studies have found lower quantities in tumour tissue compared to surrounding healthy tissue (Ye *et al*, 2008). The accumulation of both mt^{4977} and mt^{7436} in the ageing process is well documented (e.g. Cortopassi *et al*, 1990, 1992; Lee *et al*, 1994; Wei *et al*, 1996; Zhang *et al*, 1998; Mohamed *et al*, 2006;). However, the significance of these deletions in ageing is uncertain. Studies that have quantified these deletions demonstrate an increase in abundance with age, but even in the oldest individuals studied, the quantities of these deletions are minute. Corral-Debrinski and colleagues (1992) for example detected mt^{4977} at 0.007% in the heart muscle of elderly individuals with heart disease and Wei and colleagues (1996) detected this deletion at 0.06, 0.076 and 0.053% in the muscle, liver and testis of elderly individuals respectively. It is doubtful that these levels would surpass the threshold needed for detrimental cellular effect.

1.16.3 D-loop mutations

mtDNA damage is region-dependent, with the D-loop being most susceptible (Mambo *et al*, 2003). The sensitivity of the D-loop to mtDNA damage may be due to several factors:

(i) During mtDNA replication it has a unique structure, the short three-stranded 'loop', in which the parental H-strand is displaced,

with the single strand being prone to damage (ter Schegget *et al*, 1971).

(ii) The D-loop attaches the mtDNA to the mitochondrial inner membrane which leaves it exposed to mutagens (Hruszkewycz, 1988).

(iii) mtDNA damage repair process is mediated by polymerase gamma (γ) which has decreased proof-reading ability (Pinz *et al*, 1995) and may itself be a target of oxidative damage (Graziewicz *et al*, 2002).

(iv) The level of repair in the D-loop region has also been found to be lower than seen in other regions of mtDNA (Mambo *et al*, 2003), allowing mtDNA damage to accumulate in this region.

The D-loop, therefore, provides an excellent target on which to study mtDNA damage as it is not only more susceptible to damage but also less efficiently repaired than other regions of mtDNA.

The D-loop is a non-coding region and, therefore, the significance of damage within this region could be questioned. However, as the D-loop is responsible for control of transcription and expression of mtDNA, mutations in this region may affect the copy number and/or repression of gene expression of the mitochondrial genome. Damage to this region could interfere with the interaction of proteins involved in mtDNA transcription/translation by altering the recognition site or causing bending of the mtDNA and modifying the binding affinity of proteins. This could either increase the rate of replication, which could lead to higher levels of

mtDNA damage, or decrease replication, leading to a low copy number of mitochondria and reduced energy production capacity.

The non-coding region of mtDNA contains two well-characterised hypervariable segments, HVS1 (nt 16024-16383) and HVS2 (nt 57-372) which have been found to be hotspots for mtDNA alterations (Stoneking, 2000). Within these hotspots, there are areas which are particularly prone to damage. Microsatellites are regions of DNA with repetitions of a small number of base pairs. Microsatellite alterations occur at a rate much higher than seen in non-repetitive DNA, probably due to DNA polymerase slippage (Sia *et al*, 1997). A microsatellite consisting of 12-18 cytidine residues interrupted by a thymidine at nucleotide position 310 (known as the D310 region) has been found to be a hotspot of mutation in many human cancers (Sanchez-Cespedes *et al*, 2001; Wang *et al*, 2005). Mutations within the D310 region may be biologically significant as it is found within a conserved sequence block (CSB) which is thought to be involved in mtDNA replication/transcription.

Polymorphisms in this region were thought at first not to be relevant as numerous substitutions, small deletions and insertions were observed in normal human beings. However, a large number of sequence variants were found in the non-coding region of patients with mitochondrial disease, suggesting a link between mutations in this region and mutations in coding regions (Marchington *et al*, 1996). mtDNA mutations have been detected in almost all types of human cancer including uterine (Pejovic *et al*, 2004), colorectal (Lièvre *et al*, 2005), liver cancer (Nomoto *et al*, 2002) as well as in bladder, head and neck and lung tumours (Fliss *et al*, 2000). These are often located in the D-loop region. These studies indicate

that the accumulation of mtDNA mutations could be a crucial step in carcinogenesis, although more work is required to determine their functional consequence in cancer development.

1.17 Repair of oxidatively damaged DNA

One reason for increased damage of mtDNA relative to nuclear DNA was initially thought to be due to the limited mechanisms of mtDNA repair. Early studies demonstrated that, following prolonged exposure to oxidative stress, nuclear DNA damage was completely repaired, whereas mtDNA damage persisted (Yakes and Van Houten, 1997). More recent studies have demonstrated that mitochondria do have several mechanisms for DNA repair, (reviewed in Larsen *et al*, 2005). Base excision repair (BER), the principle pathway for the removal of oxidative DNA damage does occur (Fortini *et al*, 2003). BER involves the recognition and removal of damaged bases by specific glycosylases which cleave the bond between the base and the deoxyribose moiety of DNA. Once the base is removed, the apurinic/apyrimidinic site is removed by an endonuclease. DNA polymerase then fills in the gap and the nick is sealed by DNA ligase (Bogenhagen *et al*, 2001). OGG1 is the major DNA glycosylase for the removal of the 8-OHdG residue, and has been demonstrated to have a mitochondrial targeting sequence and to localise to mitochondria (Takao *et al*, 1998). OGG1 appears to be more important in removal of 8-OHdG lesions in mtDNA than nuclear DNA (de Souza-Pinto *et al*, 2001). 8-OHdG residues that escape OGG1 repair can generate misincorporation of an adenine during replication thus producing 8-OHdG/A mismatches. If this occurs, the mismatched adenine is removed by an enzyme termed hMYH which is a homologue of the *Escherichia coli* repair enzyme MutY. This is followed by

preferential insertion of a cytosine leading to the formation of 8-OHdG/C pairs which are then corrected by OGG1-mediated BER (Gao *et al*, 2004; Fortini *et al*, 2003). hMYH is encoded by a chromosomal gene, but the protein has a mitochondrial-targeting sequence enabling it to localise to the mitochondria (Ohtsubo *et al*, 2000).

Errors of replication that result in a mismatch or small loop are detected by the mismatch repair system. Recent evidence suggests that mitochondria also have the capacity for mismatch repair. Using a nicked substrate containing G/G and G/T mismatches, Mason *et al*, (2003a) observed a low level repair activity in rat liver mitochondrial extracts. However, a functional mismatch repair system is necessary to prevent microsatellite instability. Given that microsatellite instability has been observed in polycytidine tracts in the D-loop region of mtDNA (Sanchez-Cespedes *et al*, 2001; Wang *et al*, 2005), it may be that this system is not efficient enough to provide adequate repair.

Mitochondria, therefore, appear to contain several mechanisms of DNA repair. Of note, one mechanism that appears to be absent in mitochondria is nucleotide excision repair, (NER) a more complex process than BER, which involves the detection of lesions arising from distortions of the DNA helix. This means that a large group of DNA lesions may not be repaired (LeDoux *et al*, 1992).

1.18 HCV, oxidative stress and mtDNA damage

The sequelae for individuals chronically infected with HCV are often severe. Approximately 20% will develop liver cirrhosis with progression to hepatocellular

carcinoma (HCC) in 1-4% of these individuals per year. The mechanisms of HCV pathogenesis remain unclear, but oxidative stress, resulting from the host immune response or the virus itself, may play a key role in HCV-induced liver damage (Choi and Ou, 2006). In chronic viral infection there is elevated oxidative stress over a long time period which diminishes the probability of mtDNA repair (Yakes *et al*, 1997). Additionally, hepatocytes contain many mitochondria and, therefore, have high ROS production. These factors suggest that chronic HCV infection would have a high propensity to elevate levels of ROS and therefore cellular damage within infected individuals. Oxidative stress has long been known to be involved in the pathophysiology of human cancers (Franco *et al*, 2008) and it could be that its destructive effects are what drive the development of HCC in HCV-infected individuals.

The host immune response to HCV may play a role in the production of oxidative stress. HCV-infected individuals exhibit increased production of tumour necrosis factor-α (TNF-α), a cytokine important in the inflammatory response which can produce oxidative stress by stimulating the generation of ROS (Larrea *et al*, 1996). Serum levels of TNF-α have been seen to correlate significantly with severity of HCV disease (Zylberberg, 1999). Elevated levels of ROS have been detected in transgenic mice expressing HCV core protein, even with the absence of inflammation (Moriya *et al*, 2001). This suggests that the virus rather than the host immune response may be more significant in the production of oxidative stress. Accordingly, the majority of studies have focussed on the role of the virus in augmenting oxidative stress and cellular damage in infected HCV-individuals.

1.18.1 Oxidative stress in HCV-infected individuals

There is a plethora of data which demonstrate that infection with HCV is associated with increased oxidative stress, both in the liver and systemically. Most studies utilise the detection of 8-OHdG, an indicator of oxidatively-generated DNA damage, as the marker of oxidative stress. High levels of 8-OHdG have been found in leucocytes and liver tissue from patients with chronic HCV infection. Elevated levels correlated with advanced progression of disease and increased amount of liver steatosis (Shimoda *et al*, 1994; Farinati *et al*, 1999; Cardin *et al*, 2001; Fujita *et al*, 2007). Kitada *et al* (2001) detected 8-OHdG immunohistochemically in various forms of chronic liver disease, regardless of aetiology, although they did not undertake quantification for comparison between the different aetiologies. Expression of hepatic 8-OHdG in the livers of HCV-infected individuals who developed HCC was significantly higher than in those that did not develop HCC (Tanaka *et al*, 2008). Other studies have measured levels of malondialdehyde (MDA) – a marker of lipid peroxidation in HCV-infected individuals. Elevated levels of MDA were observed in these individuals when compared to controls (De Maria *et al*, 1996; Vidali *et al*, 2008). Accumulation of lipid peroxidation products were seen to be reversed by successful interferon therapy (Kageyama *et al*, 2000).

Quantitation of the oxidised and reduced forms of anti-oxidants is a useful marker of oxidative stress. Levels of the antioxidant GSH were found to be significantly decreased in patients with chronic HCV infection with a concurrent increase in the oxidised form, GSSG, suggesting a high turnover of GSH in response to liver damage (Farinati *et al*, 1995; Mahmood *et al*, 2004). Jain *et al* (2002) measured a

variety of markers of oxidative stress including pro- and anti-oxidants and found that there was clear evidence of oxidant stress in HCV-infected individuals, even in the absence of cirrhosis – demonstrating that oxidative stress occurred early in infection. Induction of MnSOD, the mitochondrial antioxidant, is enhanced in PBMCs of patients with HCV but depleted in the liver cells (Larrea *et al*, 1998), suggesting that this organ could be less protected against oxidative damage. A genetic polymorphism which maps within the mitochondrion-targeting sequence of the MnSOD gene and prevents translocation into the mitochondria was found to increase the risk of developing HCC in a cohort of HCV-infected Moroccan patients (Ezzikouri *et al*, 2008). This suggests that anti-oxidants could be vital for the prevention of oxidative stress and progression to HCC, although this finding has yet to be confirmed by other studies. Supporting these studies are the findings in patients with chronic HCV infection where the extent of liver injury was reduced significantly by the administration of anti-oxidant therapy (Houglum *et al*, 1997).

The liver is an iron-rich organ and so a plentiful source of ferrous iron (Fe^{2+}) which produces ROS through the Fenton reaction. HCV infection is associated with iron accumulation (Bonkovsky *et al*, 1997). Increased iron deposition was found to be positively correlated with levels of hepatic 8-OHdG in the livers of patients with chronic HCV infection (Fujita *et al*, 2007). Supporting this, decreases in the level of 8-OHdG were seen following iron-depletion therapy in patients with HCV (Kato *et al*, 2001). The increased iron storage in the liver tissue of HCV-infected individuals correlated with increased lipid peroxidation and anti-oxidant turnover (Farinati *et al*, 1995) indicating that excess iron storage in the liver provides a source of ROS production contributing to cellular damage.

1.18.2 HCV pathogenesis and oxidative stress

Although HCV-infected individuals demonstrate elevated markers of oxidative stress, it is difficult to determine how the virus is involved. Studies of the pathogenesis of HCV were hampered by the lack of a cell culture system permissive for HCV infection and replication. Cell lines expressing HCV sequences from chromosomally integrated cDNA constructs have gone some way to resolve this (Lohmann *et al*, 1999). Okuda and colleagues (2002) expressed the HCV core protein in 3 different cell lines and demonstrated that core expression by itself was sufficient to increase oxidative stress, lipid peroxidation and antioxidant gene expression. Other studies have produced similar results, demonstrating increased oxidative stress and anti-oxidant turnover in cell lines expressing the HCV core protein (Otani *et al*, 2005; Li *et al*, 2007). Abdalla *et al* (2005) found that expression of both the core and NS5 proteins led to increased oxidative stress and that the magnitude of ROS formation correlated with the level and length of time of core protein expression. Oxidative stress was demonstrated to be induced in both core- and NS5a-transfected cells but an earlier and more marked increase was observed in cells expressing NS5a protein (García-Mediavilla *et al*, 2005).

The HCV non-structural proteins including NS5a make up a ribonucleoprotein replication complex which is associated with the host cell's endoplasmic reticulum (ER) membrane (Mottola *et al*, 2002). It is thought that this localisation permits NS5a to induce ER stress, causing a release of Ca^{2+} which are taken up by mitochondria, resulting in increased ROS (Gong *et al*, 2001; Robinson and Marchant, 2008). The expression of NS5a protein was demonstrated to disturb intracellular calcium and trigger the elevation of ROS in mitochondria, leading to

the activation of transcription factors STAT-3 and NF-κB which are induced by oxidative stress (Gong *et al*, 2001; Waris *et al*, 2002). These processes were dramatically reduced with the addition of reagents which chelated calcium or eliminated oxygen radicals. Various deletion mutants of NS5a were also unable to induce these processes (Gong *et al*, 2001). The activation of STAT-3 and NF- κB may be beneficial to the virus as these proteins are known to be involved in cell proliferation and the expression of anti-apoptotic genes (Bromberg *et al*, 1999; Mercurio and Manning, 1999). Moreover, STAT-3 activation has been found to contribute to the stimulation of HCV replication (Waris *et al*, 2005). Thus NS5a may have a potential role in the establishment of chronic liver disease. A very recent study has indicated that other non-structural HCV proteins may be important in cellular damage. HCV NS3/4a was found to impair the efficiency of DNA repair by interacting with ataxia-telangiectasia mutated (ATM) a cellular protein kinase which is essential for response to double-stranded DNA breaks, rendering the cell more sensitive to DNA damage (Lai *et al*, 2008).

The use of cell culture systems may produce erroneous results as the quantities of proteins expressed in the cell system is far greater than seen in human infection. Expression of the entire HCV polyprotein in inducible cell lines, under the tight control of the regulatory elements of the *Escherichia coli* tetracycline resistance operon, has allowed improved simulation of HCV infection (Moradpour *et al*, 1998). With this system HCV gene expression can not only be switched on and off, but fine-tuned over a broad range by varying the concentration of tetracycline in the culture medium. Studies using such a system have supported earlier work by demonstrating that HCV proteins co-localise to the mitochondria and have several

deleterious effects including an increase in ROS, decreased mitochondrial membrane potential, decreased cellular respiratory activity and inhibition of complex I of the ETC (Piccoli *et al*, 2006). Transgenic mice which express HCV proteins at levels characteristic of human disease have been created and results using these animal models support those from cell culture studies (Moriya *et al*, 1998; Okuda *et al*, 2002; Korenaga *et al*, 2005). These studies also allowed the visualisation of the direct association of the HCV core protein with the outer mitochondrial membrane. Korenaga and colleagues (2005) also demonstrated that expression of structural proteins, including the core protein, stimulated Ca^{2+} uptake into the mitochondria which was followed by increased ROS production, oxidation of glutathione and a defective electron transport complex I, leading to an increase in complex I-mediated ROS production. They postulated that the localisation of the core protein to the outer mitochondrial membrane resulted in mitochondrial dysfunction by facilitating Ca^{2+} uptake.

Chronic inflammatory states frequently lead to the increased production of nitric oxide (NO) via inducible NO synthase (iNOS). NO reacts with O_2^- to form peroxynitrite ($ONOO^-$), which acts as a ROS, destroying cellular constituents. NO causes double-stranded DNA breaks and enhances the mutation frequency of cellular genes. In an eloquent series of studies, using both cell lines expressing various viral proteins and transgenic mice expressing the HCV core protein, Machida and colleagues (2004, 2006) have shown that the induction of both NO and ROS by HCV proteins leads ultimately to DNA damage. They first demonstrated that core and NS3 proteins induced iNOS expression and production of NO which in turn caused DNA damage, with the pathway blocked by treatment

of infected cells with iNOS inhibitors (Machida *et al*, 2004). They then demonstrated that core, NS3 and E1 proteins induced ROS production, enhanced lipid peroxidation and reduced mitochondrial membrane potential. In addition, using a mouse model, they demonstrated that the expression of the core protein induced lipid peroxidation and oxidative DNA damage in the livers of core-transgenic mice (Machida *et al*, 2006).

Cells have various cell cycle check points which ensure that repair of DNA lesions occurs before cell cycle progression resumes. Production of oxidative stress by HCV could be advantageous to the virus as its DNA-damaging effects may drive the infected cell to cell cycle arrest. Viruses are thought to replicate more efficiently in cells in an arrested state, as they can utilise fully the host cell machinery without competition from the host cell itself. Several viruses, such as the herpesviruses are known to interact with the host cell cycle control pathways (Flemington *et al*, 2001). Recent work has demonstrated that chronic HCV infection drives cells into an arrested state (Marshall *et al,* 2005). However, in a study by Choi and colleagues (2004) where human hepatoma cells expressing HCV replicons were treated with DNA-damaging peroxide, a decrease in HCV RNA was observed. This was found to occur rapidly at the level of HCV RNA replication, disrupting HCV replication complexes by reducing the amount of NS3 and NS5a. This finding is as yet unsupported, but suggests that production of ROS is detrimental to the virus, suppressing its replication.

1.19 Summary and aims

This thesis is divided into two clear parts with the continuing theme of hepatitis C virus. HCV is the most common blood-borne virus in Europe, and currently the main cause of infectious hepatitis in the UK. There is, therefore, an increasing demand on diagnostic laboratories to provide rapid assays to aid clinicians in HCV diagnosis and monitoring using accurate and sensitive state-of-the-art methods. The aims of the research described in Chapter three were to design, develop, optimise and implement rapid and inexpensive real-time PCR assays for HCV quantitation (with internal control) and genotyping to support clinical practice. An additional objective was to develop methods for defining HCV isolates at the subtype level, for epidemiological and transmission studies.

Primary infection persists in 70-80% of infected individuals with spontaneous resolution of infection in approximately 20%. Chapter three also describes the application of the fully optimised assays in a series of clinical studies to investigate the role of HCV genotype in spontaneous clearance of HCV infection and to examine the epidemiology, at subtype level, of HCV isolates circulating within the eastern region of the UK.

Chronic infection with HCV will lead to serious liver disease such as cirrhosis and fibrosis in 20% of individuals. Between 1-4% of those with cirrhosis per year will develop hepatocellular carcinoma. Infection with HCV is, therefore, very damaging and one way in which this is thought to occur is through the production of cellular oxidative stress especially through the action of viral proteins such as the core and NS5a proteins. Cellular oxidative stress causes DNA damage and mtDNA is

particularly susceptible. Accumulation of mtDNA damage decreases the bioenergetic potential of cells, but damage must reach a critical threshold level before detrimental effects are observed. Mitochondria are vitally important cellular organelles, with their major function being the generation of the cellular energy source – ATP - through the OXPHOS pathway.

Most studies examining the damaging effects of oxidative stress on DNA in individuals with HCV have focussed on detecting 8-OHdG as a marker of DNA damage. Although a useful marker of DNA damage, the amounts of oxidative modifications detected by different methods can vary considerably. There is also the possibility of introducing oxidation during DNA isolation, artificially elevating the detectable 8-OHdG. Direct examination of mtDNA to scan for and quantify specific mtDNA deletions and mutations within the mitochondrial genome is a far superior method for detection of mtDNA damage. mtDNA provides an excellent target to measure DNA damage due to its increased susceptibility to ROS. The aims of the research reported in Chapters four and five were to develop rapid PCR methods for the detection/quantitation of mtDNA damage. Chapter four describes the development of assays to detect and quantify two specific and well-documented mtDNA deletions - mt^{4977} and mt7436. Chapter five outlines the development of a method to scan for mtDNA mutations occurring within the mtDNA D-loop – a region particularly susceptible to damage.

All of the assays developed in this thesis were exploited in a clinical study of liver biopsies from patients with chronic HCV infection and other liver aetiologies. The level of mtDNA damage occurring in the livers of these patients was established.

The hypothesis that was addressed was whether individuals with HCV infection were experiencing greater levels of oxidative stress and thus mtDNA damage than those with other liver aetiologies.

CHAPTER TWO

Materials and Methods

2.1 Reagents and solutions

Reagents used were all of the highest quality (AnalaR grade or equivalent) and were stored at the appropriate temperature and conditions stated by the manufacturer. All relevant glassware and other materials used were washed with distilled and deionised water (ddH_20) before use (Optima Water Purifier, Triple Red Ltd, Buckinghamshire). Solutions were prepared with ddH_20 and, where appropriate, autoclaved at 121°C for 15 min at a pressure of 1.1 bar. Stock solutions were prepared according to published guidelines (Sambrook and Russell, 2001). Stock and working solutions are detailed in Appendix A. The ultraPURE™ DNAse, RNAse-free water used in the following methods was purchased from Invitrogen (Paisley UK, cat. no. 10977035).

2.2 Clinical specimens

2.2.1 Blood specimen collection and storage

Blood samples were taken from HCV-infected individuals attending the Hepatology Clinic at Addenbrooke's Hospital, Cambridge, as part of routine diagnosis/monitoring. The HCV genotyping assay was developed and utilised on all patients attending the clinic who had detectable HCV RNA and for whom HCV genotyping was requested as part of routine monitoring. HCV serotyping was carried out on all patients attending the clinic that had a detectable HCV antibody response by routine laboratory testing but were found to be HCV RNA negative by PCR.

Blood specimens were taken by hospital phlebotomists into labelled EDTA blood tubes. These were spun in a Centaur 1 centrifuge (R W Jennings and Company

Ltd, Nottingham UK) to separate the serum. This was aliquoted into labelled eppendorf tubes and stored at -70°C until required.

2.2.2 Liver biopsy collection and storage

Liver biopsy specimens were obtained from a total of 79 patients (55 male and 24 female, with an average age of 46.2 years). These had all attended the Planned Short Stay Unit (PSSU) at Addenbrooke's Hospital, Cambridge between 2005 and 2007. Ethical approval for liver biopsy collection and storage had been obtained from the Cambridge Local Research Ethics Committee (LREC reference number 04/Q0108/124, Appendix E) prior to the commencement of the study. A biopsy specimen was obtained from patients who had read an information sheet and signed a consent form permitting the use of their liver tissue for research purposes (Appendix F), and for which there was sufficient tissue remaining from that required for routine diagnostic/investigative purposes.

A small segment of the liver biopsy was immediately transferred to a sterile 1.5 ml eppendorf tube containing 1 ml of RNA*later*™ (Sigma, USA, cat. no. R 0901). The biopsies were kept at 4°C until collection. The RNA*later*™ was then removed with a pastette and the eppendorf, containing the biopsy transferred to a -70°C freezer for storage until use.

2.3 Nucleic acid extraction - homogenisation of liver biopsy specimens

2.3.1 Manual homogenisation

Tissue samples were manually homogenised using a sterile 1.5 ml pestle (Starlab Ltd, Milton Keynes UK, cat. no. I1415-5390) in a 1.5 ml eppendorf containing the

appropriate buffer (depending on the extraction method to be utilised, see Sections 2.4 and 2.5).

2.3.2 Automated homogenisation

Tissue samples were homogenised using the MagNA Lyser (Roche Diagnostics Ltd, Burgess Hill UK, cat. no. 03358976001) with MagNA Lyser green beads (Roche Diagnostics GmbH, cat. no. 3358941) in the appropriate buffer (depending on the extraction method to be utilised, see Sections 2.4 and 2.5). Homogenisation took place at 7000 rpm for 60 s.

2.4 Nucleic acid extraction - automated extraction methods

2.4.1 MagNAPure extractor

Nucleic acid was extracted from 200 µl of serum with a MagNAPure LC Total Nucleic Acid Isolation kit (Roche Diagnostics, Burgess Hill UK, cat. no. 3038505) using automated MagNAPure extraction equipment and the total NA variable elution protocol eluting in 60 µl elution buffer, according to manufacturer's guidelines.

2.4.2 BioRobot MDx workstation (Qiagen, Crawley UK, cat. no. 900600) using the QIAamp Virus BioRobot MDx kit (cat. no. 965652)

Lyophilised carrier RNA was dissolved in 450 µl AVE buffer. Two hundred and thirty microlitres of carrier RNA reconstituted in buffer AVE were transferred to one bottle containing 33 ml buffer AL (lysis buffer) and mixed. Liver biopsy specimens were homogenised in 350 µl of the AL/carrier RNA solution. These were transferred to sterile 2 ml microtubes (Sarstedt Ltd, Leicester, UK). The BiRobot

MDx workstation was prepared and the extraction run set up following manufacturer's guidelines. Nucleic acid was eluted in 100 µl buffer AVE.

2.5 Nucleic acid extraction - manual extraction methods

Three different manual extraction methods were evaluated for the extraction of DNA from liver biopsy specimens:

2.5.1 Modified Trizol® DNA isolation (Invitrogen Life Technologies, cat. no. 15596-018)

DNA was extracted from liver biopsies using the Trizol® reagent, but altering the protocol from the published manufacturer's guidelines to improve yield of DNA. The liver biopsy specimen was homogenised in 800 µl of Trizol® reagent, using either manual or automated homogenisation as described (Section 2.3). The homogenised sample was left to incubate for 5 min at room temperature. One hundred and sixty microlitres of chloroform (Sigma-Aldrich, Dorset UK, cat. no. 496189) were added and the tubes were shaken vigorously by hand for 15 s and then incubated at room temperature for 2 min. The sample was then centrifuged at 13000 rpm for 15 min. Following this centrifugation step, the mixture separates into a lower, red, phenol-chloroform phase, an interphase and a colourless upper aqueous phase. The upper aqueous phase which contains the RNA was carefully removed and dispensed into a fresh tube.

Two hundred and forty microlitres of absolute ethanol (Sigma-Aldrich, Dorset UK, cat. no. 32221) were added to the lower and interphase and the sample was mixed by inversion. The sample was then stored at room temperature for 2 min and the

DNA was sedimented by centrifugation at 8000 rpm for 5 min. The phenol-ethanol supernatant (containing protein) was removed. Thirty microlitres of 3 M sodium acetate (Sigma-Aldrich, Dorset, UK, cat. no. S-7899) were added and the sample was mixed briefly. Three hundred microlitres of isopropanol (Sigma-Aldrich, Dorset, UK, cat. no. 33539) were added and the sample was vortexed briefly and incubated at room temperature for 2 min. The sample was spun at 13,000 rpm for 10 min and the supernatant was carefully decanted. The pellet was washed with 0.5 ml of 70% ethanol (Appendix A), vortexed, incubated for 10 min at room temperature and spun at 13,000 rpm for 15 min. The wash, vortex and incubation steps were repeated. The DNA pellet was air-dryed for 2-5 min in an open tube. The pellet was then re-dissolved in 70 µl ultraPURE™ water. Incubation of the partially dissolved pellet for two hours at room temperature or 4°C overnight was found to improve DNA solubilisation. The DNA was stored at -20°C until use.

RNA was extracted from the upper aqueous phase and stored as a resource for future work. A 0.4 ml volume of isopropanol was mixed with the aqueous phase and the samples were incubated at room temperature for 10 min. The samples were then centrifuged at 12,000 xg for 10 min at 4°C in a Heraeus Biofuge Stratos centrifuge (Kendro Laboratory Products, Hertfordshire UK). The supernatant was discarded and the RNA pellet was washed in 0.8 ml of 75% ethanol (Appendix A). The sample was mixed by vortexing and centrifuged at 7,500 xg for 5 min at 4°C. The RNA pellet was allowed to air dry for 5 min and was then dissolved in 200 µl of ultraPURE™ water, by passing the solution a few times through a pipette tip and incubating for 10 min at 60°C. The solution was then kept at -70°C for long-term storage.

2.5.2 QIAamp Viral RNA Kit (Qiagen, UK, cat. no. 52906)

Prior to commencing the extraction, one vial of carrier RNA was added to one bottle of AVL buffer. Two hundred and eighty microlitres of prepared AVL buffer were added to either a sterile, labelled 1.5 ml eppendorf (manual homogenisation) or a MagnaLyser tube (automated homogenisation) and the biopsy specimen added. The biopsy was then homogenised in the AVL buffer as described in Section 2.3. The homogenate was removed and placed in a new sterile 1.5 ml eppendorf tube; this was incubated at room temperature for 10 min. Two hundred and eighty microlitres of absolute ethanol (Sigma-Aldrich, Dorset UK, cat. no. 32221) were added and the sample was vortexed and then pulse spun at 13,000 rpm. The mixture was added to a QIAamp spin column which was centrifuged at 8000 rpm for 1 min. The waste from the collection tube was discarded into a universal tube. The QIAamp spin column was then placed in a clean 2 ml collecting tube. Two hundred and fifty microlitres of buffer AW-1 were added to the column and this was centrifuged at 8000 rpm for 1 min. The waste from the collection tube was discarded into a new universal tube and the QIAamp spin column was placed in a clean 2 ml collecting tube. Two hundred and fifty microlitres of buffer AW-2 were added to the column and this was centrifuged at 8000 rpm for 1 min. The waste from the collection tube was discarded into the same universal tube as the previous step. The QIAamp spin column was replaced in the same collecting tube which was centrifuged at 13000 rpm to remove any residual buffer. The QIAamp spin column was then place in a labelled 1.5 ml eppendorf tube (after removing the flip-top lid with a pair of scissors). The eppendorf tube with the spin column was then placed into a heating block set at 80°C, with the column lid opened and this was incubated for 1 min. Sixty

microlitres of preheated (to 80°C) AVE buffer were added to the centre of the column and the lid closed. This was incubated for a further 5 min. The nucleic acid was then centrifuged at 8000 rpm for 1 min. The spin column was discarded and the eppendorf tube, containing the eluted nucleic acid was re-capped. The nucleic acid was stored at -20°C until use.

2.5.3 DNeasy® Blood and Tissue kit (Qiagen, Crawley UK, cat. no. 69504)

Nucleic acid was extracted from liver biopsy specimens using the DNeasy® Blood and Tissue Kit following manufacturer's guidelines. In brief, the biopsy specimen was homogenised in 180 µl Buffer ATL. Twenty microlitres of proteinase K (provided with the kit) were added and the mixture was vortexed and incubated at 56°C for 1 h. The solution was then vortexed for 15 s and 200 µl buffer AL were added to the sample which was mixed thoroughly by vortexing. Two hundred microlitres of ethanol (96-100%) were added and the sample was mixed again. The mixture was pipetted into a DNeasy Mini spin column in a 2 ml collection tube which was centrifuged at 8000 rpm for 1 min. The flow-through and the collection tube were discarded. The spin column was then placed in a new 2 ml collection tube and 500 µl of buffer AW1 were added. This was centrifuged at 8000 rpm for 1 min and the flow-through and collection tube were discarded. The spin column was then placed in a new 2 ml collection tube and 500 µl of buffer AW2 were added. This was centrifuged at 13000 rpm for 3 min and the flow-through and collection tube were discarded. The spin column was transferred to a new, labelled, 1.5 ml microcentrifuge tube and 100 µl of elution buffer AE were added directly onto the DNeasy membrane. This was incubated at room temperature for 1 min and then centrifuged at 8000 rpm for 1 min to elute the nucleic acid from the DNeasy

membrane into the microcentrifuge tube. The nucleic acid was stored at -20°C until use.

2.5.4 Salting-out method

DNA was extracted from peripheral blood mononuclear cells (PBMCs) by adapting an existing protocol (Miller *et al*, 1988). A 5 ml EDTA blood sample was spun in a Centaur 1 centrifuge for 10 min at 3000 rpm. After centrifugation, two layers are formed – the top layer comprising plasma and a bottom layer of red blood cells. The interface between the two layers contains the PBMCs (buffy coat). Using a pastette the plasma was carefully removed into a waste container. The buffy coat was then removed and transferred to a labeled 15 ml polypropylene tube (Elkay Laboratory Products, Basingstoke UK, cat. no. 2088-000). Five millilitres of red cell lysis buffer (RCLB) (Appendix A) were added to the tube, and the tube was inverted several times and left to stand for 5 min, mixing gently on two occasions. The mixture was spun in a centrifuge for 10 min at 3000 rpm. The supernatant was decanted into a waste container, leaving the white cell pellet at the base of the tube. One millilitre of RCLB was added and the pellet was resuspended using a pastette. A further 5 ml of RCLB were added and the sample incubated at room temperature for 10 min, again with occasional mixing. The sample was centrifuged as before and the supernatant discarded. The pellet was resuspended in the residual RCLB and the solution transferred to a sterile 1.5 ml eppendorf tube. One millilitre of nuclei lysis buffer (NLB) (Appendix A), 53 µl of 10% sodium dodecyl sulphate solution (SDS) (Sigma-Aldrich, Dorset, UK, cat. no. 71736) and 16 µl of proteinase K (at 10 mg/ml concentration) (Appendix A) were added to the tube

which was then vortexed for 15 s. The tube was left on a BT3 heating block (Grant Instruments, Cambridge UK) at 56°C for 2 h.

A bottle of saturated (~6M) NaCl (Appendix A) was shaken well and 0.3 ml were added to the tube which was then capped and vortexed for 10 s. In a fume cupboard, 0.7 ml of chloroform (Sigma-Aldrich, Dorset UK, cat. no. 496189) were added to the tube and it was capped and shaken vigorously for 15 s until a milky froth appeared. The tube was then vortexed for 10 s and spun on the centrifuge for 10 min at 3000 rpm. The upper layer (containing the DNA) was removed into a fresh pre-labeled 15 ml polypropylene tube, leaving 2 mm of fluid above the interface to avoid sucking up protein. An equal volume of isopropanol (Sigma-Aldrich, Dorset UK, cat. no. 33539) was added to the tube and the solution was mixed gently until the DNA was observed as a visible string-like precipitate. The string was pulled out with a sterile pastette and transferred to a fresh, sterile eppendorf tube. One millilitre of 70% ethanol (Appendix A) was added to the pellet and this was mixed gently with a pipette. The tube was spun in a micro-centrifuge for 5 min at 13000 rpm. The ethanol was gently removed with a pipette. The ethanol wash was repeated and the tube was spun as before. The tube was left to air dry for several minutes. Depending on the size of the DNA pellet, 300-400 µl of 1x TE buffer (Appendix A) were added. The tube was left at room temperature and vortexed regularly until the DNA pellet had completely dissolved. The solution was then stored at -20°C until required.

2.6 Determination of DNA concentration by spectrophotometry

A 1:100 dilution of DNA sample was prepared by adding a 5 µl aliquot of DNA to 495 µl of distilled water in a microcentrifuge tube. The DNA mixture was then

transferred to a quartz microcell cuvette and the absorbance was read at 260nm in a Model 6505 UV/VIS spectrophotometer (Jenway, Dunmow UK), using water as a blank. The DNA concentration of the sample was calculated on the basis that an optical density reading (OD) of 1.0 is equivalent to a double stranded DNA concentration of 50 µg/ml, using the equation below:

$$A_{260} \times 5 = \text{Concentration of DNA } (\mu g/\mu l)$$

2.7 Agarose gel electrophoresis

Following amplification, PCR products were monitored by 2% agarose gel electrophoresis. One point two grams of 3:1 NuSieve® agarose (Lonza, Wokingham Ltd, Berkshire UK, cat. no. 50090) were added to 60 ml 1x TBE buffer (Appendix A) in a 500 ml conical flask and the contents mixed by swirling. This was boiled in a microwave oven for approximately 90 s. The gel solution was cooled to 65°C, 20 µl ethidium bromide (2 mg/ml) (Appendix A) were added and the solution mixed by gentle swirling. Two 20 well combs and end pieces were inserted into a level 24 cm x 15 cm gel tank (Engineering and Design Plastic Ltd, Cambridge UK, cat. no. EM100). The solution was poured in and allowed to set for 30 min at room temperature. The combs were removed and 5 µl of PCR product which had been mixed with 10 µl Orange G loading buffer (Appendix A) was loaded into each gel slot. Five microlitres of PCR markers (Promega, Southampton UK, cat. no. G3161) were loaded into the first well of each row. Each marker contains ~35 ng of DNA fragment and allows approximate quantitation of PCR products by comparison with the band intensity of the markers. The gel tank was carefully flooded with ~75 ml of 1x TBE buffer and the samples were electrophoresed for ~40 min using a Shandon Vokam Power Supply (Model

SAE2761, Shandon Scientific, Cheshire UK) set at 75 Volts (V) for electrophoresis at 5 V/cm. Following electrophoresis, the gel was photographed under UV illumination, viewed and documented using the AlphaImager™ digital imaging system using AlphaEase software (Alpha Innotech Corporation, California USA).

2.8 HCV serotyping

HCV serotyping was carried out using the Murex HCV Serotyping Kit (Abbott Murex, Dartford UK, cat. no. 2G26-01), following manufacturer's guidelines. In brief, the conjugate was reconstituted by adding the whole bottle of conjugate diluent to the bottle of conjugate. This was mixed by gentle inversion and allowed to rehydrate for at least 30 min. The substrate solution was prepared by pouring the entire bottle of substrate diluent into the bottle of substrate concentrate. This was kept away from direct sunlight. The wash fluid was prepared by diluting it 1 in 20 with ddH_20.

The required number of strips was assembled in the plate frame, including one for a typing control (genotype 1). Each sample to be serotyped was incubated in eight separate microwells which are each coated with HCV peptides. Different competing solutions were added to each well as follows:

A. 10 µl of CS Type 6 to well A (specific peptides for serotypes 1, 2, 3, 4 and 5)
B. 10 µl of CS Type 5 to well B (specific peptides for serotypes 1, 2, 3, 4 and 6)
C. 10 µl of CS Type 4 to well C (specific peptides for serotypes 1, 2, 3, 5 and 6)
D. 10 µl of CS Type 3 to well D (specific peptides for serotypes 1, 2, 4, 5 and 6)
E. 10 µl of CS Type 2 to well E (specific peptides for serotypes 1, 3, 4, 5 and 6)
F. 10 µl of CS Type 1 to well F (specific peptides for serotypes 2, 3, 4, 5 and 6)

G. 10 µl of CS ALL to well G (specific peptides for all six serotypes)
H. No CS added

Eighty microlitres of sample diluent were added to wells A to H using a multi-pipette. Ten microlitres of sample or HCV typing control were added to each of the 8 wells of one strip, using a clean tip for each well. This was mixed thoroughly by pipetting up and down at least four times. The wells were covered with a lid and incubated for 30 min at 37°C. The plate was then washed using an automated ELx50 bioelisawasher (Biokit, Barcelona Spain) performing 5 wash cycles using wash fluid with a fill volume of 500 µl/well and an aspirate/wash/soak cycle of 30 s. One hundred microlitres of reconstituted conjugate were then added to each well using a multi-pipette. The plate was covered with a lid and incubated for 30 min at 37°C. The plate was then washed as before. One hundred microlitres of substrate solution were added to each well using a multi-pipette. The plate was covered with a lid and incubated for 30 min at 37°C. Fifty microlitres of stop solution (2 M sulphuric acid, Fisher Scientific, Leicestershire UK, cat. no. J/8410/PB15) were added to each well using a multi-pipette. The optical density (OD) for each well was determined by reading the absorbance at 450 nm within 15 min, using 690 nm as the reference wavelength. The instrument was first blanked on air (no plate). For each sample the 'All' OD value (AC) (well G) was subtracted from the OD value of each of the serotyping wells (A-F). The typing ratio was then calculated for the serotyping well demonstrating the highest resulting value (HT) (only if this value was >0.1). The typing ratio was calculated as follows:

$$\text{Typing Ratio} = \frac{[\text{HT-AC}]}{[\text{NC-AC}]}$$

NC = no competition (OD from well H)

AC = All competition (OD from well G)

HT= highest type (serotyping well (A-F) with highest OD)

For a valid typing signal

- NC-AC >0.1
- HT-AC>0.1
- Typing ratio >0.2

If no serotyping wells demonstrated a value of >0.1 following subtraction of the AC value, then the sample was regarded as negative. If multiple serotyping wells demonstrated a value >0.1 then the sample was regarded as non-typable.

2.9 Ultracentrifugation

Prior to HCV serotyping, serum specimens were ultracentrifuged and subjected to HCV quantitative PCR to ensure that HCV RNA was not present. The ultracentrifugation step allowed increased sensitivity in order to detect even minute amounts of HCV RNA. Ultracentrifugation was carried out on a 1 ml aliquot of serum which was transferred to a sterile 1.5 ml flat cap microcentrifuge tube and spun at 23,000 xg for 60 min in a Heraeus Biofuge Stratos centrifuge (Kendro Laboratory Products, Germany) set at 4°C. The supernatant was carefully decanted and the nucleic acid pellet was then re-suspended in 350 µl of ultraPURE™ water and extracted using the BioRobot MDx workstation as described in section 2.4.2.

2.10 Preparation of MS2 internal control

2.10.1 Re-hydration of freeze-dried MS2 phage and phage propagation

Phage MS2 (15597-B1™) and host (15597 *Escherichia coli* strain) were acquired from the American Type Culture Collection (ATCC) (www.lgcpromochem-atcc.com). The host was supplied as a lypophilised preparation and was reconstituted in #271 broth (Appendix A) and incubated overnight at 37°C aerobically. Using a sterile 1 µl loop, colonies were streaked onto a #271 agar plate (Appendix A) and incubated overnight at 37°C aerobically and stored. A colony of MS2 host was inoculated in #271 broth and incubated in an orbital incubator at 200 revolutions per minute at 37°C overnight. Freeze dried phage stock was re-hydrated in 1 ml of #271 broth under aseptic conditions.

2.10.2 Agar layer method

A high titre stock was prepared from 0.25 ml of the re-hydrated MS2 phage using the agar layer method (the remainder was stored frozen at -20°C). Five sterile universals, each containing 0.2 ml of the host and 50 µl of MS2 phage were incubated at room temperature for 10 min to allow the phage to adsorb onto the host. A control universal containing MS2 host without phage was also prepared.

To 100 ml of soft agar (5%) (Appendix A) cooled to 45°C was added 1 ml of 10% glucose (Appendix A), 0.2 ml of 1 M calcium chloride (Appendix A) and 0.1 ml of 10 mg/ml thiamine (Appendix A). Four millilitres of the soft agar (still in liquid form) were added to each of the 6 universals, mixed and then immediately poured on to fresh pre-warmed (37°C) #271 agar plates, and allowed to set. The plates were

then incubated overnight at 37°C aerobically and plaque formation was visualised the next day.

Twenty millitres of #271 broth were added to each of the 5 plates (displaying clear confluent lysis as compared to the control). The soft agar was then scraped off using a sterile spreader into two 50 ml polypropylene tubes (Elkay Laboratory Products, Basingstoke UK, cat. no. 2092-000) and the contents vigorously mixed. The agar/bacterial debris was removed by centrifugation at 3000 rpm for 25 min. The supernatant containing the phage was filtered through a 0.22 µm Millex-GP sterilising filter unit (Millipore Ireland BV, Cork, cat. no. SLGP 033 RS) and the phage stored at -20°C.

2.10.3 Determining plaque forming units

The phage stock was serially diluted (10^{-1}, 10^{-2}, 10^{-3}, to 10^{-10}) in #271 broth and 25 µl of each dilution was spotted, in triplicate, on the surface of #271 agar plates which contained an overlay of soft agar with MS2 host (0.2 ml of overnight culture). The plates were allowed to dry, incubated overnight at 37°C and visualised the next day for plaque formation. At the dilution where 20-100 plaques were visible, counts were made and the titre determined by working back with the dilution factor.

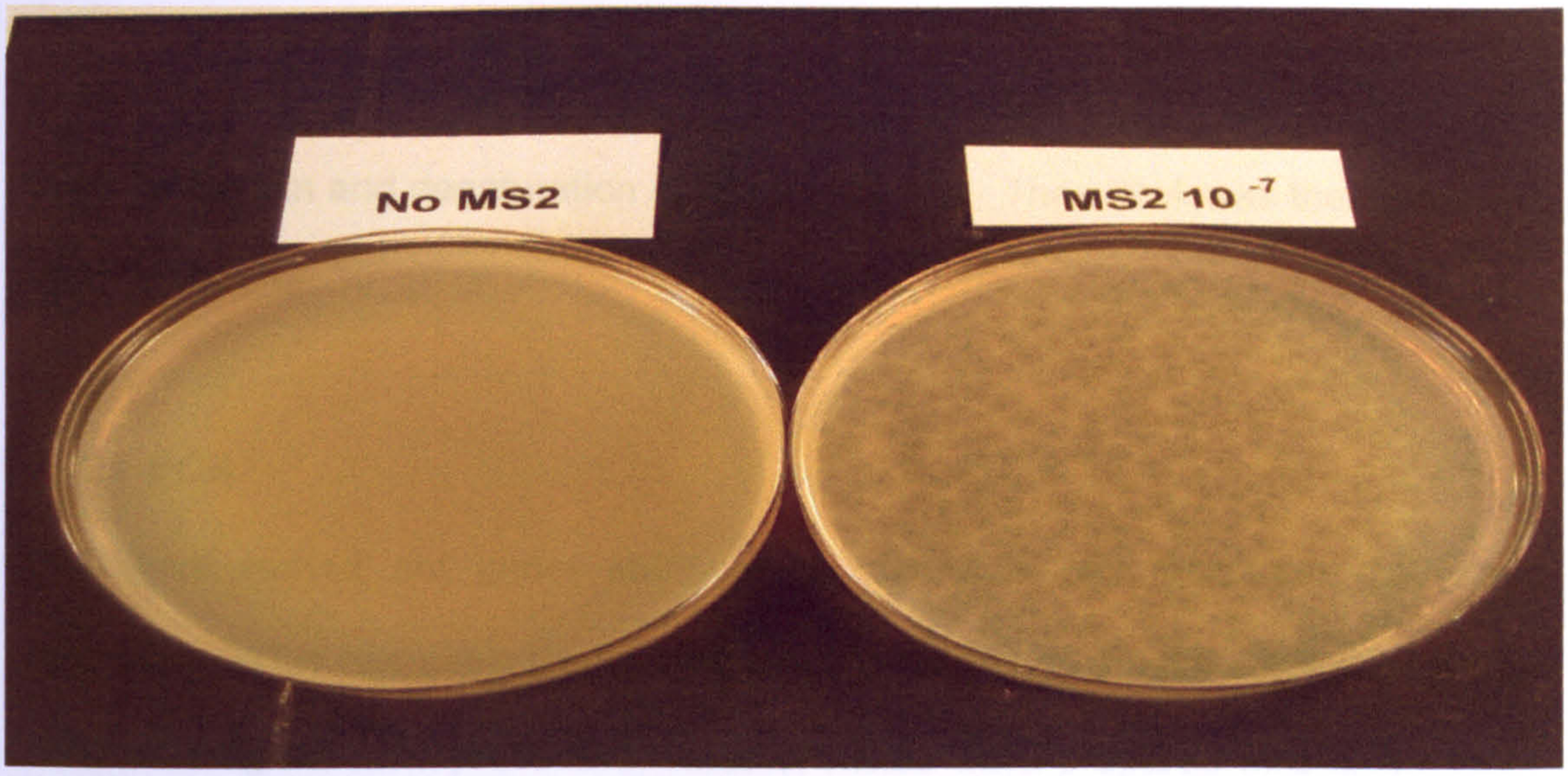

Figure 2.1: Determining plaque forming units (pfu) of MS2. The plate on the left show confluent growth of E. coli host (no MS2 added). The plate on the right shows plaques produced when a 10^{-7} dilution of MS2 was added to the host.

2.11 Reverse transcription (cDNA preparation)

Twenty microlitres of extracted RNA and 1 µl $pd(N)_6$ random hexamer (GE Healthcare, New Jersey USA, cat. no. 27-2166-01) were added to labeled 0.2 ml PCR tubes (Corbett Research, Cambridge, UK). These were placed in a PTC-200 Peltier thermal cycler (MJ Research, Waltham USA) and heated to 70°C for 5 min to unfold the secondary structure and facilitate annealing prior to reverse transcription. Meanwhile, a master mix for reverse transcription was prepared in 1.5 ml flat cap microcentrifuge tubes (StarLab Ltd, Milton Keynes UK) using M-MLV Reverse Transcriptase (RT) 200U/µl (Invitrogen, Paisley UK, cat. no. 28025-013) (Appendix C). After 5 min on the thermal cycler, the tubes containing linearised nucleic acid were transferred immediately to ice, incubated for 2 min and then pulse spun in a Micro Centaur centrifuge (MSE, London UK). Fourteen microlitres of prepared master mix were added to each tube, which were then vortexed and pulse spun. Reverse transcription took place on the thermal cycler at

37°C for 60 min and denaturation at 95°C for 5 min. The cDNA was then stored at –20°C until use.

2.12 PCR

PCR was carried out under stringent conditions in the molecular diagnostic laboratory. This has separate accommodation with clear spatial separation of the different stages in the procedure. Master mixes were prepared in a clean room and were then transferred to the extraction room where nucleic acid was extracted and samples were prepared. PCR occurred in an amplification room which contained the thermal cyclers. Any subsequent amplicon analysis, such as gel electrophoresis was carried out in the detection room. The flow of work was uni-directional with amplicons never entering the clean or extraction rooms. Each of the rooms was equipped with its own consumable items, protective clothing, reagents, pipettes and equipment.

2.12.1 Block-based PCR

Block-based (conventional) PCR assays were carried out using the *Taq* DNA polymerase kit (Invitrogen, Paisley UK, cat. no. 10342-020). This kit includes 10x PCR buffer-II (200mM Tris-HCl [pH8.4], 500mM KCl), 50 mM $MgCl_2$ and *Taq* DNA polymerase. A master mix containing the appropriate volumes of buffer, $MgCl_2$, *Taq* polymerase, dNTPS (dATP, dCTP, dGTP, dTTP) at 10 mM (Appendix A), and primers was prepared in 1.5 ml flat cap microcentrifuge tubes (StarLab Ltd, Milton Keynes UK) and aliquoted into labeled 0.2 ml PCR tubes (Corbett Research, Cambridge UK). Nucleic acid (DNA or cDNA) was then added and the mixture vortexed and pulse spun. Positive and negative controls were included in every run. PCR was carried out on a PTC-200 Peltier thermal cycler (MJ Research,

Waltham USA). Optimised master mixes and cycling conditions for all block-based PCR assays are given in Appendix C.

2.12.2 Real-time PCR

Two different thermal cyclers were used in this research, the Rotor-Gene™ 3000 (Corbett Life Sciences, Cambridge UK) and the LightCycler 1.5 (Roche Diagnostics, Burgess Hill UK).

2.12.2.1 Rotor-Gene™ 3000

The Rotor-Gene™ 3000 is a centrifugal real-time DNA amplification system. Its 4 channel multiplexing allows up to 4 different fluorescently labelled probes to be monitored in a single tube with no spectral overlap. During the run, the rotor spins at approximately 500 rpm as the tubes are thermally cycled in a low-mass air oven. The 4 channel LED source irradiates the tube from the side wall and the photomultiplier detects the energy from the base of the chamber (Figure 2.2). Each dye is excited at its peak wavelength, maximising sensitivity and reducing cross-talk between channels (Table 2.1). The detection filter wheel has six different filters, four are band pass that are used in four channel multiplex runs, the other two are high pass filters that can be used for specialised applications. The unit holds either 36 x 0.2 ml PCR tubes (Corbett Research, Cambridge UK, cat. no. 3001-001) or 72 x 0.1 ml PCR tubes (Corbett Research, Cambridge UK, cat. no. 3001-001), loaded into a carousel.

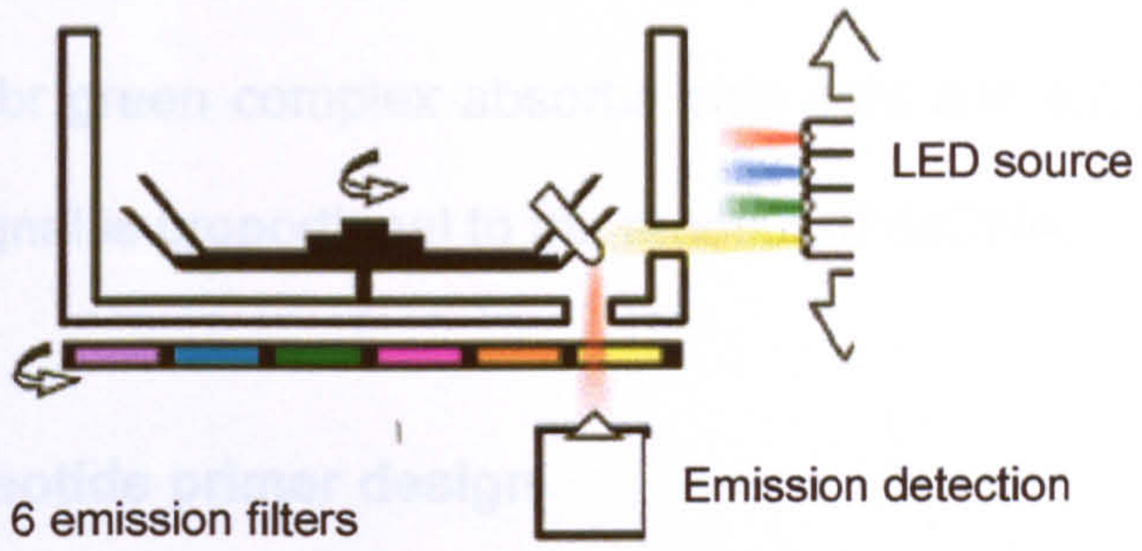

Figure 2.2: Rotor-Gene™ 3000 side view

Dye	Source	Detector
FAM	470 nm	510 nm
JOE/VIC	530 nm	555 nm
ROX	585 nm	610 nm
Cy5	625 nm	660 hp

Table 2.1: Wavelength of the source LED and detection filter for each of the probes used by the Rotor-Gene™ 3000. Hp; high pass filter used

2.12.2.2 LightCycler®

The LightCycler 1.5 Real-Time PCR System is a carousel based thermal cycler. PCR occurs in glass capillaries (Roche Diagnostics, Burgess Hill, UK, cat. no. 11909339001) which have an optimal surface-to-volume ratio to ensure rapid equilibration between the air and reaction components, resulting in rapid amplification cycles. It has three detection channels which measure fluorescence at 530, 640 and 705 nm. LightCycler® Software 3.5.3 controls the instrument and performs analyses which can be absolute quantification, melting curve analysis and mutation/SNP analysis.

Although the LightCycler can be used with fluorescent labelled dyes, in this study it was only used for non-specific detection using SYBR Green I. This fluoresecent

intercalates into double-stranded (ds) DNA and produces a fluorescent signal. The resulting DNA-Sybr green complex absorbs blue light and emits green light. The intensity of the signal is proportional to the amount of dsDNA.

2.13 Oligonucleotide primer design

Primers were designed around reference sequences extracted from National Centre for Biotechnology Information (NCBI) website (http://www.ncbi.nlm.nih.gov). The required sequence data was aligned with MegAlign software in the DNASTAR Lasergene Software package (DNASTAR Inc, Madison, USA. See www.dnastar.com). Alternatively, lengthy sequences were aligned and interrogated using the European Bioinformatics Institute website (http://www.ebi.ac.uk).

Primers were designed following published recommendations (Innis and Gelfand, 1990). Primers were designed to be 15-30 nucleotides in length with G+C content of between 40-60% and a melting temperature (Tm) of between 50-70°C. Each primer in a set was designed to have approximately equal melting temperatures. Complementarity, especially at the 3' end (to prevent primer-dimer formation) and runs of 3-4 repeats of the same base were avoided. To introduce relative instability to the 3' end of primers and to reduce non-specific priming, the number of Gs and Cs in the last 5 nucleotides at the 3' end did not exceed two. Primers were designed, where possible, to end in a G or C – the 'GC clamp' to increase stability. The primer sequence was entered onto the OligoAnalyzer 3.0 software, available on the Integrated DNA Technologies website (http://eu.idtdna.com/analyzer/Applications/OligoAnalyzer), to check for self-

complementarity leading to self-dimerisation and 'hairpin' structures. A BLAST database search of the primer sequence was carried out to ensure no homology to other sequences. If necessary, primers were modified with LNA additions (see section 1.11.1.3). Primers (including fluorescent-labelled primers) were synthesised by Metabion GmbH, Germany. LNA primers were synthesised by Proligo (www.proligo.com). Nucleotide sequences for all primers used are given in Appendix B.

2.14 Oligonucleotide probe design

Design of Taqman probes followed the same rules as those described for primer design. The probes were designed to have a Tm of around 5-10°C higher than that of the primers. The DNA strand which gave the probe more Cs than Gs was selected. The placement of a G at the 5' end was avoided. The probes were labelled at the 5' end with a specific fluorophore, either FAM, JOE(VIC), ROX or Cy5. The 3' end had an attached quencher with was either NFQ, TAMRA, or BHQ-2. All probe sequences are given in Appendix B.

2.15 Real-time PCR master mix preparation and assay set-up

2.15.1 Rotor-Gene

All Rotor-Gene PCR assays (except for HCV quantitation and β-globin quantitation) were carried out using the LightCycler® FastStart DNA Master HybProbe kit (Roche Diagnostics, Burgess Hill UK, cat. no. 12239272001). HCV quantitation was carried out using the SuperScript™ III RT/Platinum® One-Step Quantitative RT-PCR System (Invitrogen, Paisley UK, cat. no. 11732-088). β-globin quantitation was carried out using the Platinum® Quantitative PCR SuperMix-UDG

kit (Invitrogen, Paisley, UK, cat. no. 11730-025). A PCR master mix was prepared by combining the appropriate reagents in a 1.5 ml flat cap microcentrifuge tube. Following gentle mixing, the mix was dispensed in appropriate volumes into 0.1 ml (Rotor-Gene 72-sample carousel) or 0.2 ml PCR tubes (Rotor-Gene 36-sample carousel). Target DNA/cDNA was added to each appropriate tube. Positive and negative controls were included in every analysis. Optimised master mixes for all assays are given in Appendix C. The samples were then loaded into the Rotor-Gene 3000 carousel.

Amplification profiles were created for each assay, determined by optimisation experiments and are outlined in Appendix C. Prior to the commencement of every run, a calibration was carried out on all the channels which would be utilised during the run; this adjusted the gains for the channels selected. Following the completion of the run, the threshold, which determines the threshold cycle (C_T) for each sample, was set. This was normally between 0.1-0.2. If plasmid standards were used, then 'auto threshold' was selected. This gives the best line of fit for the standard curve.

2.15.2 LightCycler

A PCR master mix was prepared (LightCycler® DNA Master SYBR Green I kit; Roche Diagnostics, Burgess Hill UK cat. no.12158817001) by combining the appropriate reagents (Appendix C) in a 1.5 ml flat cap microcentrifuge tube. Following gentle mixing, this was dispensed in appropriate volumes into 20 µl LightCycler capillaries. Target DNA/cDNA was added to each appropriate capillary which was then capped. The samples were pulse spun in a LC carousel centrifuge

(Roche Diagnostics, Burgess Hill, UK, cat no. 12189682001). Optimised master mixes for all assays are given in Appendix C. The samples were then loaded into the LightCycler 1.5 for real-time PCR. Amplification profiles are outlined in Appendix C.

2.16 PCR optimisation

For each amplification reaction, optimal PCR reagent and cycling conditions were achieved by experimenting with various annealing temperatures and by varying the concentration of $MgCl_2$, PCR primers and probes according to published guidelines (Innis and Gelfand, 1990).

To determine the appropriate annealing temperature for each primer set, the melting temperature (Tm) for each primer was calculated using the OligoAnalyzer 3.0 software, as described in section 2.13. The starting annealing temperature was taken as 4°C below the average Tm for each primer set. If necessary, this temperature was increased or decreased by increments of 1-2°C until the desired specificity of product was obtained.

Once the appropriate annealing temperature was established, the product intensity was improved by applying the following reagent titration experiments:

(i) titration of $MgCl_2$

(ii) variation of primer concentration

(iii) variation of one primer with respect to the other, depending on whether the probe annealed to the plus or minus strand of DNA

(iv) variation of probe concentration

2.17 Purification of PCR products

PCR products were purified using the QIAquick® PCR Purification Kit (Qiagen, Crawley, UK, cat. no. 28106). All centrifugation steps were at 13000 rpm. Prior to purification, PCR products were electrophoresed on 2% agarose (Section 2.7) to determine the approximate concentration of each product. In brief, to purify PCR products, 5 volumes of buffer PB were added to 1 volume of the PCR sample and mixed in a 1.5 ml flat cap microcentrifuge tube (StarLab Ltd, Milton Keynes UK). The PB/PCR product mix was added to a QIAquick spin column which had been placed in a 2 ml collection tube. To bind the DNA, the sample was centrifuged for 1 min. The flow-through was discarded and the QIAquick column was replaced in the same collection tube. To wash, 0.75 ml of Buffer PE (containing 96% ethanol) were added to the QIAquick column and centrifuged for 1 min. The flow-through was discarded and the QIAquick column was placed back in the same collection tube and centrifuged for 1 min to remove any residual fluid. The QIAquick column was then placed in a 1.5 ml flat cap microcentrifuge tube (StarLab UK Ltd, Buckinghamshire). To elute the DNA, 50µl (or 30µl if the original PCR product was weak – as determined by comparison with PCR markers on gel electrophoresis) of buffer EB were added to the centre of the QIAquick membrane. The column was left to stand for 1 min and then centrifuged for 1 min to collect the product. To determine the yield following purification, purified PCR products were run on a 2% agarose gel (Section 2.7). The products were stored at -20°C until required.

2.18 ABI 3100-*Avant* genetic analyzer

The ABI 3100-*Avant* Genetic Analyzer (Applied Biosystems, Warrington UK) is a fully automated DNA analysis system which uses capillary electrophoresis.

Samples are simultaneous injected into a parallel four-capillary array using electrokinetic injection. This allows faster run times and increases run-to-run consistency. The DNA passes through a detection cell and a laser beam simultaneously illuminates the four capillaries on both sides of the array. The omitted fluorescent light is collected, separated by wavelength and focussed onto a charge-coupled device (CCD). The data is then transferred to the instrument computer where chemometric algorithmic processing transforms the data into a 4 or 5-dye electropherogram. The ABI 3100-*Avant* has multiple applications and in this study was used for both DNA sequencing and fragment analysis.

2.19 ABI 3100-*Avant* system preparation

The ABI 3100-*Avant* was prepared as outlined in the manufacturer's guidelines. The POP-6™ polymer (Applied Biosystems, Warrington UK, cat. no. 4316357) was allowed to equilibrate to room temperature. The 5 ml polymer reserve syringe and the 250 µl array-fill syringe were first primed with polymer which was then discarded. The 5 ml syringe was filled with 0.5 ml of polymer and the 250 µl syringe was completely filled with polymer. All air bubbles were removed by inverting the syringe and pushing the air bubbles out. Both syringes were screwed into the upper polymer block.

A 1x working solution of the 10x Genetic Analysis Buffer 310 (running buffer) (Web Scientific Ltd, Crewe UK, cat. no. DAD-025) was prepared by adding 2.5 ml to 22.5 ml ddH_20 in a 50 ml polypropylene tube (Elkay Laboratory Products, Basingstoke UK, cat. no. 2092-000) and mixing by inversion. The anode buffer reserve was filled to the marked level with prepared buffer and attached to the lower polymer

block. The interconnecting tube was fastened between the upper and lower polymer blocks. A 50 cm ABI 3130/3100-*Avant* capillary array (Applied Biosystems, Warrington UK, cat. no. 4333466) was installed and connected to the upper polymer block via the array ferrule knob. The detection cell was secured into the detection block. All air bubbles were removed from the system by pushing down on each of the syringe plungers in turn whilst holding down the pin valve above the lower polymer block and then releasing it to allow air bubbles to flow into the anode buffer reserve. Three autosampler reservoirs were filled to the mark with ddH_20 and the cathode reservoir with 1x running buffer and covered with septa.

Samples were loaded into a 96-well optical reaction plate, fitted with a genetic analyser septa and loaded into a 96-well autosampler tray (all included in the 3100/3100-*Avant* Genetic Analyser Autosampler Plate kit, Applied Biosystems, Warrington, UK, cat. no. 4316471)

2.20 ABI 3100-*Avant* calibration

2.20.1 Spatial calibration

A spatial calibration was carried out each time that a capillary array was installed, and as part of the weekly maintenance, as described in the users manual. This maps the position of each capillary on the CCD camera. The capillaries were filled each time the spatial analysis was performed. The peak shape and peak spacing were visually evaluated each time and the calibration accepted if satisfactory.

2.20.2 Spectral calibration

A spectral calibration was carried out when a new dye set was run for the first time or if the dyes were being run under new conditions. The spectral calibration creates a mathematical matrix to correct for the overlapping of fluorescence emission spectra for the dyes. This creates a matrix file which is then applied to samples run under similar conditions. A matrix standard set is used to generate the 'multicomponent matrix' required when analysing DNA fragments on the ABI 3100-*Avant*. The data collection software for the instrument uses the multicomponent matrix to automatically analyse the different coloured fluorescent dye-labelled samples in a single capillary. For sequencing analysis, the BigDye® Terminator v3.1 Matrix Standard Kit (Applied Biosystems, Warrington, UK, cat. no. 4336974) (dye set Z) was used. Ten microlitres of the standard were combined with 190 µl of Hi-Di™ formamide (Applied Biosystems, Warrington UK, cat. no. 4311320). This was mixed thoroughly, spun in a centrifuge and denatured at 95°C for 5 min and immediately placed on ice for 2 min. Ten microlitres of the mixture were then dispensed into four wells of a 96-well optical reaction plate which was loaded into the autosampler as described in section 2.19. The Plate Editor spreadsheet was completed for the wells that were loaded and the correct dye set and run module were selected (Spect50_POP6DefaultModule). The spectral calibration was run and accepted if the results were within acceptable limits outlined in the User Manual.

2.21 Sequencing

2.21.1 Preparation of sequencing reactions

PCR products were sequenced by automated fluorescent cycle sequencing using the BigDye® Terminator v3.1 Cycle Sequencing kit (Applied Biosystems, Warrington, UK, cat. no. 4337455). PCR products to be sequenced were first purified (section 2.17) and run on gel electrophoresis to check for adequate purification and to estimate DNA concentration.

Products were always sequenced in both directions using the forward and reverse primers at 2 pmol/µl concentrations. For each PCR product to be sequenced, two reaction mixes were made up in 1.5 ml flat cap microcentrifuge tubes one with the forward primer and one with the reverse primer. For each sequencing reaction, 4 µl of BigDye Terminator v3.1 Ready Reaction Premix (included in sequencing kit) and 2 µl of BigDye sequencing buffer (5x) (Applied Biosystems, Warrington, UK, cat. no. 4336697) were added to labelled 0.2 ml PCR tubes along with 4 pmol of the appropriate primer. Between 1 and 8 µl of purified PCR product were added and the volume made up to 20 µl with ultraPURE™ water. The amount of PCR product added was dependent upon the estimated concentration of the product, ascertained from comparison with markers of known concentration on gel electrophoresis (section 2.7). Good quality sequence data was usually obtained with the addition of 1 µl of PCR product for strong/medium bands on gel electrophoresis. All components of the sequencing mix were added in the clean room, apart from the PCR products which were added in the detection room. The sample tubes were kept on ice whilst the sequencing mix was being made.

Cycle sequencing was carried out on a PTC-200 Peltier thermal cycler (MJ Research, Waltham USA) programmed to perform the following:

Denaturation: Rapid thermal ramp to 96°C*
96°C for 1 min

25 cycles: Rapid thermal ramp to 96°C
96°C for 10 s
Rapid thermal ramp to 50°C
50°C for 5 s
Rapid thermal ramp to 60°C
60°C for 4 min

Rapid thermal ramp to 4°C and hold until ready to purify.

* rapid thermal ramp is 1°C/s

The sequencing products were then removed from the thermal cycler and spun briefly.

2.21.2 Ethanol/EDTA/sodium acetate purification and precipitation

The sequencing reactions were purified and precipitated using the ethanol/EDTA/Sodium Acetate method. A stop solution consisting of equal volumes of 125 mM EDTA (Appendix A) and 3 M sodium acetate (Sigma-Aldrich, Dorset, UK, cat. no. S-7899) was made up. Four microlitres of the solution were added to each well to be used in a 96-well optical reaction plate making sure that the solution reached the base of each well. The sequencing products were then added to each well. Fifty microlitres of absolute ethanol (Sigma-Aldrich, Dorset UK, cat. no. 32221) were added to each well using a multi-pipette and each reaction was mixed by pipetting gently up and down. The plate was sealed with transparent sealant and left to incubate for 15 min at room temperature. The plate was then spun at 2000 xg for 30 min in a Sigma 4-15°C laboratory centrifuge

(SciQuip, Shropshire UK, cat no. 10733). Immediately following centrifugation, the plate was inverted over lint-free tissue and spun up to 185 xg and then removed from the centrifuge. Seventy microlitres of 70% ethanol (Appendix A) were added to each well and the plate was spun at 1650 xg for 15 min. The plate was again inverted over lint-free tissue and spun up to 185 xg for 1 min (from when the rotor started moving) The plate was removed from the centrifuge, inverted and left to air dry for 10 min, with the plate protected from the light. The samples were resuspended in 10 µl of Hi-Di™ formamide (Applied Biosystems, Warrington, UK, cat. no. 4311320), pipetting up and down the sides of the wells to ensure the samples were fully resuspended. The prepared 96 well sample plate containing the purified sequencing products was covered with a plate septum, fixed into a plate base and covered with a plate container. The prepared plate assembly was loaded into the autosampler.

Sequencing was carried out on the ABI 3100-*Avant* Genetic Analyzer using a 50 cm capillary array (Applied Biosystems, Warrington, UK, cat. no. 4333466) using POP-6™ polymer (Applied Biosystems, Warrington, UK, cat. no. 4316357). The system was set up as described in section 2.19. The Plate Editor spreadsheet was completed for the wells that were loaded. The correct dye set (Z), mobility file (DT3100POP6{BDv3}v1.mob), run module (StdSeq50_POP6DefaultModule) and analysis module (BC-3100POP6SR_SeqOffFtOff.saz) were selected and the run was launched.

2.22 Sequence analysis and alignment

Sequences were viewed using Sequencing Analysis software v5.2 (Applied Biosystems, Warrington UK) to check the quality of the data. Good quality

sequence data was then saved and analysed using the DNASTAR Lasergene Software package (DNASTAR Inc, Madison, USA. See www.dnastar.com). This includes programmes for sequence visualisation (SeqMan), editing (EditSeq) and alignment and phylogenetic analysis (MegAlign).

2.23 PCR product cloning

PCR products were cloned using the TOPO TA Cloning® Kit for Sequencing with TOP10 chemically competent One Shot® cells (Invitrogen, Paisley UK, cat. no. K4575-01) following manufacturer's guidelines. Prior to cloning, PCR products were purified, as described in section 2.17.

2.23.1 Ligation

Ligation reactions were set up using the TOPO vector® as outlined in Table 2.2. The amount of PCR product added to the reaction mix was determined by the product yield on gel electrophoresis (section 2.7).

Reagent	
Fresh PCR product	0.5 to 4 µl
Salt solution	1 µl
Water	Add to a volume of 5 µl
TOPO vector®	1 µl
Final Volume	6 µl

Table 2.2: PCR product cloning. Reaction mix for product ligation

The reaction mix was left overnight at room temperature for maximum uptake of the PCR product into the vector.

2.23.2 Transformation

The following day a vial of One Shot® Chemically Competent *E. coli* were thawed on ice, one vial for each cloning reaction. Two microlitres of cloning reaction were added to a vial and mixed gently. The reaction was incubated on ice for 30 min. The cells were heat-shocked by placing the vials in a waterbath set to 42°C for 30 s. The vials were then immediately transferred to ice. Two hundred and fifty microlitres of room temperature S.O.C medium were added to each vial. The vial was tightly closed and shaken horizontally in an incubator at 37°C for 1 h. Following incubation, the S.O.C medium was spread onto pre-warmed LB/Ampicillin agar plates containing 50 µg/ml ampicillin (Appendix A). Different volumes, ranging from 10-200 µl were plated onto a total of five plates for each transformation to ensure that at least one plate would have well-placed colonies; additional S.O.C medium was added to low volumes to ensure even spreading over the entire plate. The plates were incubated overnight at 37°C. The following day, numbered grids were drawn on the bottom of fresh, prewarmed LB/ampicillin agar plates. Using sterile 1 µl loops, 20 individual putative transformants from the overnight incubation plates were selected and smeared diagonally within each grid square of the new plate. The plate was then incubated at 37°C overnight. The plates were covered with Parafilm™ and stored at 4°C until ready for testing.

2.23.3 Insert verification

A small quantity of cells from each of 20 streaked colonies was removed using a sterile 1 µl loop and placed individually into 30 µl ddH_2O in 1.5 ml flat cap microcentrifuge tubes. The samples were placed in a Grant BT3 heating block (Grant Instruments, Cambridge, UK) set at 95°C for 10 min and then spun for 2 min at 13,000 rpm in a microcentrifuge, to pellet down any agar or cell debris. One microlitre of the solution was subjected to colony PCR using the M13 primer pair (Appendix B) with a mastermix prepared as outlined in (Appendix C). Gel electrophoresis (section 2.7) of the PCR product was carried out to verify the presence of the insert. Absence of the insert was demonstrated by a band of 198 bp.

2.23.4 Cell harvesting

A loopful of cells from a streaked colony containing the insert was incubated overnight in a shaking incubator set at 37°C in 2 separate universals, each containing 5 ml of prewarmed LB/Ampicillin broth medium (Appendix A). The following day, cells were harvested from one of the universals by repeated centrifugation, at 13,000 rpm, of 1 ml aliquots in the same 1.5 ml flat cap microcentrifuge tube (StarLab UK Ltd, Buckinghamshire) tube leading to a sizeable bacterial pellet at the base of the tube.

2.24 Plasmids

2.24.1 Long-term storage of plasmids

The 5 ml of LB broth containing transformed cells in the duplicate universal which were not harvested for the plasmids was mixed with an equal volume of 50%

glycerol (Appendix A). The universal was clearly labelled and kept at -70°C for long-term storage.

2.24.2 Plasmid purification

Plasmids were purified using the QIAprep® Miniprep Kit (Qiagen, Crawley, UK), following manufacturer's guidelines. In brief, the pelleted bacterial cells were resuspended in 250 µl of Buffer P1. Two hundred and fifty microlitres of Buffer P2 were then added and the solution mixed thoroughly by inverting 6 times. Three hundred and fifty microlitres of Buffer N3 were then added and mixed immediately and thoroughly by inverting 6 times. The mixture was then centrifuged at 13,000 rpm, producing a compact white pellet. The supernatants were decanted into a QIAprep spin column and centrifuged for 1 min. The flow-through was discarded and the QIAprep spin column was washed by addition of 0.75 ml Buffer PE and centrifuged for 1 min. The flow-through was discarded and the spin column was centrifuged for a further 1 min to remove residual wash buffer. The QIAprep spin column was then placed in a clean 1.5 ml microcentrifuge tube. To elute the DNA, 50 µl of elution buffer (EB) were added to the centre of the QIAquick membrane. This was left to stand for 1 min and then centrifuged to collect the product. Presence of the plasmid and determination of concentration was carried out by subjecting 5 µl of eluted purified plasmid to gel electrophoresis (section 2.7). Plasmids were mixed with 50 µl of 1x TE (Appendix A) and stored at -20°C until use.

2.24.3 Plasmid quantitation

Plasmids were quantified using the PicoGreen® dsDNA Quantitation Kit and reagents (Invitrogen, Crawley, UK Molecular Probes, cat. no. P-7589 [kit], P-11495 [reagent]) following manufacturer's guidelines. The method was adapted for quantitation on the Rotor-Gene 3000.

A working solution of TE was made by diluting the 20x TE provided with the kit (100 µl into 2 ml ddH_20) in a sterile 5 ml universal. A working solution of the PicoGreen dsDNA quantitation reagent in DMSO was produced by making a 200-fold dilution (10 µl into 2 ml TE) in a sterile 5 ml universal. The solution was protected from light and used within a few hours of its preparation. To produce a low-range standard curve, the bacteriophage lambda DNA standard provided with the kit at 100 µg/ml was diluted 50-fold in TE, in sterile eppendorfs to make a 2 µg/ml working solution. This was then serially diluted 2-fold in TE as shown in Table 2.3. Each lambda standard dilution was then mixed 1:1 with PicoGreen (25 µl of standard to 25 µl of PicoGreen). This produced a set of 6 standards with a DNA concentration range from 1.562-50 ng as outlined in Table 2.3.

Standard number	Volume (µl) of lambda DNA stock	Volume (µl) of TE	Concentration of DNA	Final amount of DNA in reaction tube (ng)
1	5	245	2 µg/ml	50
2	100	100	1 µg/ml	25
3	100	100	500 ng/ml	12.5
4	100	100	250 ng/ml	6.25
5	100	100	125 ng/ml	3.125
6	100	100	65 ng/ml	1.562

Table 2.3: Production of lambda DNA standard curve for plasmid DNA quantitation using PicoGreen® dsDNA Quantitation Kit

A 1 in 10 dilution of the purified plasmid stock was made in TE (5 µl of plasmid into 45 µl TE) and then a series of four 1 in 2 dilutions in TE was made (25 µl plasmid dilution with 25 µl of TE) in sterile 0.2 ml tubes. Each dilution was then mixed with an equal volume of PicoGreen (25 µl of plasmid dilution to 25 µl of PicoGreen) in sterile flat-lid tubes. These were loaded onto the Rotor-Gene 3000 carousel and were run using the following conditions:

Hold		30°C	5 min
Cycling	8 cycles	30°C	20 s acquiring to FAM

The lambda standards were used to create a standard curve. The appropriate dilution of plasmid whose concentration fell within the standard curve was used to calculate the DNA concentration of the plasmid stock solution.

2.24.4 Plasmid linearisation

Linearisation of recombinant plasmids was carried out using the *Pst I* enzyme (Invitrogen Life Technologies, cat. no. 15215-015). The reaction buffer was diluted 1 part in 10 with ddH_20 and recombinant plasmid was added to the buffer and left to incubate at 37°C for 2.5 h.

2.25 Development of reference strand conformation analysis (RSCA) on the ABI 3100-*Avant*

2.25.1 Preparation of fluorescent labelled references (FLRs)

To create a plasmid stock of D-loop amplicon from which FLR could be continually produced, extracted nucleic acid was first amplified using the primers DloopF and DloopR (Appendix B) in an optimised block-based PCR protocol (Appendix C). The PCR product was monitored by 2% agarose gel electrophoresis (section 2.7), purified (section 2.17) and cloned (section 2.23). The purified plasmid was diluted

in a working solution of 1ng/µl herring sperm DNA (Invitrogen, Paisley, UK, cat. no. 15634-017, stock solution at 10 mg/ml) to a 10^{-6} dilution.

To create the FLR, PCR amplification of an appropriate dilution of the D-loop plasmid (found by experimentation to be 10^{-6}) was carried out as described above, substituting the DloopF primer for DloopFLab (labelled at the 5' end with FAM fluorophore). Products were monitored and purified as described before. The purified FLR was mixed with 50 µl of 10 mM EDTA (Appendix A) to inactivate the polymerase. This was stored at -70°C until required.

2.25.2 Duplex formation

To form duplexes, one microlitre of the FLR was added to a 0.2 ml microtube and mixed with 3 µl of the PCR product (generated using primers DloopF and DloopR as described in section 2.25.1). Samples were then placed in a thermal cycler and denatured at 96°C for 4 min. The temperature was then reduced slowly over a period of 5 min to 55°C and held there for 1 min to facilitate hybridisation of the complementary sense and anti-sense strands. The temperature was then reduced over a period of 5 min to 15°C and held there for 8 min.

2.25.3 Dilution of duplexes prior to RSCA

Following duplex formation, the product required dilution to produce optimum fluorescent signal intensity without 'pull-up' peaks from overloading of sample or low intensity from over-dilution. The optimised dilution protocol required the product to be first diluted 1 in 10 by adding 36 µl of ddH_20 and mixing. Ten microlitres of this dilution were then mixed with 10 µl of ddH_20 and 0.5 µl of 2500

(ROX) GeneScan size standards (Applied Biosystems, Warrington, UK) in a new 0.2 ml tube. The samples were then transferred to a 96-well optical reaction plate, fitted with a genetic analyser septa and loaded into a 96-well autosampler tray (all included in the 3100/3100-*Avant* Genetic Analyser Autosampler Plate kit, Applied Biosystems, Warrington, UK, cat. no. 4316471) and run on the ABI 3100-*Avant* analyser.

2.25.4 Spectral calibration

In this particular application, only two fluorescent dyes were run (FAM for the FLR and ROX on the size standards). The DS-30 (dye set D – 6FAM, HEX, NED and ROX) Matrix Standard Kit was used (Applied Biosytems, Warrington UK, cat. no. 4345827) to create the matrix file. A spectral calibration was performed with DS-30 as described for dye set Z in section 2.20.2 but with 5 µl in 195 µl Hi-Di™ Formamide for DS-30. After correction, the fluorescent intensities are colour-coded and displayed as peaks in the electropherogram which allows the samples and size standards to be distinguished.

2.25.5 Experimental design considerations

Before samples were run on the ABI 3100-*Avant* Genetic Analyser, certain basic design factors had to be considered:

- Fluorescent signal intensity had to be between 150-2000 relative fluorescent units (RFU)
- Optimisation of electrokinetic injection parameters
- Optimisation of electrophoresis conditions e.g. polymer type and run time for accurate detection of all fragments

Extensive experimental work was required to determine the optimal conditions in terms of fragment resolution and fluorescent signal intensity for the RSCA analysis.

2.25.6 Capillary electrophoresis

Samples were run on the ABI 3100-*Avant* Genetic Analyser (Applied Biosystems, Warrington, UK) which was prepared as described in section 2.19. A plate record for fragment analysis was created using the plate editor in the GeneScan application. Each sample was entered into the spreadsheet. The size standard dye colour was kept as the default (red) which corresponds to ROX label being present on the size standards. The appropriate dye set (D) was selected. The appropriate, optimised run module was generated in the Module Editor. All parameters of the run module had been determined experimentally to produce conditions for electrophoresis which produced optimum fluorescent signal intensity, fragment resolution and run time. The following parameters were applied in each run: injection time = 45 s, injection voltage = 2 v, run voltage = 15 v, run time = 3600 s, run temperature = 30°C with POP-6 polymer and a 50 cm capillary array *in situ*. The GS500analysis.gsp module was selected for data analysis and the samples were then run.

2.25.7 GeneMapper analysis

Following electrophoresis, fragment analysis of RSCA data was carried out using GeneMapper® software v4.0 (Applied Biosystems, Warrington, UK). To set up the software for fragment analysis, the analysis settings were configured in the GeneMapper Manager. The 'basic' peak detection algorithm was selected and 50 rfu was selected as the user-specified minimum peak height for all of the dyes. The

fragment sizes of the GeneScan-2500 ROX internal size standards (ISS) were entered into the size standard editor of the GeneMapper Manager, as a new size standard. The fragment sizes for this set of standards are shown in Figure 2.3.

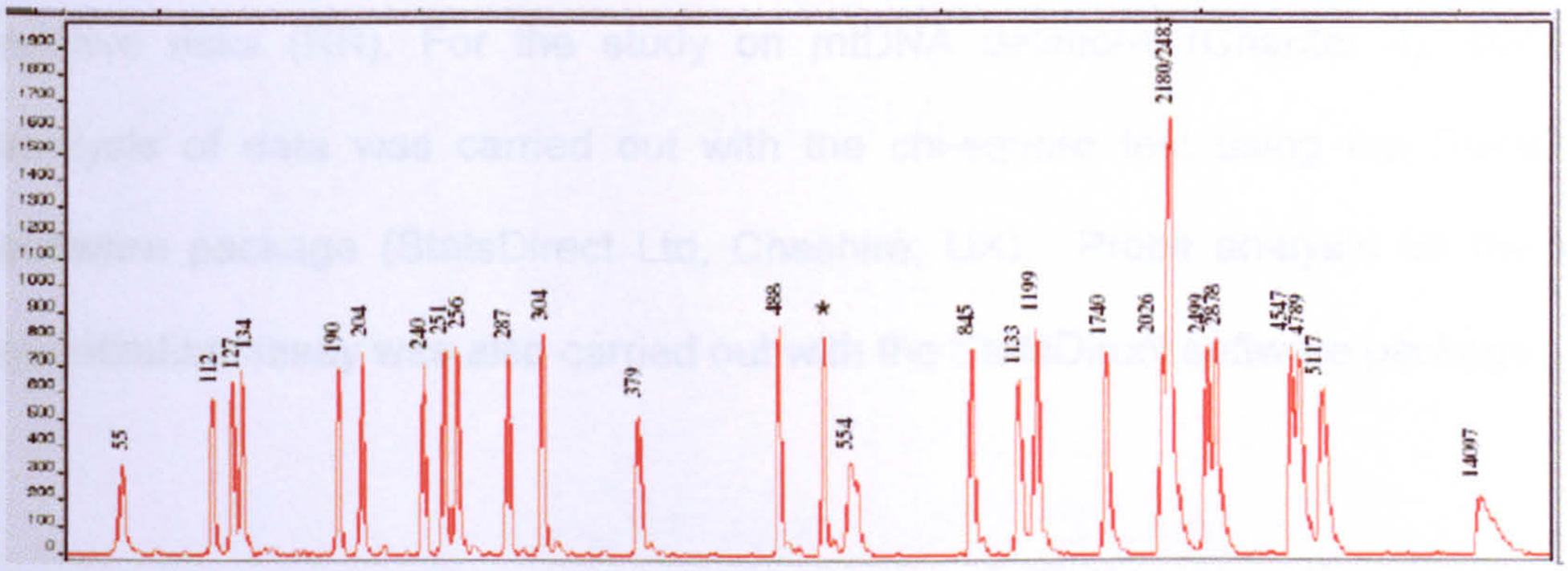

Figure 2.3: Electropherogram of the GeneScan-2500 size standards run under non-denaturing conditions. An * for the 508 bp peak denotes a peak result from abnormal migration. This peak should not be used to size samples. Taken from the GeneScan Reference Guide p5-17. (Applied Biosystems, 2000).

Following electrophoresis, sample data was imported into a new project on the software. The configured analysis method and size standards were selected. The samples were then analysed. The sample sizing quality was assessed and the peak assignments for any low quality samples was checked in the Size Match Editor and altered if necessary. The plots were displayed which enabled visualisation of the internal standards and the fragments for each sample. The migration of each fragment could be determined by the mobility value which was recorded in a sizing table for each detectable fragment.

2.26 Statistics

For the HCV clearance study, detailed statistical analysis was carried out using the SPSS statistical analysis software (SSPS Inc, Chicago, IL, USA). Mutlivariable regression analysis was performed using STATA® data analysis and statistical software (StataCorp LP, Texas, USA), using the Binreg Command to obtain relative risks (RR). For the study on mtDNA deletions (Chapter 4), statistical analysis of data was carried out with the chi-square test using the StatsDirect software package (StatsDirect Ltd, Cheshire, UK). Probit analysis for the HCV quantitation assay was also carried out with the StatsDirect software package.

CHAPTER THREE

Molecular Diagnosis/Monitoring of HCV Infection

3.2 HCV Genotyping

3.3 HCV Subtyping

3.4 HCV Quantitation

3.5 HCV Clearance Study

3.1 Overview

The increasing incidence of HCV and the resulting demand for diagnostic techniques has led to the need for rapid, sensitive and accurate methods for HCV quantitation and genotyping. Due to the potential high number of mild cases of HCV, the recent extension of the original NICE guidance by the re-named National Institute for Health and Clinical Excellence recommends that, in addition to those with moderate to severe HCV infection, patients diagnosed with mild chronic HCV should also be offered treatment (NICE, 2006). This has put further pressure on laboratories for high–throughput diagnostic techniques to support clinical practice.

The requirement for HCV isolates to be genotyped was recognised in 2004 with the publication of NICE guidance (NICE, 2004, 2006) which recommended that treatment of moderate to severe chronic HCV (and more recently for mild disease) in people over the age of 18 years should be tailored according to genotype. The gold-standard for HCV genotyping is nucleotide sequencing followed by phylogenetic analysis (Robertson *et al*, 1998; Simmonds *et al*, 2005). The 5'UTR which is highly conserved yet displays genotype-specific motifs is the preferred target (Germer *et al*, 1999). Sequencing is, however, labour-intensive and time-consuming, reducing its value in a high-throughput laboratory.

HCV genotype may also be an indicator of whether an individual is able to spontaneously resolve HCV genotype without treatment. Spontaneous viral clearance occurs in around 25% of infected individuals (Micallef *et al*, 2006). Early studies have suggested that genotype 3 infections are more likely to clear, with genotype 1 infections more likely to proceed to chronicity (Lehmann *et al*,

2004; Hwang *et al*, 2001). However, a recent study has indicated that individuals with HCV genotype 1 infections are more likely to clear the infection than those with non-1 types (Harris *et al*, 2007).

Although identification of HCV isolates at the subtype level is not yet a requirement for patient management, HCV subtyping is not merely of academic interest. It can have applications in the study of HCV evolution, epidemiology and outbreak/transmission investigations. The possibility of an association between subtype 1b, progression to chronicity and its refractory nature with regards to treatment, means that the ability to distinguish subtype 1b from non-1b subtypes could be a valuable tool in the future. Attempts have been made to use the 5'UTR for subtyping purposes, with limited success. This region is simply too conserved to have the necessary discriminatory power for subtype determination. Attention has therefore turned to other regions of the HCV genome, with the NS5b region being a prime target, due to its variability.

Real-time PCR has become increasingly important in the diagnostic laboratory and promotes itself as the best platform to provide assays necessary for the diagnosis and management of patients with HCV infection. Recent advances in probe technology include the addition of 3' minor groove binding (MGB) groups and the incorporation of locked nucleic acids (LNA). These modifications stabilise the template probe hybrid and have allowed the design of shorter probes which are highly sequence-specific over small regions and therefore ideal for genotyping assays. The ever-increasing array of fluorescent labels for these probes, along with the evolution of multi-channel, real-time DNA amplification systems, permits the design of multiplex, rapid and relatively inexpensive genotyping/subtyping assays.

Detection and quantitation of HCV viral load is important both in diagnosis and clinical management of HCV. Commercial PCR-based tests are expensive and so the development of in-house assays is advantageous. HCV can circulate in low titres in infected individuals; therefore the lower detection limit (~500 IU/ml) of some commercial kits can give rise to false-negative results with serious implications for virus transmission. False-negative results can also occur as a result of degradation of nucleic acid or inhibitors within the serum sample. An internal control (IC) is a vital component of nucleic acid amplification assays to detect false-negative results. It can be added at the extraction stage and is co-amplified with the sample. If the IC cannot be detected, this demonstrates a problem with the assay/sample which can then be re-extracted and re-tested.

3.1.1 Aims

The primary aim of the research described in this chapter was to develop an HCV diagnostic/monitoring service to support clinical practice, using the latest real-time PCR technology. These assays would need to be rapid, to provide good turn-around times in a high through-put laboratory and inexpensive for the service to be competitive. High speed and low cost could not be at a detriment to accuracy and reproducibility. The main targets were:

- to develop a real-time PCR HCV genotyping assay, capable of detecting all the currently circulating genotypes in the region of the UK covered by the hepatology service
- to develop a real-time PCR HCV quantitation assay complete with an IC, to accurately determine HCV viral load whilst removing the possibility of releasing false-negative results

- to develop an assay for the accurate subtyping of HCV isolates to provide a useful tool for epidemiological studies and transmission investigations
- to apply these techniques to elucidate the role of HCV genotype in the spontaneous clearance of HCV from certain infected individuals.

3.2 Development of an HCV genotyping assay

The HCV Taqman genotyping assay described herein was developed as a novel technique for identifying the four most common HCV genotypes seen in the UK (1-4). This assay has been improved continuously and updated. The progress of this evolution to the highly specific, accurate and sensitive method now used routinely in our diagnostic laboratory is detailed.

3.2.1 HCV genotyping primer selection and probe design

A BLAST database search (http://www.ncbi.nlm.nih.gov/BLAST) of the 5'UTR was carried out to produce a sequence databank of well characterised isolates from each of the 6 genotypes (Table 3.1). These sequences were aligned using MegAlign software (Section 2.22). The PCR primers HCV3 (NCR4) (Garson *et al*, 1990) and HCV4 (OKA1) (Okamoto *et al*, 1990) (Appendix B) have been reported previously. These primers target highly conserved regions of the 5'UTR, produce a 259 bp amplicon and were selected for their robustness. These primers had been in long-term use within the laboratory for qualitative HCV detection in a block-based nested-PCR and had been found to be highly specific and sensitive (laboratory data). As a result of the analysis of the aligned sequence data, primer HCV3 was modified slightly for improved

amplification of all genotypes (a T→G and a G→A change, in the 5' proximal third of the primer sequence) (Appendix B).

Genotype	Accession Number
1	1aAF011752, 1aAF00055302, 1aD29815, 1aD29817, 1aY10150, 1bAF483269, 1bAJ006336, 1bAJ238799,1bD31603, 1bD45867, 1bD45870, 1bD45871, 1eL38349, 1fL38350
2	2aD31604, 2aD31605,2aD45875, 2aL29462, 2bAB030907, 2bAF057147, 2bAF057148, 2bAF057149, 2bD29816, 2bD31606, 2bD45877, 2bD45878, 2bD45879, 2bL29464, 2cAF041329, 2cL29465, 2cL38319
3	3aAF057151, 3aAF057152, 3aAF057153, 3aAJ006318, 3aAJ006323, 3AJ006331, 3bD49374, 3gX91421
4	4aAF057154, 4aAF057155, 4AJ006324, 4aY11604, 4U33432, 4U81284
5	5aY13184, 5L29585, 5L29612
6	6aY12083, 6U33431

Table 3.1: Accession numbers of the reference sequences used for HCV genotyping primer and probe design. All accession numbers are preceded by the HCV subtype. All reference sequences are available in the Entrez Nucleotide database at http://www.ncbi.nlm.nih.gov/sites/entrez.

The sequence alignment was then utilised to design probes for genotypes 1-4 by looking for genotype-specific motifs within this region (Figure 3.1). Initially, seven type-specific probes were designed, two each for genotypes 1, 2 and 3 and one for genotype 4 (Appendix B and Figure 3.1) using the recommendations for probe design (Innis and Gelfand, 1990) outlined in section 2.14. In brief, all probes:

- had a Tm of around 5-10°C higher than that of the primers
- avoided the placement of a G at the 5' end
- used the DNA strand which gave the probe more Cs than Gs

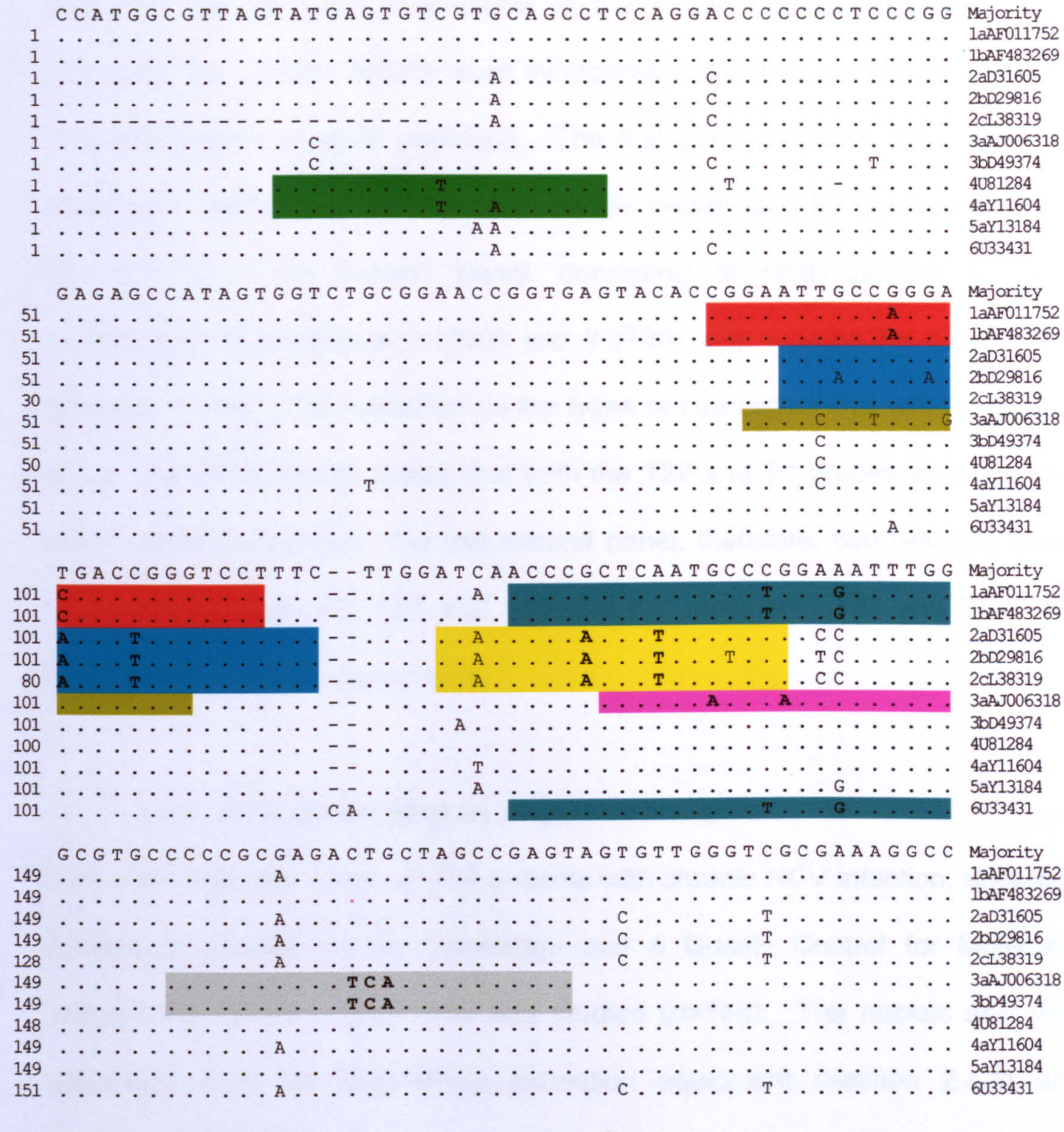

Figure 3.1: Alignment of the PCR target sequences (devoid of primer sequences) of representatives of the six major HCV genotypes displaying the site and context of each of the seven Taqman probes designed for HCV genotyping. Dashes indicate complete identity with the majority sequence. Probe sites are block shaded within their respective sequences, notated with their accession numbers prefixed by the genotype number/subtype. The 100% identity of genotype 6 with probe T11 is also highlighted. The complete sequence for each probe is given in Appendix B. *The NCT333 probe is incorporated into the improved Taqman genotyping assay described later in the chapter. In the original genotyping assay the T22 and T4 probes were both labelled with FAM and the panel was carried out as two separate Rotor-Gene runs.

Each probe was labelled with a specific fluorescent dye at the 5' end (FAM, Cy5, ROX or JOE) and a quencher at the 3' end (Tamra, BHQ-2 or NFQ) (Appendix B). These probes were incorporated into two panels for detection and confirmation of each genotype. The first panel included two probes for genotype 1 detection (T1, T11) and a single probe each for genotypes 2 (T2) and 3 (T3). The second panel, consisting of MGB probes, provided confirmation of genotypes 2 (T22) and 3 (T33) and a probe for detection of genotype 4 (T4). The restriction on the types of fluorescent dye which could be put on the MGB probes meant that both the T22 and T4 probes were labelled with a FAM fluorophore. For the second panel, therefore, two reaction mixes were needed, one with T22 and T33 and the other with T33 and T4 which required two separate assay runs.

3.2.2 HCV genotyping by sequence analysis

HCV RNA from the serum of 154 patients with chronic HCV infection, attending hepatology out-patients in Cambridge and 4 Quality Control for Molecular Diagnostics (QCMD) specimens was studied (n=158). The nucleic acid was extracted using the MagnaPure extraction equipment (Section 2.4.1) and reverse-transcribed to produce cDNA (Section 2.11). Amplification of the 5'UTR took place using the HCV3 and HCV4 primers using a qualitative LightCycler-based technique (Section 2.12.2.2 and Appendix C). PCR products were retrieved from the glass capillaries and purified (Section 2.17). The purified PCR products were sequenced using the HCV3 and HCV4 primers separately (Section 2.21). The sequences were trimmed and aligned using MegAlign software (Section 2.22). Genotype was determined through both phylogenetic analysis using the reference databank and examination of the sequence data for the characteristic genotype specific motifs, according to the classification

proposed by Simmonds *et al* (1993). Quantitation of HCV RNA (viral load) was carried out using the RealArt HCV^{TM} RG RT PCR reagents (Appendix C). Among the genotypes determined by sequencing, 78 (49%) were genotype 1, 18 (11%) genotype 2, 47 (30%) genotype 3, and 10 (6%) genotype 4. For two samples, the heterogeneity of the sequence data indicated mixed infection with more than one genotype, with insufficient clarity to identify the involved genotypes. Three samples failed to be amplified, the viral load of these were very low (<1000 IU/ml).

3.2.3 Rotor-Gene optimisation

A selection of cDNA preparations from HCV isolates of known genotype were used to optimise reaction conditions for real-time HCV genotyping on the Rotor-Gene 3000 DNA Analyser (Corbett Research). Optimisation of the assay was carried out as described in section 2.16 to ensure optimum sensitivity and specificity with no probe cross-reaction. Each panel of probes was optimised separately and reaction conditions for each panel are outlined in Appendix C.

3.2.4 Sequence-based genotyping vs. Taqman genotyping

All of the samples which had been genotyped by sequencing were subsequently genotyped using the Taqman method and results compared. Concordant results were obtained for 77/78 (99%) of the genotype 1 isolates. All of these isolates were positive with both the FAM and Cy5 probes. One genotype 1 isolate was negative in the Taqman assay, but this had a very low viral load (1,095 IU/ml). Results for genotype 2 were concordant with sequencing in 17/18 (94%) of isolates. One genotype 2 isolate (3770) was negative with both panels in the Taqman assay. This had an undetectable viral load with the RealArt quantitation assay.

With regards to genotype 3, the Taqman assay was concordant with sequencing in 43/47 isolates (91%). One isolate (2242) was negative with both panels. Analysis of sequence data demonstrated that this isolate had neither the motif for T3 or T33 probe hybridisation having reverted to the consensus sequence at both sites (Figure 3.2). This isolate had proven very difficult to genotype by sequencing, as the data were difficult to analyse. A BLAST database search using the sequence data from isolate 2242 matched it with HCV isolate JK055 (acc no D49756) (100% identity). This was an isolate from Indonesia, classified as a genotype 3k (Tokita *et al*, 1996).

Another isolate (2216) was negative only with the first panel. Sequence data analysis revealed that the specific T3 motif had altered from TCA to CCG (Figure 3.2). A further isolate, (4886) negative with both panels, was shown upon sequence analysis to have both the necessary genotype 3 motifs. This isolate had a very low viral load (1127 IU/ml) which may explain the failure of the Taqman assay.

```
Consensus  AAT GCC CGG AAA TTT GGG CGT GCC CCC GCG AGA CTG CTA G
Genotype 3 --- A-- -A- --- --- --- --- --- --- --- --- TCA --- -
T3 probe                                   --- --R --- TCA --- -...
T33 probe  --- A-- -A- --- --- --
2242       --- --- --- --- --- --- --- --- --- --- --- --- --- -
2216       --- A-- -A- --- --- --- --- --- --- --- --- -C- --- -
```

Figure 3.2: Sequence data, around the sites of the genotype 3 probes, from isolates 2242 and 2216, which could not be assigned genotype with the Taqman HCV genotyping assay. The consensus sequence is shown along with a typical genotype 3 isolate and the probe sequences for the genotype 3 probes (T3 and T33). Isolate 2242 lacks both the T3 and T33 probe-binding motifs. Isolate 2216 has the T33 probe-binding motif but has two base pair mismatches with the T3 probe-binding motif. Nucleotides identical to the consensus are indicated with a '-'. R = A or G

Isolate 4252 was detected with both the T3 and T11 probes but was negative with all other probes including T33. Sequencing analysis identified this isolate as subtype 3b and confirmed it lacked the T33 specific binding motif, consistent with the known reference subtype 3b sequence (Figure 3.3; acc no D49374). Genotype 3b isolates only contain one mismatch with the T11 probe which explains the observed cross reaction and shallow curve, devoid of a true exponential rise seen with the T11 probe for this isolate.

```
Consensus  AAT GCC CGG AAA TTT GGG CGT GCC CCC GCG AGA CTG CTA G
Genotype 3 --- A-- -A- --- --- --- --- --- --- --- --- TCA --- -
T3 probe                                   --- --R --- TCA --- -...
T33 probe  --- A-- -A- --- --- --
4252       --- --- --- -G- --- --- --- --- --- --- --- TCA --- -
T11 probe  --- --- T-- -G- --- --
```

Figure 3.3: Sequence data, around the sites of the genotype 3 probes, from isolate 4252, which could not be assigned genotype with the Taqman HCV genotyping assay. The consensus sequence is shown along with a typical genotype 3 isolate and the probe sequences for the genotype 3 probes (T3 and T33). The T11 (genotype 1) probe sequence data is also shown to demonstrate the mismatch of 4252 with this probe. Dashes indicate nucleotides identical to the consensus. R = A or G.

No Taqman probe in the first panel had been designed to detect genotype 4. However, it was seen that 6/10 (60%) of the genotype 4 samples were positive for Cy5 but not FAM, differentiating them from genotype 1 isolates. This trait was observed probably as a consequence of genotype 4 isolates having only two mismatches with the T11 probe (Figure 3.1). Genotype 4 isolates share exact sequence identity to genotype 3b at this site; therefore, as with the genotype 3b, cross-reaction occurred. Sequence data for the T11 probe site was examined to ascertain why only 60% of the genotype 4 isolates cross-reacted. No explanation in terms of sequence or viral load arose to account for these findings. Genotype 4 isolates could be distinguished from genotype 1 isolates as they were positive with only one of the two genotype 1 probes (Cy5). Moreover, curves with this probe were also distinct from that seen with

genotype 1 isolates as they were shallow without a true exponential rise (Figure 3.4). This could be used as a probable marker for genotype 4 detection.

The other four genotype 4 isolates were negative with the first panel of Taqman probes. All (n = 10) of the genotype 4 isolates were positive with the T4 MGB probe. Interestingly, 2 of the 10 were QCMD samples and represented the genotype 4 sequence (Figure 3.1, acc no U81284) containing a single mismatch (A–G) with the T4 MGB probe, demonstrating that the probe could tolerate this single mismatch found in some genotype 4 isolates. Reassuringly, no cross-reaction was observed with any of the type 1 isolates which would contain two mismatches with this probe.

(A) Panel one - Genotype 1 probe T11

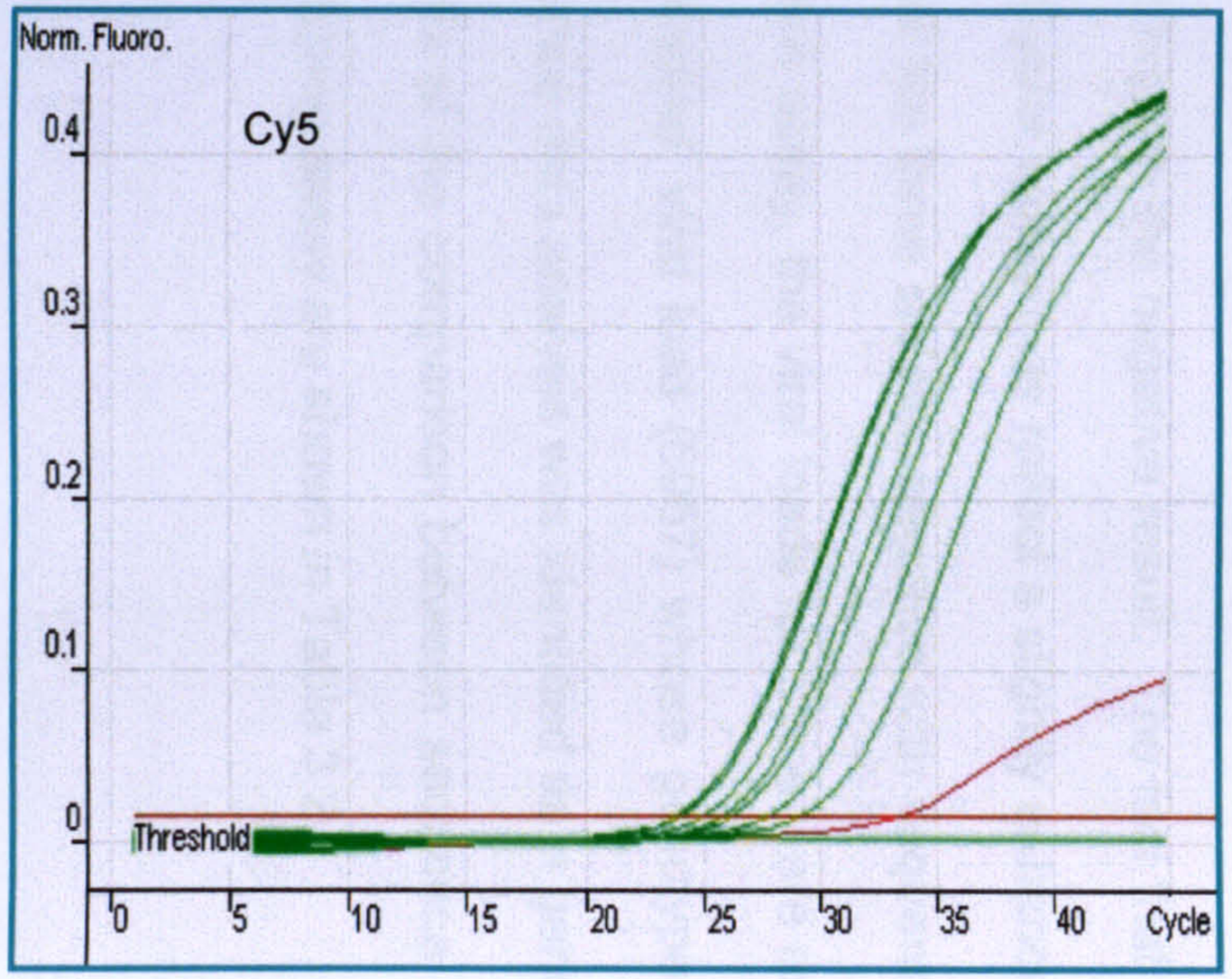

(B) Panel two – Genotype 4 probe T4

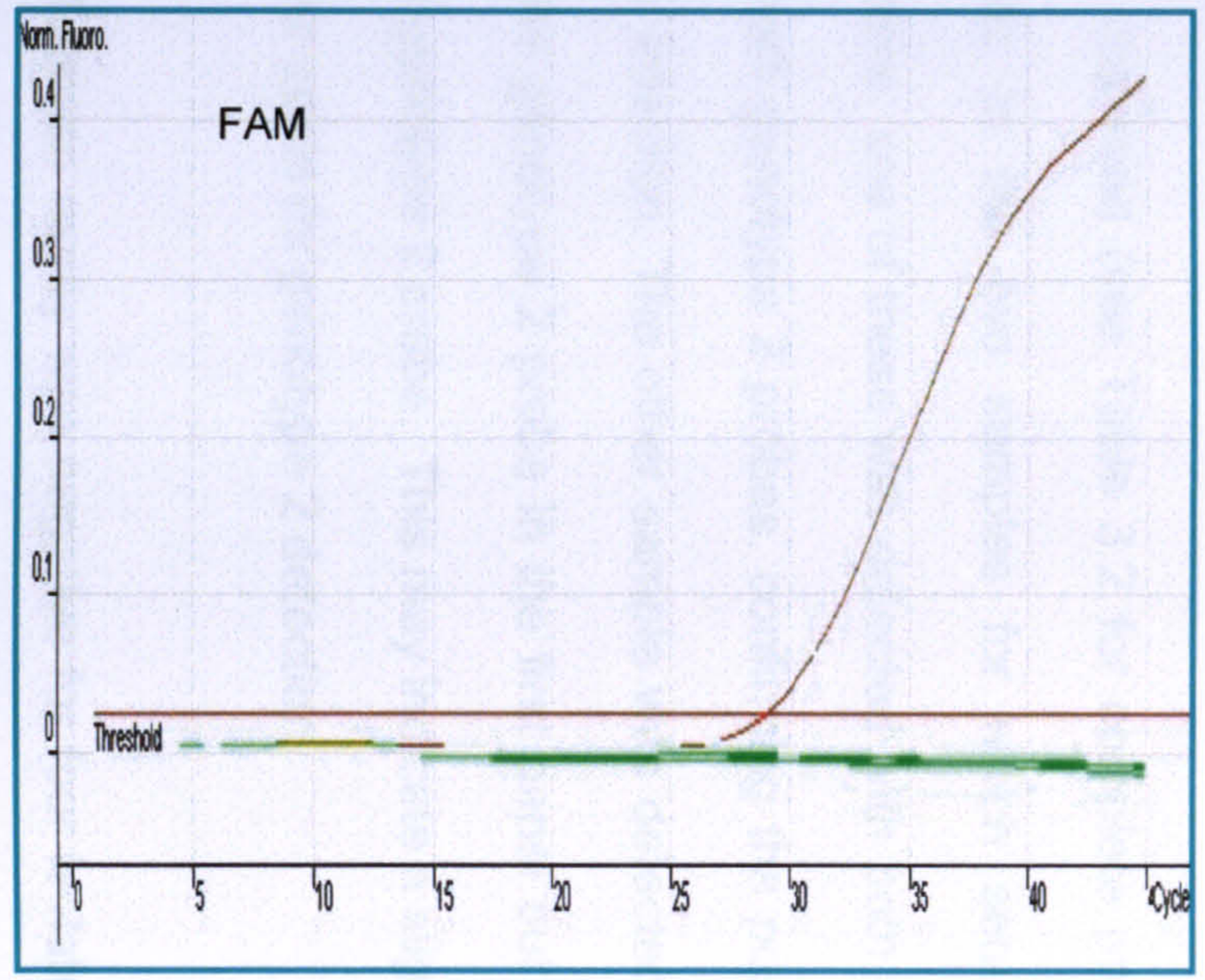

Figure 3.4: The genotyping trait observed in 60% of genotype 4 isolates. The Rotor-Gene graphs show a selection of genotype 1 isolates (green) and a genotype 4 isolate (red). (A) The genotype 4 isolate demonstrates a non-exponential curve with the genotype 1 probe T11(Cy5) in panel one. The genotype 1 isolates demonstrate true exponential curves with this probe. (B) The genotype 4 isolate demonstrates a true exponential curve with the genotype 4 probe T4(FAM) in panel two. The genotype 1 isolates are negative with this probe.

With the exception of the few cases outlined above, the sequence data confirmed the presence of the expected sequence motifs for all the designed probes in all the other isolates and no other unexpected probe cross reactions were observed (see Table 3.2 for complete probe patterns observed). With regards to the two samples for which sequencing had indicated mixed infections, one of these was detected with both type 1 probes in the first panel and both genotype 2 probes, confirming the possibility of a mixed genotype 1 and 2 infection. The other sample was detected with both genotype 1 probes and the genotype 2 probe in the first panel but was negative with the second panel genotype 2 probe. This may indicate a slight reduction in sensitivity of the second panel for genotype 2 detection.

The Taqman assay was negative for four isolates (one each of genotype 1, 2 and two genotype 3) genotyped successfully with the LightCycler. They all had very low viral loads (1095, undetectable and 1127 IU/ml respectively), which could explain the negative result. The fact that they could be amplified with the LightCycler assay may reflect a slightly enhanced sensitivity of the latter assay. Two of the three isolates negative with sequencing were also negative with the Taqman assay, the viral loads for these were extremely low. A sample with an 'undetected' viral load (6957) whose genotype could not be ascertained with sequence data analysis was identified as a genotype 1 with the Taqman assay. Results of the comparison between sequence analysis and the Taqman HCV genotyping assay are shown in Table 3.2.

No of isolates (ID)	Sequence Result	Taqman Result	Probe Patterns						
			T1	T11	T2	T3	T22	T33	T4
77	Genotype 1	Genotype 1	+	+	-	-	-	-	-
17	Genotype 2	Genotype 2	-	-	+	-	+	-	-
43	Genotype 3	Genotype 3	-	-	-	+	-	+	-
6	Genotype 4	Genotype 4	-	+	-	-	-	-	+
4	Genotype 4	Genotype 4	-	-	-	-	-	-	+
2	Negative	Negative	-	-	-	-	-	-	-
1 (3492)	? Mixed	Mixed 1 and 2	+	+	+	-	+	-	-
1 (5493)	? Mixed	? Mixed	+	+	+	-	-	-	-
1 (6050)	Genotype 1	Negative	-	-	-	-	-	-	-
1 (3770)	Genotype 2	Negative	-	-	-	-	-	-	-
1 (2242)	Genotype 3	Negative	-	-	-	-	-	-	-
1 (4886)	Genotype 3	Negative	-	-	-	-	-	-	-
1 (2216)	Genotype 3	?	-	-	-	-	-	+	-
1 (4252)	Genotype 3b	?	-	+	-	+	-	-	-
1 (6957)	Negative	Genotype 1	+	+	-	-	-	-	-
158									

Table 3.2: Concordance between genotype results for the 158 HCV isolates assigned genotype via sequenced-based and Taqman genotyping assays. The HCV Taqman assay probe pattern for each of the isolates is shown. Non-concordant results (n=7, 4.4%) are indicated in red type.

3.2.5 Improvements to the Taqman HCV genotyping assay

Following optimisation of the genotyping assay and incorporation into routine use, failings of the Taqman genotyping assay were identified and four major improvements/additions to the original protocol were made:

3.2.5.1 Positive controls

A limitation of the original Taqman genotyping assay was the absence of positive controls for each genotype. This is important to detect false negatives due to probe breakdown or user error when setting up the assay. During the initial development of the assay, stored HCV cDNA from previously identified genotype 1, 2, 3 and 4 isolates were included in every run as positive controls for each probe. However, these could not be stored long-term due to cDNA degradation and were not always available for the less common genotypes (2 and 4). Positive controls were created by isolating the PCR product of a high titre positive for each genotype; purifying it (Section 2.17) and producing

plasmid clones of this region (Section 2.23). The plasmid DNA was purified (Section 2.24.2) and quantified for each genotype (Section 2.24.3). A dilution of plasmid for each genotype, which was sufficiently high to be consistently detected, but not to pose a contamination risk was included with each panel on each run. Plasmid stock was prepared for long term storage at -20ºC (Section 2.24.1).

3.2.5.2 New T22 probe

Subsequent to the initial development of the genotyping assay, the advance in probe technology meant that an LNA® probe with a Cy5 attachment became available. In the original assay, panel two could not be carried out as a single run as the probes for genotypes 2 and 4 were both labelled with a FAM fluorophore. A new Cy5-labelled T22 LNA probe was designed (Appendix B). This was identical in sequence to the original T22 probe, but had LNA additions incorporated at conserved positions within the probe. This was tested against a panel of isolates previously identified as genotype 2. This probe could successfully detect all genotype 2 isolates. The probe was incorporated into panel two and tested against a set of genotype 2, 3 and 4 isolates to ensure that the reaction conditions were adequate for the new probe, no cross-reaction with other probes occurred and to ensure that there was no loss of sensitivity of the panel. As a result of this new probe, the HCV Taqman genotyping assay was streamlined with a reduction from three to two assay runs per test. The second panel now contained probes for genotype 2 and 3 confirmation and for genotype 4 detection with no compromise to the assay.

3.2.5.3 New NCT333 probe

Routine genotyping using the original assay identified three isolates that were negative with the T3 (panel one) probe but positive with the T33 (panel two) probe. Sequence analysis identified that these isolates had no mismatches with the T3 probe. It was therefore thought that the failure of the T3 probe was due to a stronger stringency and reduced sensitivity with panel one.

Since a spare channel (ROX) was available with panel two and due to the high number of genotype 3 isolates seen in our region (around 46%), it was decided to design a further genotype 3 probe (NCT333) which would act as a confirmatory probe if T3 was negative. The reference databank was interrogated for a further genotype 3 specific motif in the 5'UTR. A putative motif was identified (Figure 3.1) and a Taqman probe, NCT333, labelled with a ROX fluorophore was designed (Appendix B). This probe was tested against all genotype 3 isolates identified during assay development and it detected each of them, including those that were negative with the T3 probe. The probe was incorporated into panel two and tested against a set of genotype 2, 3 and 4 isolates to ensure that the reaction conditions were adequate for the new probe and to ensure that no loss of sensitivity or cross-reactivity occurred with the other probes. The new probe was found to have no effect on the efficiency/specificity of panel two as all isolates were correctly genotyped with no loss of sensitivity.

3.2.5.4 Additional probe – NS53

With the original assay, several HCV isolates failed to be correctly genotyped as they were positive with the panel one T3 probe but negative with the panel two T33 probe (and subsequently found also to be negative by the new NCT333

probe). Sequence analysis determined that these isolates lacked the specific probe-binding motifs of the T3 and NCT333 probes whilst maintaining the T3 probe-binding site. A BLAST database search, with the generated sequence data, indicated that these isolates were subtype 3b which indeed lacked panel two genotype 3 probe-binding motifs (Figure 3.5).

```
Consensus          TCA ATG CCC GGA AAT TTG G
T33                --- --A --- A-- --- --- -
Subtype 3b         --- --- --- --- --- --- -


Consensus          CCC GGT CAT CCC GGC AAT TC
NCT333             --- --- --C --- A-- G-- --
Subtype 3b         --- --- --- --- --- G-- --
```

Figure 3.5: Mismatches occurring with subtype 3b isolates at the T33 and NCT333 probe-binding sites. Nucleotides identical to the consensus are indicated with a '-'. The NCT333 probe is on the reverse strand and it is this sequence that is indicated.

The relative infrequency of this probe pattern result indicated that subtype 3b was not commonly observed. However, to ensure complete coverage of the genotyping assay for all observed subtypes, especially with the high prevalence of genotype 3 within our region, it was deemed prudent to design a further genotype 3 probe to identify subtype 3b isolates specifically. This would remove the need to undertake sequencing of these isolates. No further genotype 3 specific motifs were available in the 5'UTR, therefore, attention was shifted to the NS5b region. This is amplified using the subtyping primers (NS5bF2 and NS5bR) described further in the subtyping section (3.3). Using a sequence alignment of reference sequences of the NS5b region from genotype 3 isolates (see Table 3.3 and Figure 3.6), a probe was designed around a genotype 3-specific motif in the NS5b region. There were no suitable motifs

that were specific for subtype 3b isolates and so the probe was designed to detect all subtypes of genotype 3. This probe, NS53, was labelled with a ROX fluorophore (Appendix B). Reaction conditions for this additional probe were optimised using a panel of genotype 3 isolates, including subtype 3b isolates. A subset of isolates of non-3 genotype was also tested to check for probe cross-reaction. The fully optimised reaction conditions are given in Appendix C. This probe would be utilised to confirm an isolate as genotype 3 in the absence of a confirmed genotype 3 probe pattern with panels one and two.

Subtype	Accession Number
3a	AJ291256, AY003970, D17763*, D28917*
3b	AF279121, AY443346, AY443347, AY515261, D49374*

Table 3.3: Accession numbers of the reference sequences used for the design of the NS53 probe. All reference sequences are available in the Entrez Nucleotide database at http://www.ncbi.nlm.nih.gov/sites/entrez.
* indicates full-length genome.

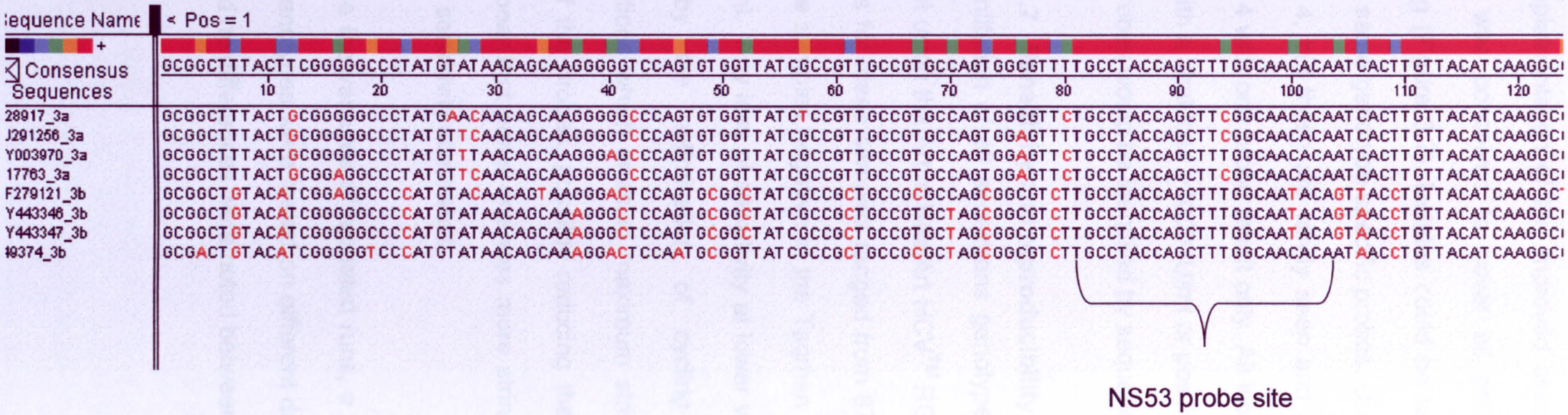

Figure 3.6: Design of the NS53 probe at a conserved site within the NS5b region of genotype 3 isolates. Degenerate nucleotides were incorporated at the two sites where degeneracy occurred. Note that the NS53 probe is on the reverse strand.

3.2.6 HCV genotyping algorithm

To aid implementation of the improved assay into routine diagnostic use, an algorithm was conceived to cover all permutations seen in routine HCV genotyping (Figure 3.7). Isolates could be assigned a genotype if positive by two of the same genotype-specific probes. Only a single probe was available for genotype 4, but these are rarely seen and could be considered a confirmed genotype 4 with one probe result only. All isolates which were negative with all probes, with a viral load >1000 IU/ml or positive with non-concordant genotype-specific probes would be identified by sequence analysis.

3.2.7 Sensitivity and reproducibility

HCV quantitation of all specimens genotyped using the Taqman assay was carried out using the Artus RealArt HCV^{TM} RG RT PCR reagents (Appendix C). Viral loads for these samples ranged from 872 to 21,920,463 IU/ml. The viral load of the samples negative in the Taqman assay ranged from undetected to 6053 IU/ml. Any loss of sensitivity at lower viral loads was likely to have been caused by the optimisation of cycling temperature and magnesium concentrations which enabled maximum stringency and minimal non-specific binding of the probes, possibly reducing the sensitivity. From the results, it would appear that panel one was more stringent than panel two which would reduce its sensitivity somewhat.

To analyse the variance of repeated runs, a selection of isolates from each of the four genotypes were tested on different days. Every sample could be typed clearly and no differences were noted between results on the respective days.

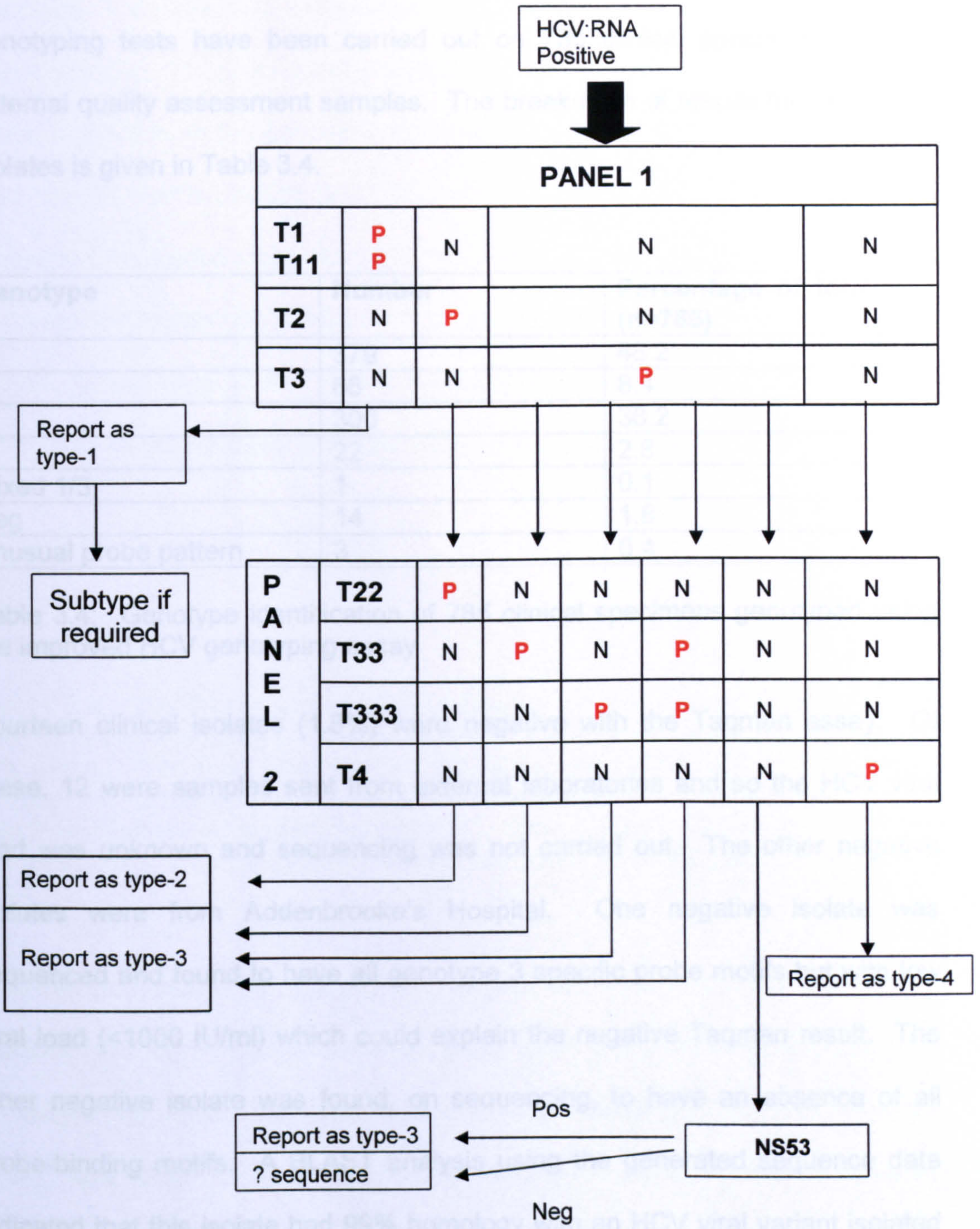

Figure 3.7: An algorithm for Taqman HCV genotyping. All isolates can be assigned a genotype if positive by two of the same genotype-specific probes (except for genotype 4 which has a single probe). All isolates negative with all probes, with a viral load >1000 IU/ml and all isolates giving ambiguous probe results would be identified by sequence analysis. P; positive, N; negative.

3.2.8 Incorporation of the improved Taqman HCV genotyping assay into routine use

Following its modifications, the improved Taqman HCV genotyping assay was put into routine use in the diagnostic laboratory. To date (May 2008), 809 genotyping tests have been carried out on 785 clinical specimens and 24 external quality assessment samples. The breakdown of results for the clinical isolates is given in Table 3.4.

Genotype	Number	Percentage of total(%) (n=785)
1	379	48.2
2	66	8.4
3	300	38.2
4	22	2.8
Mixed 1/3	1	0.1
Neg	14	1.8
Unusual probe pattern	3	0.4

Table 3.4: Genotype identification of 785 clinical specimens genotyped using the improved HCV genotyping assay

Fourteen clinical isolates (1.8%) were negative with the Taqman assay. Of these, 12 were samples sent from external laboratories and so the HCV viral load was unknown and sequencing was not carried out. The other negative isolates were from Addenbrooke's Hospital. One negative isolate was sequenced and found to have all genotype 3 specific probe motifs but with low viral load (<1000 IU/ml) which could explain the negative Taqman result. The other negative isolate was found, on sequencing, to have an absence of all probe-binding motifs. A BLAST analysis using the generated sequence data indicated that this isolate had 99% homology with an HCV viral variant isolated from Jakarta, Indonesia (JK049, acc. no. D49762.1). This isolate had been classified into a '10a' genetic group, which is now assigned to a subset of genotype 3 (Tokita *et al*, 1996; Simmonds *et al*, 2005).

Three isolates (0.4%) displayed unusual probe patterns with the improved Taqman assay and could not be assigned a genotype, according to the algorithm. Two isolates (15554 and 16284) were found to be positive with both genotype 1 probes and demonstrated a non-exponential curve with the T3 probe in panel one and negative with panel two. These were sequenced and found to have both the genotype 1 probe-motifs and a one basepair mismatch with the T3 probe-binding motif (Figure 3.8). A BLAST analysis using the generated sequence data indicated that these isolates had 98% homology in the amplified region with a subset of 27 subtype 1a isolates. Identical sequence homology was seen at the T3 probe-binding site with these reference isolates which had all been isolated in South America (e.g. acc no AM 400879).

```
Consensus    CCC CGC GAG ACT GCT AGC CGA GT
T3 probe     --- --- R-- -TC A-- --- --- --
15554/16284  --- --- A-- -TC G-- --- --- --
AM400879     --- --- A-- -TC G-- --- --- --
```

Figure 3.8: The T3 probe sequence indicating (in red) the genotype 3-specific motif and the one basepair mismatch of clinical isolates 15554 and 16284 with this probe. The exact homology of clinical isolate 15554 with HCV reference isolate accession number AM400879 (available at http://www.ncbi.nlm.nih.gov/sites/entrez) from South America is also demonstrated. Dashes indicate nucleotides identical to the consensus. R = A or G.

One clinical isolate was negative with all probes with a non-exponential cross-reaction with the T11 (Cy5) probe on panel one. A BLAST analysis, using the generated sequence data, identified this as genotype 5. The HCV Taqman assay was able to assign genotype identity to 98% of clinical isolates. Regarding the 24 external quality assessment isolates, the Taqman genotyping assay successfully genotyped 21/24 (87.5%). The other isolates were negative and were found, on sequencing, to belong to genotype 5.

Concerning the epidemiology in the Eastern region, a breakdown of the 773 clinical isolates successfully genotyped using the improved HCV Taqman genotyping assay and sequencing of discrepant isolates is given in Table 3.5.

Genotype	**Number**	**Percentage of total (%) (n=773)**
1	381	49.2
2	66	8.5
3	302	39.1
4	22	2.8
5	1	0.1
Mixed 1/3	1	0.1
Sex		
Male	490	63.4
Female	259	33.5
Unspecified	24	3.1

Table 3.5: Epidemiology of HCV isolates in the Eastern region

3.3 HCV Subtyping

3.3.1 Description of subtyping assays

With a clear rationale for the need for an HCV subtyping tool, two assays have been developed for this purpose, focussing on the NS5b region. The first is a generic assay which is a non-probe based method using SybrGreen to detect all known HCV subtypes. This method assigns HCV subtype by direct sequencing of a 383 bp NS5b fragment followed by phylogenetic analysis against a databank of reference isolates of known subtype. The second subtyping assay is a Taqman probe-based method which enables subtype 1b isolates to be differentiated from 'non-1b' genotype 1 subtypes.

3.3.2 Primer design and reference databank preparation

To design primers for the subtyping assays, a reference databank of isolates from all common subtypes was prepared by retrieving reference strain sequence data from NCBI and other sources (e.g. Sandres-Sauné *et al*, 2003; Simmonds *et al*, 2005) (Table 3.6). The reference sequences were aligned with the MegAlign software in the DNASTAR Lasergene software package, using the Clustal W method. Primers were then designed which target the most conserved regions of the NS5b gene. Several different primers were tested on a panel of HCV isolates, and the most sensitive, NS5F2 and NSFR, (Appendix B) were selected for use in the subtyping assays. These primers amplify a 383 bp fragment of the NS5b gene. Figure 3.9 shows a subset of the alignment of reference strains used to design the primers, and indicates the conserved nature of the primer sites and the necessity for a certain level of degeneracy within the primers to allow for the known sequence variation in HCV isolates.

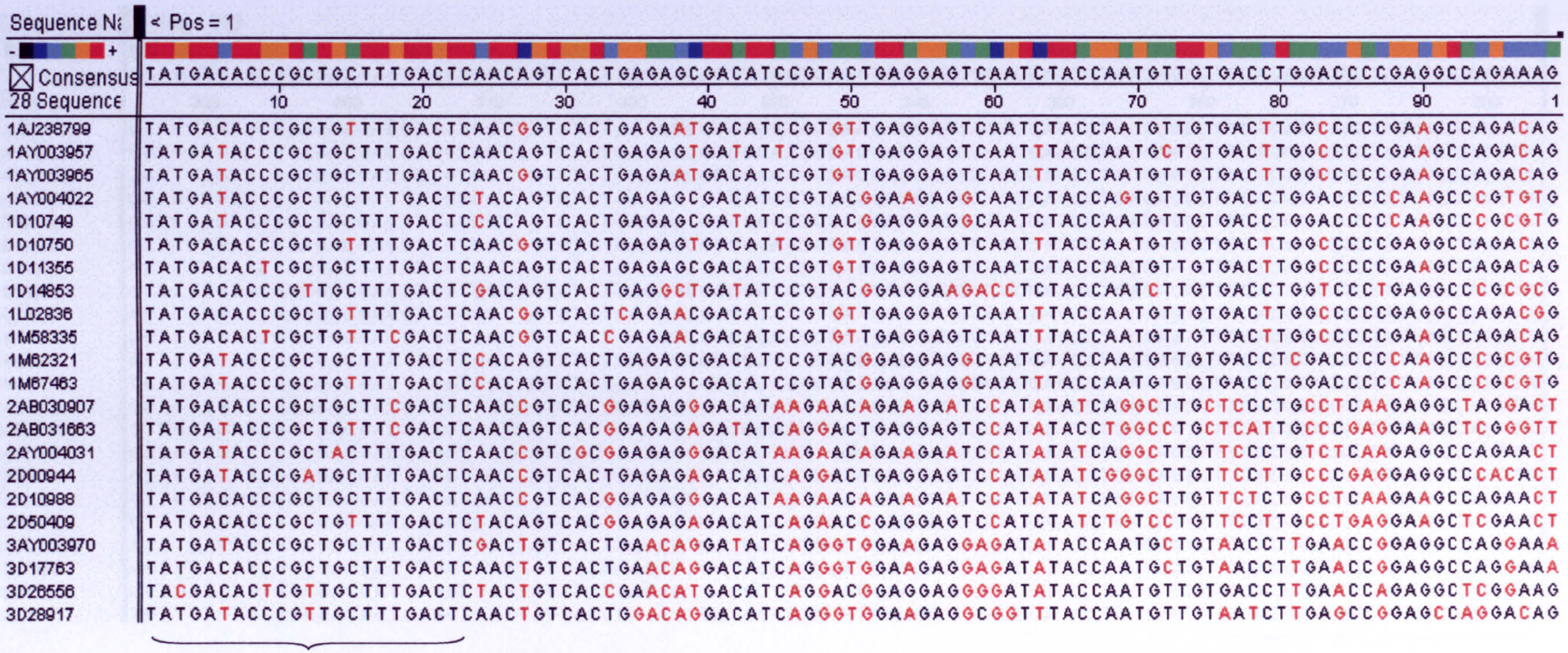

5′ TATGAYACCCGCTGYTTYGACTC 3′

NS5bF2 primer (nt 8256-8278)

Figure 3.9 (continued overleaf): A subset of the alignment of reference sequences used to design the NS5bF2 and NS5bR primer pair for HCV subtyping. Accession numbers of the reference sequences are shown. All reference sequences are available in the Entrez Nucleotide database at http://www.ncbi.nlm.nih.gov/sites/entrez. Nucleotide position is relative to HCV type 1a sequence; acc no M62321. This alignment demonstrates the positioning of the primers in the most conserved regions of the NS5b gene and indicates the necessity for degeneracy within the primer sequences to allow for sequence variation. Y= C or T, R= A or G, N= A, C, G or T.

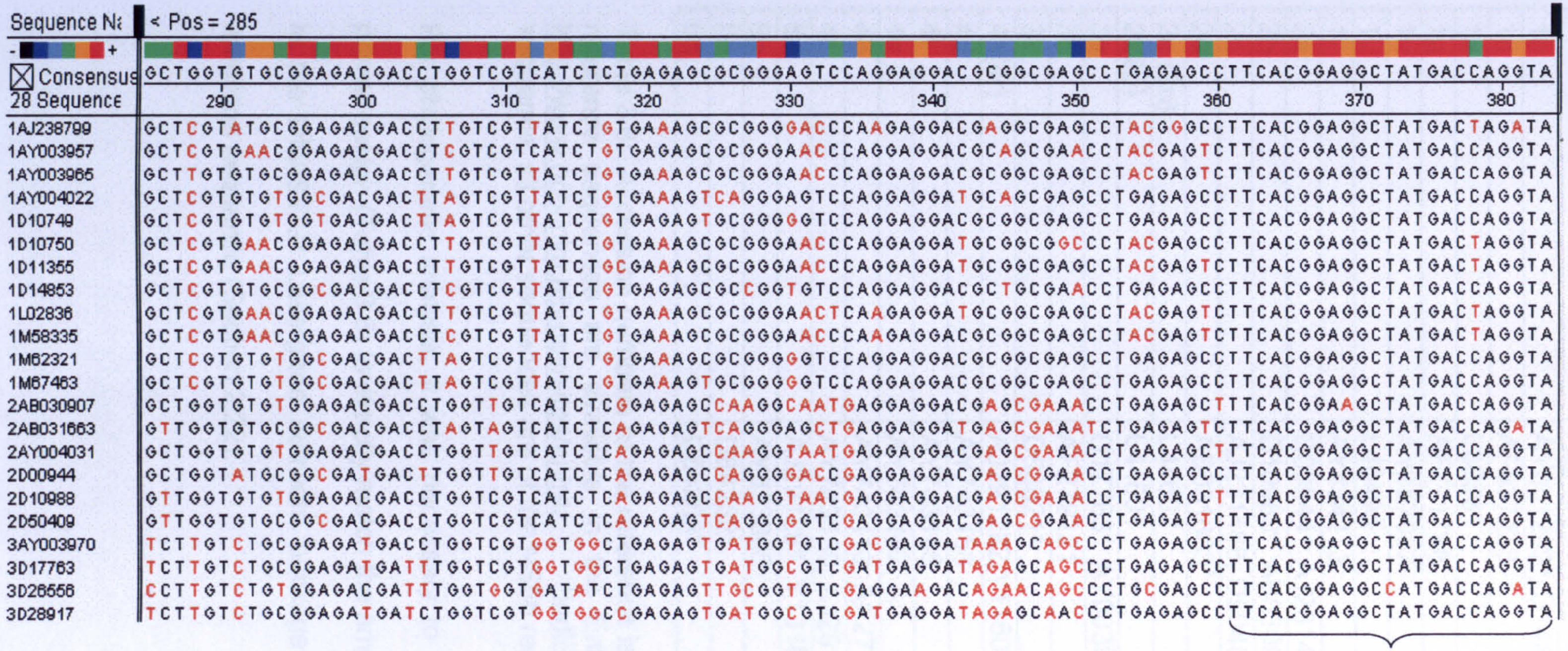

Figure 3.9 continued.

Subtype	Accession Numbers
1a	D10749*, M62321*, AJ291247, AY004022
1b	AY003957, AY003965, AJ291273, AJ238799*, AJ849954, AJ849955, AY003957
1c	AY051292*, D14853*
1d	AF037233
1e	L38361
1g	AF271798
1h	AY257087
1i	L48495
1j	AY434113
2a	D00944*, AJ231479
2b	D10988*, AB030907*
2c	AJ231468, D50409*
2d	AB031663*
2e (2n)	L44602
2f(2p)	L44601
3a	D17763*, AY003970, D28917*
3b	AF279121
3k	D63821*
4a(4r)	AJ291282,Y11604
4d	AY743168
4f	AY743145
4k	AY743167
4o	AY743113, AF271815
4r	AY743159, AJ291282
5a	AJ291281, Y13184*
6a	AY973866
6b	D84262*
6d	D84263*

Table 3.6: Accession numbers of the reference isolates for HCV subtyping. All reference sequences are available in the Entrez Nucleotide database at http://www.ncbi.nlm.nih.gov/sites/entrez. *indicates complete genome sequence, all other sequences are of the NS5b region only.

For phylogenetic analysis, it was necessary to trim the sequences used for primer design (Table 3.6) to exactly match the amplicon (383 bp), using EditSeq in the DNASTAR Lasergene software package to exactly match the target amplicon sequence (Section 2.22).

3.3.3 Generic HCV subtyping assay

To develop the generic HCV subtyping assay, a real-time PCR method using SybrGreen on the Rotor-Gene 3000 was developed to amplify part of the NS5b gene using the NS5F2 and NS5R primers. A subset of cDNA preparations of isolates previously genotyped using the Taqman genotyping assay was selected to optimise reaction conditions. Optimisation experiments included a range of isolates from different genotypes to ensure that the assay was equally sensitive across all commonly seen genotypes (1-4). The fully optimised PCR conditions are outlined in Appendix C.

3.3.4 Evaluation of HCV generic subtyping assay

To evaluate the HCV generic subtyping assay, it was used on 50 isolates which had previously been subtyped using the TRUGENE™ NS5b and the TRUGENE™ HCV 5'NC (which targets the 5'UTR) commercial assays by another laboratory (Visible Genetics, Cambridge). Following amplification with the optimised SybrGreen method, the PCR products were purified (Section 2.17) and sequenced in both directions using the NS5b primers (Section 2.21). The sequence data was trimmed to the correct size (if necessary) and imported into the reference databank in the MegAlign programme (Section 2.22). The sequences were aligned using the Clustal W method. The phylogenetic tree was examined and subtype was assigned according to phylogenetic relatedness to the reference isolates. In the evaluation study, genotype was concordant between all three assays. A comparison of subtyping results between the three assays for 50 HCV isolates is shown in Table 3.7. The 5'NC assay failed to assign subtype for 12 (24%) of samples. These were eleven genotype 1 isolates and one genotype 4 isolate. The TRUGENE™ NS5b assay and the generic HCV subtyping assay were concordant with all subtypes, with

the exception of one isolate which was negative with the generic HCV subtyping assay (subtype 2b, by the commercial NS5b assay), due to poor sequence data. The TRUGENE™ 5'NC assay had two discordant subtyping results, an isolate assigned as subtype 1b was identified as a 1a by both NS5b assays and a subtype 2a isolate by the 5'NC assay was a 2b by the NS5b assays. Two isolates failed to be amplified by both of the NS5b assays. These were identified as a 1a and a 3a by the 5'NC assay.

Genotype/subtype	Commercial assays		In-house assay
	TRUGENE™ 5'NC	TRUGENE™ NS5b	Generic HCV Typing
1	11	-	-
1a	13	24	24
1b	6	5	5
2a	2	1	1
2b	4	4	3
2c	-	1	1
4	1	-	-
4a	1	1	1
4d	-	1	1
3a	12	11	11
Neg	-	2	3

Table 3.7: Results from the subtyping of 50 isolates by the commercial TRUGENE™ 5'NC and NS5b assays and the in-house generic HCV subtyping assay. The Trugene NS5b and the Generic HCV Typing assays were concordant with all subtypes, with the exception of one isolate which was negative with the in-house assay. The Trugene 5'NC assay failed to assign subtype for 12 (24%) of samples.

3.3.5 Clinical study

The generic HCV subtyping assay was used on 121 clinical isolates from patients attending the hepatology clinic at Addenbrooke's Hospital, Cambridge. This included 83 males aged between 26-82 years and 38 females aged between 24-72 years. These had been previously genotyped using the HCV Taqman genotyping assay, described in section 3.2. Of these 121 samples, 113 (93.4%) were successfully amplified using the NS5b assay. Eight of the specimens could not be amplified using the NS5b assay. A further four specimens were amplified but produced sequence data of a quality which was too poor to allow phylogenetic analysis. Of the remaining 109 (90.1%) samples successfully amplified and subjected to direct sequencing of the NS5b region, there was 100% concordance with the Taqman assay with regards to assignation of genotype. The NS5b assay classified the 109 specimens into seven different subgroups by phylogenetic analysis. HCV subtype distribution was 1a, 46 (42.2%), 1b, 17 (15.6%), 2a, 4 (3.7%), 2b, 5 (4.6%), 3a, 32 (29.4%), 3b, 2 (1.8%) and 4a, 3 (2.8%). Thus the most prevalent subtypes were 1a followed by 3a then 1b. Figure 3.10 shows an example phylogenetic tree demonstrating the subtyping of unknown clinical isolates.

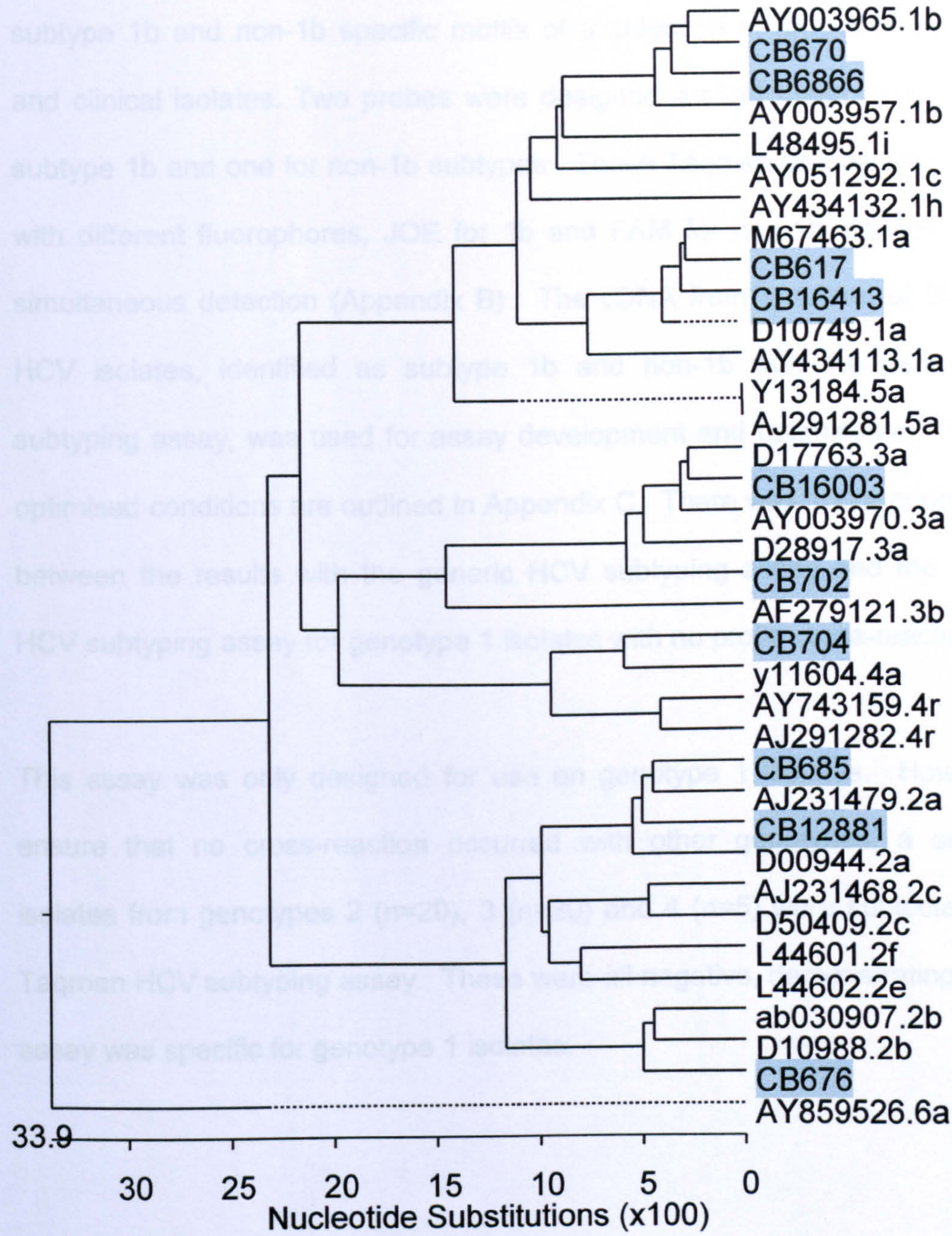

Figure 3.10: An example phylogenetic tree showing a subset of reference isolates used for HCV subtyping. Accession numbers of the reference isolates are shown followed by their subtype assignation. All reference sequences are available in the Entrez Nucleotide database at http://www.ncbi.nlm.nih.gov/sites/entrez. 'Unknown' (clinical) isolates are highlighted.

3.3.6 Taqman HCV subtyping of genotype 1 isolates

To develop an assay for subtyping of genotype 1 isolates, the NS5b reference databank was interrogated to identify subtype 1b and non-1b specific motifs in the region between the NS5bF2 and NS5bR primers. Figure 3.11 shows the subtype 1b and non-1b specific motifs of a selection of reference sequences and clinical isolates. Two probes were designed around these motifs, one for subtype 1b and one for non-1b subtypes. These Taqman probes were labelled with different fluorophores, JOE for 1b and FAM for non-1b isolates to allow simultaneous detection (Appendix B). The cDNA from a subset of 20 clinical HCV isolates, identified as subtype 1b and non-1b with the generic HCV subtyping assay, was used for assay development and optimisation. The fully optimised conditions are outlined in Appendix C. There was 100% concordance between the results with the generic HCV subtyping assay and the Taqman HCV subtyping assay for genotype 1 isolates with no probe cross-reaction.

This assay was only designed for use on genotype 1 isolates. However, to ensure that no cross-reaction occurred with other genotypes, a subset of isolates from genotypes 2 (n=20), 3 (n=20) and 4 (n=5) were subjected to the Taqman HCV subtyping assay. These were all negative, demonstrating that the assay was specific for genotype 1 isolates.

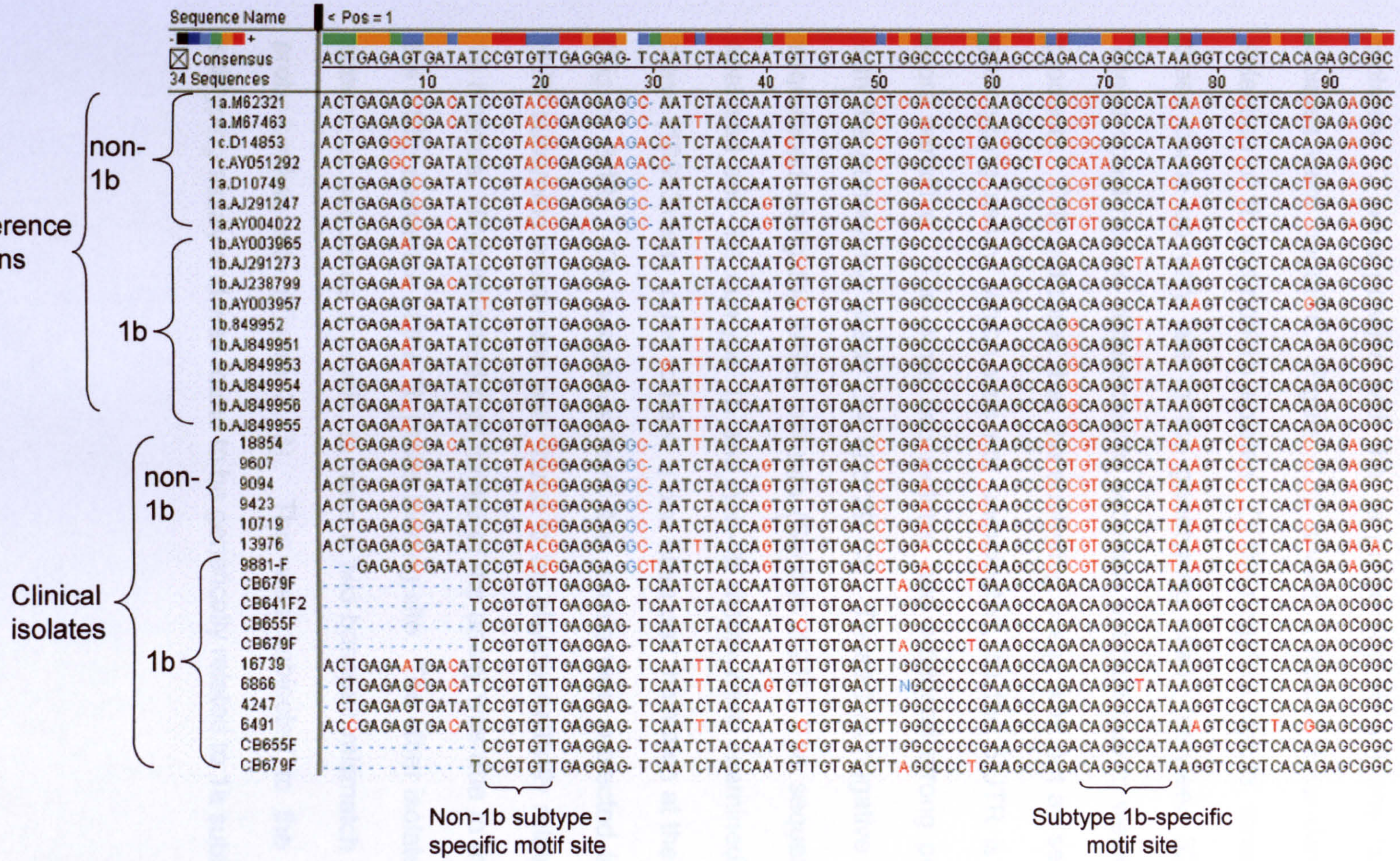

Figure 3.11: A sequence alignment of a section of the HCV NS5b region (nt 8286-8379 relative to HCV type 1a sequence; acc no M62321, available at http://www.ncbi.nlm.nih.gov/sites/entrez) demonstrating the non 1-b and 1b subtype-specific motifs around which the subtyping probes were designed. The alignment shows a number of reference strains (available at http://www.ncbi.nlm.nih.gov/sites/entrez) and sequenced clinical isolates.

3.3.7 Taqman HCV subtyping of clinical isolates

The 1b/non 1b subtyping assay was used to subtype 108 clinical isolates which had been identified as genotype 1 in the Taqman genotyping assay. Of these isolates, 77 were positive with the 1a probe and 26 with the 1b probe. Five isolates were negative. Figure 3.12 shows a typical Rotor-Gene run with a selection of 1b and non-1b isolates. Of the negative results, three out of five of these came up very late in the genotyping assay (between 32 and 35 Ct). These could not be sequenced to ascertain subtype due to weak amplification products. This indicated that the subtyping assay was not as sensitive as the genotyping assay, which was not unexpected, as the 5'UTR is known to be more sensitive. The other two isolates had produced strong positive results with the genotyping assay (24 and 29 Ct). These two negative isolates were sequenced using the NS5b primers (Section 2.21). The sequence data was analysed and the subtype 1b and non-1b motifs were examined. The first of these (16653) was found to have a one base pair mismatch at the 1b probe site (Figure 3.13). The sequence from this isolate was subjected to the generic HCV subtyping assay and was found to be phylogenetically related to subtype 1b isolates. This indicated that failure of the assay was due to the mutation of the NS5b sequence at the 1b probe binding site. The other isolate (13350) was shown, by sequence analysis, to have a two basepair mismatch at the non-1b probe-binding site (Figure 3.13). This was subjected to the generic HCV subtyping assay and was found to be genetically related to 1a subtypes.

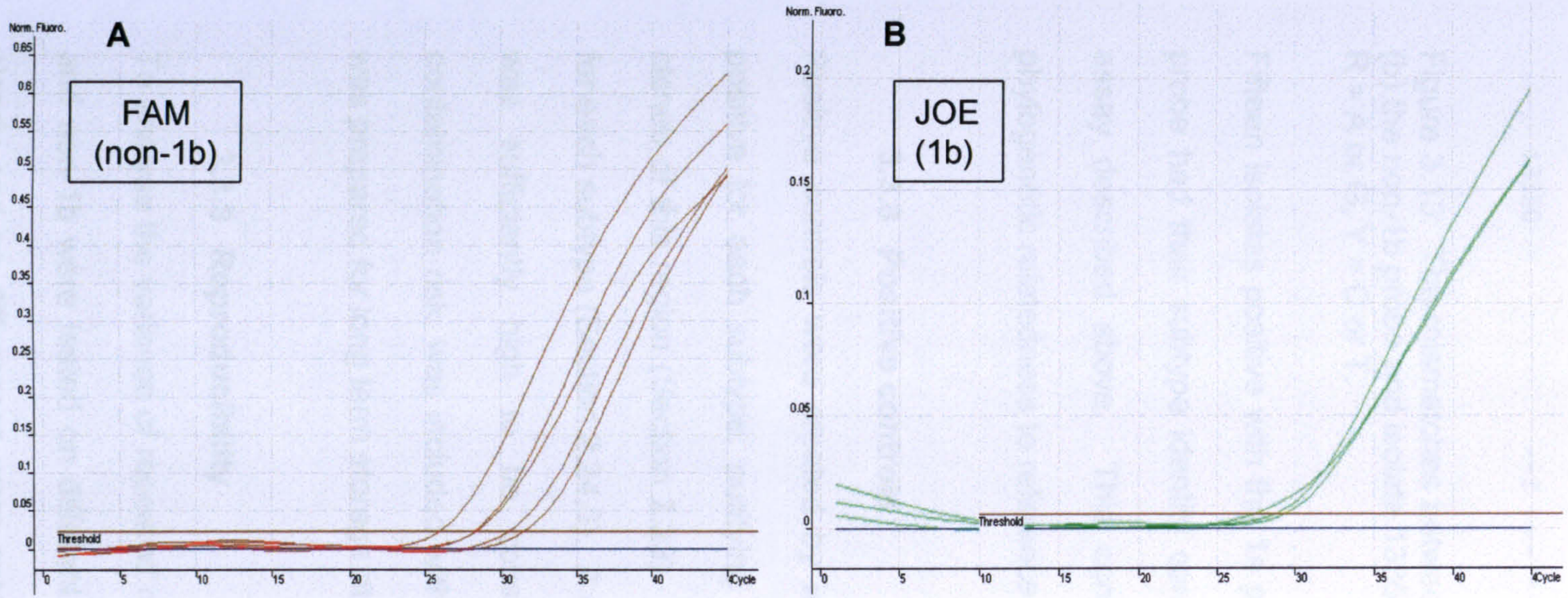

Sample	Ct		Subtype
	FAM	JOE	
3175	-	29.56	1b
18354	-	28.91	1b
5223	-	27.53	1b
3332	30.71	-	1a
5023	31.72	-	1a
4247	28.51	-	1a
6737	26.15	-	1a
16739	28.44	-	1a
water	-	-	negative

Figure 3.12: Rotor-Gene graphs demonstrating a selection of clinical isolates subtyped using the Taqman HCV subtyping assay. Graph A shows five isolates positive with the FAM-labelled non-1b probe. Graph B shows three isolates positive with the JOE-labelled 1b probe. Each isolate is positive with one probe only. Ct; threshold cycle.

a. 1b probe CCG AAG CCA GRC AG

16653 --- -G- --- -A- --

b. Non-1b probe GAY ATC CGT ACG GAG GAG GCA ATC TA

13350 --T --- --- -T- --- --- --- --A -

Figure 3.13: The mismatches between (a) the 1b probe and isolate 16653 and (b) the non-1b probe and isolate 13350. Mismatches are indicated in blue type. R = A or G, Y = C or T.

Fifteen isolates positive with the 1a probe and ten isolates positive with the 1b probe had their subtype identity confirmed using the generic HCV subtyping assay described above. This confirmed the subtype assignation through phylogenetic relatedness to reference strains.

3.3.8 Positive controls

Positive controls were created by isolating the PCR product of a high titre positive for each subtype; purifying it (Section 2.17) and producing plasmid clones of this region (Section 2.23). The purified plasmid DNA was quantified for each subtype (Section 2.24.3). A dilution of plasmid for each subtype, which was sufficiently high to be consistently detected, but to not pose a contamination risk, was included with each panel on each run. Plasmid stock was prepared for long term storage at -20 ºC (Section 2.24.1).

3.3.9 Reproducibility

To analyse the variance of repeated runs, a selection of isolates identified as 1b and non-1b were tested on different days. Every sample could be subtyped clearly and no differences were noted between the results on the respective days.

3.3.10 Use of the NS5b subtyping assays in a possible nosocomial transmission

The advantage of having access to HCV subtyping assays was demonstrated with the occurrence of a possible transmission situation. It was necessary to identify whether nosocomial transmission of HCV had occurred between two individuals. The clinical scenario involved two patients who were admitted to hospital and were being treated in adjacent beds on the same ward. One patient (A) was a known HCV-positive individual. Another patient (B) who was not thought, at the time, to be HCV positive was subsequently found, post-admission to be infected with the virus. Patient B claimed that his/her lifestyle did not leave him/her 'at risk' of HCV and that his/her infection must have been acquired from patient A, whom he/she knew to be HCV positive. This has important medico-legal issues regarding HCV transmission within the hospital setting and could have involved substantial compensation to patient B if nosocomial transmission had occurred. The HCV subtyping (and genotyping) assays were vital to establish the relatedness of the HCV isolates from patients A and B to determine if nosocomial transmission was a possibility. The HCV isolates from both patients were genotyped with the Taqman assay and were found to be genotype 1. The isolates were then subjected to the 1b/non-1b assay and were both found to be non-1b subtype. Finally the isolates were subjected to the generic subtyping assay. Analysis of the sequence data and of the phylogenetic tree indicated that there were 18 nucleotide differences between the two isolates (Figure 3.14). This level of variation (5.14% disparity) indicated that it was highly unlikely that transmission of the virus had occurred between these two individuals.

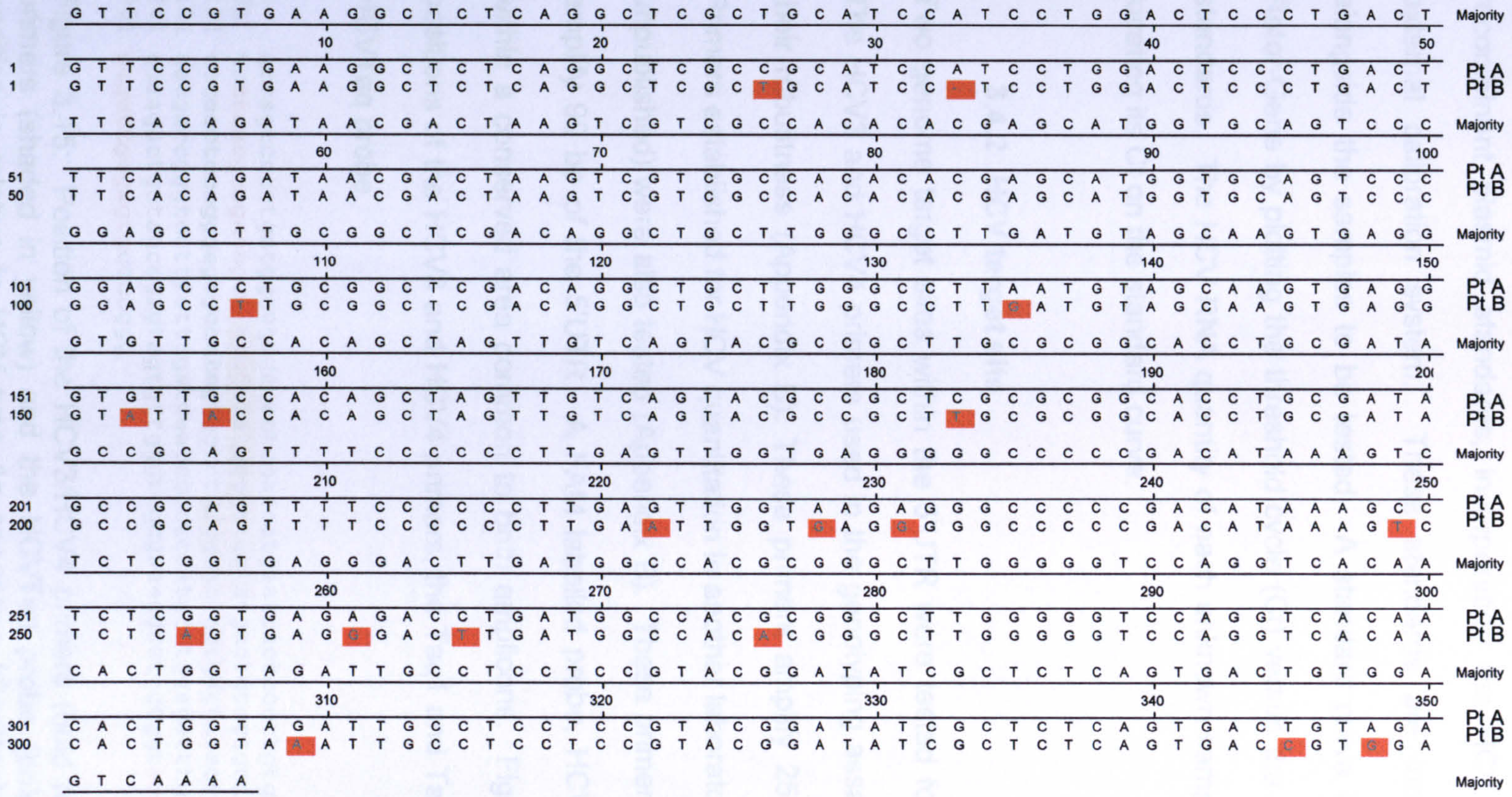

Figure 3.14: Sequence alignment of a region of the NS5b gene (nt 8276-8625 relative to HCV type 1a sequence; acc no M62321, available at http://www.ncbi.nlm.nih.gov/sites/entrez) of HCV isolates from two HCV positive patients, patient A (Pt A) and patient B (Pt B) involved in a possible nosocomial HCV transmission. The sequence data illustrates the 18 nucleotide differences (shaded in red) within the 350 base pair region (5.14% disparity), demonstrating that nosocomial transmission was extremely unlikely. Note that the reverse sequence is shown in this alignment.

3.4 HCV Quantitation

3.4.1 HCV quantitation assay description

An HCV quantitation assay was designed which would use a serial dilution of recombinant plasmid standards, incorporating the HCV target site, as an external calibration system. These standards are included in each run alongside the samples to be tested. A standard curve is generated by the Rotor-Gene by plotting the threshold cycle (Ct) versus the concentration of the standards. The HCV RNA quantity of each unknown sample is determined by locating its Ct on the standard curve.

3.4.2 HCV target site

Two genome target sites within the 5'UTR were tested for HCV quantitation. The HCV3 and HCV4 primers used in the genotyping assay were selected for their robustness (Appendix B). These primers amplify 259 bp of the 5'UTR. Primers established for HCV quantitation in another laboratory (Grant & Garson, unpublished) were also tested (Appendix B). These primers – Taq1 and Taq2, amplify 90 bp of the 5'UTR. A FAM labelled probe, HCVTaq was designed within a conserved area common to both amplicons. Figure 3.15 shows the positions of the HCV3 and HCV4 primers, the Taq1 and Taq 2 primers and the HCVTaq probe.

```
1   gccagccccctgatgggggcgacactccaccatgaatcactcccctgtgaggaactactg
61  tcttcacgcagaaagcgtctagccatggcgttagtatgagtgtcgtgcagcctccaggac
121 ccccccctcccgggagagccatagtggtctgcggaaccggtgagtacaccggaattgccag
181 gacgaccgggtcctttcttggatcaacccgctcaatgcctggagatttgggcgtgccccc
241 gcaagactgctagccgagtagtgttgggtcgcgaaaggccttgtggtactgcctgatagg
301 gtgcttgcgagtgccccggg
```

Figure 3.15: Position of the HCV3/HCV4 primers (bold red font), Taq1/Taq2 primers (shaded in yellow) and the HCVTaq probe (bold black font). The position is relative to HCV type 1a sequence (GenBank accession number M62321). Note the overlap of the HCV4 and Taq1 primer sites.

In a direct head-to-head comparison of twenty clinical samples tested on the same day, the assay generating a shorter amplicon shifted the crossing point an average of 3.4 Ct to the left (SD 2.12 Ct) (Table 3.8), thus showing increased sensitivity. The shorter amplicon was therefore selected for further development.

Sample ID	HCV3 and HCV4 259 bp amplicon	Taq 1 and Taq 2 98 bp amplicon	Ct Variation
	Ct		
6924	22.4	22.1	0.3
7929	27.6	25.2	2.4
8555	26.2	22.1	4.1
8769	25.3	22.7	2.6
6175	26.7	22.9	3.8
6433	22.6	22.1	0.5
5545	22.6	20.8	1.8
9881	26.3	25	1.3
7718	36.9	30.1	6.8
7847	27.4	22.5	4.9
7857	28.5	24	4.5
8938	26.4	22.6	3.8
6193	25.5	21.9	3.6
6484	25.8	20.7	5.1
6525	39.3	31.1	8.2
6080	26.4	25.7	0.7
886	21.9	21.3	0.6
7586	27.3	23	4.3
6026	26.5	22.2	4.3
2202	27.9	24.1	3.8
			Average: 3.4

Table 3.8: A comparison of the threshold cycles (Ct) of twenty clinical samples amplified using primers which generated either a 259 bp (primers HCV3 and HCV4) or a 90 bp (primers Taq1 and Taq2) amplicon from the 5'UTR. The difference in Ct values between amplification with each primer set is shown. This table illustrates that primers Taq1 and Taq2 are superior.

3.4.3 Production and quantitation of plasmid standard

A plasmid standard was created by cloning the 259 bp 5'UTR amplicon, using the HCV3 and HCV4 primers derived from a genotype 4 isolate into the Topo TA vector (Section 2.23). Sequencing, using the M13 primer pair (Appendix B), was carried out to determine that the amplicon had been correctly incorporated into the plasmid (Section 2.21). The plasmid standard was linearised with the *Pst I* restriction enzyme (Section 2.24.4) and serially diluted in polyA for long-term storage. The plasmid was quantified and pinned to the World Health Organisation (WHO) HCV RNA standard (96/798) which has a known titre of $5x10^4$ IU per vial. Triplicates of the WHO standard dilutions (neat to 10^{-3}) were run alongside triplicates of the HCV plasmid standard (Figure 3.16) to quantify each plasmid dilution.

The 10^{-8} plasmid dilution was then repeated ten times in a single run and an average IU calculated (Figure 3.17). The 10^{-8} plasmid was found to have an average of 40,913 IU/ml. The IU of the surrounding plasmid dilutions was then extrapolated from this figure. Plasmids dilutions from 10^{-6} to 10^{-10} were deemed to have a sufficient dynamic range (4,091,300 to 409 IU/ml) to be incorporated into the HCV quantitation assay. These plasmids would be used as standards in each run, along with a positive and negative control. Ten microlitre aliquots of each plasmid dilution were made in polyA and stored at -70°C and thawed before use.

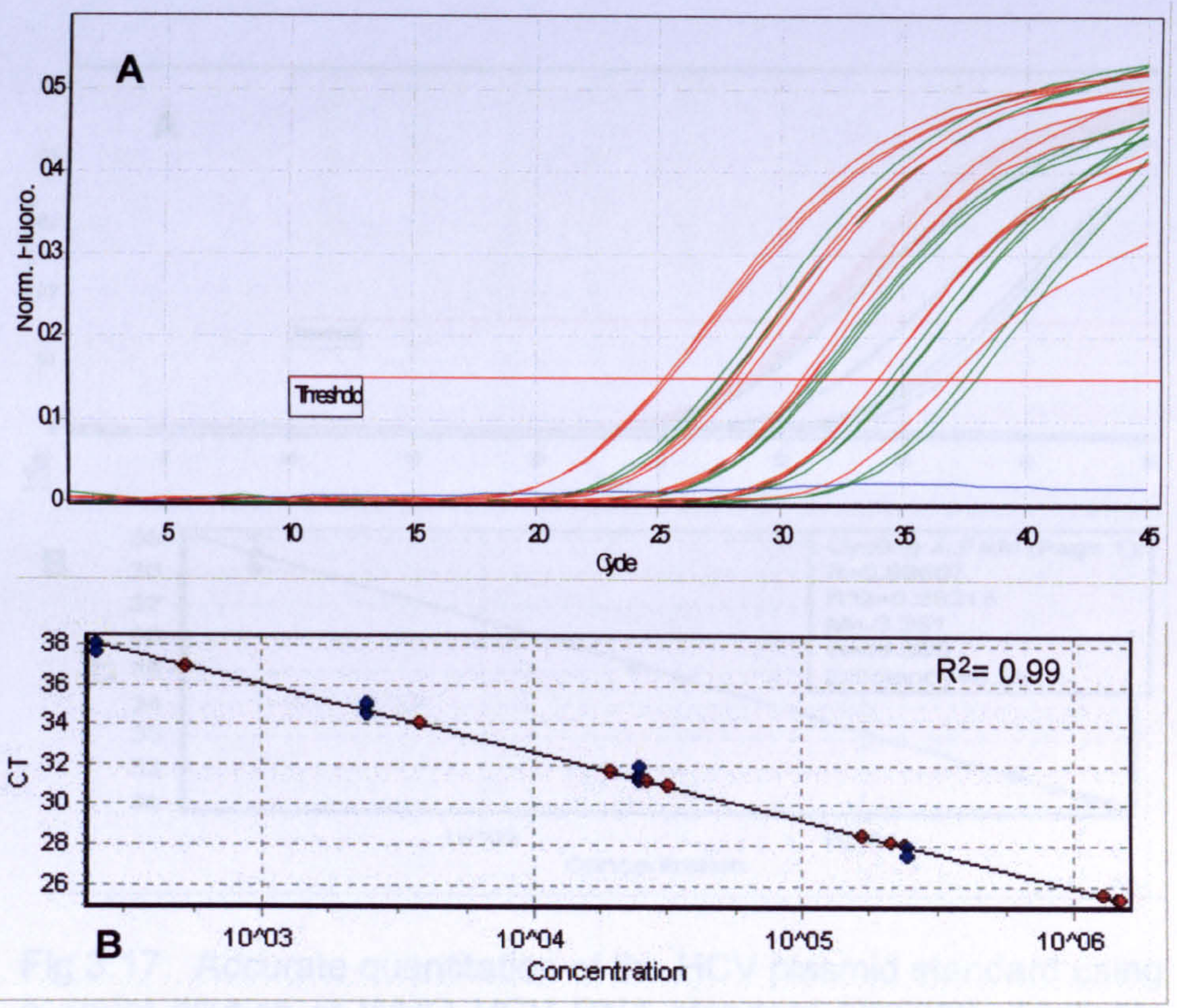

Figure 3.16: Quantitation of the HCV plasmid standard using a serial dilution of WHO HCV RNA standard (96/798). Triplicate dilutions of the WHO standard (green lines on graph A) each with known concentration were used to create a standard curve (B). Triplicate dilutions of the plasmid standards (red lines on graph) were run alongside and were quantified by extrapolation from the standard curve. The R^2 value is an indicator of run efficiency. S; standard, U; unknown.

	Sample	Type	Given Conc (IU/ml)	Calc Conc (IU/ml)
	WHO neat	S	250,000	249,442
	WHO neat	S	250,000	261,146
	WHO neat	S	250,000	344,289
	WHO -1	S	25,000	22,193
	WHO -1	S	25,000	17,238
	WHO -1	S	25,000	19,500
	WHO -2	S	2,500	2,030
	WHO -2	S	2,500	2,766
	WHO -2	S	2,500	1,940
	WHO -3	S	250	255
	WHO -3	S	250	352
	plasmid -6	U		1,513,448
	plasmid -6	U		1,496,856
	plasmid -6	U		1,320,628
	plasmid -7	U		242,788
	plasmid -7	U		217,106
	plasmid -7	U		167,743
	plasmid -8	U		32,156
	plasmid -8	U		26,451
	plasmid -8	U		27,556
	plasmid -9	U		3,848
	plasmid -9	U		3,844
	plasmid -9	U		3,892
	plasmid -10	U		535

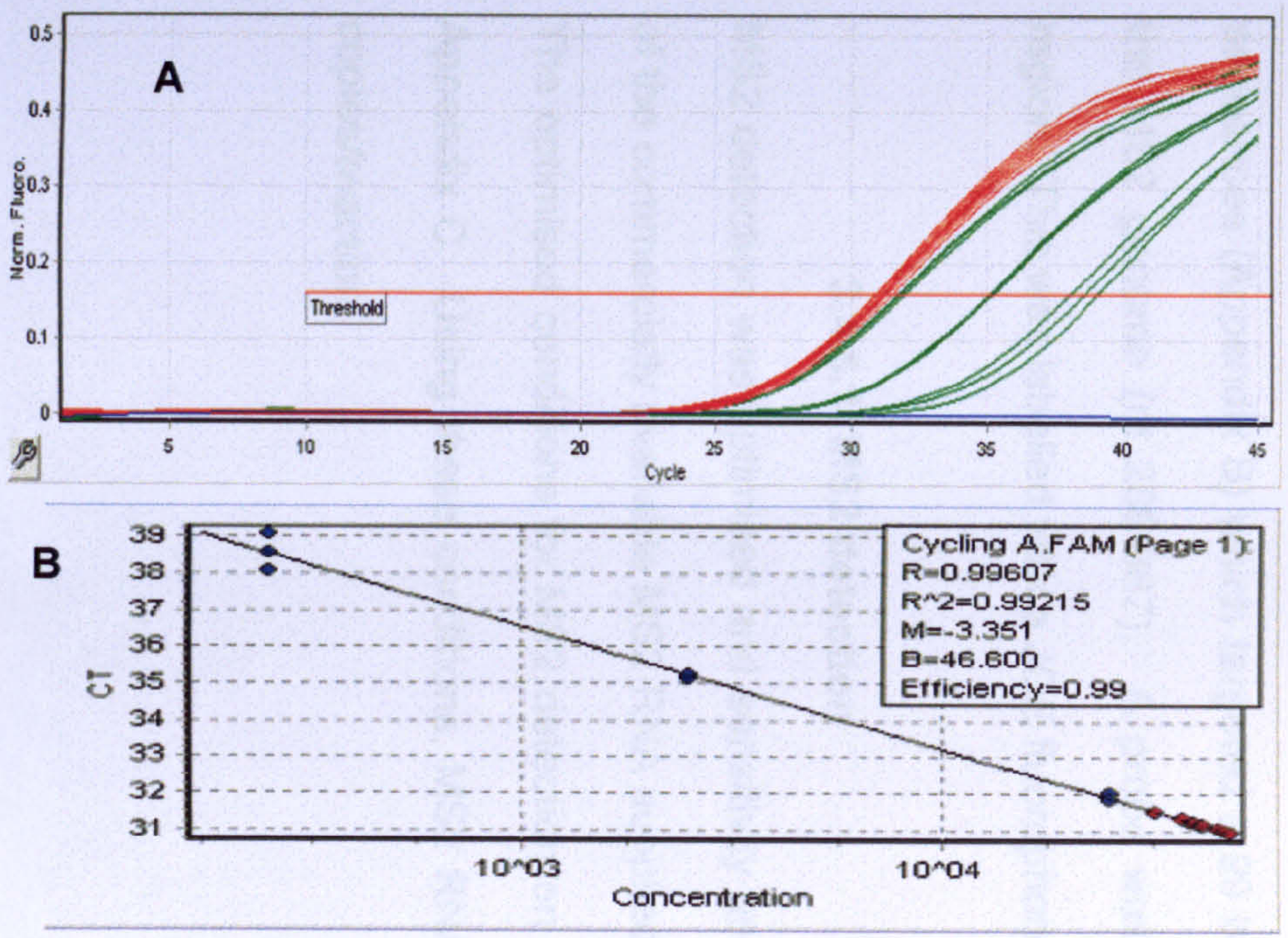

Fig 3.17: Accurate quantitation of the HCV plasmid standard using a serial dilution of WHO HCV RNA standard (96/798). Triplicate dilutions of the WHO standard (green lines on graph A) each with known concentration were used to create a standard curve (B). Ten replicates of the 10^{-8} plasmid standard dilution (red lines on graph A) were run alongside and were quantified by extrapolation from the standard curve. S;standard, U; unknown.

	Sample	Type	Given Conc (IU/ml)	Calc Conc (IU/ml)
	WHO -1	S	25,000	
	WHO -1	S	25,000	
	WHO -1	S	25,000	
	WHO -2	S	2,500	
	WHO -2	S	2,500	
	WHO -2	S	2,500	
	WHO -3	S	250	
	WHO -3	S	250	
	WHO -3	S	250	
	Plasmid -8	U		47,496
	Plasmid -8	U		41,203
	Plasmid -8	U		39,609
	Plasmid -8	U		46,362
	Plasmid -8	U		41,377
	Plasmid -8	U		38,718
	Plasmid -8	U		31,868
	Plasmid -8	U		44,634
	Plasmid -8	U		40,722
	Plasmid -8	U		36,691

3.4.4 HCV quantitation optimisation

To determine the optimal conditions for HCV quantitation (without MS2) the plasmid standards were used in a series of optimisation experiments using the SuperScript™ III Platinum® One-Step Quantitative RT-PCR System. This is a one-step system which incorporates the reverse transcription step, thus removing the need for a separate cDNA preparation step. A serial dilution of a high titre HCV RNA extract was utilised to produce an assay with optimum sensitivity.

3.4.5 MS2 internal control

Sequence data for MS2 was obtained from NCBI (www.ncbi.nlm.nih.gov, accession number NC_001417) and used to design the primer oligonucleotide sequences (Appendix B) which targeted a 99 bp region, close to the 5' end of the MS2 genome (nt 289-387). A probe was designed within the amplified region. This was labelled with a JOE fluorophore (Appendix B).

3.4.5.1 MS2 detection

MS2 detection was optimised and sensitivity ascertained using a serial dilution of the commercially available MS2 RNA supplied at a concentration of 0.8 µg/µl. The optimised conditions for MS2 detection on the Rotor-Gene are outlined in Appendix C. Using these conditions, MS2 RNA could be detected down to 2 copies/reaction.

3.4.5.2 MS2 bacteriophage propagation

From plating assays (Section 2.10.3) the stock solution of MS2 phage was calculated to have $2.3x10^9$ pfu/ml. Using MS2 RNA as standards, the genome copy number was calculated as 9.18 per pfu of stock. Thus the phage stock had an estimated $2.1x10^{10}$ genome copies/ml.

Determination of optimal input of IC per extraction was carried out by producing a 10-fold serial dilution to 10^{-8} of MS2 phage in PBS from the stock solution and adding 20 µl of the lower dilutions (10^{-3} to 10^{-8}) to the extraction tray along with 200 µl of HCV-negative serum prior to MagNAPure extraction (Section 2.4.1). This indicated that 20 µl of a 10^{-5} dilution (in PBS) of stock was the most reliable input per extraction for reproducible MS2 detection. At this dilution, the MS2 was detected at ~27 Ct (Figure 3.18). Below this dilution, the MS2 was detected late, ~31.5 Ct at the 10^{-6} dilution and was detected inconsistently at lower dilutions.

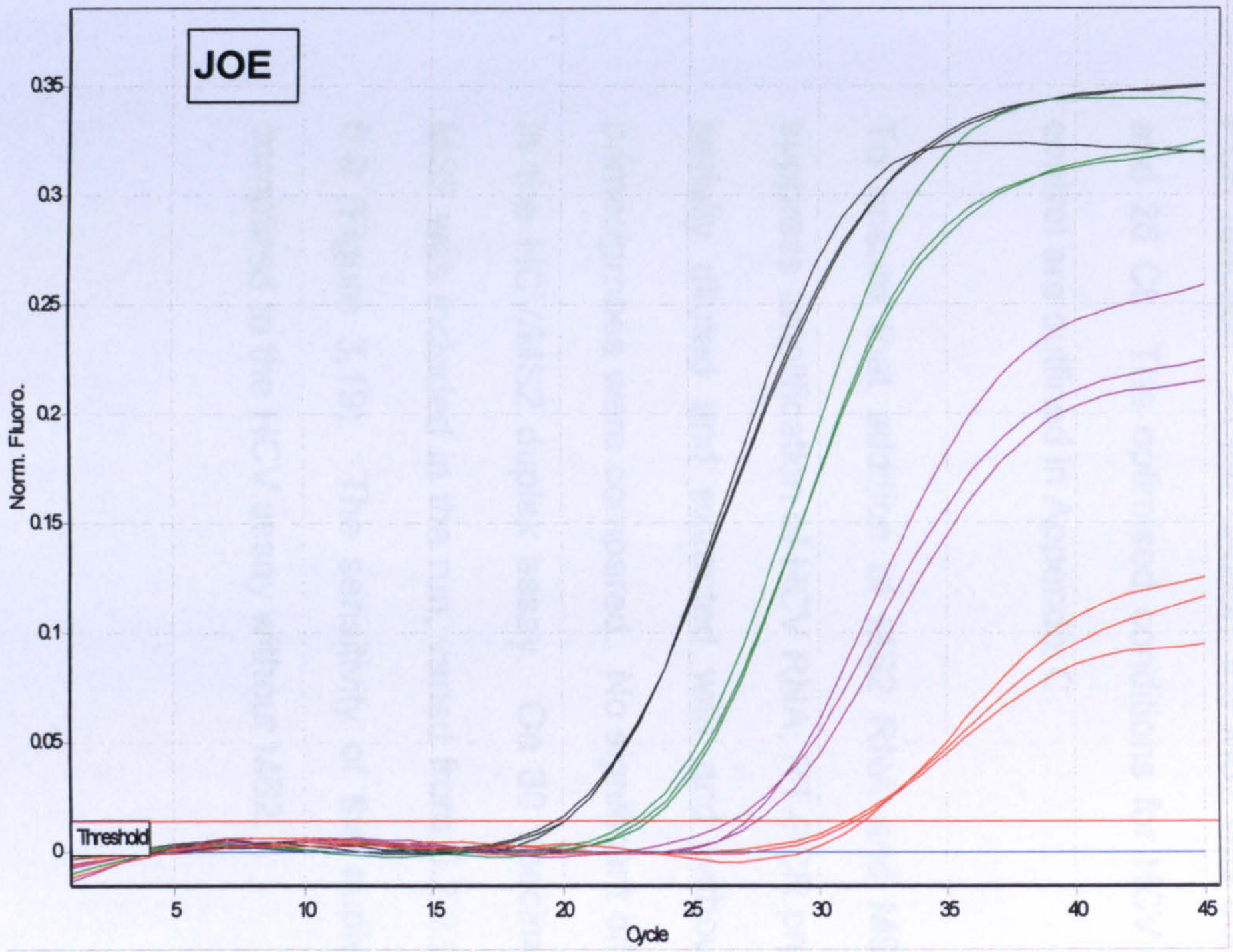

	MS2 dilution	Ct
	MS2 -3	20.07
	MS2 -3	19.77
	MS2 -3	20.08
	MS2 -4	23.43
	MS2 -4	22.78
	MS2 -4	23.14
	MS2 -5	27.19
	MS2 -5	27.56
	MS2 -5	26.57
	MS2 -6	31.17
	MS2 -6	31.44
	MS2 -6	31.76
	Water	negative

Figure 3.18: Determination of optimal input of MS2 internal control per extraction. Twenty microlitres of each MS2 dilution (10^{-3} to 10^{-6}) were added to the MagnPure extraction tray along with 200 µl of HCV negative serum. These were run in triplicate on the Rotor-Gene and detected on the JOE channel, which is shown. Detection was inconsistent below the 10^{-6} dilution.

3.4.5.3 Implementation of MS2 into the HCV quantitation assay

The HCV quantitation assay with internal control was optimised primarily to HCV target detection, to ensure that the sensitivity and amplification efficiency were not compromised by the presence of MS2. The conditions for HCV quantitation were not altered from the optimisation experiments. The primer/probe concentrations for MS2 detection were reduced to the minimum which could consistently detect the MS2 (2 pmol for each primer and the probe). Because the reaction was not optimal for MS2 detection, a higher dilution (10^{-4}) than expected needed to be added to the extraction tray prior to nucleic acid isolation. This equates to 4600 pfu per extraction and, therefore, in the case of a 60 µl elution followed by addition of 5 µl of extract, 383 pfu (3516 copies) per PCR reaction. At this dilution, the MS2 was consistently detected between 24 and 26 Ct. The optimised conditions for HCV quantitation with MS2 internal control are outlined in Appendix C.

To ensure that addition of MS2 RNA and MS2 primer and probes did not suppress amplification of HCV RNA, RT-PCR profiles of clinical serum samples serially diluted and extracted with and without addition of MS2 RNA and primer/probes were compared. No significant difference in viral load was noted in the HCV/MS2 duplex assay. On 30 specimens the difference in Ct when MS2 was included in the run, varied from 0.2-2.39 with an average variance of 0.9 (Figure 3.19). The sensitivity of the duplex assay was not reduced as compared to the HCV assay without MS2.

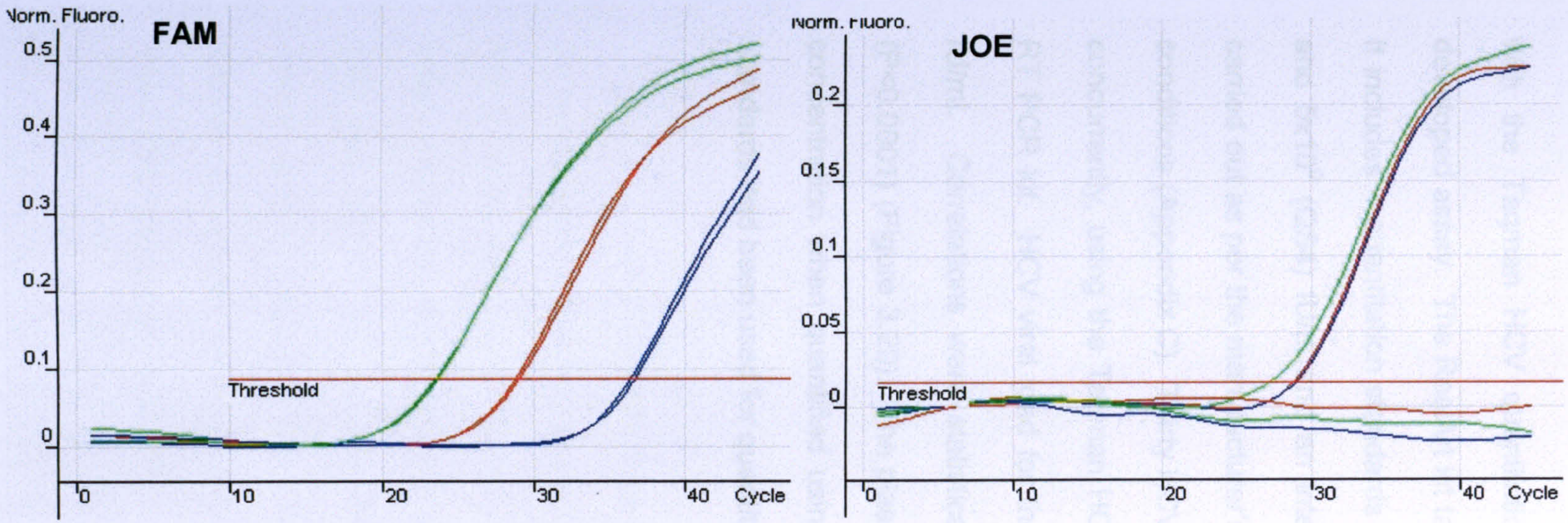

Clinical sample	Ct – FAM channel		Variation
	+ MS2	- MS2	
A	29.02	28.82	-0.2
B	36.39	36.67	+0.28
C	23.66	23.55	-0.11

Figure 3.19: Assessing the effect of addition of MS2 to the HCV quantitation assay. This figure shows three clinical HCV isolates (A, B and C) which were subjected to the HCV quantitation assay with and without the addition of MS2 to the extraction tray and MS2 primers/probes to the master mix. The FAM channel (HCV detection) shows that there is negligible difference in Ct value when each sample is run with or without MS2. This is demonstrated in the table which shows the variation in Ct value for each clinical specimen. The JOE channel shows the detection of MS2 from the clinical samples with MS2 incorporated.

3.4.6 Correlation between the Taqman assay and a commercial HCV RNA quantitation assay

The RealArt™ HCV RG RT PCR kit (Corbett Research) was used in parallel with the Taqman HCV quantitation assay to check the accuracy of the developed assay. The RealArt kit targets a 240 bp region of the HCV genome. It includes 4 quantitation standards of $5x10^3$ (QS1), $5x10^2$ (QS2), $5x10^1$ (QS3) and $5x10^0$ (QS4) IU/µl and an internal control. The commercial assay was carried out as per the manufacturer's guidelines and recommended Rotor-Gene conditions (Appendix C). Thirty HCV positive clinical specimens were quantified concurrently, using the Taqman HCV/MS2 assay and the RealArt™ HCV RG RT PCR kit. HCV viral load for the specimens ranged from 72 to 6,539,133 IU/ml. Correlations were statistically significant between these two assays ($P<0.0001$) (Figure 3.20). The plasmid dilutions were also given an equivalent concentration when quantified using the Artus standards as when the WHO standards had been used for quantitation.

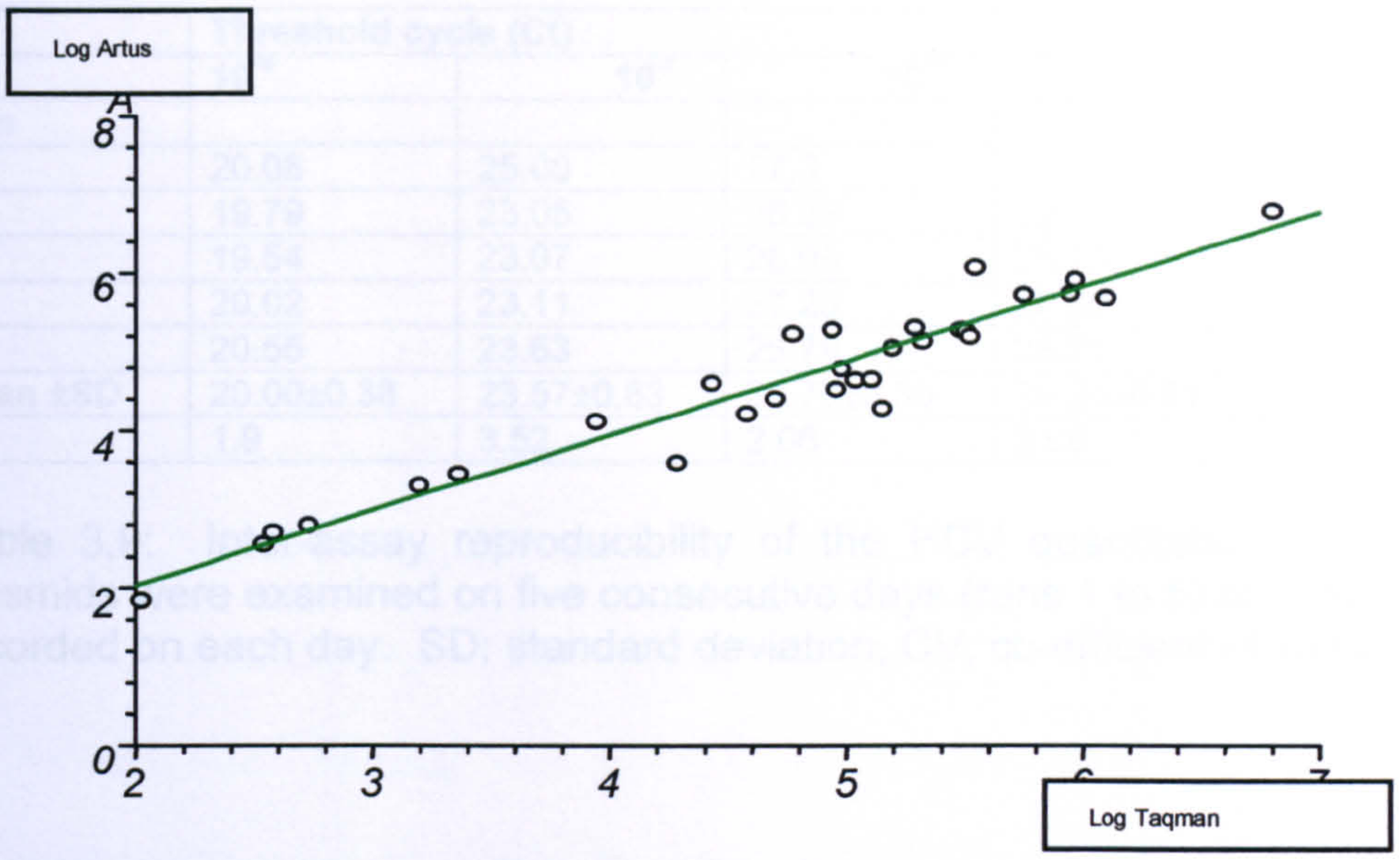

Equation: Log Artus = 0.7937 Log Taqman + 1.3631
Correlation coefficient (r) = 0.964722 (r^2 = 0.930689)

Figure 3.20: Simple linear regression of commercial HCV quantitation vs. in-house Taqman assay. Thirty HCV positive clinical specimens were quantified concurrently, using the Taqman HCV/MS2 assay and the RealArt™ HCV RG RT PCR kit. An R^2 value of 0.93 demonstrates good linear relationship between the two assays.

3.4.7 Precision and range of quantitation

To evaluate the inter-assay reproducibility, plasmid dilutions (4,091,300 to 409 IU/ml) were examined on five separate consecutive days. Table 3.9 demonstrates that the co-efficient of variation (CV) of Ct values was between 1.48 and 3.52%. To evaluate the reproducibility within a run (intra-assay), clinical samples were run in triplicate to check for variations in Ct, the co-efficients of variation for a set of 7 clinical specimens (A-G) is outlined in Table 3.10. This ranged from 0.6-2.9%.

	Threshold cycle (Ct)				
	10^{-6}	10^{-7}	10^{-8}	10^{-9}	10^{-10}
Run					
1	20.08	25.00	27.3	30.11	32.40
2	19.79	23.05	26.36	29.10	31.40
3	19.54	23.07	26.05	28.70	31.13
4	20.02	23.11	27.28	29.59	31.76
5	20.55	23.63	26.79	28.71	31.51
Mean ±SD	20.00±0.38	23.57±0.83	26.76±0.55	29.24±0.61	31.66±0.47
CV	1.9	3.52	2.06	2.09	1.48

Table 3.9: Inter-assay reproducibility of the HCV quantitation assay. The plasmids were examined on five consecutive days (runs 1 to 5) and the Ct value recorded on each day. SD; standard deviation, CV; co-efficient of variation

	Threshold Cycle (Ct)						
	A	B	C	D	E	F	G
Run							
1	20.16	23.76	27.92	31.28	21.78	26.65	30.5
2	20.62	23.45	26.95	30.6	21.56	25.3	30.63
3	20.44	22.59	27.02	30.3	21.58	26.58	30.28
Mean ±SD	20.41 ±0.23	23.27 ± 0.61	27.3 ± 0.54	30.73 ±0.5	21.64 ±0.12	26.18 ±0.76	30.47 ±0.18
CV	1.14	2.6	1.98	1.63	0.55	2.9	0.6

Table 3.10: Intra-assay reproducibility of the HCV quantitation assay. Triplicates of 7 clinical specimens (A-G) were quantified in a single run and the average Ct value calculated. SD; standard deviation, CV; co-efficient of variation

The accuracy of the quantitation assay was also verified using the OptiQuant® HCV RNA Quantification Panel (AcroMetrix, cat. no. 94-2011). This is a panel of seven samples at pre-determined levels calibrated against the WHO standard, ranging from negative to $5x10^6$ IU/ml. Using the plasmids as standards, the correct quantities were assigned for each member of the OptiQuant® panel.

3.4.8 Limit of detection and linearity

Probit analysis to determine the lower detection limit of the HCV/MS2 duplex assay was performed (Section 2.26). The 10^{-9} plasmid dilution (4103.9 IU/ml) was further diluted to produce a series containing 300, 150, 100, 75, 50, 25 and 5 IU/ml. These were run in replicates of 10 each in a single run and the number of positives per dilution was counted. From these results, a probit analysis was performed. This calculated the sensitivity of the assay to be 25 IU/ml (6.3-38.6 at 95%CL). The linearity was found to be excellent over the dynamic range covered by the plasmid standards with a slope of ~1.0 on the $\log_{10}$ scale on all assay runs.

3.4.9 Genotype sensitivity

The NIBSC HCV RNA genotype panel for nucleic acid amplification techniques (NIBSC code 02/202) was used to assess the capability of the HCV quantitation assay to detect all six genotypes. This panel consists of six vials each representing one of the six major genotypes at a concentration of 1000 IU/ml for each genotype. These were extracted and subjected to the HCV quantitation assay. All six genotypes could be detected using the assay. The sensitivity of the assay did not vary according to genotype. All six genotypes had a Ct value between 30.3 and 31.8 (Figure 3.21).

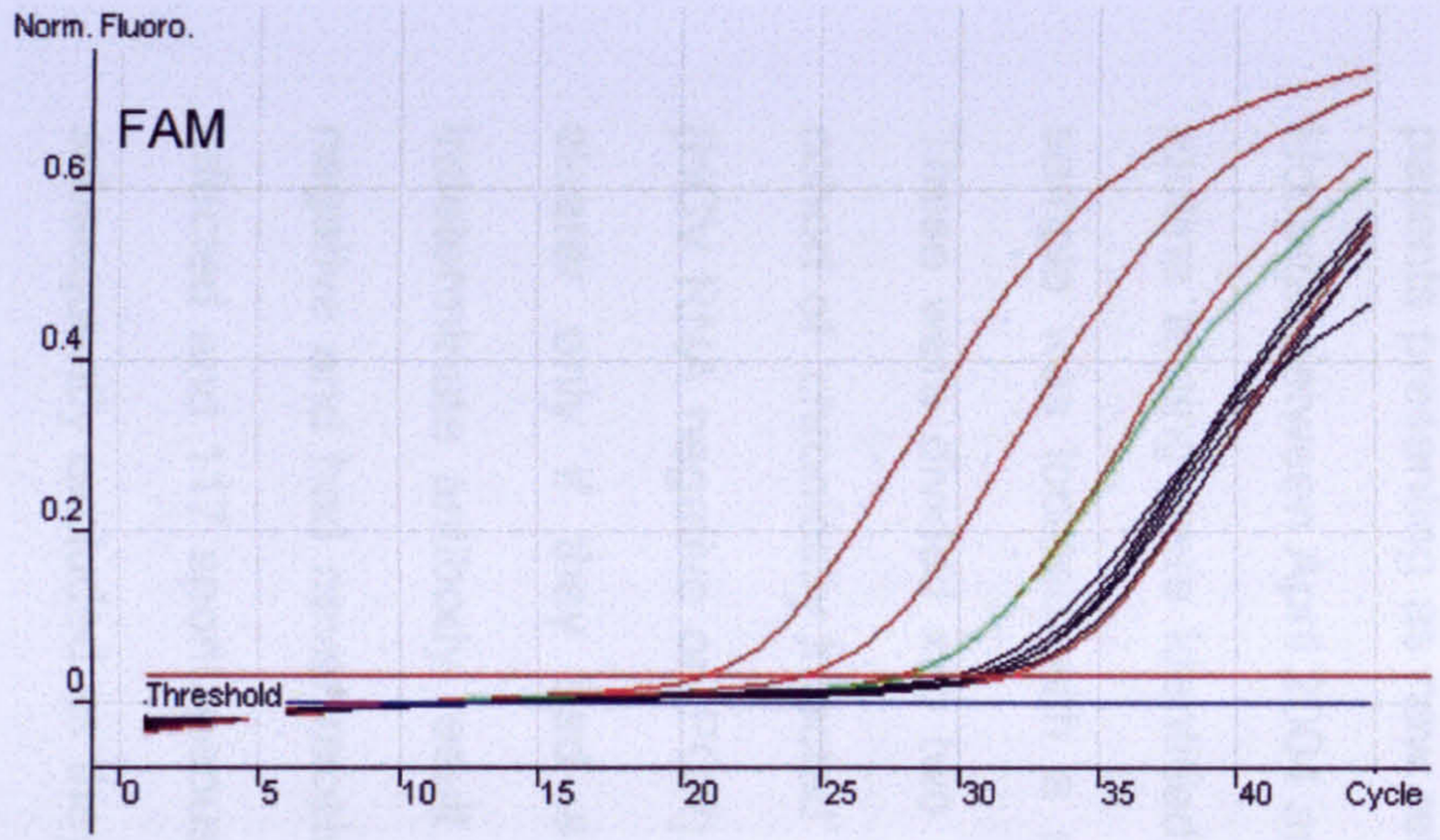

Figure 3.21: Assessing the genotype sensitivity of the Taqman HCV quantitation assay using the NIBSC HCV RNA genotype panel. All six HCV genotypes could be detected with equal sensitivity. The red lines on the Rotorgene graph are a dilution of plasmid standards used to create the standard curve for quantitation. The six black lines are the NIBSC HCV genotypes 1-6. The green line is the HCV positive control, included in each run. S;standard, U; unknown.

	Name	Type	Ct	Given Conc (IU/ml)	Calc Conc (IU/ml)
	Plasmid -6	S	21.24	4,091,300.00	3,983,908.30
	Plasmid -7	S	24.84	409,130.00	408,970.70
	Plasmid -8	S	28.35	40,913.00	44,346.00
	Plasmid -9	S	32.21	4,091.00	3,877.50
	HCV POS	U	28.53		39,577.80
	GENOTYPE 1	U	31.37		6,599.90
	GENOTYPE 2	U	31.37		6,591.50
	GENOTYPE 3	U	31.77		5,107.30
	GENOTYPE 4	U	30.3		12,906.00
	GENOTYPE 5	U	31.35		6,653.30
	GENOTYPE 6	U	30.98		8,424.20
	WATER	Negative	Negative		Negative

3.4.10 Implementation of the HCV quantitation assay into routine use

The HCV quantitation assay with MS2 internal control has been carried out on ~6000 clinical specimens. From the optimisation experiments, it was decided that any specimen which was found to be HCV RNA negative with an MS2 Ct of >29 would be re-extracted and re-tested. Of the clinical samples tested, 10 (0.17%) were found to be HCV RNA negative with MS2 not detected, or detected at Ct >26 and were re-extracted and re-tested. All of these isolates were found to be HCV RNA negative on repeat, with positive MS2.

3.5 HCV clearance study

The Taqman genotyping, subtyping and quantitation assays described in this chapter were all utilised in a study which was designed to investigate whether viral genotype was associated with the ability to clear HCV spontaneously. All patients presenting as new referrals to the hepatology clinic at Addenbrooke's Hospital between April 2004 and April 2007 who were HCV antibody positive by routine testing were identified; a total of 370 individuals. Of these, a serum sample was located with a sufficient volume for testing in 336 individuals. These were divided into two cohorts dependent on their HCV PCR result, a cohort of 'chronically infected' (HCV RNA positive) and 'spontaneous clearers' (HCV RNA negative on PCR). An individual was identified as a spontaneous clearer only if they had a positive antibody result (all those with an indeterminate antibody result were excluded), had always tested HCV RNA negative and had never received treatment for HCV. In total, 219 chronically infected and 117 spontaneous clearers were identified. Fifteen clearers were subsequently excluded as they were found to have been previously treated for HCV.

For the HCV RNA positives, infecting genotype was ascertained using the fully optimised Taqman HCV genotyping assay described in section 3.2. Three isolates had ambiguous results and required sequencing for confirmation. Two of these isolates were positive with the two genotype 1 probes but also had a cross-reaction with the T3 probe in panel one of the genotyping assay (Section 3.2). Sequence analysis indicated that with one isolate (10719), there was a one basepair mismatch with the T3 probe (as seen with isolate 15554, described in section 3.2.8, Figure 3.8). The other isolate which displayed this pattern (18854) demonstrated a strong cross-reaction with the T3 probe and was seen, on sequence analysis, to have a mix of genotype 1 (CCG) and genotype 3 (TCA) specific motifs at the T3 probe-binding site (Figure 3.22). This isolate did not display any other genotype 3 specific motifs. To rule out the possibility of a recombination event, this isolate was also subtyped using the NS5b region, with the methods described in section 3.3 and was found to be subtype 1a. These isolates (10719 and 18854) were both reported as genotype 1. One isolate (12394) was positive with all genotype 1 and 3 probes. This was found, by sequencing, to be a mixed genotype 1 and 3 infection, and was excluded from the study. Table 3.11 shows the genotyping results for the 218 patients successfully genotyped and included in the clearance study.

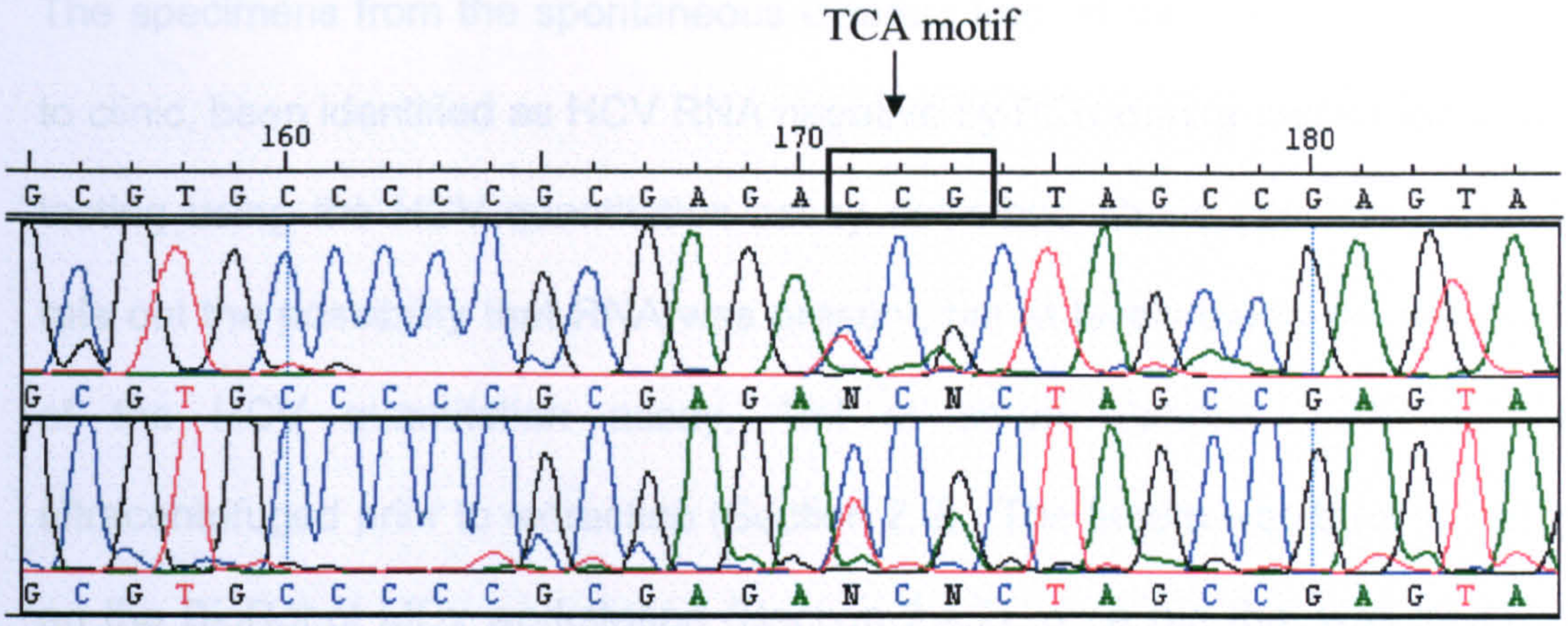

Figure 3.22: Sequence data from isolate 18854 which was positive with both genotype 1 probes and cross-reacted with the T3 probe. The genotype 3-specific TCA motif is shown which demonstrates the mixed sequence, displaying elements of both genotypes 1 and 3 at this motif.

For the spontaneous clearers, the infecting genotype was ascertained by serotyping using the Abbot Murex HCV Serotyping kit, following manufacturer's guidelines (Section 2.8). In total, 102 specimens were serotyped. Thirty-seven isolates were negative and 3 were mixed/non-typable by serotyping and were excluded from the analysis, leaving a cohort of 62 isolates successfully serotyped (Table 3.11).

	HCV - chronics	**HCV-clearers**
Genotype	**Number (%)**	
1	98 (45.0)	40 (64.5)
2	16 (7.3)	4 (6.5)
3	102 (46.8)	16 (25.8)
4	2 (0.9)	0
5	0	1 (1.6)
6	0	1 (1.6)
	n= 218	**n= 62**

Table 3.11: HCV genotyping and serotyping results of isolates included in the HCV clearance study.

The specimens from the spontaneous clearers had, at the time of presentation to clinic, been identified as HCV RNA negative by PCR during routine laboratory testing using the HCV quantitation assay described above (Section 3.4). To rule out the possibility that RNA was present, but at levels below the sensitivity of the HCV quantitation assay, 1ml of serum (where available) was ultracentrifuged prior to extraction (Section 2.9). The serum was then extracted on the BioRobot MDx workstation (Section 2.4.2), on a run that was free from HCV RNA positive specimens, and amplified using the HCV quantitation assay. HCV RNA remained undetectable in all sera ultracentrifuged prior to extraction; MS2 was amplified in these samples within the acceptable range.

The clinical details for all individuals for whom a serum specimen was available (n=336) were collated. These included sex, age, ethnicity (white or non-white), country of birth (UK or non-UK), mode of HCV acquisition (IDU or known transfusion), alcohol consumption (< or >21 units per week for males and < or >14 units for females), age at infection and duration of infection. The duration of infection was calculated as the date of sample - age at infection. For each individual, infecting genotype was reported either as type 1 or non-1 type. Statistical analysis was carried out using SSPS package (Section 2.26) to compare the chronically infected and spontaneous clearers cohort. Univariable analysis was carried out on the cohort of individuals for whom a HCV genotyping/serotyping result was available (n=280), comparing those who had tested positive for HCV RNA (n=218) with those who were presumed to have spontaneously cleared the virus (n=62). The clinical details for this cohort and univariable analysis for each patient characteristic are shown in Table 3.12.

	Chronics n=218 (%)	Clearers n=62 (%)	Statistic (with 'not knowns' excluded)	P value (with 'not knowns' excluded)
Male	137 (62.8)	44 (71.0)	$\chi^2 = 1.39$	0.24
Female	81 (37.2)	18 (29.0)		
UK	81 (37.2)	34 (54.8)	$\chi^2 = 9.82$ ($\chi^2 = 9.22$)	0.007 (0.002)
Non-UK	41 (18.8)	3 (4.8)		
Not-known	96 (44.0)	25 (40.3)		
White	174 (79.8)	47 (75.8)	$\chi^2 = 4.64$ ($\chi^2 = 1.44$)	0.098 (0.383)
Non-white	18 (8.3)	2 (3.2)		
Not-known	26 (11.9)	13 (21.0)		
IDU	134 (61.5)	49 (79.0)	$\chi^2 = 12.16$ ($\chi^2 = 0.04$)	0.002 (0.953)
Transfusion	24 (11.0)	9 (14.5)		
Not-known	60 (27.5)	4 (6.5)		
<21 (M) or <14 units (F) alcohol	123 (56.4)	38 (61.3)	$\chi^2 = 0.492$ ($\chi^2 = 0.492$)	0.782 (0.552)
>21 (M) or >14 units (F) alcohol	88 (40.4)	22 (35.5)		
Not known	7 (3.2)	2 (3.2)		
Type 1	98 (45.0)	40 (64.5)	$\chi^2 = 7.39$	0.007
Non-1 type	120 (55.0)	22 (35.5)		
Mean age at infection (yrs)*	22.6	19.2	t= 2.79	0.006
Mean duration of infection (yrs)*	20.9	22.2	t= 0.76	0.448

Table 3.12: Characteristics and univariable statistical analyses comparing those who tested positive for HCV RNA and those who tested negative for HCV RNA. *age at infection (and therefore duration of infection) was unknown for 105 cases.

Univariable analysis suggested that HCV PCR negatives (clearers) were significantly more likely to be UK-born (P=0.007), have type 1 infection (P=0.007) and be younger at infection (P=0.006). To investigate whether the association between viral type and viral clearance was independent of other potential confounding factors (sex, age at infection, country of birth), a multivariable logistic regression analysis was undertaken in STATA using the Binreg Command to obtain relative risks rather than Odds Ratios (OR) (Table 3.13). Age at infection was unknown for 105 individuals and so these cases were excluded from the multivariable analysis (leaving 175 individuals eligible for inclusion). Factors included in the model were age at infection and country of birth (as these two factors were found to have significant effects in the univariable analysis (see table 3.12). Sex was also included because of its reported influence on viral clearance in other studies (see Section 3.6.4). Multivariable analysis demonstrated that a statistically significant association remained between viral serotype and viral clearance (RR=1.75, 95%CI: 1.151-2.663; P=0.009). Additionally, age at infection was also seen to be significantly independently associated with PCR negativity (OR=1.849, 95%CI: 1.531, 2.233; P=<0.001). These results suggest that those individuals who acquired their infections at a younger age and who had type 1 infections were more likely to clear them. Individuals who had type 1 infections were nearly twice (1.8x) as likely to clear them. Similarly, the risk of clearing nearly doubled (1.8x) for every 10 years younger individuals were at infection. Although those born outside the UK were significantly less likely to clear in the univariable analysis, this was no longer statistically significant after adjusting for the other factors (Table 3.13). However, the point estimate for the relative risk of clearance was less than 0.5 suggesting this could still be important, in particular considering that the loss of

statistical significance was probably a combination of adjustment for the other factors and also loss of study power due to missing data for age at infection.

Factors	RR	P	95%CI
Sex (male vs. female)	1.374	0.268	0.784, 2.409
Genotype (1 vs. non-1)	1.751	0.009	1.151, 2.663
Age at infection (per 10 year decrease)	1.849	<0.001	1.531, 2.233
Country (baseline UK born) Non-UK Not known	 0.423 0.666	 0.204 0.050	 0.112, 1.598 0.444, 0.999

Table 3.13: Multivariable logistic regression for the 175 individuals for whom complete data were available. RR; relative risk.

Further univariable analyses comparing those individuals included in the multivariable analysis (n=175) with those from whom serum specimens were available (n=336) but were excluded from any statistical analysis (n=161), were undertaken. The results of these analyses are given in Appendix D.

Regarding the two factors which were shown to be significantly associated with viral clearance (age at infection and genotype), no significant difference in age at infection was found between those included and excluded from the study (P=0.220). With regards to genotype, the analysis demonstrated that there was a significant difference between those included and those excluded from the study. This simply illustrates that the distribution of genotypes in the final sample entering the multivariable analysis varied from that in the original sample (χ^2=55.156, P=<0.001).

3.6 Discussion

3.6.1 HCV genotyping

The gold-standard for HCV genotyping is sequencing of the genome followed by phylogenetic analysis. However, this is impractical on a large scale basis in a clinical laboratory. Real-time PCR has recently been identified as a rapid, sensitive and specific method for HCV genotyping with two groups recently recognising its potential (Schröter *et al*, 2002; Bullock *et al*, 2002) These protocols used FRET (hybridisation) probes to identify different genotypes using melt curve analysis on the LightCycler detection system. Two formats have been described using either three sets of probes and two channels (Schröter *et al*, 2002) or a single set of probes within a single channel (Bullock *et al*, 2002; Haverstick *et al*, 2004). Although accurate and sensitive, this method does, however use amplification products created from separate RT-PCR assays, requiring tubes containing amplicons to be opened prior to the genotyping step which introduces the possibility for contamination.

The development of the Taqman HCV genotyping assay described in this chapter was the first published report using Taqman probes for HCV genotyping (Rolfe *et al*, 2005). An alternative Taqman-based HCV genotyping assay, using a complicated 96-well PCR plate method with each sample being amplified in four adjacent wells with probes matching genotypes 1, 2, 3 or 4 respectively, was simultaneously developed (Lindh and Hannoun, 2005). This lacked sensitivity compared to the Taqman method described here (10,000-20,000 IU/ml lower detection limit for most genotypes) and also showed cross-reaction between genotype 1 and 4 probes.

The Taqman HCV genotyping assay has been continually improved and enhanced over the past two years whilst in routine use by sequencing of isolates which failed to be genotyped and designing/incorporating new probes as required. The current HCV Taqman assay is extremely specific and sensitive. Of the 773 clinical isolates that have been genotyped with the latest version (excluding the external laboratory specimens which were negative but not sequenced), only 5 (0.6%) have required sequencing for identification. Failure of the Taqman HCV genotyping assay is due either to very low viral load (<1000 IU/ml) or base mutations at a probe binding site. The strict algorithm requires all isolates to be positive with two probes (except genotype 4) and, as a result, even if a mismatch has occurred at one probe site, then the genotype will not be confirmed. Of the isolates that have been positive with one probe, and subsequently sequenced, the initial probe result was always correct. HCV genotyping of all patients presenting at Addenbrooke's Hospital, Cambridge gives a clear indication of the epidemiology of chronic HCV infection in Cambridge and the surrounding region between 2005 and 2007 (Table 3.5). The findings mirror those of other studies on the epidemiologically of HCV infection in the UK which have also demonstrated that genotypes 1 and 3 predominate (Watson *et al*, 1996; Harris *et al*, 1999; Mohsen *et al*, 2001). In the Eastern region, genotype 1 infection is more common that genotype 3 infection (49.2% vs. 39.1%). This does not reflect the results from a recent large sentinel surveillance study (n= 2208) which demonstrated that genotype 3 is slightly more common than genotype 1 infection (HPA, 2006).

This assay was designed to identify the four most common genotypes (1-4) seen in the Eastern region of the UK. The assay is not designed to detect genotypes 5 or 6. These are singled out as a result of their negativity or non-

specific probe reactivity (genotype 6) in the Taqman genotyping assay and are sequenced to confirm their identity. There has only been one genotype 5 isolate from a clinical specimen which had a non-exponential curve with the T11 probe. Genotype 6 isolates have been part of external quality assurance schemes. A genotype 6 result can be predicted by an unusual probe pattern of a positive result with only the T11 probe (Cy5) in panel one, which earmarks the isolate for sequencing. At present, genotypes 5 and 6 are seen predominantly in South Africa and South East Asia, respectively. A limitation of the assay, would, therefore be its bias towards UK-based HCV genotypes. This could lessen its utility in countries where genotypes 5 and 6 predominate. It could also pose a problem if the UK HCV epidemiology alters dramatically in the coming years. Detailed analysis of the 5'UTR region has identified that there are no motifs which could be used to differentiate genotypes 5 and 6. At present only 1 clinical isolate (and three external quality assessment samples) have failed to be genotyped by the HCV Taqman assay and were found to be genotypes 5. The sequencing burden is therefore very low. If, in future years, the numbers of genotypes 5 and 6 increased, then changes would need to be made in the HCV genotyping assay. Attention would need to be focused on an alternative target with genotype 5 and 6-specific motifs. A further multiplex Taqman PCR assay could be developed and any isolates negative with the Taqman assay described herein could be subjected to a second genotype 5 and 6-specific genotyping assay.

Data published from studies using the TRUGENE™ 5' NC genotyping kit (Bayer Diagnostics) and the VERSANT™ HCV Genotype Assay (LiPA), version 1 (line probe assay) indicate that the HCV Taqman genotyping assay compares very favourably against these commercial genotyping kits. The genotyping

efficiencies of these two commercial assays was found to be 94.8% (n=96) (Germer *et al*, 2003). These assays have recently been updated for enhanced subtype discrimination which may have slightly improved their genotyping capacity (Ross *et al*, 2007; Ross *et al*, 2008). The Taqman HCV genotyping assay is superior to the TRUGENE™ 5'NC genotyping kit as it does not require the lengthy sequencing and data analysis steps. The line probe assay has equivalent specificity to the Taqman genotyping assay, demonstrating between 97-100% concordance with sequencing (Haushofer *et al*, 2003; Zheng *et al*, 2003), but lacks the sensitivity seen by the Taqman assay with a lower limit for typing reported to be around 20,000 IU/ml (Zheng *et al*, 2003).

The HCV Taqman genotyping assay focuses on a single region of the HCV genome. Consequently this assay, as with all commercially available techniques, would have limitations if widespread recombination existed (Simmonds *et al*, 2005). At present, reports of recombinant forms of HCV are limited (Noppornpanth *et al*, 2006, Legrand-Abravanel *et al*, 2007). A recombinant consisting of structural genes from genotype 2 and non-structural genes from genotype 1b has been reported in St Petersburg, Russia (Kalinina *et al*, 2002, 2004). Recombination has been reported in other flaviviruses, such as the dengue virus (Holmes *et al*, 1999; Tolou *et al*, 2001) so it is plausible that HCV recombination could occur in patients with multiple exposures. With the availability of a subtyping method using the NS5b region, there is the possibility of detecting recombination events as both the 5' and a region close to the 3' end (NS5b) of the HCV genome can be interrogated to verify whether a recombination event has occurred. This, of course, would only be useful if recombination was suspected.

The field of HCV diagnosis and monitoring is not stationary and continues to evolve as new techniques become available. Indeed, since the development of the Taqman HCV genotyping assay, other techniques for genotyping have been published. Pyrosequencing, a method of DNA sequencing based on a chemiluminescent enzymatic reaction (Ronaghi *et al*, 1998), has been used recently to determine HCV genotype (Elahi *et al*, 2003) and appears to identify successfully isolates to the subtype level, despite the short (237 nt) region of the 5'UTR targeted. Pyrosequencing has also recently been used successfully to identify minority HCV genotypes in multitypic HCV infection (Buckton *et al*, 2006) which appears, on examination, to be a rare event, even in people at high risk of repeated HCV infection.

With the updated NICE guidance recommending that all patients, regardless of disease severity, should be offered interferon therapy, and the resulting increased demand for HCV genotyping, the development of a rapid assay for genotyping to support clinical practice was required. The HCV Taqman genotyping assay is fast without compromising reliability, sensitivity and reproducibility. It also compares favourably in terms of cost when compared with sequencing, both in terms of the price of consumables and in worker costs per man hour. A worthwhile future development would be to develop this method into an assay which could both quantify and genotype in a single assay which would dramatically increase throughput for monitoring HCV infection.

3.6.2 HCV subtyping

Several groups maintain that their methods for HCV genotyping can also define isolates at the subtype level. The INNO-LiPA HCV II, manufactured by Innogenetics, is one such example (Stuyver *et al*, 1993; Andonov and

Chaudhary, 1995). Several studies have demonstrated that the line assay is unsuitable for subtyping purposes (Ansaldi *et al* 2001: Halfon *et al* 2001; Nolte *et al*, 2003). In particular, it has been demonstrated to be unreliable in the differentiation between 1a/1b, 2a/2c and in assigning subtype to genotype 4 isolates. The original INNO-LiPA assay has been replaced by a new 'improved' version (Versant HCV Genotype Assay 2.0), with the addition of core probes. Concordance with genotype and subtype with sequencing reference was improved from 37.5% with the original version, to 64.7% with the new version, but still lacked subtyping capability (Bouchardeau *et al*, 2007). In a study using 110 clinical specimens, Ross *et al* (2007), this assay showed improved discriminatory power, particularly with regards to discriminating between 1a and 1b subtypes when compared to the first generation line assay. However, despite the use of the additional sequence information derived from the core region, the second generation kit was still unable to make a distinction between 2a and 2c strains. The TRUGENE™ 5'NC genotyping kit also has difficulty in determining subtype with an accuracy of only 74% when compared to sequencing of the NS5b region (Halfon *et al*, 2001). Many subtyping assays target the 5'UTR which, although containing genotype-specific motifs, lacks the variability needed for subtype discrimination. Subtypes 1a and 1b, for example, share 98.8% homology in this region. The discrimination between 1a and 1b subtypes is based on a single nucleotide substitution, an A-to-G transition at position -99 which occurs in subtype 1b isolates, but is also apparent in subtype 1a isolates (Chen and Weck, 2002). The target of choice for subtyping is the NS5b region of the HCV genome which has been shown to provide the necessary resolution for subtyping purposes.

This chapter describes the development of two subtyping assays which serve different purposes. The generic HCV subtyping assay, based on sequencing of a region of the NS5b gene can be used for all HCV genotypes. This was developed with the express interest of providing a powerful tool for epidemiological studies. As demonstrated by the use of this assay in a suspected nosocomial HCV transmission, the importance of a reliable sequence-based method to investigate suspected transmissions is also vital. The second, Taqman probe-based HCV subtyping assay is a rapid, real-time assay for discrimination between 1b and non-1b isolates. At present, the evidence related to the increased risk associated with subtype 1b infection of disease severity (Zein *et al*, 1996; Amoroso *et al*, 1998; Hwang *et al*, 2001), non-response to treatment (Nousbaum *et al*, 1995; Manesis *et al*, 1997) and development of hepatocellular carcinoma (HCC) (Silini *et al*, 1996; Bruno *et al*, 1997) is controversial (Benvegnù *et al*, 1997; Nakano *et al*, 2001, 2001a). This could be due to the mis-classification of subtypes due to the poor resolution of the subtyping assays used. This assay could be utilised in a study to clarify the relevance of subtype 1b in HCV infection and could find a future use as a high throughput method for identification of subtype 1b if this were to become necessary in HCV monitoring.

The 5'UTR is favoured for genotyping as its highly conserved nature aids the design of primers which target sites with very low sequence variability, reducing the possibility of mismatches, therefore increasing assay sensitivity and reducing false-negative results. The NS5b region is a much more recalcitrant target by virtue of its most beneficial feature – its variability; making primer design difficult. However, by creating a large reference databank of the NS5b region of all known HCV subtypes, primers for the subtyping assays described

here could be designed around the most conserved region, adding degenerate nucleotides where necessary. The comparison of the 1b/non-1b subtyping assay with the genotyping results indicated (by failure to subtype low positive genotype 1 isolates), that the subtyping assay was slightly less sensitive than the genotyping assay. However, it was highly specific and could accurately subtype all genotype 1 isolates with Ct values <32.

The specificity and sensitivity of the generic HCV subtyping assay mirror the results of studies using either a prototype commercial (Othman *et al*, 2004) or an in-house (Sandres-Sauné *et al*, 2003) HCV subtyping system based on the NS5b region. The NS5b subtyping assays demonstrated superiority over the TRUGENE™ 5'NC assay in terms of subtyping, with 24% of isolates failing to have subtype assigned using the 5'NC assay. The failure of the TRUGENE NS5b and the HCV generic subtyping assays to amplify 2 and 3 isolates respectively (Table 3.7) indicates that the NS5b region is less robust than the 5'UTR with variation at the primer-binding sequences causing lower sensitivity.

Through the creation of a generic system for HCV subtyping, a large reference databank of trimmed 'ready-to-use' reference sequences, tailored to our developed assay, has been produced. This is available as a FASTA file to diagnostic laboratories. Laperche and co-workers (2006) have recently carried out a multicentre study in which they provided laboratories with expertise in sequencing techniques a consensus reference databank and some HCV isolates. The accuracy of genotype/subtype assignation was higher in these laboratories than it had been previously without the provision of a reference databank (Laperche *et al*, 2005, 2006).

3.6.3 HCV quantitation

Commercially available assays for HCV quantitation are being continually improved and updated. The latest real-time PCR-based assays such as the Cobas Taqman HCV assay and the Abbott Real-Time HCV assay benefit from high throughput, automation and large dynamic range with sensitivity down to tens of IU/ml (Halfon *et al*, 2006; Germer *et al*, 2005; Sizmann *et al*, 2007). Commercial assays have the disadvantage of being much more costly than in-house assays, often relying on specific reagents and equipment. Companies do not disclose the primer/probe sequences of their products and so there is not the opportunity for isolate characterisation as can occur when an in-house assay is developed.

The limit of detection, the lowest level of HCV RNA that can be detected consistently (>95% of the time) is a critical determinant of a successful HCV quantitation assay. A patient who has a negative HCV RNA result at the end of treatment is seen as a 'responder' and therapy terminated. However, if the detection assay is not sufficiently sensitive, it may be that there is still a low level of circulating HCV RNA and the patient may relapse (Sarrazin *et al*, 2000). Another requirement of HCV quantitation assays is linearity over a large dynamic range to enable accuracy over a wide range of HCV viral loads. Linearity is assessed by the degree to which the standard curve approaches a straight line – a slope of 1.0 on the $\log_{10}$ scale. Good linearity means that observed changes in viral level reflect actual changes, not those due to biases.

An ideal HCV RNA quantitation assay would have a lower detection limit of 5-50 IU/ml and a 6-7 $\log_{10}$ linear range to eliminate the need for both quantitative and qualitative assays and would be equally sensitive across all genotypes. It would

be a one-step protocol, use reliable and reproducible standards which can be stored long-term without degradation and have a dependable internal control to detect false-negative results. The Taqman assay was developed with these points in mind. As a single-step assay it reduces labour and prevents contamination which can occur in a two-step or nested-PCR process. The amplicon produced is small (90 bp) which aids amplification and increases the sensitivity of the assay when compared to one generating a larger amplicon, as seen in direct head-to-head comparisons with a larger amplicon. The use of plasmid standards as an external calibration system allows a broad dynamic range, with detection down to 25 IU/ml – a sensitivity not achieved by many non real-time PCR-based assays. The high upper range of the assay – with the highest plasmid concentration of over 4 million IU/ml means that samples do not require dilution prior to testing. Plasmid dilutions with IU values greater than 4 million could always be incorporated into the assay, if viral loads were found to be outside the scope of the standard curve. The linearity of the developed assay is excellent over the wide range of viral loads covered by the plasmid standards (4,091,300 to 409 IU/ml). This enables quantitation over the wide range of HCV viral loads observed pre-, during and post-treatment to accurately assess whether a $2\log_{10}$ viral decline has occurred and thus whether treatment should be continued or terminated.

The Taqman HCV quantitation assay utilises recombinant DNA plasmids to produce the standard curve. The PicoGreen dsDNA quantitation reagent, the ultrasensitive fluorescent nucleic acid stain was used to quantify the plasmids. This has several advantages over determination via absorbance which suffers from interference caused by contaminants, inability to distinguish between DNA and RNA and the large contribution of nucleotides and single-stranded nucleic

acids to the signal. It may be argued that, as HCV is an RNA virus, then an RNA template should be used to create the external calibration curve, rather than the recombinant DNA used in this assay. However, Pfaffl and Hageleit (2001), in a direct comparison of recombinant RNA and recombinant DNA as external calibrators, found the latter to be more sensitive, reproducible, stable and with a larger quantification range. The choice of a genotype 4 isolate for use in the recombinant plasmid was to enable contamination issues to be easily detected, as genotype 4 isolates are seen very rarely in our region. Linearisation of the plasmid prior to use was carried out so that the standards better reflected the linear HCV RNA genome, making quantitation more accurate. *Pst I* was selected as the restriction enzyme for linearisation as the site of cleavage is found once in the TopoTA vector and not in the 5'UTR amplicon, enabling a single cleavage and a linear molecule to be produced. The plasmids are diluted in a DNA carrier (herring sperm DNA) and are checked every six months by re-quantifying using the WHO standards to ensure no degradation has occurred. The Ct values of the plasmids have not increased over time, indicating that they are stable, even when stored long-term (data not shown). Moreover, the incorporation of an external quality standard with every run has demonstrated a consistent value every time.

A further requirement of a HCV quantitation assay is that it is equally sensitive across all genotypes. This should be achieved by targeting the 5'UTR of the genome, which is highly conserved. However, poor genotype performance is an old problem in HCV RNA quantitation (Mellor *et al*, 1999) and remains a contentious issue, even with more recent commercial HCV quantitation assays (Colson *et al*, 2006; Gelderblom & Beld, 2007). Many of the published developed assays do not test for genotype sensitivity and could, therefore, be

under-estimating viral load. The equal sensitivity of the developed HCV Taqman HCV quantitation assay across all genotypes (1-6) indicates that this assay is not affected by genotype.

One of the central aspects of the developed Taqman quantitation assay is the incorporation of MS2 bacteriophage as an internal control to monitor inhibition or RNA degradation. Optimisation of the MS2-specific real-time assay, using MS2 RNA demonstrated that MS2 detection was highly sensitive, with a limit of 2 genome copies/reaction. As a non-competitive IC, MS2 was not expected to interfere with viral amplification. However, to minimise the risk of competition between target and IC, the primer concentration for MS2 detection was reduced on incorporation into the HCV assay. Even at low MS2 primer concentration the 10^{-4} dilution of MS2 could still be reproducibly detected at 26 $^{+}$/-3 Ct with no compromise to the detection of HCV.

For an IC to be useful in a clinical setting it must be produced easily, versatile (to be used in a number of different assays) and stored for long periods without degradation. The MS2 bacteriophage meets all these criteria. It is easily propagated on standard media, and high stock yields can be produced. We have stored both the stock solution and aliquots of the working solution for over a year at -20°C with no increase in Ct value, indicating that MS2 has long-term stability. It is also versatile, and could be used as in IC in all RNA virus detection/quantitation assays. We have introduced it into our enterovirus, influenza and norovirus (Rolfe *et al*, 2007) detection assays, using exactly the same conditions as outlined above, and these assays are now used routinely in our laboratory. Figure 3.23 illustrates the use of MS2 in these assays and the reproducibility of its detection in each assay. Others have also recently

favourably described the use of MS2 bacteriophage as an IC, using an alternative target site (Dreier *et al*, 2005, 2006). The internal controls which are supplied with many commercial kits are incorporated into the master mix and can therefore only monitor the amplification process. MS2, by being included in the extraction tray, allows the assay to be monitored from the outset and can therefore identify faults with the extraction and reverse transcription processes in addition to inhibition during amplification. If a laboratory does not wish to propagate the bacteriophage, then the commercially available purified MS2 RNA itself provides an IC which can be added (at very low concentration) to a master mix. Experimental data indicates that 0.5 µl of a 10^{-6} dilution ($2x10^3$ copies) is sufficient for detection. This will, of course, not monitor the extraction process but will detect inhibition occurring during reverse transcription and amplification steps.

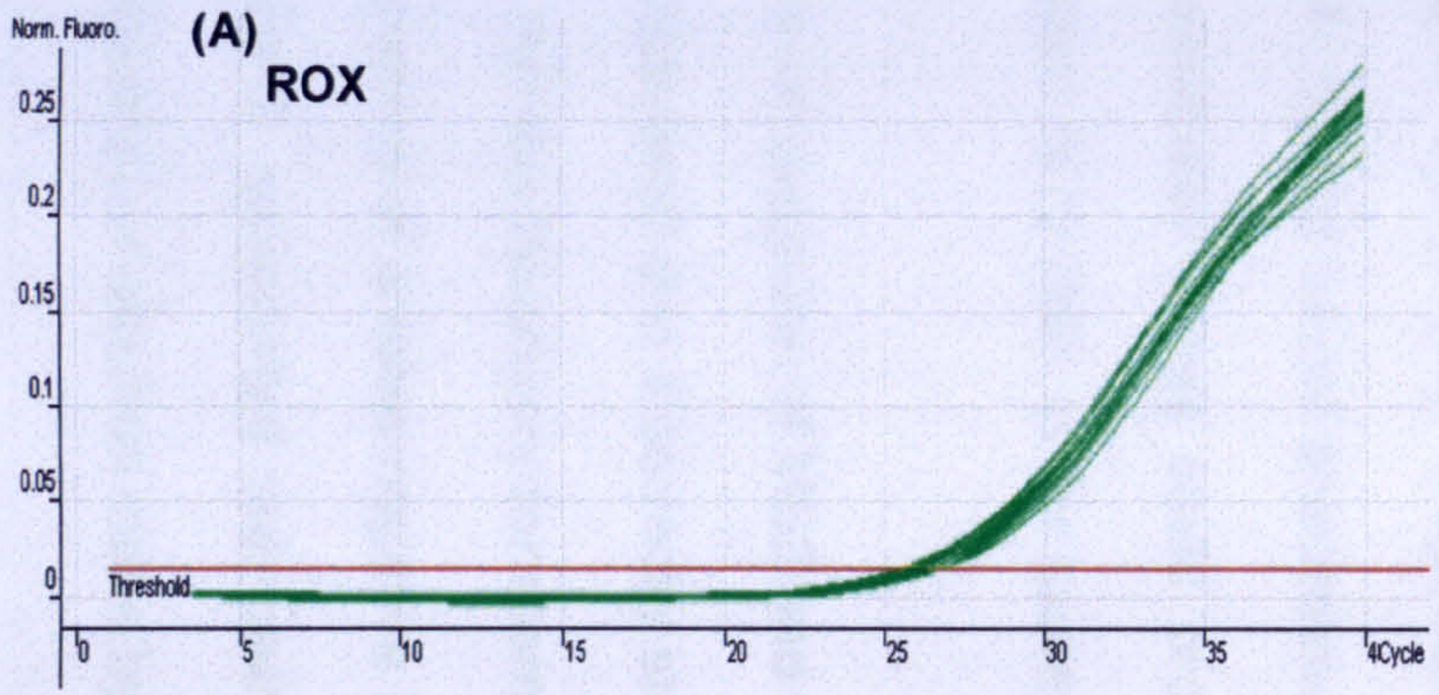

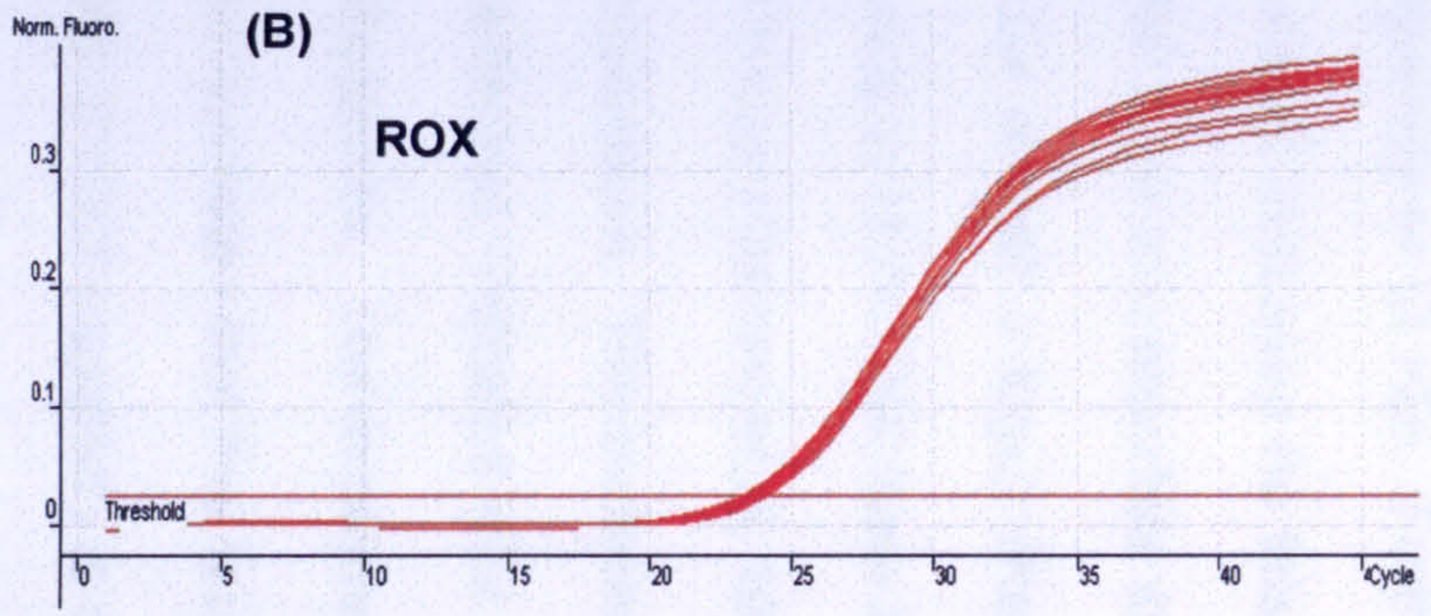

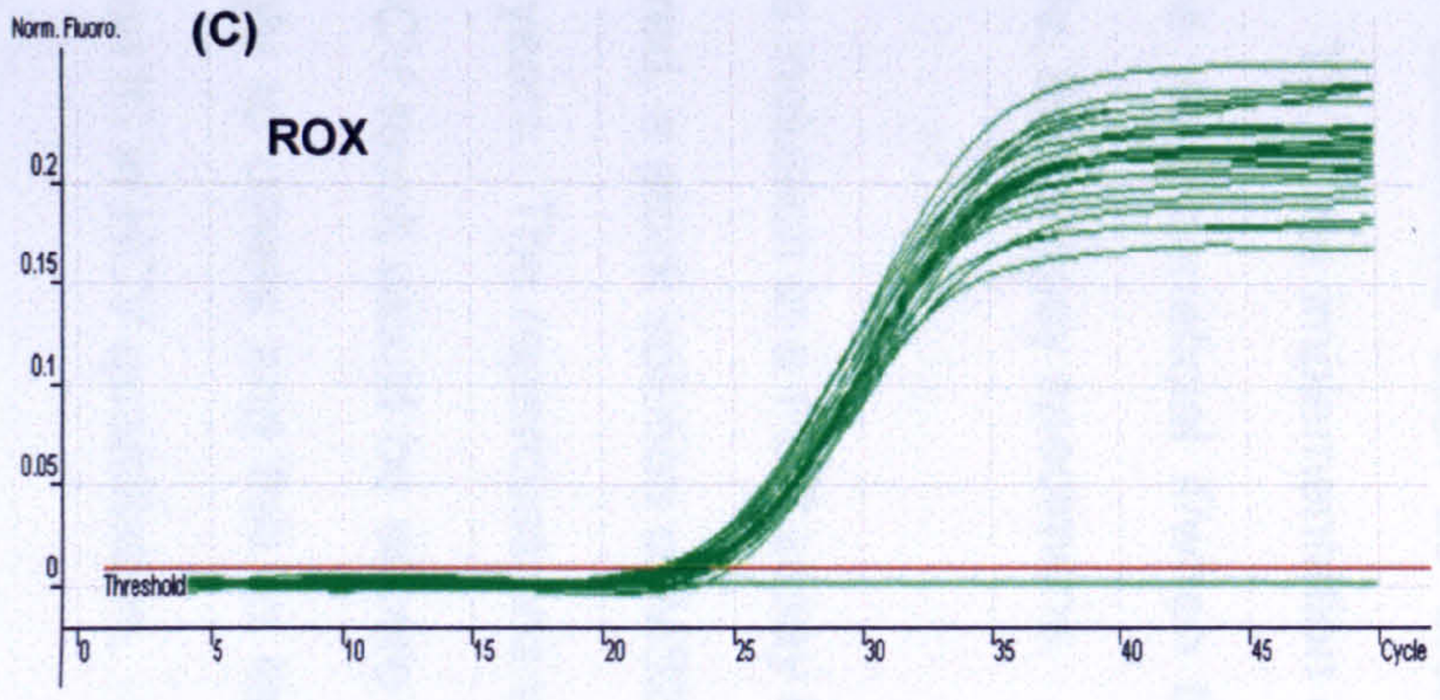

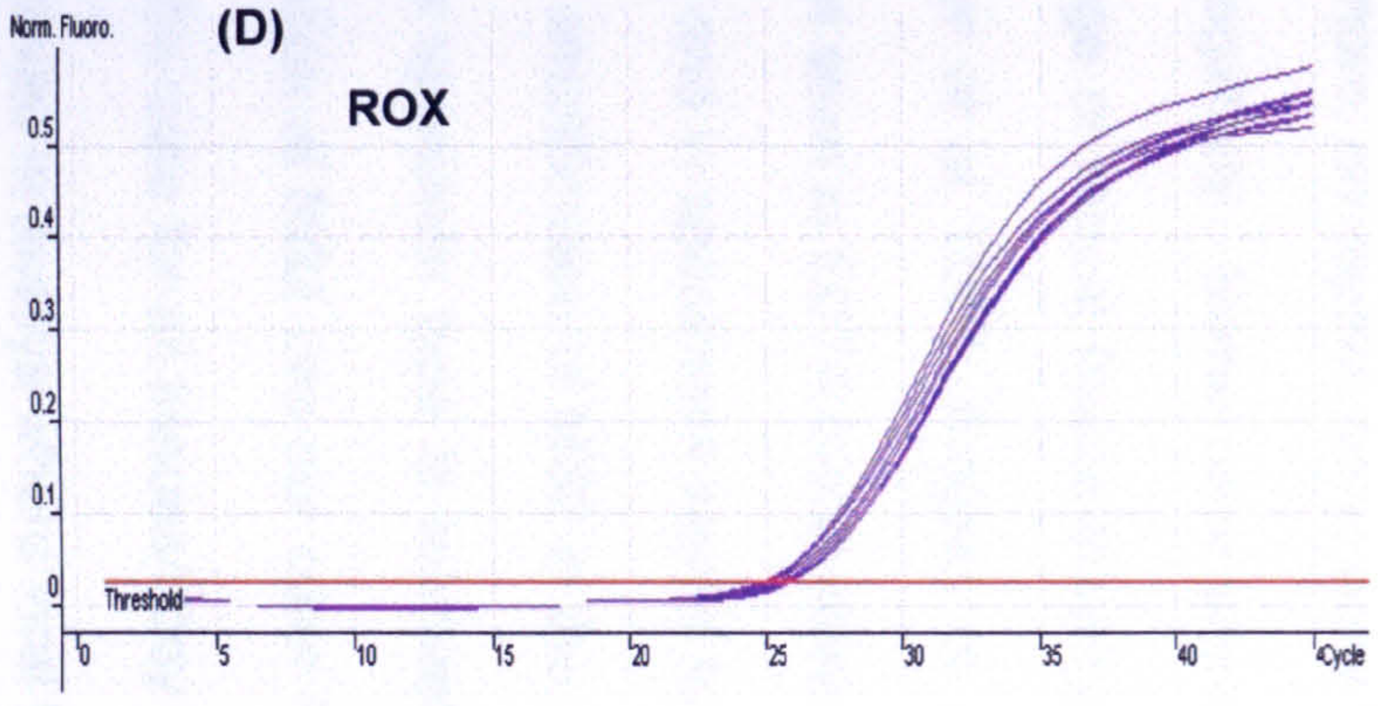

Figure 3.23: The implementation of MS2 internal control into the (A) enterovirus, (B) influenza H5, (C) norovirus and (D) respiratory viruses assays. For these assays the MS2 probe was labelled with a ROX fluorophore.

The need for an internal control in the HCV quantitation assay could be questioned, as only 0.17% (n=6000) of tests required repeating, due to MS2 negativity or Ct >29. Furthermore, on repeat, none were found to be HCV RNA positive, indicating no false-negativity. Some have argued that losses of HCV RNA from inappropriate storage or repeat freeze-thawing are negligible (in the order of half a log_{10}) (Kessler *et al*, 2001; Krajden *et al*, 1999). Significant losses in HCV RNA have been seen in EDTA blood stored at 4°C for more than 48 hours (Damen *et al*, 1998) and in specimens stored for long periods at room temperature. The successful amplification of MS2 in the vast majority of serum specimens indicates that this specimen type is relatively free from inhibitory substances. The implementation of MS2 into our other RNA virus assays has demonstrated that this is not the case for all tissues/body fluids. A much higher level of MS2 negativity is observed in assays where viral RNA is extracted from tissue specimens, respiratory specimens such as bronchoalveolar lavages (BALs) and faecal specimens. Thus the implementation of MS2 into the HCV quantitation assay could prove very beneficial if/when the assay is used to detect HCV RNA in, for example, liver biopsy specimens.

The propagation of MS2 and its inclusion in a PCR assay is inexpensive. Once propagated and if correctly stored, a stock solution of MS2 will provide a supply to last the laboratory for many years. The repercussions which could follow the reporting of a false-negative HCV result would be severe and could mean that HCV is transmitted unknowingly to others and this in itself should justify the valuable contribution made by an IC in HCV quantitation.

3.6.4 HCV clearance study

Early treatment of HCV can prevent chronicity. However, interferon therapy has severe side effects and is costly. Spontaneous clearance occurs in around twenty to thirty per cent of people with acute hepatitis C (Santantonio *et al*, 2002; Micallef *et al*, 2006). It would be advantageous to be able to identify these people prior to therapy. Spontaneous clearance is thought to occur within 3 months of infection (Gerlach *et al*, 2003) and so delaying treatment of individuals who are likely to clear the virus spontaneously is feasible. For the strategy of delayed treatment to be possible, there would have to be very clear predictors of the factors, either host or viral, which were strongly predictive of spontaneous clearance. Excessive alcohol intake, co-infection with HIV and black ethnicity have been linked to a decreased likelihood of spontaneous clearance (Thomas *et al*, 2000; Piasecki *et al*, 2004) whilst female sex (Alric *et al*, 2000; Micallef *et al*, 2006; Wang *et al*, 2007), symptomatic infection (Gerlach *et al*, 2003) and HBV co-infection (Piasecki *et al*, 2004) have been found to be significantly associated with HCV clearance.

Studies on the influence of HCV genotype have suggested that infection with genotype 1b is more likely to proceed to chronicity (Amoroso *et al*, 1998; Hwang *et al*, 2001). A study of male prisoners in Germany with a high prevalence of IDU (98%) found the prevalence of genotype 3 infection to be significantly higher among individuals who had cleared the virus (Lehmann *et al*, 2004). Thus these studies suggest that genotype 1 infections are less likely to clear than non-type 1 infections. A recent systematic review of 31 longitudinal studies, however, has found no association between viral clearance and infecting genotype (Micallef *et al*, 2006).

For an individual to be identified as a spontaneous clearer there must be an absence of HCV RNA in the serum. Studies of spontaneous HCV clearance have relied on routine methods of HCV RNA detection, and often do not state the sensitivity of the HCV quantitation/detection assays used. Increasing the sensitivity of HCV RNA detection is possible by ultracentrifugation of the serum prior to nucleic acid extraction (Forman and Valsamakis, 2004; Bartolomé *et al*, 2007). McHutchinson *et al*, (1999) used ultracentrifugation of serum samples, prior to extraction, to look for the presence of HCV RNA in patients who had relapsed following termination of therapy. Using this technique, they detected HCV RNA in 58% of relapser patients (n=12) at week 12 and 50% (n=14) at week 24. These specimens had all been negative by routine HCV PCR. The HCV quantitation assay described in this Chapter and utilised for the HCV clearance study, demonstrates excellent sensitivity (25 IU/ml, section 3.4.8). However, to guarantee HCV RNA negativity in the serum of presumed spontaneous clearers, serum specimens from this cohort were subjected to routine HCV RNA detection and then re-tested using this method following serum ultracentrifugation prior to nucleic acid extraction. Neither method detected HCV RNA in the sera from any of the spontaneous clearers in the cohort.

The possibility of occult HCV infection in individuals presumed to have cleared the virus cannot be ruled out. Occult HCV infection is a recently characterised entity which is defined as the presence of HCV RNA in the liver without serum HCV RNA (Castillo *et al*, 2004). It can be recognised in two clinical situations: in anti-HCV negative, serum HCV RNA negative patients with abnormal LFTs, and in anti-HCV positive subjects with normal LFTs and without serum HCV-RNA (Carreño, 2006). In a study on presumed spontaneous clearers (anti-HCV

positive, serum HCV-RNA negative patients with normal LFTs), the genomic HCV RNA strand was detected in the liver of 85% of these individuals (n=12), with HCV replication in all of these patients (Carreño *et al*, 2006). Interestingly, all the infections were found to be with subtype 1b. These findings suggest that the term 'spontaneous clearer' must be used with care, as these individuals may still have genomic HCV RNA in their liver tissue.

The study described herein supplemented the recent work of Harris and colleagues (2007). They had ascertained the infecting type in a large cohort of individuals who were chronically infected with HCV (n=508) or had spontaneously resolved their infection (n=96). This study demonstrated that the prevalence of genotype 1 in those who had cleared the virus was 69% and in those that had remained HCV RNA positive was 51%, suggesting that individuals with HCV genotype 1 infections were more likely to spontaneously clear the virus than those infected with non-1 types (OR 0.47, 95% CI 0.29–0.78, P= 0.003). The cohort used in this study (Harris *et al*, 2007) consisted of patients enrolled in the UK HCV National Register. Most of these patients (90%) had been traced during the National HCV Lookback Programme and had acquired their infection at a known date via transfusion of infected blood (prior to routine HCV screening) (Harris *et al*, 2000). Unlike the study of Harris *et al* (2007), many of the patients in the present study would have been ascertained by virtue of their clinical symptoms and hence referred to the hepatology clinic for further investigation post testing. As such, cohorts of patients from tertiary referral centres are more likely to be biased towards symptomatic disease. Also, unlike in the study by Harris and colleagues, date of infection would be a crude estimate, as high risk activities would give an uncertain date for HCV transmission.

The results from the HCV clearance study described in this chapter support the findings of Harris and colleagues (2007) and strengthen the argument that genotype 1 infections are more likely to clear spontaneously. Infecting genotype was significantly associated with PCR negativity in both univariable and multivariable statistical analyses. Individuals who had type 1 infections were nearly twice (1.8x) as likely to clear them. An additional finding suggested that those who acquired their infections at a younger age were more likely to clear them, with the risk of clearing nearly doubling (1.8x) for every 10 years younger individuals were at infection. One hundred and seventy five individuals were included in the multivariable analysis (62.5% of the 280 individuals genotyped/serotyped for the study). Non-inclusion in this analysis (n=105) was the result of missing data relating to unknown dates of infection for many of the individuals in the cohort. Although, a comparison of the clinical characteristics of individuals included in the multivariable analysis with those excluded from the study (Appendix D) did reveal a number of statistical differences between the two groups, none of these differences were likely to invalidate the findings of the study.

The indication that genotype 1 infections are more likely to clear than non-type 1 infections is contrary to other studies (Amoroso *et al*, 1998; Hwang *et al*, 2001; Lehmann *et al*, 2004). Although viral clearance could be more likely in genotype 1 infections, it is thought that, in those individuals with a chronic genotype 1 infection, disease may be more severe (Nousbaum *et al*, 1995; Pozzato *et al*, 1994; Lopez-Labrador *et al*, 1997; Tanaka *et al* 1998; Harris *et al*, 2007). The link between younger age at infection and increased likelihood of HCV clearance, demonstrated in the study described herein, does not appear to have been previously reported in the literature. However, younger age at

infection has recently been found to be associated with spontaneous clearance in childhood HCV infection (Yeung *et al*, 2007) and older age at infection is thought to be linked to increased risk of progression to cirrhosis (Minola *et al*, 2002). It is pertinent to mention that in the study described herein the age of infection was, for the majority, a crude estimate which relied on each individual's recollection of risk incident. For those, such as IDUs, who are continually involved in risk behaviour, the age of infection may be highly inaccurate. The association between younger age at infection and increased likelihood of clearance is not surprising as the immune system is more responsive and able to fight infection at a young age and degenerates during the ageing process.

This study has demonstrated that age at infection and HCV genotype are factors which are strongly associated with the ability to clear HCV spontaneously. In theory, this could be used as factors in identifying individuals who are likely to clear the virus spontaneously, without the need for treatment. However, these factors are likely to be only two of a number of factors which work together to influence the outcome of HCV infection.

3.7 Summary

The primary aim of the research described in this chapter was to develop an HCV diagnostic/monitoring service to support clinical practice, using the latest real-time PCR technology. This aim was achieved with:

- Development of a state-of-the-art HCV genotyping assay, one of the first to be described and the first published report of using Taqman probes for HCV genotyping (Rolfe *et al*, 2005). The HCV genotyping assay has

been continually updated and improved and it will shortly form part of a Hepatitis C Virus protocols book (Rolfe *et al*, in press).

- Development of an accurate HCV quantitation assay with an internal control to prevent false-negatives. The internal control can also be used effectively in other RNA virus detection/quantitation assays (Rolfe *et al*, 2007).
- Development of an HCV subtyping assay, shortly to be published, (Rolfe *et al*, in press) which has already proved its worth in resolving a possible nosocomial HCV transmission investigation.

In addition the application of these techniques to elucidate the role of HCV genotype in spontaneous clearance of HCV has supported earlier work (Harris *et al*, 2007) in suggesting a link between HCV genotype 1 and spontaneous resolution of HCV infection. It has also provided new evidence, not reported in the literature of an association between younger age at infection and spontaneous viral clearance, which warrants further study.

In terms of future work, the epidemiology of HCV genotypes is dynamic and will continue to change. The HCV genotyping assay will need to be continually monitored to ensure that sequencing of isolates is kept at a minimum. If the sequencing burden increases, as genotypes such as 5 and 6 become more prevalent or as new variants arise, then the assay will need to be re-examined and further developed as appropriate. If knowledge of HCV subtype gains importance in terms of tailoring of interferon therapy or in identifying subtypes which are recalcitrant to therapy, then the same will apply to the HCV subtyping assay.

CHAPTER FOUR

Detection and Quantitation of mt^{4977} and mt^{7436} Mitochondrial DNA Deletions Using Real-time, Three-primer PCR

4.1 Overview

Oxidative stress within cells can result in damage to all cellular constituents including DNA, proteins and lipids. mtDNA is more vulnerable to oxidative damage than nuclear DNA (Yakes and Van Houten, 1997). mtDNA damage can be in the form of mutations, rearrangements, duplications and deletions. The most frequently examined mtDNA deletion is one of 4977 bp, referred to as the 'common deletion' or mt^{4977}. This deletion, spanning from nt 8469-13447, results in the damage or removal of major structural genes essential for the enzyme complexes of the OXPHOS pathway as well as five tRNA genes. A less prevalent, but well documented deletion is that of 7436 bp (identified henceforth as mt^{7436}), spanning from nt 8648-16085. Both of these deletions are flanked by homologous direct repeat sequences (Class I mtDNA deletions). For mt^{4977} this is 13 bp in length whilst for mt^{7436} it is 12 bp in length. It is thought that these repeat sequences create hot-spots for mtDNA deletion (Samuels *et al*, 2004).

The accumulation of both mt^{4977} and mt^{7436} in the ageing process is well documented (Lee *et al*, 1994; Zhang *et al*, 1998; Mohamed *et al*, 2006). The decrease in bioenergetic function seen in the ageing process is thought to result from the prolonged exposure of mtDNA to oxidative stress, resulting in the accumulation of mtDNA damage (Wei *et al*, 1998) – the so-called 'mitochondrial theory of aging' (Harman, 1972). Although the age-associated increase in these two deletions is well documented, the levels detected are extremely small (often <1%) (Wei *et al*, 1996; Corral-Debrinski *et al*, 1992). Cells can exist in a state of heteroplasmy where wild-type (wt) mtDNA subsists alongside damaged/deleted mtDNA. A deleterious effect is generally demonstrated once the proportion of damaged mtDNA rises above a threshold. This threshold level

varies from 50-90% depending on the mutation and tissues concerned (Hayashi *et al*, 1991; Porteous *et al*, 1998; Sciacco *et al*, 1994).

HCV infection is known to produce large amounts of cellular oxidative stress leading to increased DNA damage (Farinati *et al*, 1999; Kitada *et al*, 2001; Cardin *et al*, 2001). This is thought to be due to the effects of the virus itself, especially the core and NS5a proteins (Machida *et al*, 2004, 2006; Gong *et al*, 2001; Korenaga *et al*, 2005; Okuda *et al*, 2002; Otani *et al*, 2005) and the body's inflammatory response to HCV infection (Larrea *et al*, 1998). Respiratory chain defects have also been observed in the cirrhotic liver, suggesting damage to mitochondria (Müller-Höcker *et al*, 1997; Barbaro *et al*, 1999). Cells chronically infected with HCV could, therefore, be expected to demonstrate high levels of mtDNA deletions resulting from the long-term exposure to oxidative stress.

Early studies relied on visualisation of amplicons on agarose gel or by southern blot analysis to quantify mtDNA deletions. Neither of these methods is particularly accurate and southern blot analysis lacks the sensitivity necessary for detecting low level mtDNA deletions. Attention has turned to methods which can both detect and quantify mtDNA deletions relative to wt mtDNA (Pogozelski *et al*, 2003; Bai and Wong, 2005). This chapter describes the development of real-time PCR assays to detect and quantify mt^{4977} and mt^{7436}. The assays are based on the three-primer PCR method described by Sciacco and colleagues (Sciacco *et al*, 1994) which has been transferred to a real-time PCR platform for this study. Quantitation of the deletions and of wt mtDNA is achieved by reference to plasmid standards containing known quantities of the specific

mtDNA amplicon; with the quantity of each deletion calculated relative to wt mtDNA.

This chapter describes the application of the fully optimised assays to study the extent of mtDNA damage – in the form of major deletions – in the livers of patients chronically infected with HCV. The cohort studied includes 79 patients undergoing liver biopsy as part of routine investigations at Addenbrooke's Hospital between 2005 and 2007. These individuals all suffer from liver disease due to HCV or an alternate liver pathology. This study investigates whether the high level of oxidative stress reported in HCV infection results in increased mtDNA damage in comparison to other liver aetiologies.

4.2 Development of experimental procedures

4.2.1 Ethical approval

Prior to commencement of the study, ethical approval was obtained from the Cambridge Local Research Ethics Committee (LREC) (LREC reference number 04/Q0108/124, Appendix E) and the study was approved by the Addenbrooke's Hospital Research and Development Office. Patients were given an information sheet and a consent form to sign prior to inclusion in the study (Appendix F).

4.2.2 Analysis of various homogenisation/extraction methods to isolate DNA from liver biopsy specimens

Several methods and combinations for tissue homogenisation and nucleic acid extraction were assessed to determine which produced the best yield of total DNA from liver biopsy specimens. Two methods of homogenisation were tested – manual and automated (Section 2.3). Four extraction methods were evaluated (Section 2.4). Three of these were manual extraction protocols - using (i) Trizol® reagent, (ii) QIAamp Viral RNA kit or (iii) DNeasy® Blood and

Tissue kit. The fourth method was automated extraction using the Qiagen Bio Robot MDx. The protocols were all carried out on 1 mg of fresh pig's liver, to ensure consistency of results and to conserve human liver tissue samples. Figure 4.1 illustrates the yields achieved by the various combinations of homogenisation and extraction methods. Regardless of extraction protocol, automated homogenisation was found to be superior to manual homogenisation, in terms of yield of DNA. Of the three extraction procedures tested, manual extraction using the DNeasy Blood and Tissue kit was deemed the best in terms of ease, quality and yield of DNA. The major problem with the Trizol® reagent extraction procedure was the poor re-suspension of the DNA pellet. This was not achieved successfully despite different approaches to aid solubilisation including overnight incubation at room temperature, 4°C or heating to 60°C. Automated extraction using the Qiagen Bio Robot MDx was comparable to the manual method using the DNeasy® Blood and Tissue kit in terms of quality and yield of extracted DNA. However, the manual method was more suitable for use on small batches of liver biopsy specimens, and was therefore selected for DNA extraction in this study.

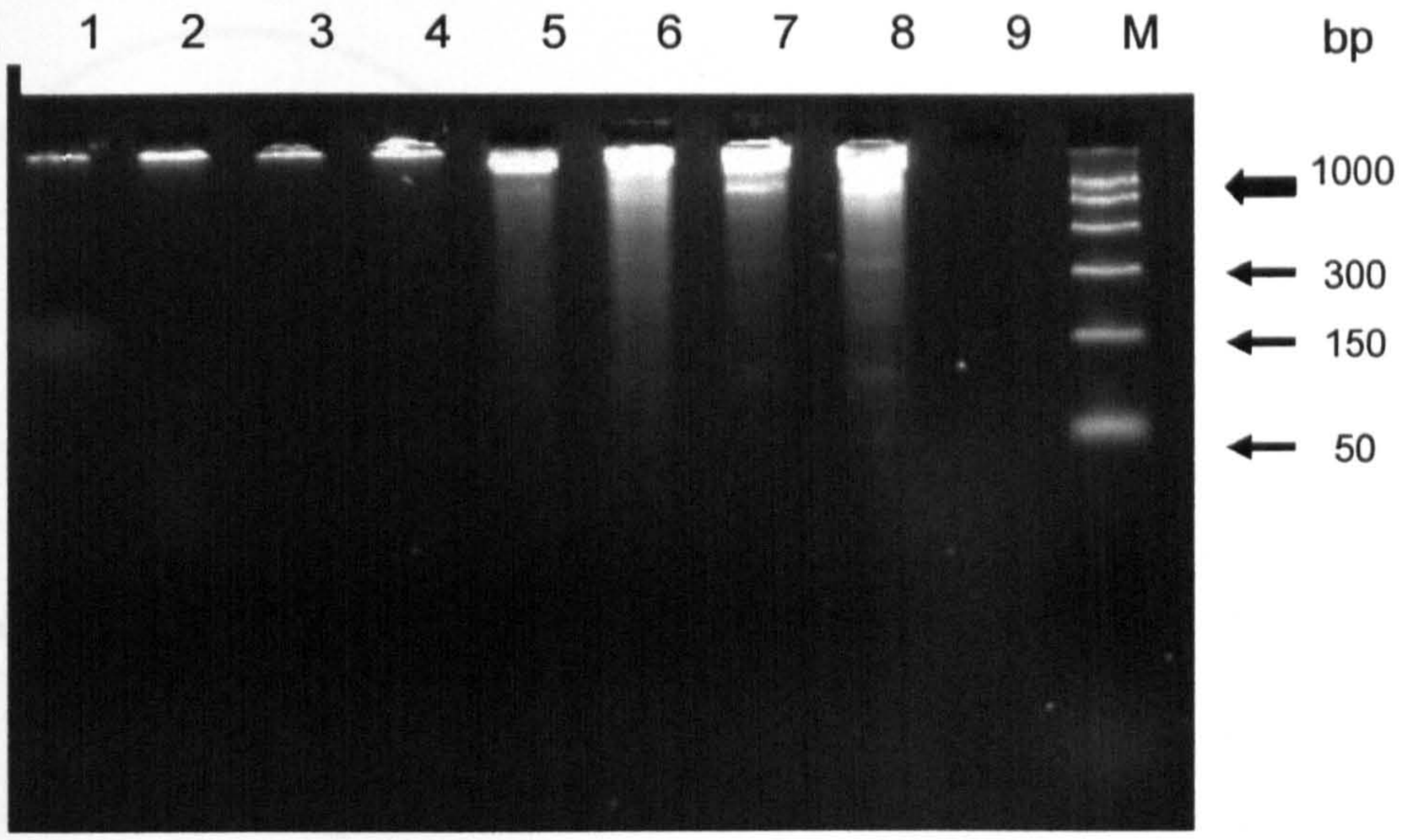

Figure 4.1: Agarose gel electrophoresis of DNA yields from different homogenisation/extraction methods. Lanes 1-4; manual homogenisation, lanes 5-8; automated homogenisation. Lanes 1 and 5; Trizol® extraction, lanes 2 and 6; QIAamp Viral RNA kit, lanes 3 and 7; Qiagen Bio Robot MDx; lanes 4 and 8; DNeasy® kit. Lane 9; water, M; PCR markers, bp; base pairs.

4.2.3 Primer design

The method used for quantitation of mtDNA deletions in this study is based on three-primer PCR, an approach developed by Sciacco and colleagues (Sciacco *et al*, 1994). As its name suggests and as illustrated in Figure 4.2, this method requires three primers. Primer 1 is common to both deletion and wt mtDNA amplification products and hybridises to a region outside the deletion. Primer 2 hybridises to a region inside the deletion, and primer 3 to the other side of the breakpoint from primer 1. Primers 1 and 2 amplify a region representing wt mtDNA. Primers 1 and 3 are located sufficiently far apart so that an amplification product is produced only if a large mtDNA deletion has taken place.

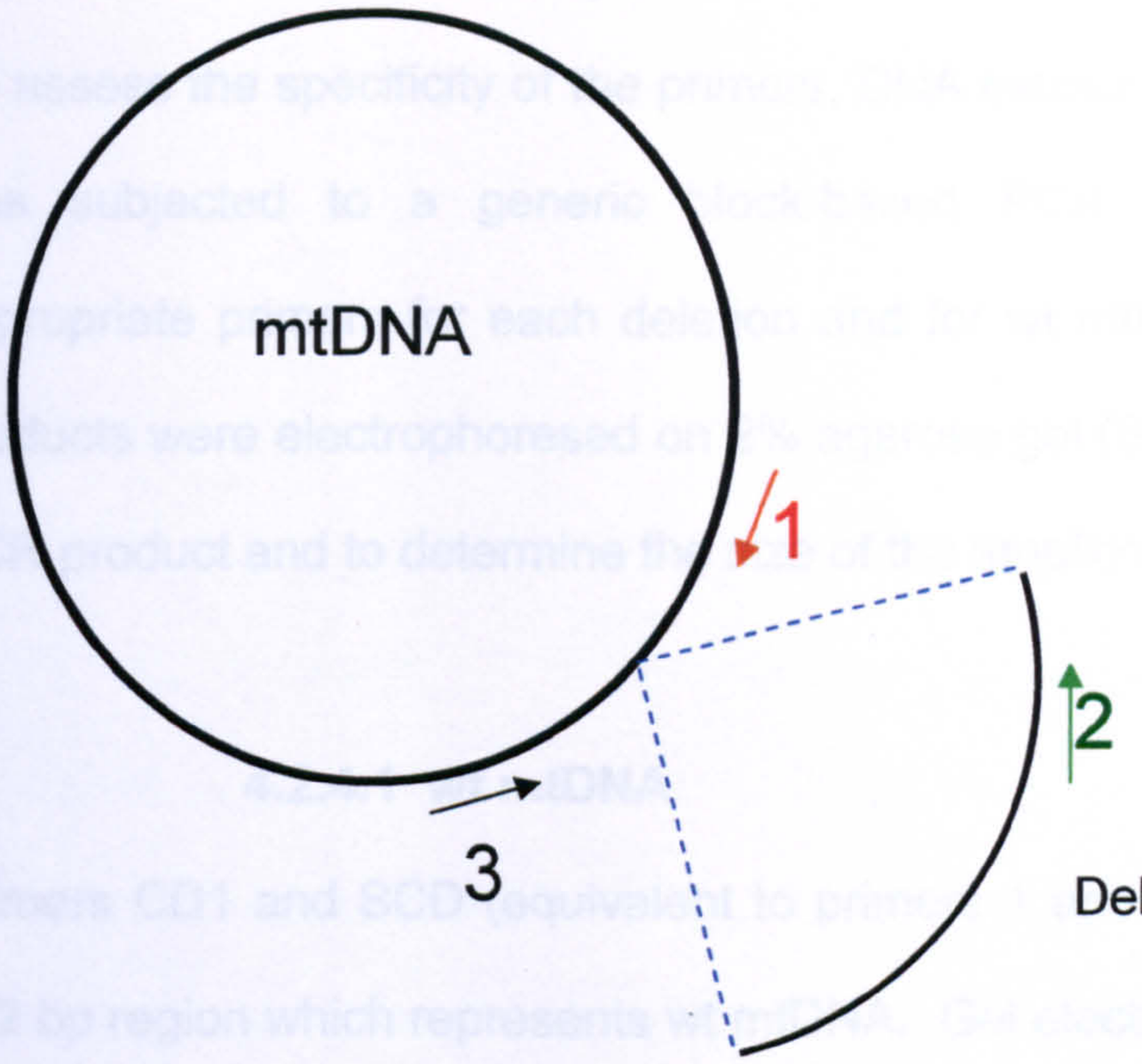

Figure 4.2: Schematic representation of three-primer PCR. The mtDNA molecule illustrated has a large deletion. The deletion is detected using primers 1 and 3 which are only in sufficiently close proximity for amplification if the mtDNA molecule harbours the deletion. Amplification of wt (undeleted) mtDNA with primers 1 and 2 will only occur if the deletion is not present, as the primer 2 site is within the deleted region.

All primers were designed according to general published guidelines (Innis and Gelfand, 1990) using the revised Cambridge Reference Sequence (rCRS) (accession number AC_000021) of the mitochondrial genome. To avoid positioning the primers at sites with a high frequency of polymorphisms, the Human Mitochondrial Genome Database (mtDB), available at http://www.genpat.uu.se/mtDB/index.html was consulted. This identifies the polymorphisms at each nucleotide site within the mtDNA genome and their frequency. The primers for mt^{4977} detection and quantitation (CD1, CD2 and SCD) are based around those of Ross and colleagues (Ross *et al*, 2002) which were originally designed to quantify mt^{4977} using a conventional (block-based) PCR approach. These primers were modified to increase their melting temperature. All primer sequences are given in Appendix B.

4.2.4 PCR specificity

To assess the specificity of the primers, DNA extract from several liver biopsies was subjected to a generic block-based PCR (Appendix C) using the appropriate primers for each deletion and for wt mtDNA detection. The PCR products were electrophoresed on 2% agarose gel (Section 2.7) to visualise the PCR product and to determine the size of the amplicon.

4.2.4.1 wt mtDNA

Primers CD1 and SCD (equivalent to primers 1 and 2 in Figure 4.2) amplify a 412 bp region which represents wt mtDNA. Gel electrophoresis following block-based PCR amplification using the CD1-SCD primer pair demonstrated one amplification product of the correct size for each DNA extract (Figure 4.3). To confirm the specificity of the PCR assay, the amplified fragments were sequenced as described (Section 2.21) and were confirmed as wt mtDNA sequence.

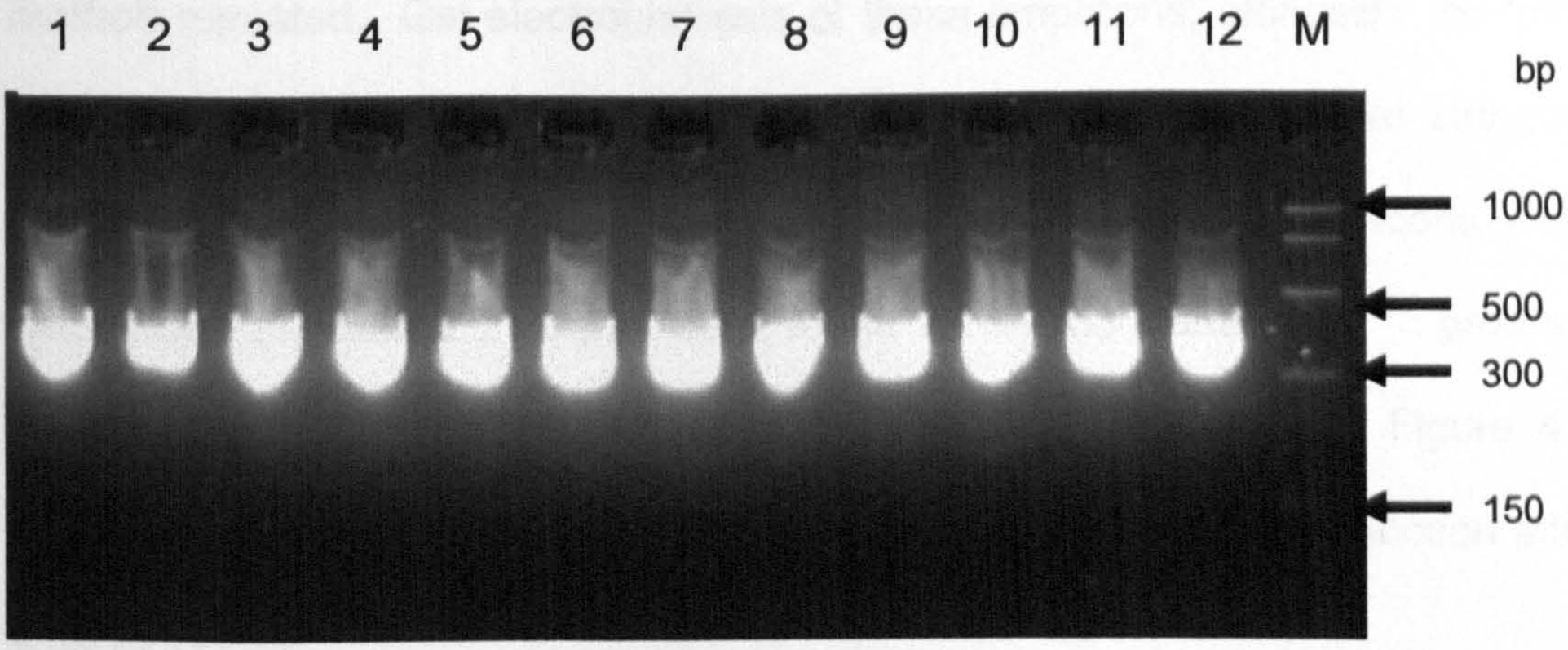

Figure 4.3: Image of wt mtDNA PCR products following separation on a 2% agarose gel. Lanes 1-12; liver DNA extracts, M; PCR markers, bp; base pairs

4.2.4.2 mt^{4977}

Primers CD1 and CD2 (equivalent to primers 1 and 3 in Figure 4.2) are designed to amplify a 271 bp region flanking mt^{4977}. Gel electrophoresis following block-based PCR amplification using the CD1-CD2 primer pair demonstrated a single band on the gel, which appeared to be of the correct size. Sequencing of the amplicons (Section 2.21) identified that a mis-priming event had occurred. The CD1 primer had annealed at a site similar in sequence to the target site and this had resulted in the amplification of a PCR product of 247 bp. This was 24 bp smaller than that expected. The site of mis-annealing was seen to be within the mt^{4977} deletion site, thus if efficient amplification was occurring then it would be expected that the isolated levels would be as high as seen with wt mtDNA. The low level of the misprime PCR product, compared to wt mtDNA, indicated that amplification was not efficient due to the reduced complementarity of the CD1 primer and the site to which it (mis)-anneals.

The stringency of the block-based PCR was increased (Appendix C) and the method repeated. Gel electrophoresis of these amplicons, alongside the 'mis-prime' product indicated that the PCR products formed using more stringent conditions were slightly larger (Figure 4.4, lane 9). These amplicons were sequenced (Section 2.21) and were found to be the correct mt^{4977} product. These all had identical sequences at the deletion junction site. Figure 4.5 shows a section of the sequence data, demonstrating the deletion junction after a 13 bp repeat.

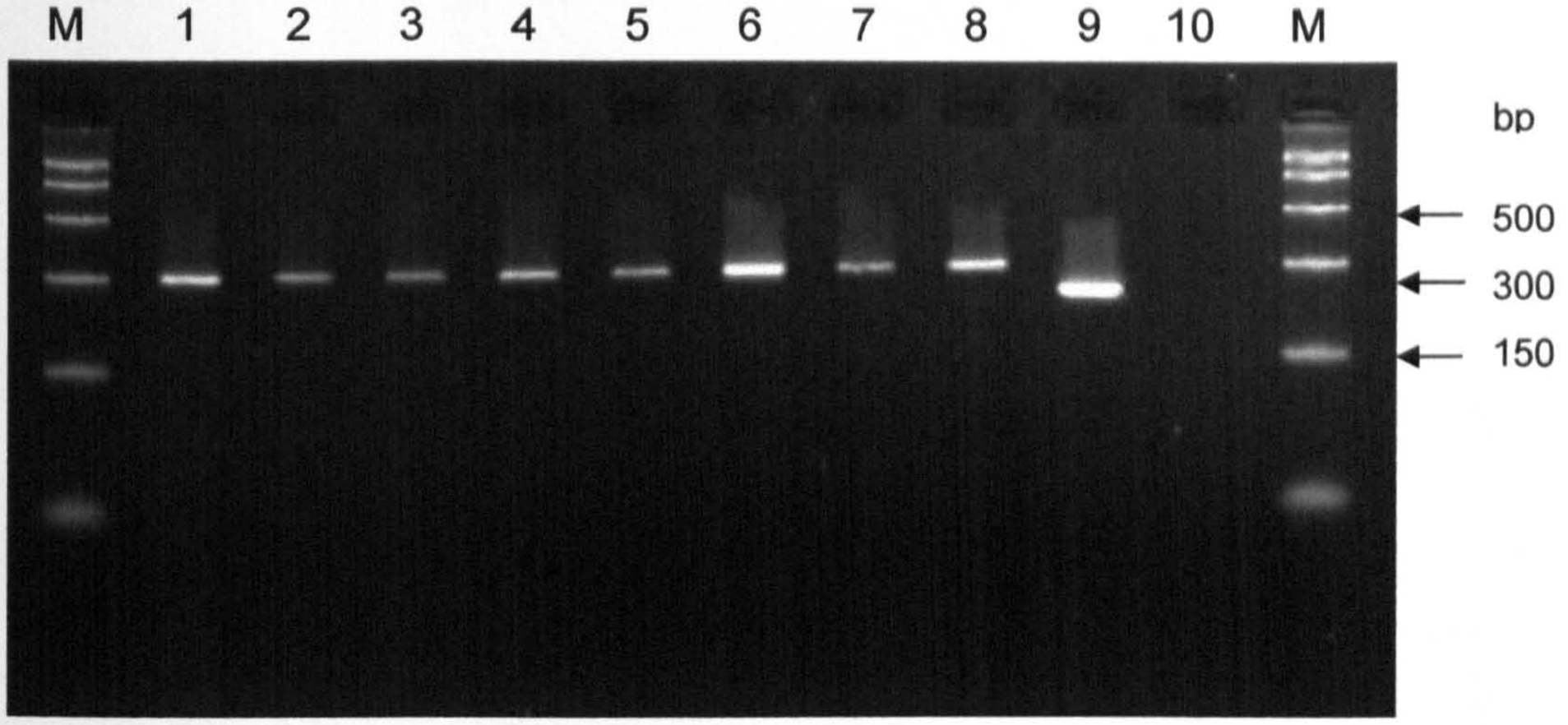

Figure 4.4: Image of mt^{4977} mtDNA PCR products following separation on a 2% agarose gel. Lanes 1-8; liver biopsy samples, lane 9; misprime amplicon, lane 10; water. M; PCR markers. All products were sequenced to confirm identity.

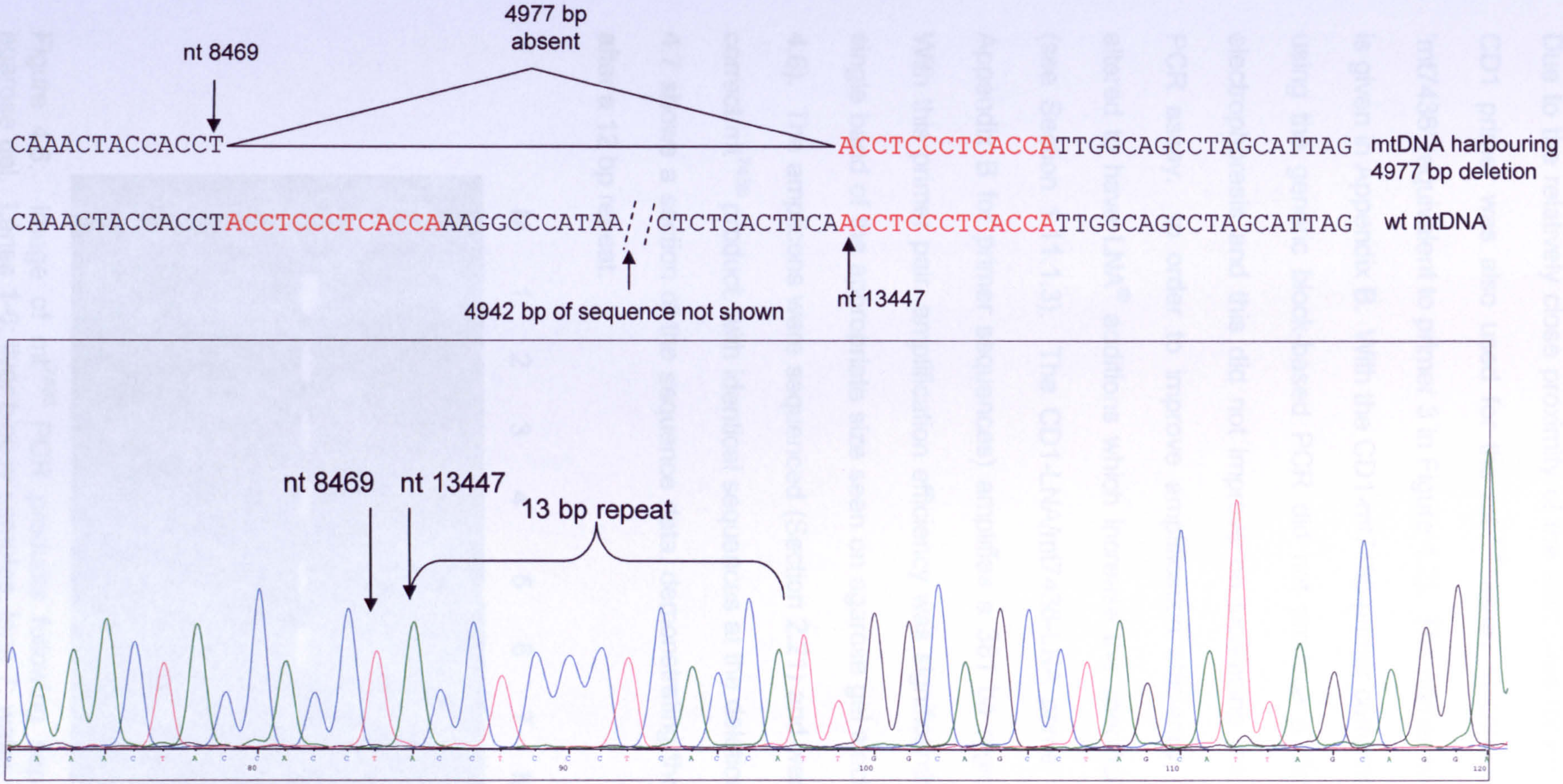

Figure 4.5: Sequence data from an mt^{4977} amplicon, indicating the specificity of the amplification and demonstrating the site of the deletion between a 13 bp repeat. One of the repeat sequences is removed in the deletion. The wt mtDNA sequence is also shown. The 13 bp repeat is indicated in red type.

4.2.4.3 mt^{7436}

Due to the relatively close proximity of the start sites for mt^{4977} and mt^{7436}, the CD1 primer was also used for the mt^{7436} assay in combination with primer 'mt7436' (equivalent to primer 3 in Figure 4.2). The primer sequence of mt7436 is given in Appendix B. With the CD1-mt7436 primer combination, amplification using the generic block-based PCR did not produce a distinct band on gel electrophoresis and this did not improve on increasing the stringency of the PCR assay. In order to improve amplification efficiency, the primers were altered to have LNA® additions which increase the specificity of hybridisation (see Section 1.11.1.3). The CD1-LNA/mt7436-LNA primer combination (see Appendix B for primer sequences) amplifies a 381 bp region flanking mt^{7436}. With this primer pair, amplification efficiency was significantly improved with a single band of the appropriate size seen on agarose gel electophoresis (Figure 4.6). The amplicons were sequenced (Section 2.21) and were found to be the correct mt^{7436} product, with identical sequences at the deletion junction. Figure 4.7 shows a section of the sequence data, demonstrating the deletion junction after a 12 bp repeat.

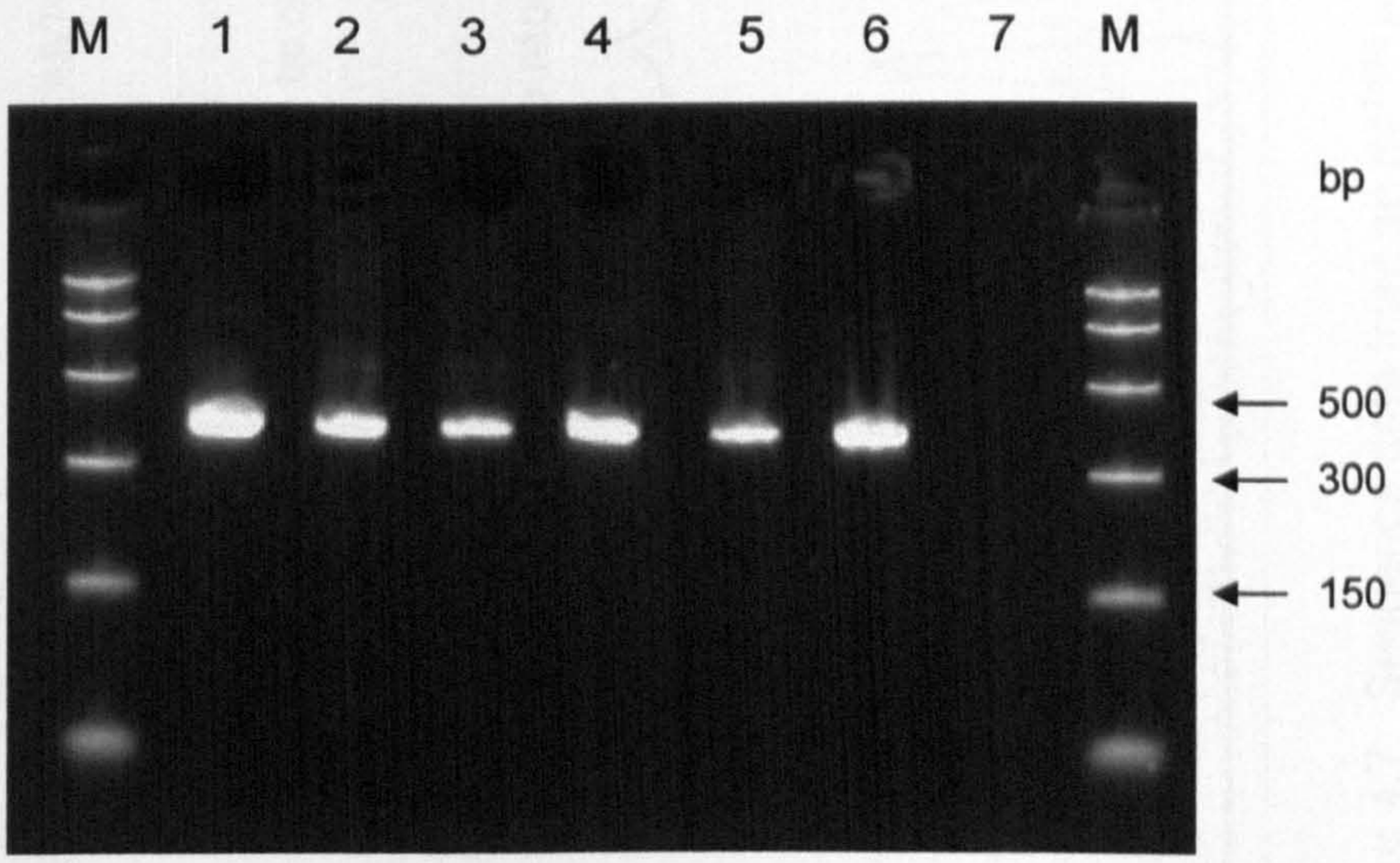

Figure 4.6: Image of mt^{7436} PCR products following separation on a 2% agarose gel. Lanes 1-6; liver biopsy samples, lane 7; water, M; PCR markers. All products were sequenced to confirm identity.

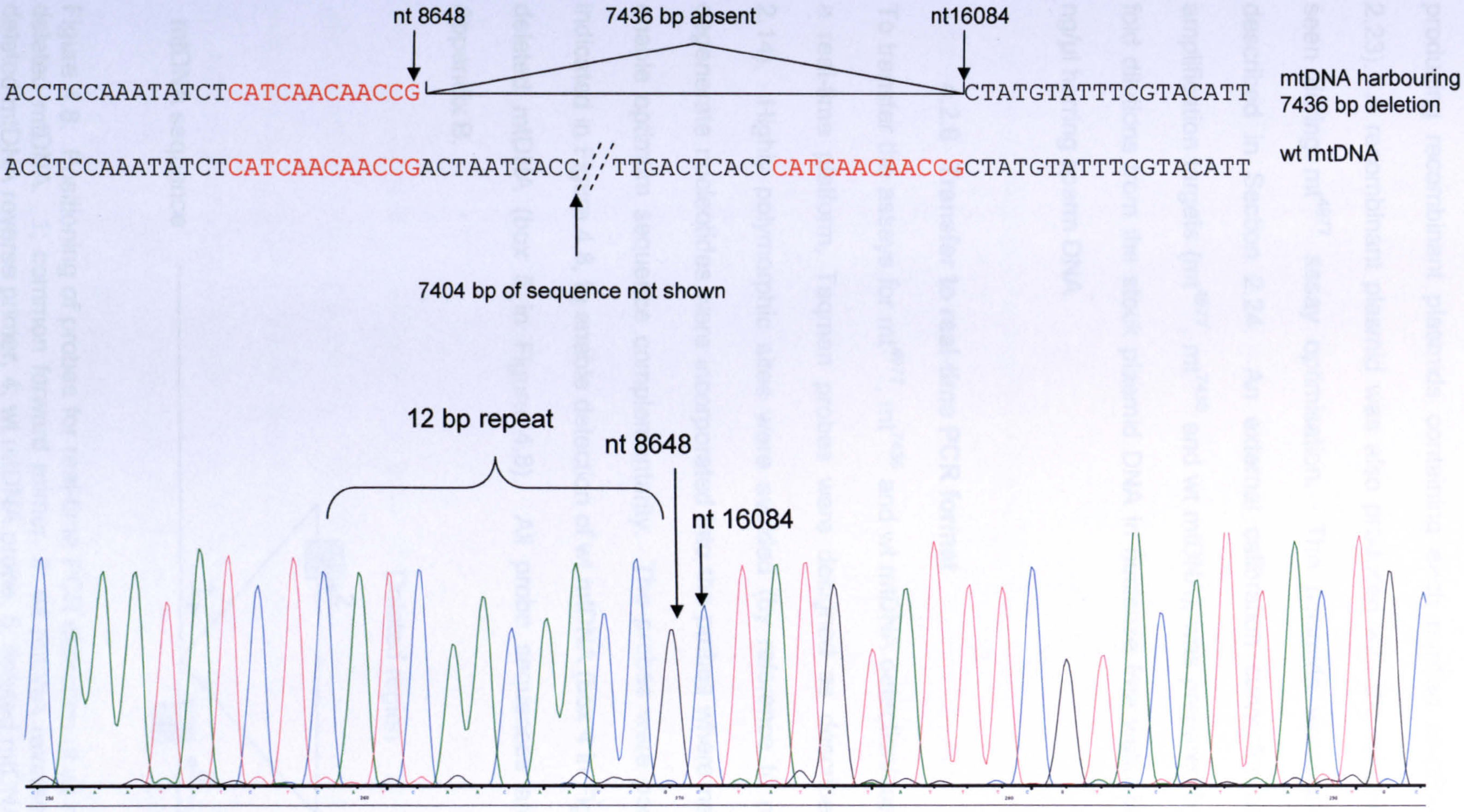

Figure 4.7: Sequence data from an mt^{7436} amplicon, indicating the specificity of the amplification and demonstrating the site of the deletion directly after a 12 bp repeat. The wt mtDNA sequence is also shown. The 12 bp repeat is indicated in red type.

4.2.5 Production of plasmid standards

The wt and deleted (mt^{4977} and mt^{7436}) mtDNA standards were constructed by producing recombinant plasmids containing each purified amplicon (Section 2.23). A recombinant plasmid was also produced with the misprime product seen during mt^{4977} assay optimisation. The plasmids were quantified as described in Section 2.24. An external calibration curve for each of the amplification targets (mt^{4977}, mt^{7436} and wt mtDNA), was prepared by serial 10-fold dilutions from the stock plasmid DNA in nuclease free water containing 1 ng/µl herring sperm DNA.

4.2.6 Transfer to real-time PCR format

To transfer the assays for mt^{4977}, mt^{7436} and wt mtDNA detection/quantitation to a real-time platform, Taqman probes were designed as described (Section 2.14). Highly polymorphic sites were avoided (by reference to mtDB), and degenerate nucleotides were incorporated into the probes where necessary to enable optimum sequence complementarity. The probes were positioned as indicated in Figure 4.8, to enable detection of wt mtDNA (box 4 in Figure 4.8) or deleted mtDNA (box 5 in Figure 4.8). All probe sequences are given in Appendix B.

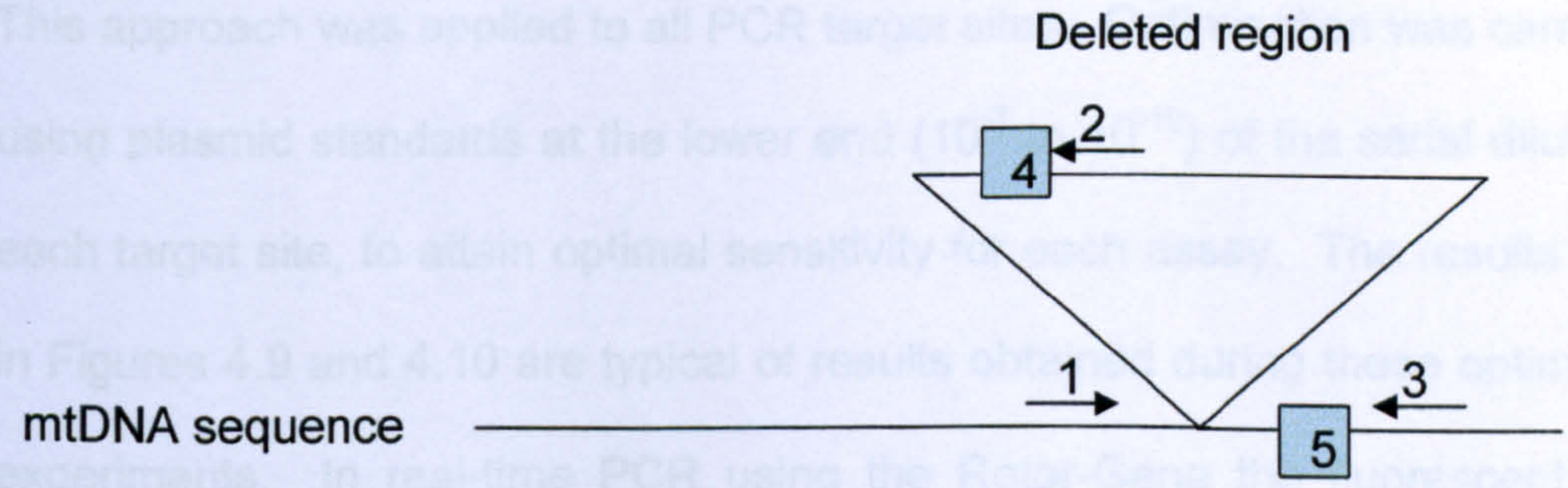

Figure 4.8: Positioning of probes for real-time PCR detection of wt mtDNA and deleted mtDNA. 1; common forward primer, 2; wt mtDNA reverse primer, 3; deleted mtDNA reverse primer, 4; wt mtDNA probe, 5; deleted mtDNA probe.

4.2.7 Optimisation of PCR assays

For each primer pair used in this study, optimal PCR reagent and cycling conditions were achieved by varying the concentration of $MgCl_2$, primers and probes and by experimenting with various annealing temperatures (Section 2.16). To determine the appropriate annealing temperature for each primer set, the starting annealing temperature was taken at 5°C below the average melting temperature (Tm) for each primer set. The temperature was then increased or decreased by increments of 2°C to achieve optimum yield of product.

Once the appropriate annealing temperature was established, the product intensity was improved by applying the following reagent titration experiments:

(i) titration of $MgCl_2$ at 1.0 mM, 1.5 mM, 2.0 mM, 2.5 mM, 3 mM, 3.5 mM and 4 mM. (Figure 4.9)

(ii) variation of primer concentration at 0.15 μM, 0.2 μM and, 0.3 μM

(iii) variation of the concentration of one primer with respect to the other, depending on whether the probe annealed to the plus or minus DNA strand (Figure 4.10)

(iv) variation of probe concentration

This approach was applied to all PCR target sites. Optimisation was carried out using plasmid standards at the lower end (10^{-7} to 10^{-10}) of the serial dilution for each target site, to attain optimal sensitivity for each assay. The results shown in Figures 4.9 and 4.10 are typical of results obtained during these optimisation experiments. In real-time PCR using the Rotor-Gene the fluorescent signal (Figures 4.9 and 4.10, y axis) increases in direct proportion to the amount of PCR product in the reaction. The initial copy number can be calculated from the cycle number (Figures 4.9 and 4.10, x axis) at which a detection threshold is

crossed; the threshold cycle (C_T). Each PCR assay was optimised to produce the best fluorescent signal and the highest C_T for each of the plasmid standards, to attain optimal sensitivity to detect very low levels of mtDNA deletions. The fully optimised master mixes and Rotor-Gene conditions for each of the assays are outlined in Appendix C.

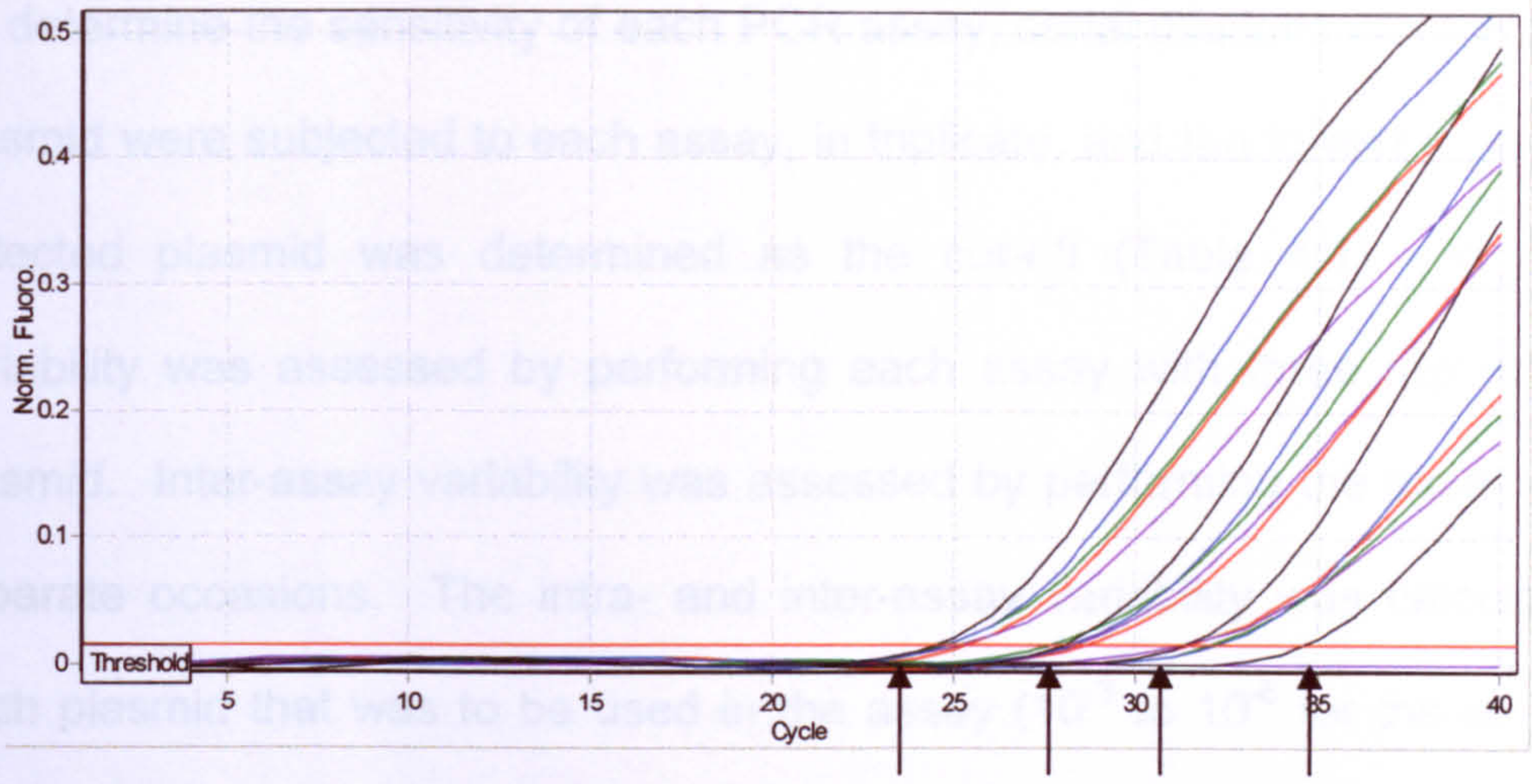

Figure 4.9: Optimisation of mt^{4977} assay - titration of $MgCl_2$. Black line; 4 mM $MgCl_2$, blue line; 3.5 mM $MgCl_2$, green line; 3 mM $MgCl_2$, red line; 2.5 mM $MgCl_2$, purple line; 2 mM $MgCl_2$. At 1 mM $MgCl_2$ all were negative. A serial dilution of plasmid standards at the lower end (10^{-7} to 10^{-10}) was used for optimisation experiments. Note the increased sensitivity at 4 mM, with the detection of the lowest plasmid dilution (10^{-10}), which is missed with the other titrations.

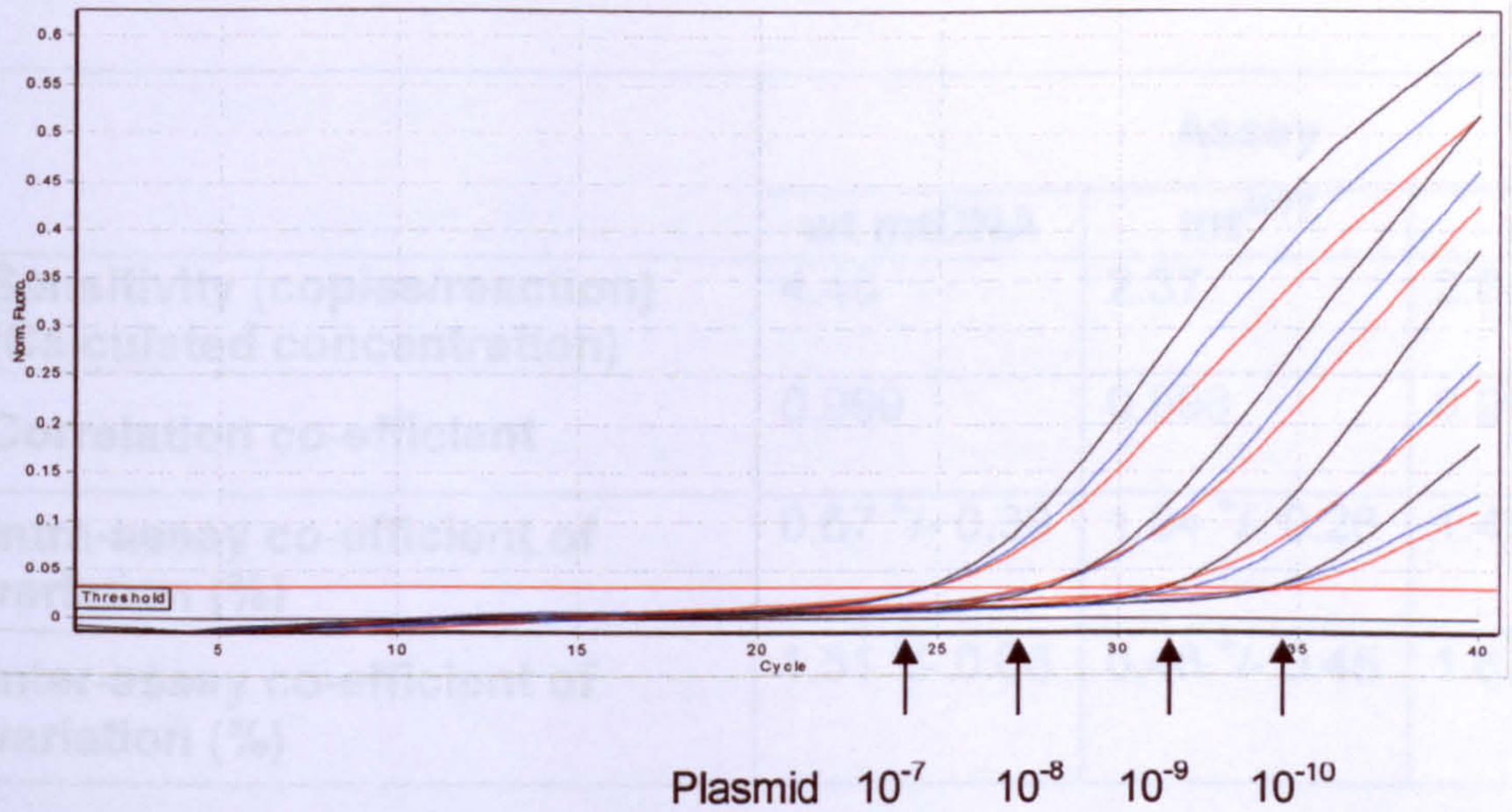

Figure 4.10: Optimisation of mt^{4977} assay - varying one primer with respect to the other. In this example the probe anneals to the reverse strand and so increasing the concentration of the reverse primer improves the Ct and shape of the curve. Black line; 10 pmol forward primer and 20 pmol reverse primer, Blue line; 20 pmol forward primer and 10 pmol reverse primer, red line; 10 pmol forward primer and 10 pmol reverse primer.

4.2.8 Sensitivity and reproducibility of the real-time PCR assays

To determine the sensitivity of each PCR assay, serial dilutions of each specific plasmid were subjected to each assay, in triplicate, and the lowest reproducibly detected plasmid was determined as the cut-off (Table 4.1). Intra-assay variability was assessed by performing each assay with three replicates per plasmid. Inter-assay variability was assessed by performing the assay on four separate occasions. The intra- and inter-assay variability was calculated for each plasmid that was to be used in the assay (10^{-3} to 10^{-6} for the wt mtDNA assay and 10^{-6} to 10^{-10} for the mt^{4977} and mt^{7436} assays. The intra- and inter-assay co-efficient of variation was calculated (Table 4.1). Each PCR assay could detect down to single copy numbers of deleted (mt^{4977} and mt^{7436}) or wt mtDNA. The intra- and inter-assay variability was in the region of 1% for each of the assays as shown in Table 4.1.

	Assay		
	wt mtDNA	**mt^{4977}**	**mt^{7436}**
Sensitivity (copies/reaction) (Calculated concentration)	4.40	2.37	2.86
Correlation co-efficient	0.999	0.998	0.999
Intra-assay co-efficient of variation (%)	0.67 +/- 0.39	1.04 +/- 0.26	1.49 +/- 0.67
Inter-assay co-efficient of variation (%)	1.51 +/- 0.66	0.46 +/- 0.45	1.67 +/- 0.59

Table 4.1: The sensitivity, inter- and intra-assay variability of the mt^{4977}, mt^{7436} and wt mtDNA detection/quantitation assays.

4.2.9 Normalisation of data

Normalisation of data was carried out by reference to the ß-globin gene, a single copy-number chromosomal gene (2 copies/human genome) with an assay used routinely in the diagnostic laboratory (Dr Hamid Jalal, personal communication). This is a real-time PCR assay which utilises a series of four plasmid standards with known quantity of ß-globin DNA (1.7 to 1700 copies/µl) to quantify the gene in clinical specimens. An external calibration curve for the β-globin amplification target was prepared by serial 10-fold dilutions from the stock DNA in nuclease free water containing 1 µg/µl poly A RNA. Primers, probes and Rotor-Gene conditions for this assay are described (Appendices B and C). Total mtDNA content was calculated by the ratio of wt mtDNA: ß-globin. This pins the data to a reference and ensures that mitochondrial proliferation/depletion had not occurred within the cells.

4.3 Clinical study

4.3.1 Cohort characteristics

Liver biopsy specimens were collected from patients undergoing this procedure in the Planned Short Stay Unit (PSSU) at Addenbrooke's Hospital, as part of their clinical management, between May 2005 and August 2007. Following the stipulations of the ethical approval, liver biopsies were only collected from patients who were aged between 18 and 75 years, had been given a patient information sheet (Appendix F) to allow informed decision and had given their written consent (Appendix F) for their biopsy to be stored and used for this study. Biopsy specimens were only received when there was sufficient material for research analysis over and above that required for standard diagnostic pathology.

A total of 79 liver biopsies were collected for this study. The male to female ratio was 2.3:1. The patients were aged between 20 and 70 years, with an average age of 46.2 years. Forty-two (53.2%) of the patients had undergone a liver biopsy due to HCV infection either as the sole aetiology (n=32) or in association with another liver pathology (n=10). Thirty seven (46.8%) had undergone liver biopsies for other liver pathologies. Table 4.2 outlines the clinical characteristics of the patient cohort described in this study. Further cohort characteristics are given in Appendix G.

	Number	Average age (years)	Male: female
HCV	32	46.4 (30-70)	5:3
HCV + HBV	2	44.8 (26-63)	9:1
HCV + HIV	1		
HCV + alcohol	7		
	n=42		
HBV	8	33.8 (22-62)	3:1
NAFLD/NASH	5	48.4 (40-58)	5:0
Alcohol	10	54.4 (41-65)	7:3
Autoimmune	3	45.7 (20-66)	2:1
Other	11	47.3 (32-68)	6:5
	n=37		

Table 4.2: Clinical characteristics of the 79 patients from whom liver biopsy specimens were received for this study.

For each HCV-infected individual, the infecting genotype was identified using the Taqman HCV genotyping assay described in Chapter Three. Of the forty-two HCV infected individuals there were twenty-six (61.9%) genotype 1 infections, two (4.8%) genotype 2 infections, eleven (26.2%) genotype 3 infections and one (2.4%) genotype 4 infection. For two patients (4.8%), the HCV viral load was too low for HCV genotyping. For the virally infected individuals, the liver viral load was also determined. For the HCV-infected individuals, this was carried out using the HCV quantitation assay described in Chapter Three. HCV viral load varied from undetectable to 35,668,285 IU/ml.

The HBV viral load was determined using an assay already established within the diagnostic laboratory (Aliyu *et al*, 2004). HBV viral load varied from $3.4x10^3$ to $3.1x10^6$ IU/ml. The liver biopsy specimens all underwent histopathological investigation by Consultant Pathologists as part of standard diagnostic procedures. The pathology report for each liver biopsy specimen was interrogated to determine the stage of fibrosis within the sample (none, minimal, mild, mild/moderate, moderate, moderate/severe, severe or cirrhosis) and, in the case of specimens which had a viral aetiology, grade of inflammation was also recorded (none, minimal, minimal/mild, mild, mild/moderate, moderate).

4.3.2 mtDNA deletion detection/quantitation

Liver biopsy specimens were stored and the DNA extracted as described in Section 4.2. The extracted DNA from each liver biopsy was subjected to each assay, using the optimised conditions (Appendix C)

- mt^{4977} detection/quantitation
- mt^{7436} detection/quantitation
- wt mtDNA detection/quantitation
- ß Globin gene detection/quantitation

For each batch of livers, the assays to detect the deletions, wt mtDNA and the ß-globin gene were all carried out within days of each other to ensure no loss of accuracy due to DNA degradation following prolonged storage. For each liver biopsy, following real-time PCR, the amplicons were subjected to agarose gel electrophoresis (Section 2.7) as a safeguard to ensure specificity of amplification. A very low dilution of the 'misprime' plasmid was also included in the mt^{4977} assay to ensure that this event was not occurring in the real-time assay. Agarose gel electrophoresis of the 'misprime' amplicon and PCR products from the mt^{4977} assay indicated that all amplification products from the

liver biopsies were of the correct size. Ten PCR products from the $mt^{4977}$and mt^{7436} assays were sequenced (Section 2.21) as an extra safeguard to ensure specificity of amplification. The products all gave the expected sequence. The deletion junction of all the products was as expected for both the $mt^{4977}$and mt^{7436} deletions.

Appendix G gives a full summary of the results obtained for all 79 patients investigated in this study. Figures 4.11, 4.12 and 4.13 demonstrate typical real-time amplification Rotor-Gene reports for the mt^{4977}, mt^{7436} and wt mtDNA assays respectively. Quantitation of mt^{4977} and mt^{7436} was reported as a ratio of the quantity of the specific deletion to the quantity of wt mtDNA. For mt^{4977} this ranged from $2.14x10^{-3}$ to $1.84x10^{-6}$. In one liver (LB4), mt^{4977} could not be detected. For mt^{7436}, the ratio ranged from $2.6x10^{-4}$ to $2.38x10^{-7}$. mt^{7436} was not detected in 10 (12.7%) liver biopsies.

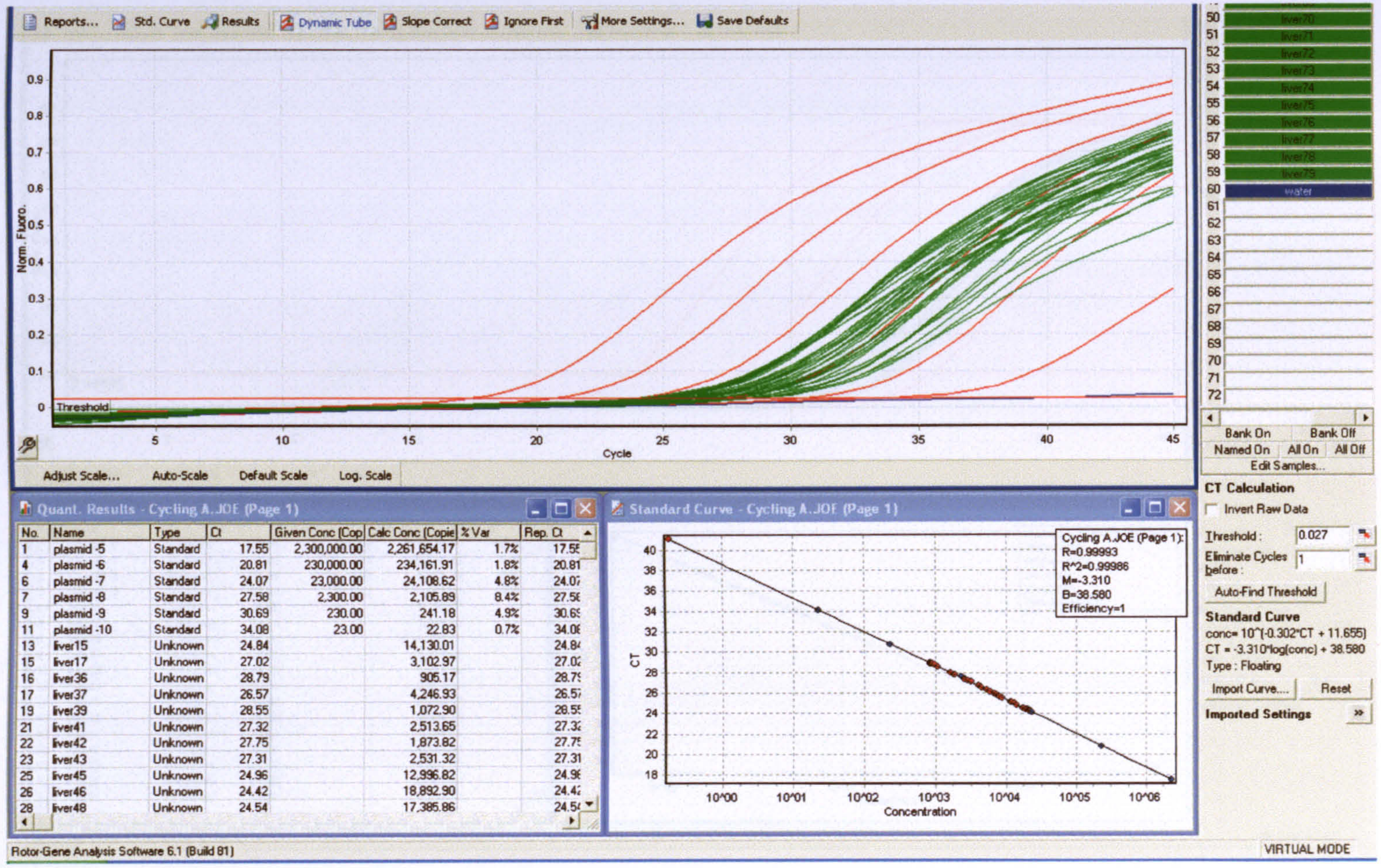

Figure 4.11: A typical Rotor-Gene report for the mt^{4977} detection/quantitation assay. Plasmid standards are shown in red. Liver biopsy specimens are shown in green. The standard curve is also shown (R^2=0.99).

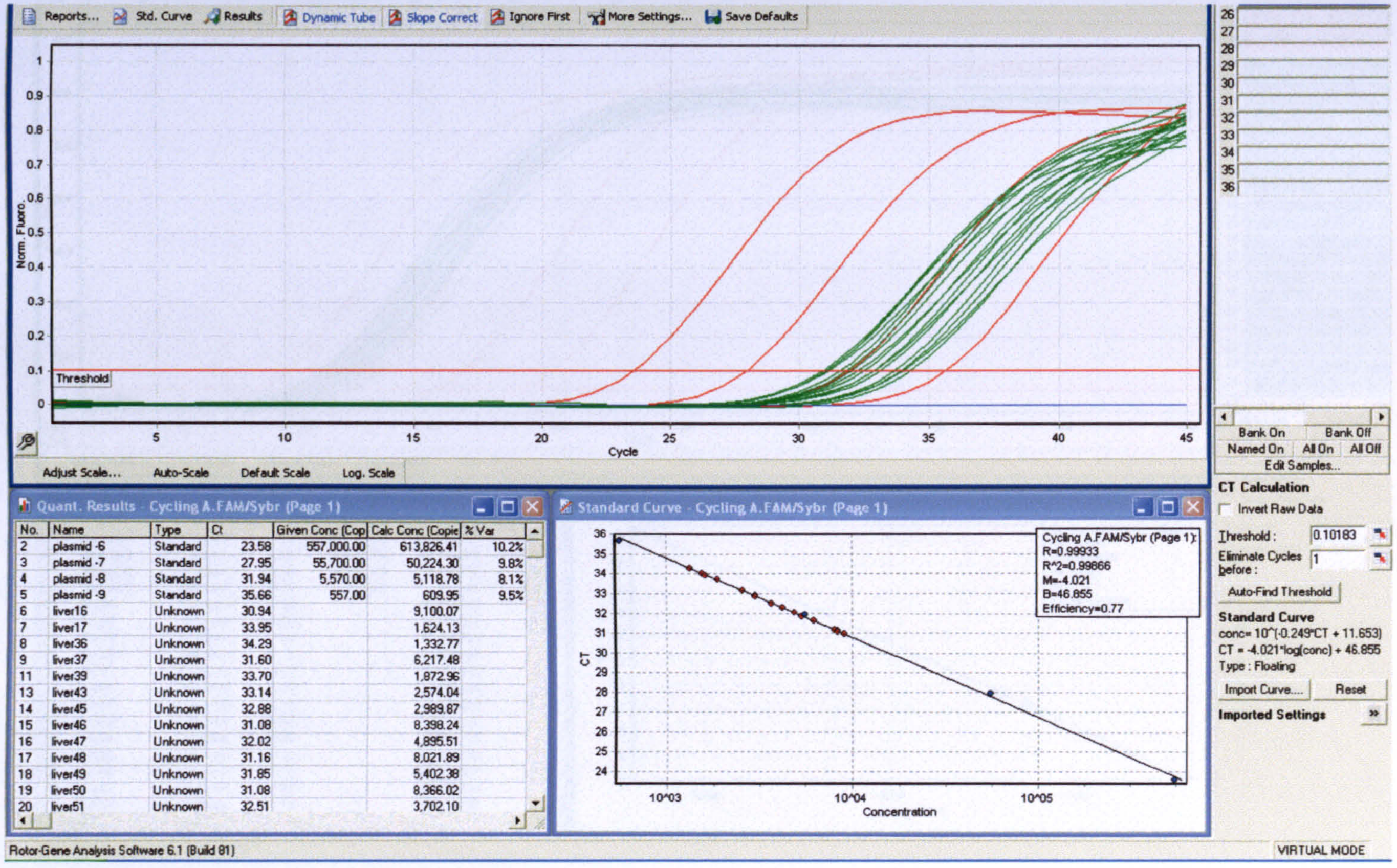

Figure 4.12: A typical Rotor-Gene report for the mt^{7436} detection/quantitation assay. Plasmid standards are shown in red. Liver biopsy specimens are shown in green. The standard curve is also shown (R^2=0.99).

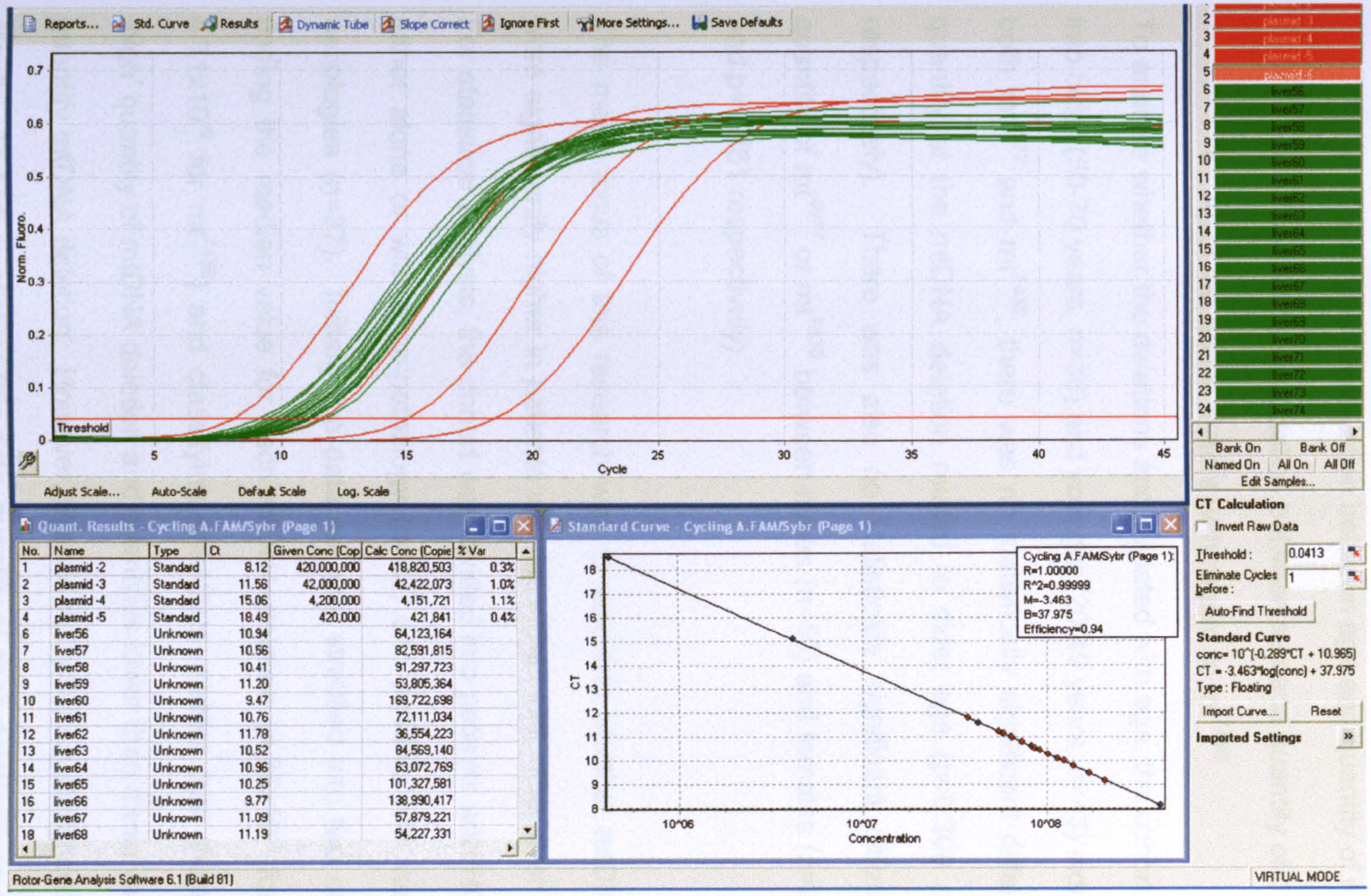

No.	Name	Type	Ct	Given Conc [Cop	Calc Conc [Copie	% Var
1	plasmid -2	Standard	8.12	420,000,000	418,820,503	0.3%
2	plasmid -3	Standard	11.56	42,000,000	42,422,073	1.0%
3	plasmid -4	Standard	15.06	4,200,000	4,151,721	1.1%
4	plasmid -5	Standard	18.49	420,000	421,841	0.4%
6	liver56	Unknown	10.94		64,123,164	
7	liver57	Unknown	10.56		82,591,815	
8	liver58	Unknown	10.41		91,297,723	
9	liver59	Unknown	11.20		53,805,364	
10	liver60	Unknown	9.47		169,722,698	
11	liver61	Unknown	10.76		72,111,034	
12	liver62	Unknown	11.78		36,554,223	
13	liver63	Unknown	10.52		84,569,140	
14	liver64	Unknown	10.96		63,072,769	
15	liver65	Unknown	10.25		101,327,581	
16	liver66	Unknown	9.77		138,990,417	
17	liver67	Unknown	11.09		57,879,221	
18	liver68	Unknown	11.19		54,227,331	

Figure 4.13: A typical Rotor-Gene report for the wt mtDNA detection/quantitation assay. Plasmid standards are shown in red. Liver biopsy specimens are shown in green. The standard curve is also shown (R^2=0.99).

Statistical analysis of the data was carried out using the chi-square test (Section 2.26). Several null hypotheses (H_0) were tested:

- There is no association between HCV infection and quantity of mt^{4977}
- There is no association between age and quantity of mt^{4977}
- There is no association between sex and quantity of mt^{4977}
- All of the above factors with regard to mt^{7436}

To analyse whether the deletions accumulated with age, the cohort was divided into older (50-70 years, n=36) and younger (20-49 years, n=43) individuals. For both mt^{4977} and mt^{7436}, there was no statistically significant difference in the quantity of the mtDNA deletion related to older age (p=0.309 and p=0.505 respectively). There was also no statistically significant difference in the quantity of mt^{4977} or mt^{7436} between males (n=55) and females (n=24) (p=0.284 and p=0.761 respectively).

The major focus of this research was to examine whether mtDNA deletions were significantly higher in patients with HCV than with other liver pathologies. For statistical analysis, the cohort was divided into patients with HCV infection, either alone or with a co-pathology (n=42) and patients with non-HCV liver aetiologies (n=37). Initially the data set was stratified into two categories by finding the median value for each mtDNA deletion ($4.36x10^{-5}$ for mt^{4977} and $4.71x10^{-6}$ for mt^{7436}) and classifying quantities greater than these values as 'high' quantity of mtDNA deletion and quantities lower than these values as 'low' quantity mtDNA deletion. However, this did not produce statistically significant results. To further analyse this data, quantity of each deletion was stratified into five categories (0 to10^{-3}, 10^{-3} to 10^{-4}, 10^{-4} to 10^{-5}, 10^{-5} to 10^{-6} and 10^{-6} to 10^{-7}). The data was analysed in an r x c contingency table to look for a trend within

the data. For mt^{4977} the chi-square value fell just outside statistical significance (p=0.0932). For mt^{7436} there was a significant difference between HCV and non-HCV liver aetiologies (p=0.008). However, from the data trend, it is impossible to determine whether a greater level of the deletion was occurring in HCV-infected or non-HCV infected individuals. Table 4.3 shows the contingency table for this data.

mt^{7436}		HCV	Non-HCV	
0 to10^{-3}	O	4	7	11
	E	5.4	4.6	
10^{-3} to 10^{-4}	O	0	4	4
	E	2.2	1.8	
10^{-4} to 10^{-5}	O	9	11	20
	E	10.8	9.2	
10^{-5} to 10^{-6}	O	20	13	33
	E	17.8	15.2	
10^{-6} to 10^{-7}	O	10	1	11
	E	5.9	5.1	
				Total: 79

Table 4.3: Contingency table for mt^{7436} quantity in HCV-infected vs. non-HCV infected individuals. O; observed, E; expected. Chi-square for this data set is 11.8, p=0.008.

4.3.3 mt^{7420} – a novel deletion?

Gel electrophoresis of the mt^{7436} products revealed that one biopsy (LB3) was negative by real-time PCR but showed an amplification product of the correct size on the gel. This liver biopsy was re-amplified with the CD1-mt7436 primer pair and again showed a product of similar size to the mt^{7436} product on agarose gel electrophoresis (Figure 4.14).

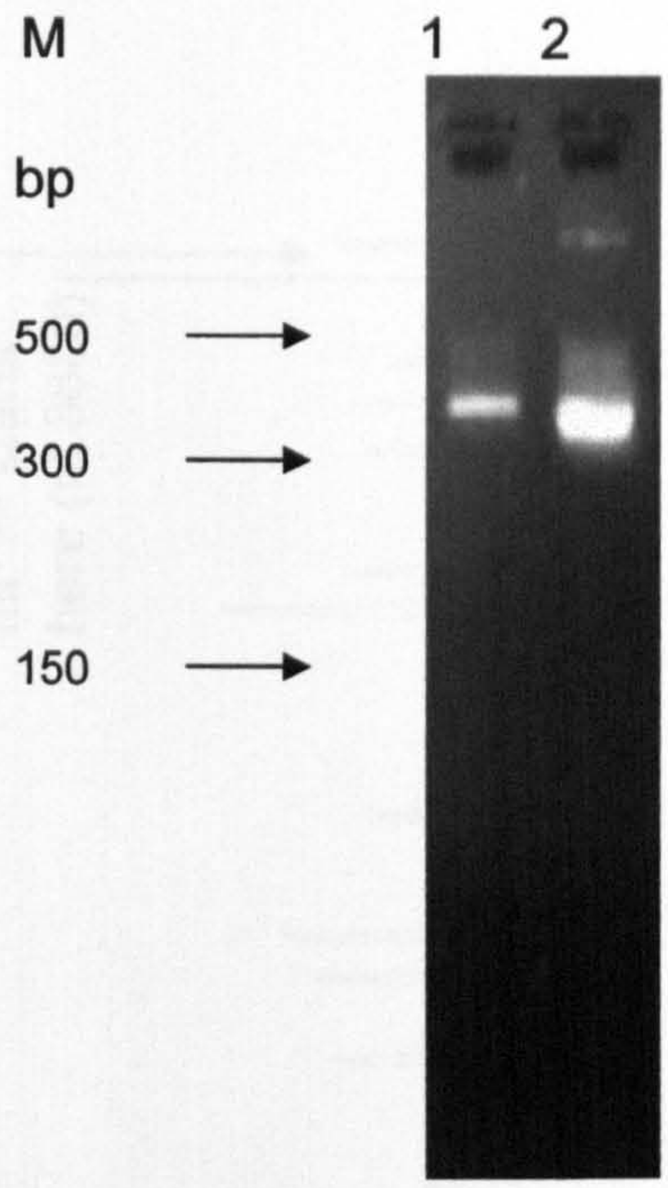

Figure 4.14: Image of mt^{7436} PCR products following separation on a 2% agarose gel illustrating LB3 (lane 1) which is similar in size to the mt^{7436} amplification product (lane 2) but negative on the mt^{7436} real-time PCR assay. M; PCR markers.

This amplification product from LB3 was sequenced (Section 2.21) using the CD1-LNA-mt7436 primer pair. The sequence data indicated that LB3 contained a mixture of two mtDNA species (Figure 4.15). Analysis of the sequence data, with reference to the rCRS (AC_000021), indicated that the majority sequence consisted of a region surrounding a deletion of 7420 bp (referred to henceforth as mt^{7420}) occurring between nt 8690 and nt 16109. This deletion begins 40 nt after mt^{7436} and ends 24 nt after mt^{7436} making the deletion 16 nt smaller than mt^{7436} (Figure 4.16). The sequence data also provided evidence as to why mt^{7420} was not detected with the mt^{7436} probe, as the mt^{7436} probe site lies within the mt^{7420} deletion site (Figure 4.17). From the sequence data, the minority sequence could not be interpreted. The possibility of contamination could not be ruled out.

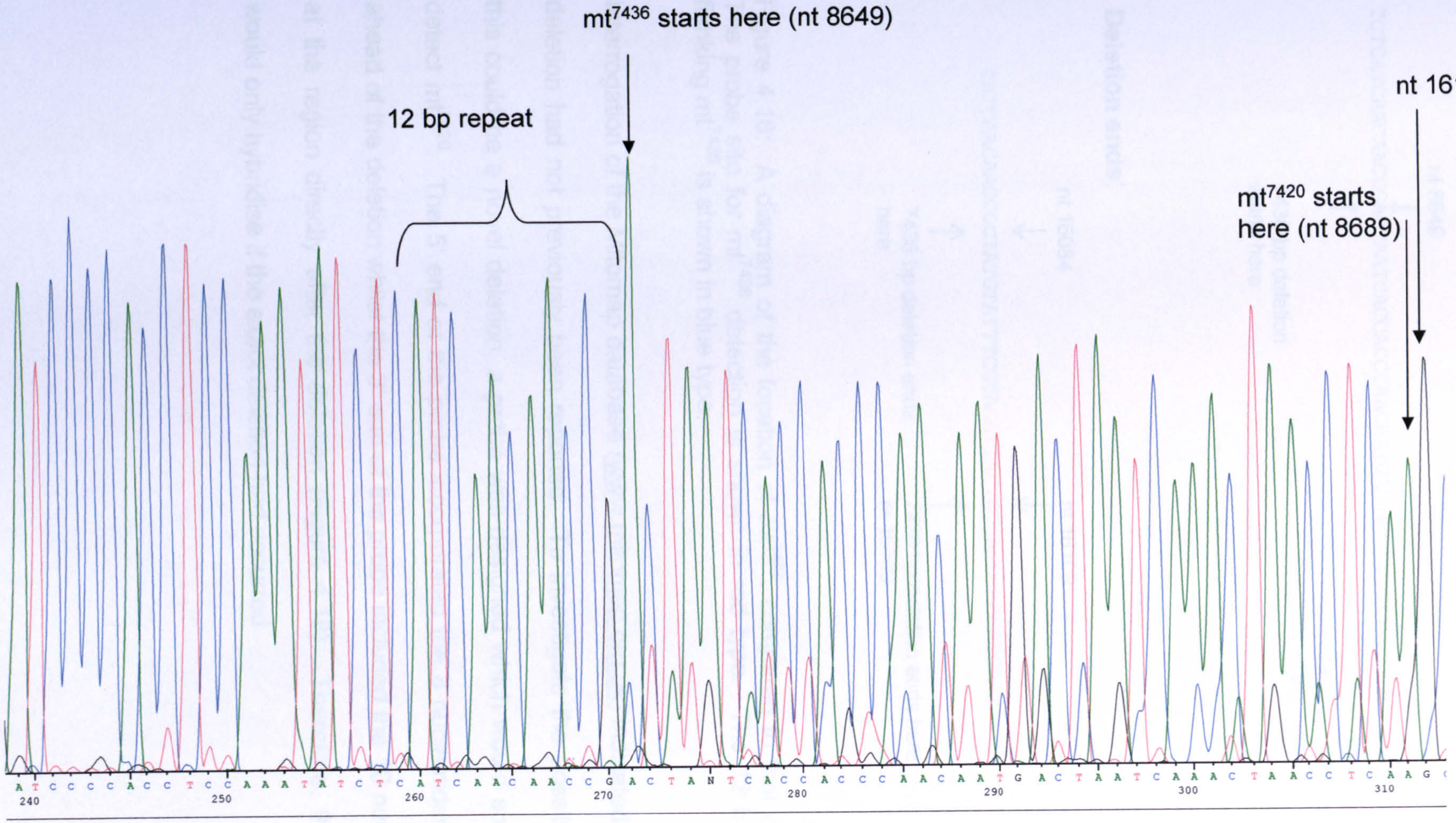

Figure 4.15: Sequence data demonstrating the mix of mt^{7436} and a novel mt^{7420} deletion observed in liver biopsy 'LB3'. mt^{7420} is the majority sequence, the minority species cannot be characterised.

Deletion begins:

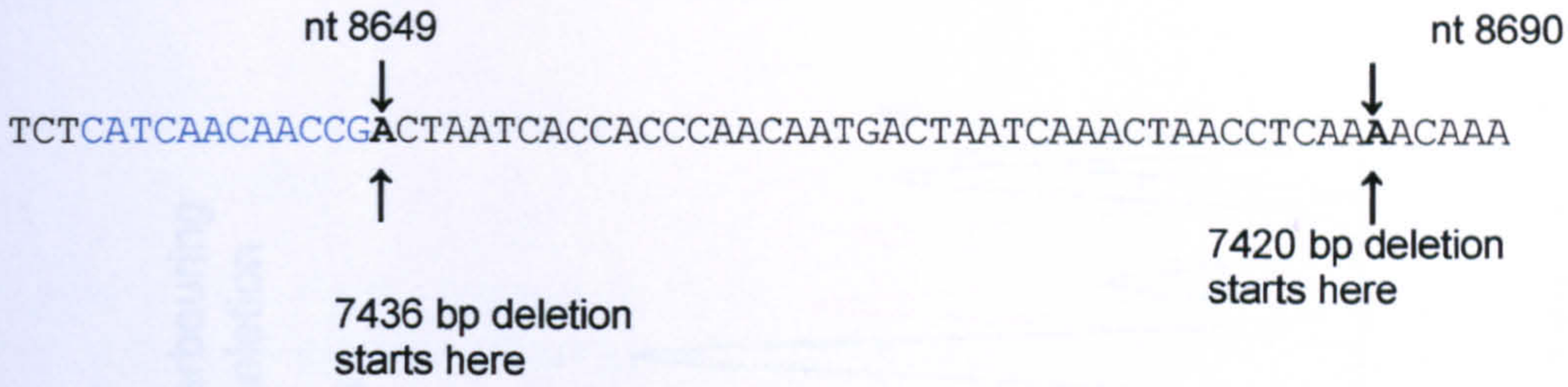

Deletion ends:

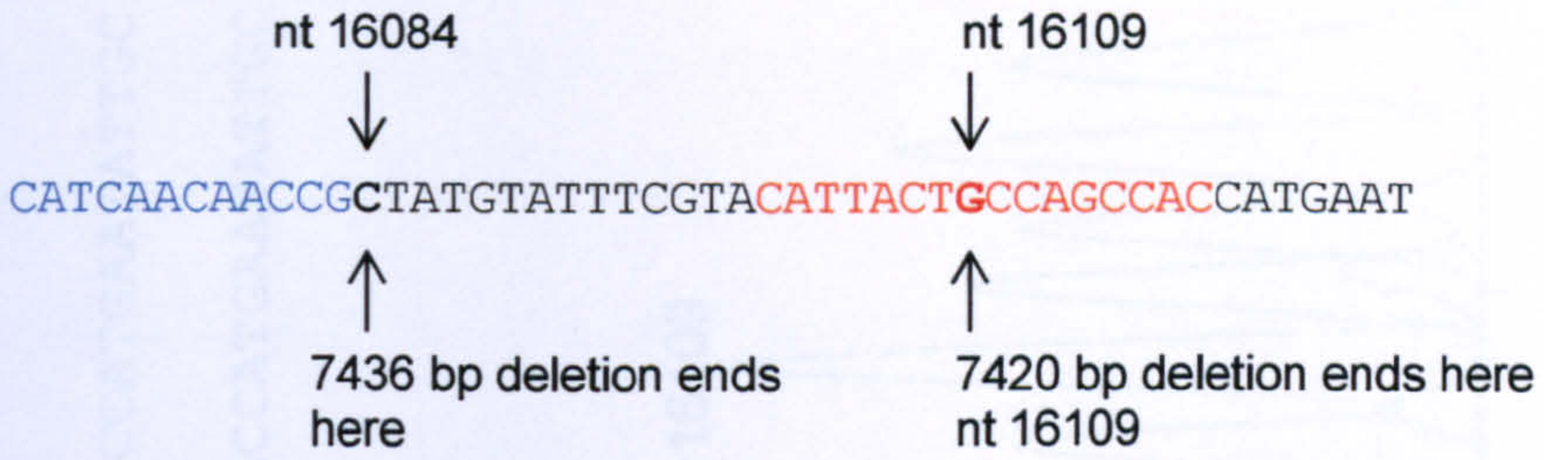

Figure 4.16: A diagram of the location of mt^{7420}, compared to that of mt^{7436}. The probe site for mt^{7436} detection is shown in red type. The 12 bp repeat flanking mt^{7436} is shown in blue type.

Interrogation of the Mitomap database (www.mitomap.org.uk) indicated that this deletion had not previously been reported. To investigate the possibility that this could be a novel deletion, a probe was designed which would specifically detect mt^{7420}. The 5' end of the probe incorporated the 8 nucleotides directly ahead of the deletion whilst the 3' end of the probe included the 10 nucleotides at the region directly after the deletion (Figure 4.18). Therefore, the probe would only hybridise if the exact deletion had occurred.

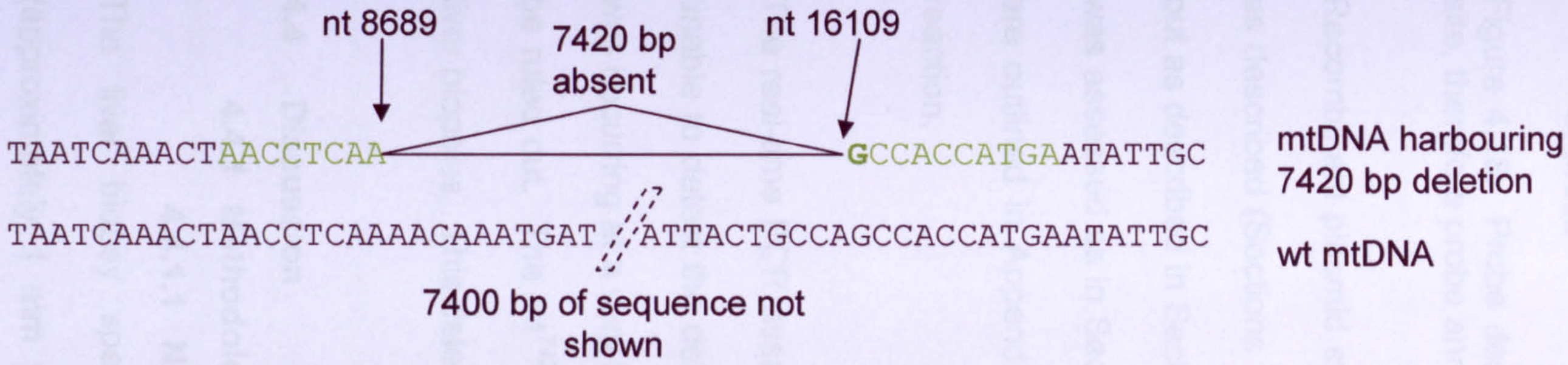

Figure 4.17: Sequence data demonstrating the position of the mt^{7420} deletion. The probe site designed to detect mt^{7420} is shown in green type.

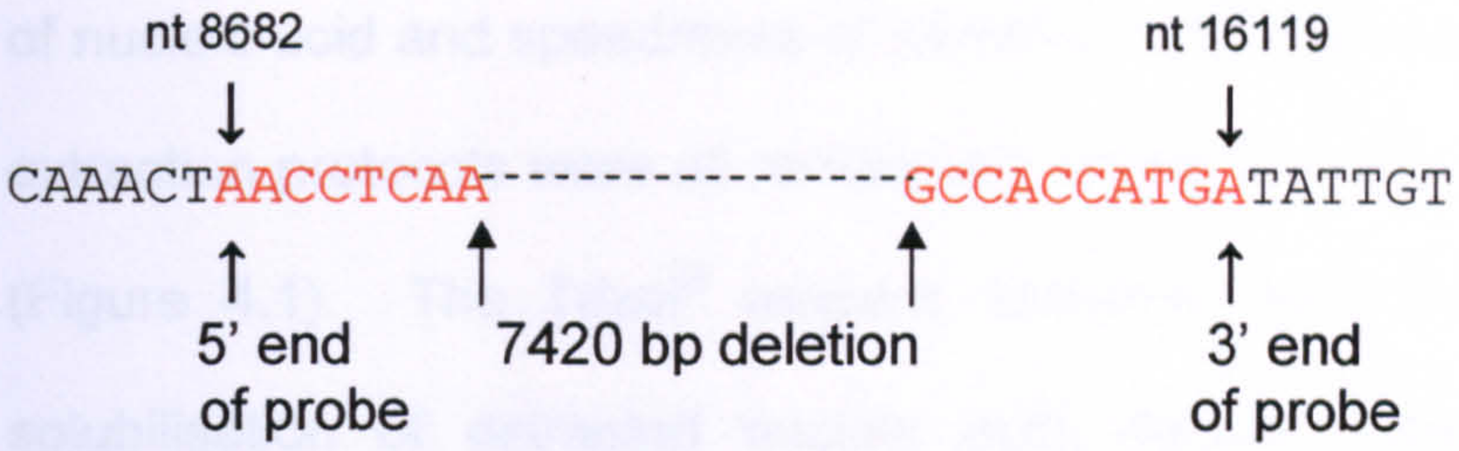

Figure 4.18: Probe design to detect mt^{7420}. The deletion is within the probe site, therefore probe annealing will only be possible if the deletion has occurred.

Recombinant plasmid standards containing the mt^{7420} amplicon were produced as described (Sections 2.23 and 2.24). Optimisation experiments were carried out as described in Section 4.2.7 and sensitivity and reproducibility of the assay was assessed as in Section 4.2.8 (data not shown). Fully optimised conditions are outlined in Appendix C. The sensitivity of the assay was 25 copies per reaction.

The real-time PCR assay for mt^{7420} detection was carried out on LB3 but was unable to detect the deletion in this liver. This could indicate that the deletion was occurring at a very low level. The possibility that it is a PCR artefact cannot be ruled out. The mt^{7420} detection assay was carried out on the remaining 78 liver biopsies. This deletion was not detected in any of these liver biopsies.

4.4 Discussion

4.4.1 Methodology

4.4.1.1 Nucleic acid homogenisation/extraction

The liver biopsy specimens received for this study were very small (approximately 1 mm thick and 4 mm long). It was, therefore, vital that homogenisation and extraction techniques produced the best yield of nucleic acid for further analysis. With this in mind, two methods of homogenisation (manual and automated) and four extraction protocols were tested. Automated homogenisation was superior to manual homogenisation, in terms both of yield

of nucleic acid and speed/ease of carrying out the procedure. The nucleic acid extraction protocols were all remarkably similar in terms of yield of nucleic acid (Figure 4.1). The Trizol® reagent, however, was inferior due to the poor solubilisation of extracted nucleic acid, despite several alterations to the protocol in an attempt to improve this. All of the extraction methods had the added advantage of isolating RNA, in addition to DNA, which provides a useful resource which could be utilised in the future for gene expression studies. The liver biopsy specimens were collected over a two year time period and were homogenised and extracted shortly after receipt. Due to the small batches of tissue which required extraction on each occasion, the manual kit which provided the best yield (DNeasy® Blood and Tissue kit) was selected.

4.4.1.2 Three-primer PCR

The three-primer PCR method used in this study was first described by Sciacco and colleagues (Sciacco *et al*, 1994) to detect and quantify mt^{4977} in patients with mitochondrial myopathy. This conventional-PCR approach has been adapted and utilised by others (Ross *et al*, 2002) to study this deletion in association with the ageing process. Until very recently, there had been no reports of the transfer of the three-primer method to a real-time PCR platform. In 2007, Poe and colleagues published results on the development of a three-primer real-time PCR assay using molecular beacons (Poe *et al*, 2007). This multiplex format simultaneously detects a 7522 bp mtDNA deletion and wt mtDNA in a single reaction. Standards for quantitation were produced from PCR products, which may not show long-term stability. This assay was developed on a cybrid cell line, which had been constructed to contain around 75% deleted mtDNA, far greater than would be observed *in vivo*.

The study described in this chapter further developed the three-primer PCR methodology to enable its conversion to a real-time PCR platform using Taqman technology to detect mt^{4977}. An additional assay was designed, using this methodology to detect another large mtDNA deletion – mt^{7436}. Quantitation of the deletions is carried out by reference to external plasmid standards. Accurate quantitation of mtDNA deletions cannot be determined without establishing their proportion relative to undeleted (wt) mtDNA. In addition to deleted mtDNA, the developed assay also detects and quantifies undeleted mtDNA to allow absolute quantitation of each deletion relative to wt mtDNA. Furthermore, the developed protocol includes a method for calculating mtDNA copy number by reference to a single-copy number gene (β-globin). mtDNA content is equivalent to the wt mtDNA copy number divided by the copy number of the β-globin gene. This additional assay, used only in a handful of other studies on mtDNA deletions (e.g. Cote *et al*, 2002; Chabi *et al*, 2003) ensures that mtDNA proliferation or depletion has not occurred which could have an effect on the results. The β-actin gene is often used for this purpose. However, it was decided, for this study, to use an assay already utilised in the laboratory for the quantitation of *Chlamydia trachomatis* in clinical specimens.

The fully optimised assay described in this chapter is excellent in terms of specificity, sensitivity and reproducibility. Following the early problems with mis-priming, sequencing of a selection of deletion amplicons demonstrated that the specific mtDNA deletion (either mt^{4977} or mt^{7436}) was amplified each time. Optimisation using plasmid standards demonstrated that all the assays were able to detect down to single copy numbers and were highly reproducible, even at low levels of mtDNA deletions. This proved to be an extremely important feature of the assay, as all mtDNA deletions were found to occur at extremely

low levels. Without a highly sensitive assay, detection of these deletions would have been impossible. This may be an explanation for the failure to detect mtDNA deletions in early studies using conventional-PCR and southern blot analysis which are far less sensitive for mtDNA deletion detection (Bai and Wong, 2005). With a PCR assay which is detecting very low copy numbers, attaining the same result on each run is extremely important. The developed assays display very low inter- and intra-assay variability (Table 4.1) demonstrating that results are reproducible even at the lower limits of detection.

Several studies have combined the detection of deleted and wt mtDNA in a single, multiplex assay (Pogozelski *et al*, 2003; Poe *et al*, 2007). Shorter targets are known to be amplified preferentially to longer targets and so these assays were designed to amplify short targets of similar size. However, wt mtDNA will be in far greater excess than deleted mtDNA and this would mean that a multiplex assay would be prone to differential bias of amplification despite the size-matched targets. To completely eliminate the possibility of biased amplification of wt mtDNA in the study described herein, it was decided to keep each assay as a monoplex format – with separate assays for mt^{4977}, mt^{7436} and wt mtDNA detection/quantitation. Each of the assays were carried out on a liver biopsy within a short time period to ensure no loss of sensitivity/accuracy due to DNA degradation.

In addition to three-primer PCR, a further method was developed during this research to detect and quantify mtDNA deletions. This was designed to quantify the amount of mtDNA in two different regions of the genome; one which is rarely deleted and the other that is absent in the majority of mtDNA molecules harbouring large deletions. This has been carried out by several

other groups (He *et al*, 2002; Bai and Wong, 2005). Attempts to develop a similar assay for use in this study, targeting the origin of replication (Ori), a region which cannot be deleted in replicating mitochondria and the ND4 gene, which is located in the commonly deleted region of mtDNA, were unsuccessful. A real-time PCR assay was designed which amplified targets of identical size from both these regions. However, the ND4 gene which should have been at a lower quantity than the Ori gene, if mtDNA deletions were occurring, was actually detected in greater abundance (data not shown). This could have been due to an increased reaction efficiency of the ND4 detection/quantitation assay compared to the Ori detection/quantitation assay.

4.4.2 mt^{4977}/mt^{7436} and liver disease

Many different mtDNA deletions have been described (see www.mitomap.org). It was decided, for this study to detect and quantify two mtDNA deletions which have already been described, rather than to look for novel deletions. The two deletions, mt^{4977} and mt^{7436} were chosen due to their large size (4977 and 7436 bp respectively) which eliminates a large part of the 16,569 bp mitochondrial genome. These deletions remove many of the genes which are essential for the OXPHOS pathway and would therefore have an adverse effect on the bioenergetic potential of cells if they accumulated to a significant proportion.

mt^{4977} and mt^{7436} were also selected as there have been very few studies investigating their prevalence in liver disease, with all published studies focusing on hepatocellular carcinoma (HCC). Early studies (Yamamoto *et al*, 1992; Fukushima *et al*, 1995; Kotake *et al*, 1999; Nishikawa *et al*, 2001) were carried out on Japanese subjects using conventional PCR. Kotake *et al* (1999) found that the levels of mt^{4977} and mt^{7436} were similar between normal and

chronically infected livers but were approximately one third in livers with cirrhosis and markedly lower in liver with HCC. Yamamoto and colleagues (Yamamoto *et al*, 1992), on comparing hepatic tumour tissue and surrounding cirrhotic liver of 10 patients with liver cancer, found multiple deletions in the cirrhotic liver tissue of all the individuals, but no deletions in the tumour portion. They did not isolate mt^{4977} but did detect mt^{7436} and a 7079 bp deletion. Fukushima *et al* (1995) detected mt^{4977} in the majority (65%, n=20) of non-tumour portions of adult patients with HCC. mt^{4977} was not seen in cirrhotic liver from paediatric patients (0%, n=16). They suggested that ageing, rather than cirrhotic changes in the liver were responsible for the accumulation of this deletion. The frequency of mtDNA deletion was significantly lower in tumour tissue (25%, n=28) compared to normal liver (65.5%, n=55). These early studies demonstrated that HCC is associated with lower levels of mtDNA deletions, but do not agree on whether cirrhotic liver tissue demonstrated increased levels of the deletions. In a later study, using conventional PCR, but with multiple, overlapping primers to screen the entire mitochondrial genome, Nishikawa and colleagues (Nishikawa *et al*, 2001) failed to isolate any deletions from either cancerous or non-cancerous liver tissue from Japanese individuals with HCC. The studies outlined above all suggest that mtDNA deletions are decreased in patients with HCC. This could be due to the rapid proliferation of cells in cancerous tissue. Large deletions in mtDNA diminish the capability for oxidative phosphorylation of mitochondria and so with the rapid growth of tumour cells, these will be at a disadvantage and will be eliminated or diluted out, with only mitochondria with fully functional mtDNA surviving.

These early studies have several limitations. They were all carried out using conventional (block-based) PCR, which is less sensitive than real-time PCR.

The deletion amplicons in these studies were large, ranging from 800-1000 bp. PCR tends to amplify longer products less efficiently than shorter ones and so the efficiency of PCR amplification may have been inferior, under-estimating the presence of the deletions or may have produced artefacts (Kajander *et al*, 1999). Two of the studies (Fukushima *et al*, 1995; Kotake *et al*, 1999) did not involve sequence analysis to verify the identity of the amplified products. This chapter describes a problem with mispriming where the misprime product was similar in size to the expected mtDNA deletion product. Specificity of PCR amplification should not be presumed without definitive identification of amplicons by sequence analysis. These early studies could not accurately quantify deletions, as quantitation of deletion amplicons was achieved by autoradiography of PCR products or by southern blot analysis, which have limited sensitivity especially of low quantity products. Although wt mtDNA was amplified, no attempt was made to quantify the levels of identified deletions relative to wt mtDNA.

More recent studies on the association of mtDNA deletions in liver disease have utilised real-time PCR techniques. Shao *et al* (2004) have employed real-time PCR with plasmid standards for both wild-type and deleted mtDNA to detect/quantify mtDNA deletions in HCC and hepatocellular nodular hyperplasia (HNH) in Chinese individuals (Shao *et al*, 2004). This group did not detect mt^{4977}, but instead isolated a novel 4981 bp deletion. They found the ratio of mitochondria with this deletion compared to wt mtDNA (indicated in brackets) to be significantly higher in HCC (0.00092) than in paired non-cancerous liver tissue (0.000) and HNH tissue (0.0000374); a result which contradicts earlier studies (Yamamoto *et al*, 1992; Fukushima *et al*, 1995; Kotake *et al*, 1999). However, as these results show, even in HCC, the ratio of deleted to wt mtDNA

is extremely low (0.00092). This study utilised paraffin-embedded liver tissues, requiring xylene and alcohol treatment pre-PCR, a process which may, itself, have resulted in DNA damage. Despite finding a high number of mtDNA mutations in individuals with chronic HCV infection (without HCC), Nishikawa and colleagues (2005) could detect no deletions in these individuals, suggesting that hepatocytes with deletions may be eliminated.

4.4.3 Clinical study

As described above, there is a paucity of research on mtDNA deletions in association with liver disease and the vast majority were carried out before the advent of real-time PCR. All the published studies on mtDNA deletion in association with HCV have been carried out on individuals of Chinese or Japanese origin. This study is the first to examine mtDNA deletions in a cohort of patients with liver disease residing in the UK. As outlined above, the early studies using conventional PCR lack sensitivity and do not accurately quantify the mtDNA deletions that were detected. The two, more recent studies using real-time PCR do not agree on whether mtDNA deletions are elevated in liver cirrhosis. This is, therefore, an area which warrants further investigation. The aim of the study described in this chapter was to examine whether levels of mtDNA deletions are higher in the liver tissue of patients infected with HCV. Due to the obvious ethical implications, it was impossible to obtain liver specimens from healthy livers. Therefore, it was decided to compare HCV-infected individuals with those undergoing biopsy for other liver aetiologies. As discussed in Chapter One, HCV is known to result in high levels of oxidative stress in infected individuals (Shimoda *et al*, 1994; Farinati *et al*, 1995; Farinati *et al*, 1999; Cardin *et al*, 2001; Jain *et al*, 2002, Mahmood *et al*, 2004; Fujita *et al*, 2007; Tanaka *et al*, 2008). This is thought to be through the interactions of

viral proteins including the core and NS5 proteins (Gong *et al*, 2001; Okuda *et al* 2002; Waris *et al*, 2002; Abdalla *et al*, 2005; García-Mediavilla *et al*, 2005; Korenaga *et al*, 2005; Otani *et al*, 2005; Piccoli *et al*, 2006; Li *et al*, 2007). It is therefore, not unreasonable to hypothesise that HCV-infected individuals would demonstrate much higher levels of mtDNA damage in the form of large deletions than non-HCV-infected individuals.

The clinical study examined a cohort of 79 individuals undergoing a liver biopsy. Approximately half (n=42) patients were infected with HCV. The remaining 37 individuals had undergone a biopsy for a variety of other liver pathologies including HBV, high alcohol intake and auto-immune disease (Appendix G). As expected, levels of wt mtDNA were high, ranging from 802,967 to 283,445,467 copies per reaction (3 µl liver biopsy DNA). Levels of mt^{4977} ranged from 0 (in one liver biopsy) to 54,738 copies per reaction (3 µl liver biopsy DNA). Levels of mt^{7436} ranged from 0 (in ten liver biopsies) to 33,991 copies per reaction (3 µl liver biopsy DNA). Although, in terms of copy number, these levels of mtDNA deletions appear quite high, it is important to examine them in relation to wt mtDNA. When defined as a ratio of deleted:wt mtDNA, levels of mt^{4977} ranged from $1.84x10^{-6}$ to $2.14x10^{-3}$ copies per reaction. For mt^{7436}, levels of mtDNA harbouring this deletion ranged from $2.38x10^{-7}$ to $2.6x10^{-4}$ copies per reaction. It is apparent, from these results, that the levels of deleted mtDNA are very low in all of the individuals studied. It must be noted, however, that liver biopsy specimens remove only a tiny fraction of the liver, the average liver biopsy samples only 1/100,000 of the whole liver (Hübscher, 2007). Thus one cannot rule out the possibility of sampling variation depending on which part of the liver (damaged or non-affected) was extracted in the biopsy specimen. Statistical analysis of the data indicated no statistically significant difference between

quantities of mt^{4977} between HCV-infected and non-HCV-infected individuals (p=0.0932). There was also no association between the amount of this deletion and the age (p=0.309) or sex (p=0.284) of the individuals. For mt^{7436} there was also no significant difference in the amount of this deletion and the age (p=0.505) or sex (p=0.761) of the individuals. The results for mt^{7436} did reach statistical significance when the comparison was between HCV-infected and non-HCV infected individuals (Table 4.3, p=0.008). This indicates a trend with respect to this deletion, however when the data was studied, it was impossible to determine whether individuals with HCV were accumulating a greater or lower level of this deletion. The cohort size for this study was small (n=79), and this may be why many of the results did not reach statistical significance, thus an extension of the study, recruiting further individuals, would be required.

The mt^{4977} deletion has been found to accumulate with age (Cortopassi *et al*, 1990, 1992; Lee *et al*, 1994; Wei *et al*, 1996; Zhang *et al*, 1998; Mohamed *et al*, 2006). It was therefore important to take into account the effect of age in the cohort of patients studied. The mean age of patients studied was 46.2 ($^{+}$/-11.6) years, and it is therefore not surprising to detect both deletions in the majority of individuals. However, no statistically significant increase in the levels of the deletions in older (50-70 years) compared to younger (20-49 years) individuals was observed for either mt^{4977} (p=0.309) or mt^{7436} (p=0.505). This may indicate that these deletions are present at very low levels in tissues regardless of the age of an individual, a result similar to that seen with mt^{4977} in lymphocytes (Ross *et al*, 2002). With the absence of a control group of healthy liver specimens, it is impossible to determine whether the levels of deletions are greater in liver disease than in healthy liver. The very low level of mtDNA deletions in individuals in this study reflects the findings of several studies

looking at the accumulation of mtDNA deletions in the ageing process. These studies have identified mtDNA deletions within tissues, at levels of less than 1% (Liu *et al*, 1998; Zhang *et al*, 1998). The very low levels of mtDNA deletions seen in this study would argue against physiologic significance. Large deletions such as mt^{4977} and mt^{7436} would have an extreme effect on the ability of single mitochondria to function, as they remove many genes essential for the enzyme complexes of the OXPHOS pathway. However, the co-existence of damaged mtDNAs with wt mtDNAs in a state of heteroplasmy within individual cells allows normal function to be maintained. The threshold level of mtDNA deletion beyond which normal function cannot be maintained is not certain. Cybrids containing different levels of mtDNA harbouring large deletions demonstrate significant bioenergetic defects only when the proportions of the deleted mtDNA is in the region of 50-60% of the total (Hayashi *et al*, 1991; Porteous *et al*, 1998). Patients presenting with symptomatic mitochondrial myopathy associated with large mtDNA deletions demonstrated 20-80% of deleted mtDNA in muscle biopsies (Holt *et al*, 1989). This is far greater than the very low levels of mtDNA deletions observed in this study and therefore a bioenergetic defect as a result of the deletions is extremely unlikely.

It would appear, from these results that mtDNA deletions are not accumulating within these individuals. There are several possible hypotheses as to why this occurs. Traditionally, it was thought that mitochondria harbouring large deletions had a replicative advantage due to their smaller, partially deleted, genomes, and could repopulate organelles significantly faster than wild-type genomes in the same cell (Linnane *et al*, 1989; Diaz *et al*, 2002). However, mitochondria harbouring large deletions would have bioenergetic defects making energy-requiring processes such as replication difficult. A later

hypothesis – the 'survival of the slowest' (de Grey, 1997) suggested that defective mitochondria harbouring deletions could accumulate due to a decreased rate of degradation. This was thought to be due to the production of fewer perhydroxyl radicals due to a reduced proton gradient resulting in less membrane damage than non-defective mitochondria.

The low levels of mtDNA deletions seen in this study and in several studies looking at mtDNA deletions in ageing tissues suggests that mtDNA deletions are not able to accumulate to significant levels with cells. There is a growing body of evidence which suggests that mitochondria harbouring deletions are more susceptible to apoptosis. Apoptosis, or programmed cell death, is a process which plays an important role in the removal of unwanted cells, and mitochondria are recognised as key players in its regulation. Liu and colleagues (Liu *et al*, 2004, 2007) using cybrid human cells harbouring different proportions of mt^{4977} demonstrated that deletions in mtDNA increase the susceptibility of human cells to apoptosis triggered by exogenous stimuli. This was found to be more pronounced in cells harbouring high levels of the deletion. Similarly Schoeler and colleagues found that cybrid cells harbouring mt^{4977} were sensitised to apoptosis even when the deletion occurred at low levels (Schoeler *et al*, 2005). Results from a study by Peng and colleagues suggest that small amounts of mt^{4977}-induced mitochondrial defects may accelerate the cell towards apoptosis (Peng *et al*, 2006).

mtDNA deletions are known to accumulate preferentially in post-mitotic tissue such as muscle and nervous tissue and are lower in mitotic tissues such as the liver, in which the cells are being continually replaced so that the function of the organ can be maintained (Cortopassi *et al*, 1992). In dividing cells, it may be

that deletions are lost as a result of negative (purifying) selective pressure, since mitochondrial dysfunction may hamper cell division. In post-mitotic tissues, the damaged mitochondria lead to no essential disadvantage to cell survival. The mitochondria harbouring deletions would be able to replicate, perhaps with the replicative advantage of smaller molecules. The liver undergoes rapid cell turnover and apoptosis, which could remove any mtDNA changes/deletions. Previous studies on liver have shown that this organ does not demonstrate age-associated mutations that are seen in post-mitotic tissues (Kovalenko *et al*, 1998; Kopsidas *et al*, 2000). The difference between mitotic and post-mitotic tissues may also explain why deletions are seen at very low levels (Kotake *et al*, 1999; Shao *et al*, 2004) or appear to be absent in the tumour tissue of HCC (Yamamoto *et al*, 1992; Nishikawa *et al*, 2001) in that the cells with a fully functional complement of mtDNA proliferate more efficiently in tumour tissue and become predominant, 'diluting out' any cells which harbour damaged mtDNA molecules. This may also explain why mtDNA deletions were seen at such a low level in this study. Even if the presence of HCV was resulting in an increase in oxidative stress and thus damaged mtDNA molecules, these may not have any replicative advantage and may be removed during the high cell-turnover which occurs in the liver tissue.

The lack of a healthy control group does introduce certain limitations to the study. The comparison of HCV-infected against non-HCV infected individuals is not ideal. Whilst HCV infection is widely acknowledged for its propensity to result in increased oxidative stress; that is not to say that other liver pathologies are not associated with oxidative stress. Ethanol consumption is known to cause an increase in ROS (Cahill *et al*, 1997; Bailey *et al*, 1999; Reinke, 2002) and mt^{4977} has been observed in alcoholics, especially those with microvascular

steatosis, a lesion that is caused by impaired mitochondrial function (Mansouri *et al*, 1997; Fromenty *et al*, 1995). Wheelhouse *et al* (2005) have found mt^{4977} in liver tissue of patients with HCC resulting from HBV infection. Hepatic mitochondria are compromised in NASH and NAFLD (Pessayre and Fromenty, 2005). Mitochondrial abnormalities have been observed in the liver mitochondria of patients with NASH, but no evidence of the common deletion has been reported (Caldwell *et al*, 1999).

One of the major disadvantages of this technique is that it is specific to individual deletions. It could be that, although large deletions are occurring only at very low levels, other types of mtDNA damage that accumulate during oxidative stress (e.g. mutations, resulting from oxidation of bases) may be occurring at high levels, but remain undetected by this assay. However, as has been shown with the isolation of a possible novel deletion (mt^{7420}), this assay does have some capacity to detect other deletions. The inability to detect mt^{7420} in any of the liver biopsies (apart from LB3 where it was first isolated), cannot rule out the possibility of it being a PCR artefact rather than a true deletion. The failure of the mt^{7420}- specific real-time PCR assay to detect the deletion in LB3 is puzzling but reinforces the possibility of a PCR artefact or, alternatively, the presence of the deletion below the detection level of the real-time PCR assay.

4.4.4 Future work

The difficulty in obtaining liver biopsy specimens sufficient in size to be used for research purposes in addition to routine diagnostic requirements has meant that the cohort size of the clinical study (n=79) was small. With the continued collection of liver biopsies, it is hoped to continue this study which may increase the statistical significance of the results obtained thus far.

In the present study, the assays failed to detect any significant levels of mtDNA deletions in the cohort of individuals studied. However, this research has resulted in the development of a sensitive tool which can be used to detect and quantify two major mtDNA deletions. This method is extremely versatile and could be used to detect these deletions in a variety of settings. For example the technology could be used as a biotool to examine the effect of administration of mutagens to cells *in vitro*. Additionally, it could be used to study these deletions in other syndromes and clinical disease, where mtDNA damage may be occurring at higher, more significant levels. mtDNA damage is known, for example to be associated with highly active anti-retroviral therapy (HAART) in HIV patients (Miro *et al*, 2000; Bartley *et al*, 2001; Zaera *et al*, 2001) resulting in lipodystrophy (abnormal fat changes).

The developed assay also has the added advantage of being able to detect mtDNA depletion/proliferation by reference to a nuclear gene (β-globin). There are several reports of mtDNA depletion/proliferation in individuals with mitochondrial disease (Bai *et al*, 2004; Bai and Wong, 2005), oesophageal cancer (Tan *et al*, 2006) and in HIV-infected patients on HAART (Coté *et al*, 2002; de Mendoza *et al*, 2004). It is hoped to transfer the methodology developed in this Chapter for other applications including the further study of mtDNA depletion/proliferation.

CHAPTER FIVE

Detection of Mitochondrial DNA Damage in the D-loop Region using Reference Strand Conformation Analysis (RSCA)

5.1 Overview

The displacement or D-loop of mtDNA (nt 16024-576) serves as the main site for mitochondrial genomic replication and transcription (Kasamatsu and Vinograd, 1974). It is known as the 'control region' as it contains the signals that regulate mitochondrial RNA and DNA synthesis (Clayton, 1982) (Figure 5.1). mtDNA is more prone to oxidative damage than nuclear DNA and the D-loop region is particularly susceptible (Mambo *et al*, 2003), due partly to the unique three-stranded loop structure which forms during mtDNA replication (Kasamatsu *et al*, 1971). Two hotspots of mutation within the D-loop are the hypervariable segments HVS1 (nt 16024-16383) and HVS2 (nt 57-372) (Figure 5.1) (Stoneking *et al*, 2000). Due to its role in regulating the transcription and replication of mtDNA, alterations in the D-loop may change the rate of mtDNA replication. This could result either in a reduced copy number of mtDNA, or an increase in the production of mutated mtDNA. Several studies have sequenced the D-loop region to look for mutations, especially in individuals with cancer. However, direct sequencing is relatively insensitive at detecting DNA mutations and will not easily identify low-frequency differences below 20% (Hancock *et al*, 2005). Sequencing is also a time-intensive process with substantial data analysis.

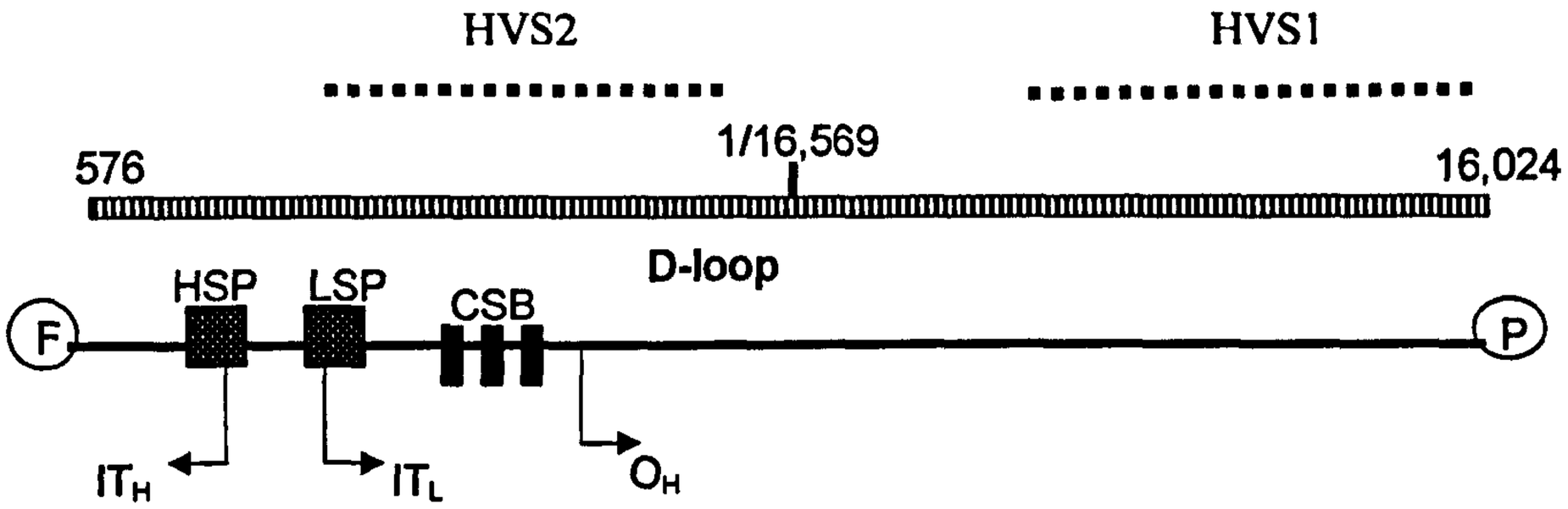

Figure 5.1: Schematic map of the 1.1 kb mtDNA D-loop region (nt 16024-576). The signals that control mitochondrial RNA and DNA synthesis are illustrated. HSP/LSP; heavy/light strand promoter, IT_H/IT_L; initiation of heavy/light strand transcription, F, P; tRNAs for phenylalanine and proline respectively, CSB; conserved sequence blocks. Also shown are the locations of the two hypervariable segments HVS1 (nt 16024-16383) and HVS2 (nt 57-372). The figure is not drawn to scale.

Reference strand conformation analysis (RSCA) is a heteroduplex-based technique which detects differences in DNA conformation when two dissimilar but related single-stranded DNA sequences are hybridised to each other, forming heteroduplexes (Section 5.2, Figure 5.2). Mismatched base pairs result in conformational changes within the heteroduplex leading to retardations in electromobility, compared to identically matched sequences (homoduplexes), when subjected to electrophoresis. RSCA utilises a fluorescent labelled reference (FLR) which forms one strand of each of the homo- and heteroduplexes. The technique has recently been transferred from polyacrylamide gel separation of duplexes to automated capillary-based electrophoresis systems with laser-based instrumentation and computer software; improving its accuracy and reproducibility. RSCA provides a platform to study mtDNA damage/mutation in the D-loop region. Unlike other applications for which RSCA has been developed, its use would not be to identify specific mutations but to analyse the region to determine the number

of D-loop 'species' harbouring different types of mtDNA damage. The number of D-loop species would be indicative of the amount of damage occurring within mtDNA and a marker of the overall cellular DNA damage. The D-loop is highly polymorphic and varies from individual to individual. It would therefore be usual for one heteroduplex to be seen, unless the region in a particular individual was identical to the FLR (thus forming a homoduplex). If mtDNA damage was present, different types (mutations, deletions and insertions) would result in different mismatched base pairs with the FLR. Each mtDNA D-loop species would be observed as a heteroduplex, each with a different mobility on electrophoresis. The number of heteroduplexes would be indicative of the level of mtDNA damage within an individual. This would provide a useful scanning tool to identify mtDNA damage in the D-loop region which could then be further analysed to discover the nature of the damage.

This chapter describes the development and optimisation of an RSCA-based technique to scan for mtDNA damage occurring within the D-loop region of the mitochondrial genome. The fully optimised technique is then applied in a clinical study to examine the extent of mtDNA damage in the liver tissue of a cohort of patients undergoing a liver biopsy as part of routine diagnostic investigation either as a result of HCV infection or an alternate liver aetiology. Oxidative stress leads to mtDNA damage (Sections 1.15 and 1.16) and HCV is known to result in increased levels of oxidative stress within infected individuals (Section 1.18). The repeated necrosis and regeneration of liver tissues associated with chronic viral hepatitis may also lead to the accumulation of mtDNA mutations (Nishikawa *et al*, 2001). This study aimed to identify whether mtDNA damage was occurring in the

liver tissue of HCV-infected individuals to a greater extent than those with other liver pathologies. Detection of D-loop species by RSCA could be applied as a useful diagnostic tool to determine the extent of DNA damage occurring within cells subjected to oxidative stress.

5.2 Reference strand conformation analysis (RSCA)

RSCA is a technique which can detect dissimilarity (mismatches, deletions or insertions) between two DNA strands which may differ by as little as one nucleotide. In RSCA, a locus-specific fluorescent labelled reference (FLR) is made, by PCR amplification, using a primer with a fluorescent dye at the 5' end. Only one of the primers has the fluorescent dye attached, and so only one strand of the FLR is labelled. The FLR is then mixed with an unlabelled PCR product from the same locus of the sample to be tested. A process of denaturation followed by annealing takes place which allows hybridisation of sense and anti-sense DNA strands. This may occur between strands of the same sample (forming homoduplexes) or between the FLR and the test sample (forming heteroduplexes). The heteroduplexes will have regions in which the nucleotide sequence is complementary to the FLR strand and regions where sequence mismatches lead to the formation of bulges and loops. Homoduplexes (perfectly matched sequences) have a different migration pattern from heteroduplexes (mismatched sequences) when subjected to electrophoresis (Figure 5.2). The conformation, mobility and therefore migration profile of each heteroduplex is unique and influenced by the number and position of the mismatches. Even a single nucleotide difference between the sample and the FLR will result in an altered mobility of the heteroduplex. Since the fluorescent label is present exclusively on

one strand of the FLR, only duplexes formed with this strand will be visualised (Argüello *et al*, 1998, 1998a).

5.2.1 Capillary electrophoresis using the ABI 3100-*Avant*

RSCA was originally developed as a tool for human leucocyte antigen (HLA) typing and was of value in donor/patient matching for bone marrow transplantation. HLA genes are the most polymorphic in the human genome and RSCA was found to be a technique which could accurately and reproducibly identify the many different HLA alleles, albeit using several different FLRs to improve resolution due to the high level of polymorphism (Argüello *et al*, 1998, 1998a; Ramon *et al*, 1998). Initially, duplexes were separated in a non-denaturing polyacrylamide gel by electrophoresis in an automated sequencer. However, gel-based RSCA has several limitations. Its low resolution means that it cannot always distinguish between closely-linked sequence variations. It is not easy to standardise and reproducibility is difficult to achieve as variations in polyacrylamide gel composition, buffer and temperature can affect the rate of mobility, resulting in both lane-to-lane and gel-to-gel variability. This method is also very time-consuming, with gel running times up to 16 hours, greatly reducing its utility as a high-throughput screening tool.

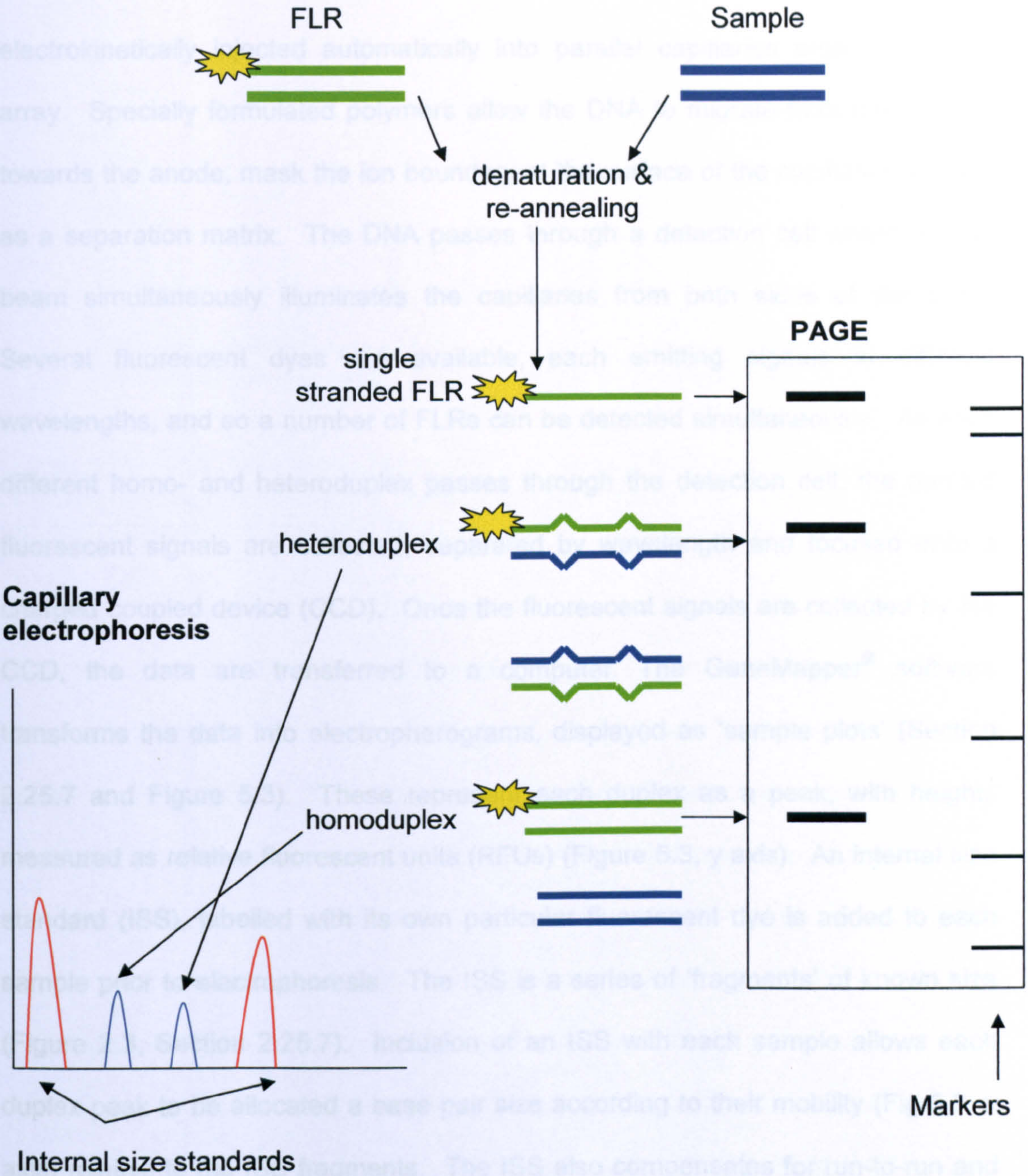

Figure 5.2: A schematic diagram of RSCA. The sample is mixed with the FLR and allowed to denature and re-anneal, either with itself (forming a homoduplex) or with the FLR (forming a heteroduplex). The duplexes are then separated by electrophoresis and those containing the labelled FLR strand are detected. Separation can be by polyacrylamide gel electrophoresis (PAGE) with detection on an automated sequencer. More recently, duplex separation has been transferred to capillary electrophoresis with detection via a charged coupled device (CCD).

The recent development of capillary electrophoresis-based RSCA techniques has led to renewed interest in this method. With capillary electrophoresis, samples are electrokinetically injected automatically into parallel capillaries organised in an array. Specially formulated polymers allow the DNA to migrate from the cathode towards the anode, mask the ion boundary at the surface of the capillaries and act as a separation matrix. The DNA passes through a detection cell where a laser beam simultaneously illuminates the capillaries from both sides of the array. Several fluorescent dyes are available, each emitting signals at different wavelengths, and so a number of FLRs can be detected simultaneously. As each different homo- and heteroduplex passes through the detection cell, the emitted fluorescent signals are collected, separated by wavelength and focused onto a charged coupled device (CCD). Once the fluorescent signals are collected by the CCD, the data are transferred to a computer. The GeneMapper® software transforms the data into electropherograms, displayed as 'sample plots' (Section 2.25.7 and Figure 5.3). These represent each duplex as a peak, with heights measured as relative fluorescent units (RFUs) (Figure 5.3, y axis). An internal size standard (ISS), labelled with its own particular fluorescent dye is added to each sample prior to electrophoresis. The ISS is a series of 'fragments' of known size (Figure 2.3, Section 2.25.7). Inclusion of an ISS with each sample allows each duplex peak to be allocated a base pair size according to their mobility (Fig 5.3, x axis) relative to the ISS fragments. The ISS also compensates for run-to-run and capillary-to-capillary variations, allowing excellent reproducibility.

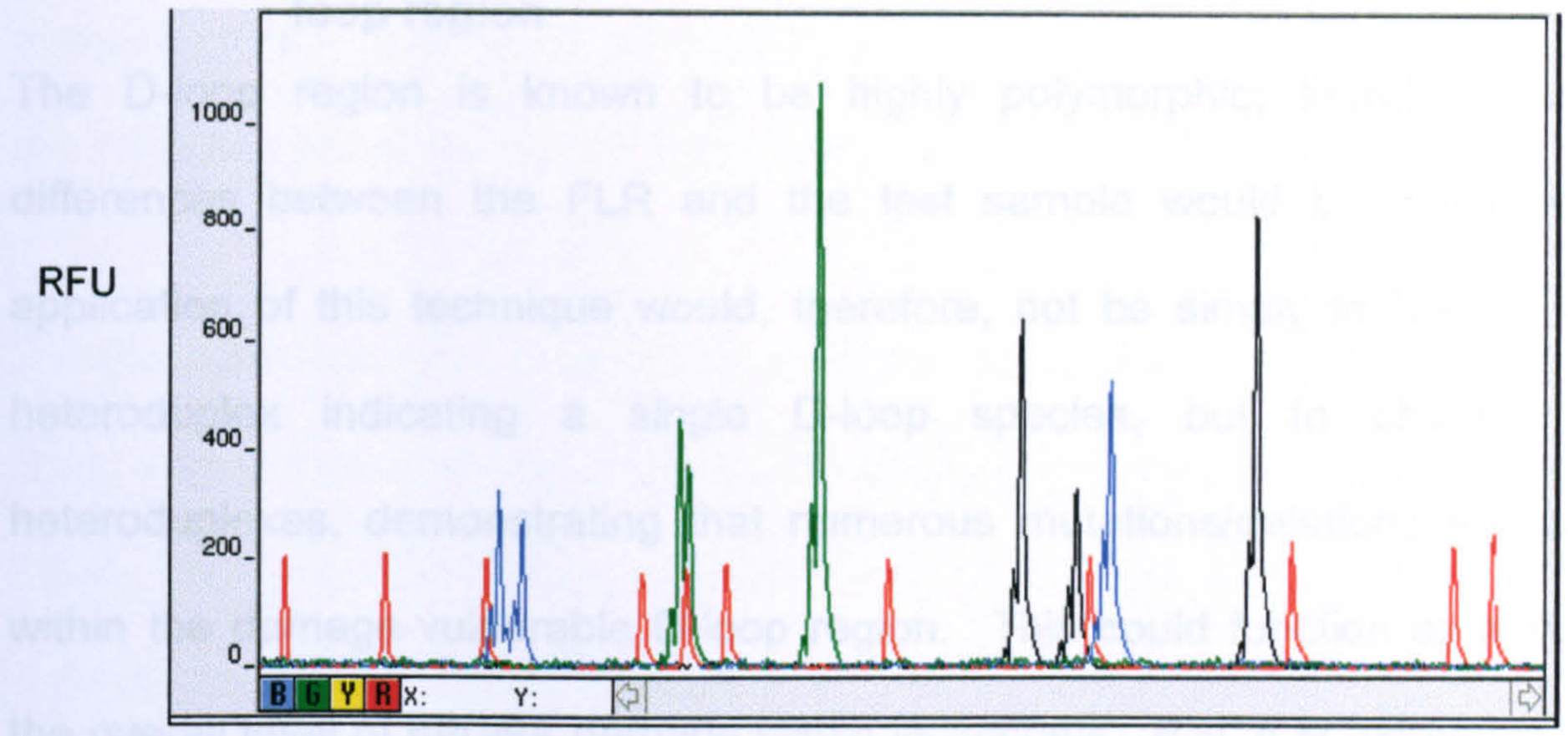

Figure 5.3: A four-dye electropherogram: The figure demonstrates a run where four different fluorescent dyes have been used, each emitting a signal at a particular wavelength which are collected by the CCD. RFU; relative fluorescent unit.

Capillary electrophoresis RSCA is carried out on Applied Biosystems Genetic Analyzers such as the ABI 3100-*Avant* where it is run as 'fragment analysis'. Fragment analysis has a wide range of applications including microsatellite genotyping, forensics, SNP genotyping, mutation detection and sizing-only applications. Unlike gel-based protocols, this method allows automation, is far less time-consuming and labour intensive and reduces cost. In addition, a wide range of polymers are available (unlike the gel-based method which relies solely on polyacrylamide). These polymers offer lower viscosity and improve separation and resolution. In addition the ISS offers a vast improvement over the PCR markers utilised in gel-based methods which are run separately from samples, at the edge of each gel, making accurate determination of the extent of migration difficult. The transfer of HLA-typing from gel-based to capillary electrophoresis greatly improved the resolution and throughput of this method (Turner *et al*, 1999, 2001).

5.2.2 Application of capillary RSCA to detect damage in the mtDNA D-loop region

The D-loop region is known to be highly polymorphic; therefore nucleotide differences between the FLR and the test sample would be expected. The application of this technique would, therefore, not be simply to identify a single heteroduplex indicating a single D-loop species, but to observe several heteroduplexes, demonstrating that numerous mutations/deletions are occurring within the damage-vulnerable D-loop region. This could function as a marker of the overall level of mtDNA damage within individuals. RSCA is extremely relevant to this application as the aim is not to detect a single, specific mutation, but, instead to act as a scanning method to detect various alterations within a defined region. Each distinct species would have a specific migration profile and therefore each heteroduplex would represent a particular damaged D-loop species. The number of species would therefore be representative of the extent of mtDNA damage occurring within the target region.

5.3 Development of experimental procedures

5.3.1 Primer design and D-loop amplification

The revised Cambridge reference sequence (rCRS) of the mitochondrial genome (available at www.mitomap.org or GenBank accession number AC_000021), was examined and one of the two hypervariable segments of the D-loop region (HVS1, nt 16024-16383) was chosen as the target for RSCA. Due to the highly polymorphic nature of this region and to ensure greatest sensitivity, the primers were designed within sequences where there are a minimal number of reported polymorphisms (Ingman and Gyllensten, 2006, www.genpat.uu.se/mtDB/index.html). The discriminatory power of RSCA should be increased when targeting a large

region as this would demonstrate greater sequence divergence. With this in mind, a region of 457 bp of HVS1 (nt 15973 -nt 16430) was targeted. The sequences of the designed primers (DLoopF and DLoopR) are given in Appendix B.

For the optimisation of D-loop amplification and subsequent RSCA development, DNA was extracted from six randomly chosen liver biopsies (LB3, LB26, LB33, LB34, LB46 and LB47) using the DNeasy® extraction protocol as described in Section 2.5.3. These DNA extracts were utilised in all optimisation experiments.

Amplification of HVS1 was carried out using a block-based PCR method, with primers DLoopF and DLoopR. PCR conditions were optimised as described in Section 2.16. Fully optimised conditions for D-loop amplification are given in Appendix C. The primers were found to be specific and sensitive for the HVS1 region of the D-loop. First, the amplicons were subjected to agarose gel electrophoresis (Section 2.7) and were found to be of the correct size (457 bp) (Figure 5.4). Second, the PCR products were purified (Section 2.17), sequenced (Section 2.21) and aligned with the rCRS (Section 2.22) which confirmed that the correct region was amplified.

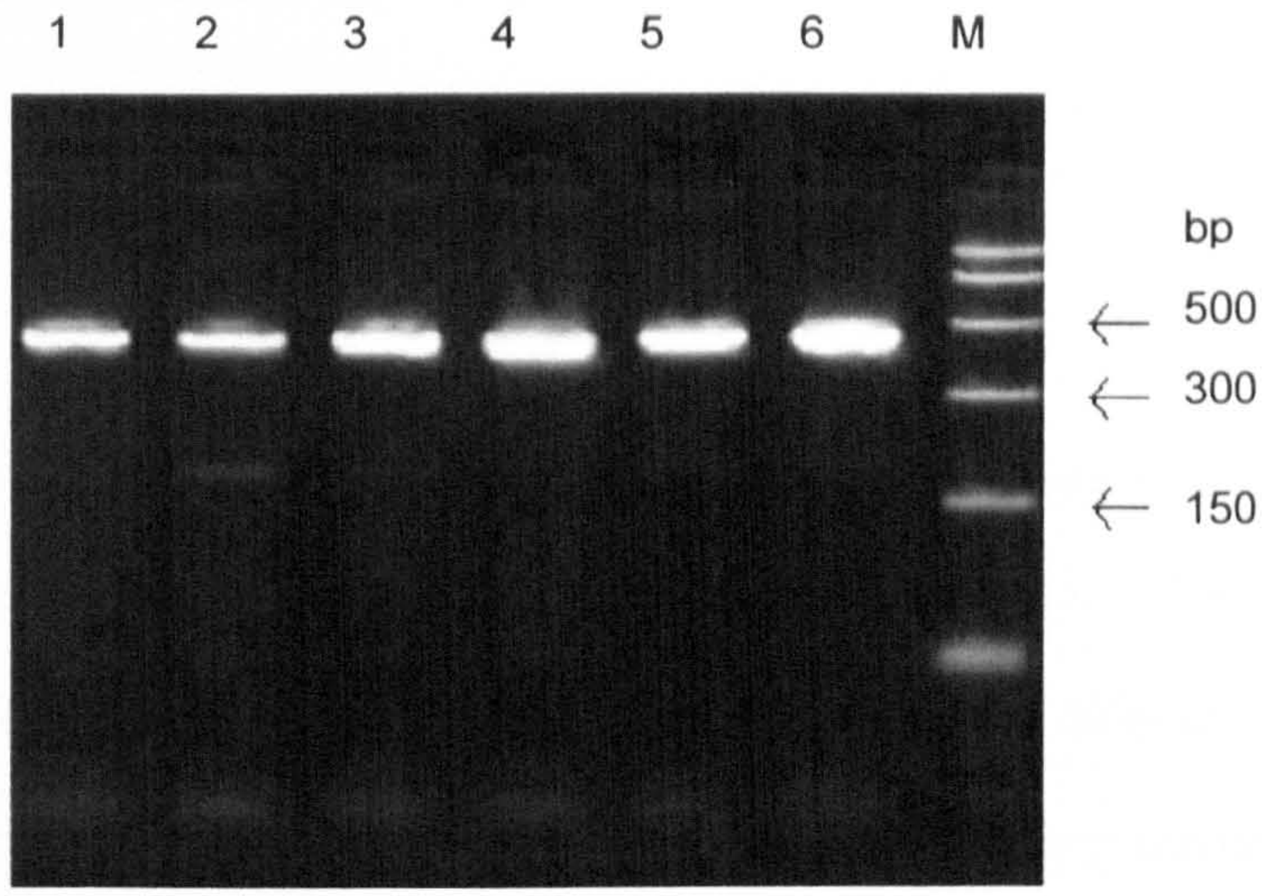

Figure 5.4: Image of HVS1 PCR products following separation on a 2% agarose gel. Extracted DNA from six liver biopsy specimens (lanes 1-6) was amplified using the D-loop primers (DLoopF and DLoopR). The image demonstrates the specificity of amplification, the amplicons are of the correct size (457 bp) and there are no other bands which would be indicative of primer non-specificity. M; PCR markers, bp; base pairs.

5.3.2 Selection of an FLR

The FLR is used as a reference sequence against which 'unknown' samples are compared. The best resolution of homoduplexes from heteroduplexes is achieved when there are a greater number of nucleotide differences between the FLR and the 'unknowns'. If the differences between the FLR and the 'unknown' are minimal, the heteroduplexes will migrate very close to the homoduplex and make it difficult to distinguish the heteroduplexes. In order to select an FLR for HVS1 which would display a high number of nucleotide variations, different sources were investigated. DNA from peripheral blood mononuclear cells (PBMCs) was extracted from the blood of two healthy laboratory volunteers (KR and MC) using the salting-out method (Section 2.5.4). The D-loop region was amplified and the amplicons

sequenced as described above. These sequences, along with those from the amplified liver biopsy specimens (LB3, LB26, LB33, LB34, LB46 and LB47) were aligned against the rCRS.

The sequenced amplicons all displayed nucleotide differences from the rCRS at the amplified region of HVS1 (Figure 5.5 and Table 5.1). The percentage divergence was calculated from the number of nucleotide differences from the rCRS in the 457 bp amplicon (Table 5.1). One of the laboratory workers (MC) had a HVS1 demonstrating the highest level of sequence divergence (6 nucleotide differences, 1.31% divergence) when compared to the rCRS. This was selected as the FLR for RSCA.

Source	Number of nucleotide differences from rCRS	Divergence (%)
LB3	5	1.09
LB26	5	1.09
LB33	3	0.66
LB34	1	0.22
LB46	3	0.66
LB47	2	0.44
KR	2	0.44
MC	6	1.31

Table 5.1: Divergence between D-loop amplicons from different sources and the rCRS. D-loop amplicons from 6 liver biopsies (LB3, LB26, LB33, LB34, LB46 and LB47) and two healthy volunteers (KR and MC) were sequenced. The sequences were aligned and compared against the revised Cambridge reference sequence (rCRS). The number of nucleotide differences between each sequence and the rCRS were counted and the percentage divergence, within the 457 bp amplicon, calculated.

Figure 5.5 (continued overleaf): An alignment of the D-loop amplicons sequenced for FLR selection. DNA from two volunteers (KR and MC) and 6 liver biopsy specimens (four shown in this figure - LB3, LB26, LB33 and LB34) was amplified and sequenced. The alignment compares all sequences against the revised Cambridge reference sequence (rCRS). Nucleotides that differ from the reference sequence are shaded in red. MC demonstrates the greatest number of nucleotide differences in the 457 bp sequence, of which 416 bp are shown in this figure.

```
     ACTATCACACATCAACTGCAACTCCAAAGCCACCCCTCACCCACTAGGATACCAACAAACCTACCCATCC  rCRS
     ACTATCACACATCAACTGCAACTCCAAAGCCACCCCTCACCCACTAGGATACCAACAAACCTACCCATCC  Majority
                220       230       240       250       260       270       280
211  ACTATCACACATCAACTGCAACTCCAAAGCCACCTCTCACCCACTAGGATACCAACAAACCTACCCATCC  LB3-F
211  ACTATCACACATCAACTGCAACTCCAAAGCCACCCCTCACCCACTAGGATACCAACAAACCTACCCATCT  LB26-F
211  ACTATCACACATCAACTGCAACTCCAAAGCCACCCCTCACCCACTAGGATACCAACAAACCTACCCATCT  B33-F
211  ACTATCACACATCAACTGCAACTCCAAAGCCACCCCTCACCCACTAGGATACCAACAAACCTACCCACCC  B34-F
211  ACTATCACACATCAACTGCAACTCCAAAGCCACCCCTCACCCACTAGGATACCAACAAACCTACCCACCC  KR-F
211  ACTATCACACATCAACTGCAACTCCAAAGCCACCCCTCACCCACTAGGATACCAACAAACCTACTCACCC  MC-F

     TTAACAGTACATAGTACATAAAGCCATTTACCGTACATAGCACATTACAGTCAAATCCCTTCTCGTCCCC  rCRS
     TTAACAGTACATAGTACATAAAGCCATTTACCGTACATAGCACATTACAGTCAAATCCCTTCTCGTCCCC  Majority
                290       300       310       320       330       340       350
281  TTAACAGTACATAGTACATAAAGCCATTTACCGTACATAGCACATTACAGTCAAATCCCTTCTCGTCCCC  LB3-F
281  TTAACAGTACATAGTACATAAAGCCATTTACCGTACATAGCACATTACAGTCAAATCCCTTCTCGTCCCC  LB26-F
281  TTAACAGCACATAGTACATAAAGCCATTTACCGTACATAGCACATTACAGTCAAATCCCTTCTCGTCCCC  B33-F
281  TTAACAGTACATAGTACATAAAGCCATTTACCGTACATAGCACATTACAGTCAAATCCCTTCTCGTCCCC  B34-F
281  TTAACAGTACATAGCACATAAAGCCATTTACCGTACATAGCACATTACAGTCAAATCCCTTCTCGTCCCC  KR-F
281  TTAACAGTACATAGCACATAAAGCCATTTACCGTACATAGCACATTACAGTCAAATCCCTTCTCGTCCCC  MC-F

     ATGGATGACCCCCCTCAGATAGGGGTCCCTTGACCACCATCCTCCGTGAAATAAAATATCCCGCAA     rCRS
     ATGGATGACCCCCCTCAGATAGGGGTCCCTTGACCACCATCCTCCGTGAAATAAAATATCCCGCAA     Majority
                360       370       380       390       400       410
351  ATGGATGACCCCCCTCAGATAGGGGTCCCTTGACCACCATCCTCCGTGAAATAAAATATCCCGCAA     LB3-F
351  ATGGATGACCCCCCTCAGATAGGGGTCCCTTGACCACCATCCTCCGTGAATAAAATTATCCCGCAA     LB26-F
351  ATGGATGACCCCCCTCAGATAGGGGTCCCTTGACCACCATCCTCCGTGAAATAAAATATCCCGCAA     B33-F
351  ATGGATGACCCCCCTCAGATAGGGGTCCCTTGACCACCATCCTCCGTGAAATAAAATATCCCGCAA     B34-F
351  ATGGATGACCCCCCTCAGATAGGGGTCCCTTGACCACCATCCTCCGTGAAATCAAATATCCCGCAA     KR-F
351  ATGGATGACCCCCCTCAGATAGGGGTCCCTTGACCACCATCCTCCGTGAAATAAAATATCCCGCAA     MC-F
```

Figure 5.5: Continued.

5.3.3 Cloning of HVS1

In order to create a stock of HVS1 amplicon for FLR production, the purified PCR product from laboratory worker MC, which had been selected for use as an FLR, was introduced into the pCR®-TOPO cloning vector as described in Section 2.23. Insert verification was carried out using colony PCR as described to confirm the effective production of a recombinant plasmid. The PCR products generated during colony PCR were sequenced in both directions to eliminate the possibility of sequence artefacts and to ensure accuracy of data generated. The cells were harvested and the plasmids purified (Section 2.24.2). This process created a recombinant plasmid containing the 457 bp region of HVS1 which could be continually used as the source from which the FLR was synthesised.

5.3.4 Generation of FLR

An FLR was created from the recombinant plasmid as described in Section 2.25.1. This involved utilising the same block-based PCR conditions for D-loop amplification as described above (Section 5.3.1 and Appendix C), but replacing the DLoopF primer with one, identical in sequence, but with a FAM-fluorophore at the 5' end (DloopFLab, Appendix B).

5.3.5 Optimisation of duplex formation and dilution

Duplex formation was carried out using a method adapted from Argüello *et al* (1998) and outlined in Section 2.25.2. This involves mixing sample D-loop amplicons with the prepared FLR in a 3:1 ratio (3 µl sample to 1 µl FLR) and allowing the PCR products to denature and re-anneal either with strands of the same sample or with the FLR and the 'unknown'. It was found that utilising PCR

amplicons which had been purified (Section 2.17) prior to duplex formation produced better results than non-purified products as there was less background noise on RSCA (data not shown).

Following duplex formation, products are very concentrated and require dilution to achieve peaks suitable for RSCA. This is a critical step in the process as over-dilution of samples will reduce sensitivity, producing smaller heteroduplex peaks which may be difficult to detect. Insufficient dilution results in over-loading which can produce so-called pull-up peaks from bleed-through of other dyes. The peak heights are measured in relative fluorescence units (RFUs) which are dependent on the amount of product which is loaded into the capillary. It is important that the protocol is optimised to produce a strong fluorescent signal with the minimum of background 'noise'. For the ABI 3100-*Avant*, the target peaks should be >100 and <2000 RFU. Several RSCA protocols (e.g. Mattocks *et al*, 2007) adopt a dilution protocol in which the products of duplex formation are diluted in a two-step process. To establish the optimum dilution of products to be loaded into the capillary, a range of different dilution combinations were assessed to produce peaks within the specified RFU range, with no loss of sensitivity (Figure 5.6). For example, a two-step process in which the duplex product was first diluted 1 in 10 (4 µl of product in 36 µl ddH_20) and then 1 in 2 (10 µl of first dilution product in 10 µl ddH_20). Peak size is also dependent on injection time of capillary electrophoresis and so optimisation of dilution factor was carried out concurrently with optimisation of injection time. The final dilution protocol is outlined in Section 2.25.3 and corresponds to run B in Figure 5.6.

5.3.6 Optimisation of capillary electrophoresis

Several different parameters including polymer type, run temperature, injection time/voltage and run time can affect the resolution and separation of homo- and heteroduplexes. The run time must be sufficient to allow all of the internal size standards to pass the detection cell. The injection time controls the peak size and must be sufficient to result in target peaks of >100 and <2000 RFU with good resolution of homo- and heteroduplexes. On the ABI 3100-*Avant*, a module editor can be utilised to alter these parameters to create and save the optimised run conditions. Three polymers were investigated; GeneScan, POP-4 and POP-6 polymer. GeneScan polymer was found to be non-compatible with the capillary array. POP-6 polymer had increased resolution of separation when compared to POP-4 polymer (data not shown) and was therefore selected. The optimisation of electrophoresis conditions was carried out on an experimental basis. Optimisation of capillary electrophoresis was carried out by injecting the same samples multiple times using a range of run times (30, 45, 60, 120 mins) and injection parameters (10, 15, 30, 45 and 60 sec) (Figure 5.6). The fully optimised conditions are outlined in Section 2.25.6. The data was collected and analysed using GeneMapper® software (Section 2.25.7).

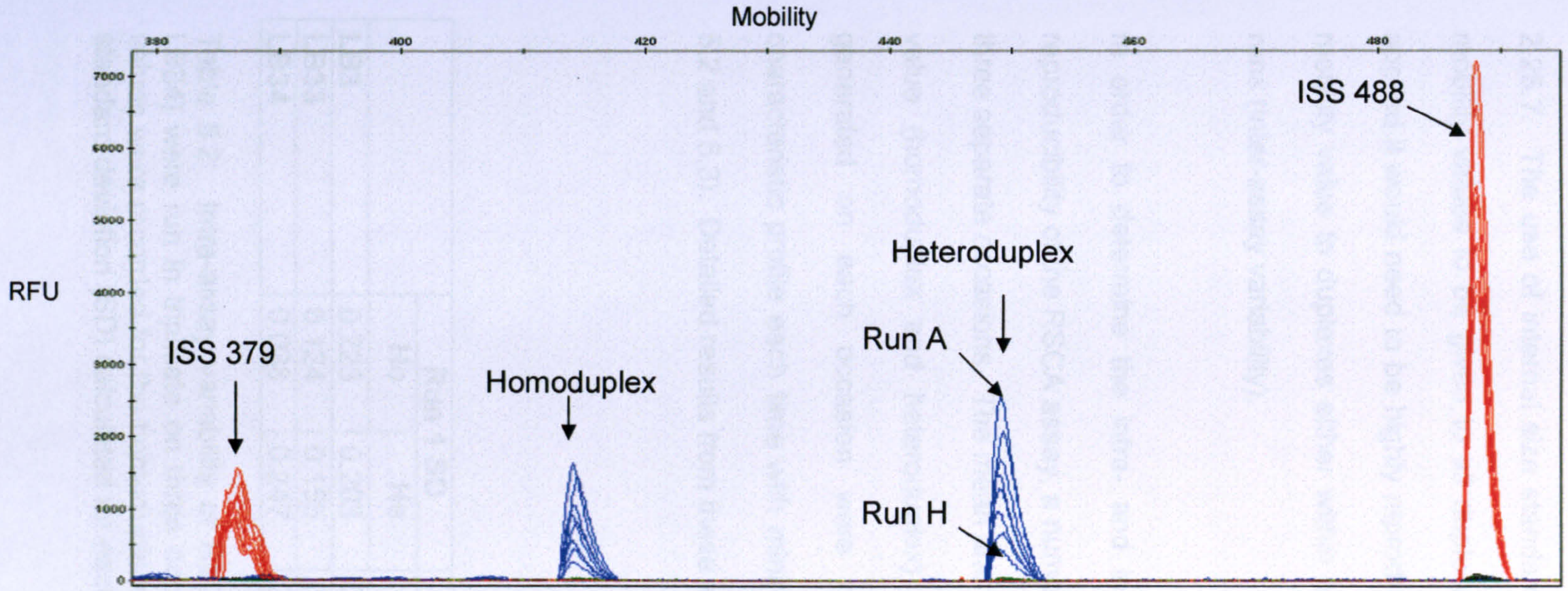

Run	1st dilution	2nd dilution	Injection time (s)
A	1 in 10	4 in 1	45
B	1 in 10	1 in 2	45
C	1 in 20	-	45
D	1 in 10	4 in 1	30
E	1 in 10	1 in 2	30
F	1 in 20	-	30
G	1 in 30	-	45
H	1 in 30	-	30

Figure 5.6: Optimisation of capillary electrophoresis: duplex dilution and injection times. Different run parameters were tested and eight are shown here (runs A-H, see table). The two stage duplex dilution protocol prior to capillary electrophoresis and the injection time of products during electrophoresis were varied, all other parameters were kept constant. The figure shows sample plots for each run. In this figure, the eight runs (A-H) have been merged into a single sample plot, to aid visualisation. ISS; internal size standard, with mobility value given, RFU; relative fluorescent unit.

5.3.7 Intra- and inter-run variation

RSCA data was analysed using GeneMapper software as described in Section 2.25.7. The use of internal size standards allows accurate base pair sizing and mobility values to be given to all duplexes. For this method to be successfully applied it would need to be highly reproducible with no difference in assignation of mobility value to duplexes either within a run (intra-assay variability) or between runs (inter-assay variability).

In order to determine the intra- and inter-run variability and therefore overall reproducibility of the RSCA assay, a number of samples were run in triplicate on three separate occasions. The mean and standard deviation (SD) for each mobility value (homoduplex and heteroduplex) was calculated. The RSCA profiles generated on each occasion were highly reproducible and generated a characteristic profile each time with minimal intra- and inter-run variation (Tables 5.2 and 5.3). Detailed results from these analyses are given in Appendix H.

	Run 1 SD		Run 2 SD		Run 3 SD	
	Ho	He	Ho	He	Ho	He
LB3	0.223	0.203	0.126	0.633	0.363	0.212
LB33	0.124	0.155	0.0757	0.116	0.214	0.107
LB34	0.038	0.247	0.256	0.204	0.380	0.344

Table 5.2: Intra-assay variability of RSCA. Three specimens (LB3, LB33 and LB34) were run in triplicate on three occasions (runs 1, 2 and 3). The mobility values were recorded for the homoduplexes (Ho) and heteroduplexes (He) and the standard deviation (SD) calculated for each triplicate on each run.

	Homoduplex SD	Heteroduplex SD
LB3	0.309	0.387
LB33	0.202	0.185
LB34	0.340	0.338

Table 5.3: Inter-assay variability of RSCA. Figures shown are the standard deviations (SD) of the mobility values for the homoduplex and heteroduplex species of three specimens (LB3, LB33 and LB34) run in triplicate on three occasions.

5.3.8 Assessing the sensitivity of RSCA

An assay developed for detection of mtDNA damage would need to be highly sensitive to ensure detection of all species of damaged mtDNA, including those present at very low levels. To test the sensitivity of the optimised RSCA assay, DNA extracts from two liver biopsy specimens were mixed prior to D-loop PCR amplification to simulate two D-loop species occurring within the same individual. Different mixtures were prepared with one liver biopsy being the minority species.

The D-loop region was then amplified and duplexes formed with the FLR, as described previously. Capillary electrophoresis of each mixture was carried out in triplicate to ensure that detection of the minority species occurred reproducibly at low levels. Figure 5.7 illustrates an example run, in which two liver biopsies (LB3 and LB26) were mixed prior to D-loop amplification so that one liver biopsy represented the minority species (see table in Figure 5.7). In this figure, two heteroduplexes are observed for each mixture which corresponds to the two liver biopsy specimens. The minority species could be detected accurately and reproducibly at the 2% level. Below this only one heteroduplex is seen, as the minority species could not be detected when it constituted less than 2% of the mixture.

Mixture	LB3 (µl)	LB26 (µl)	% of minority LB
1	20.0	0	0
2	19.8	0.2	1
3	19.6	0.4	2
4	19.2	0.8	4
5	18	2	10
6	2	18	10
7	0.8	19.2	4
8	0.4	19.6	2
9	0.2	19.8	1
10	0	20	0

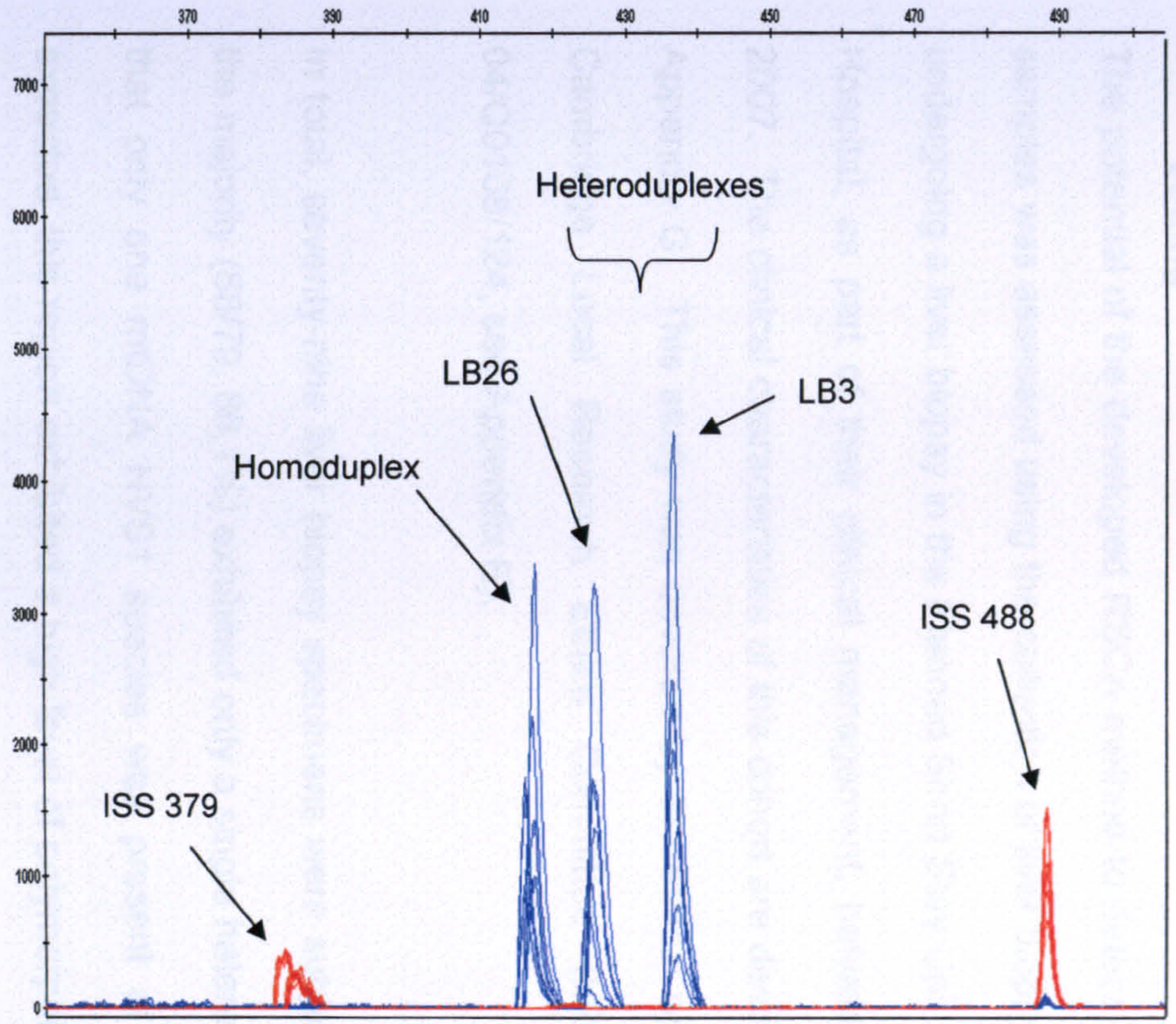

Figure 5.7: Assessing the sensitivity of RSCA. The DNA from two liver biopsy specimens (LB3 and LB26) were mixed prior to D-loop amplification. The table demonstrates a selection of the DNA mixes in which one liver biopsy was the minority 'species'. Five microlitres of each mixture was subjected to D-loop amplification, duplex formation and RSCA as described. The figure shows the sample plots of the ten RSCA runs, corresponding to each mixture, which have been merged to aid visualisation. Two heteroduplexes are formed corresponding to the two liver biopsies in the mixture. Only one heteroduplex is observed for mixtures 1, 2, 9 and 10 as the minority species could not be detected at this level. The intensity of the fluorescent signal corresponds to the relative amount of liver biopsy in the mixture. The RSCA assay could detect the minority species with a sensitivity of 2%. ISS = internal size standard, mobility value given.

5.4 Evaluation of RSCA to detect mtDNA D-loop damage in the clinical setting

The potential of the developed RSCA method to detect mtDNA damage in clinical samples was assessed using the collection of liver biopsy specimens from patients undergoing a liver biopsy in the Planned Short Stay Unit (PSSU) at Addenbrooke's Hospital, as part of their clinical management, between May 2005 and August 2007. The clinical characteristics of this cohort are described in Section 4.3.1 and Appendix G. This study was covered by the ethical approval obtained from the Cambridge Local Research Ethics Committee (LREC) (reference number 04/Q0108/124, see Appendix E).

In total, seventy-nine liver biopsy specimens were subjected to RSCA. Of these, the majority (68/79, 86.1%) exhibited only a single heteroduplex species, indicating that only one mtDNA HVS1 species was present at a detectable level. As expected, this region exhibited a high level of polymorphism. Of the 68 individuals demonstrating a single heteroduplex, 31 different mobility values for the heteroduplex were observed (Appendix I). The mobility value for the heteroduplexes ranged from 420.1 – 474.0. Ten of these liver biopsy specimens were sequenced and the sequence data examined for evidence of other D-loop HVS1 species (data not shown). The sequences of these liver biopsies clearly demonstrated only a single HVS1 species.

Eleven livers (13.9%) displayed multiple heteroduplex species, ranging from 2 to 5 species. Patient characteristics and number of heteroduplexes seen are outlined in Table 5.4. All biopsy specimens exhibiting multiple heteroduplexes were re-amplified and RSCA repeated to ensure reproducibility of results. In all cases,

identical results were seen on repeat analysis. Figure 5.8 demonstrates a selection of RSCA profiles of liver biopsy specimens demonstrating multiple heteroduplexes.

		Patient Characteristics		
Liver ID	**Heteroduplexes**	**Age**	**Sex**	**Liver Aetiology**
LB9	3	35	M	Unknown
LB10	3	44	M	HCV, genotype 1
LB36	2	53	M	HCV, genotype 1
LB41	2	31	M	HBV
LB48	2	63	F	Alcoholic liver disease
LB50	5	29	M	HBV
LB52	4	47	F	HCV, genotype 2. Diabetes
LB58	4	33	M	HCV, genotype 4
LB70	4	52	M	HCV, genotype 1
LB72	3	60	M	?ASH/?NASH
LB76	4	57	M	?dysplasia

Table 5.4: Clinical characteristics of the patients displaying multiple heteroduplexes on RSCA. HBV; hepatitis B virus, ASH; alcoholic steatohepatitis, NASH; non-alcoholic steatohepatitis.

Five (45.5%) individuals with multiple heteroduplexes were infected with HCV. The average age of patients demonstrating multiple heteroduplexes was 45.8 years which did not differ significantly from the average age of individuals demonstrating only a single heteroduplex species (46.4 years). There was an under-representation of females with multiple heteroduplexes. Females made up 32% of individuals displaying a single heteroduplex, but only 18% of individuals demonstrating multiple heteroduplexes.

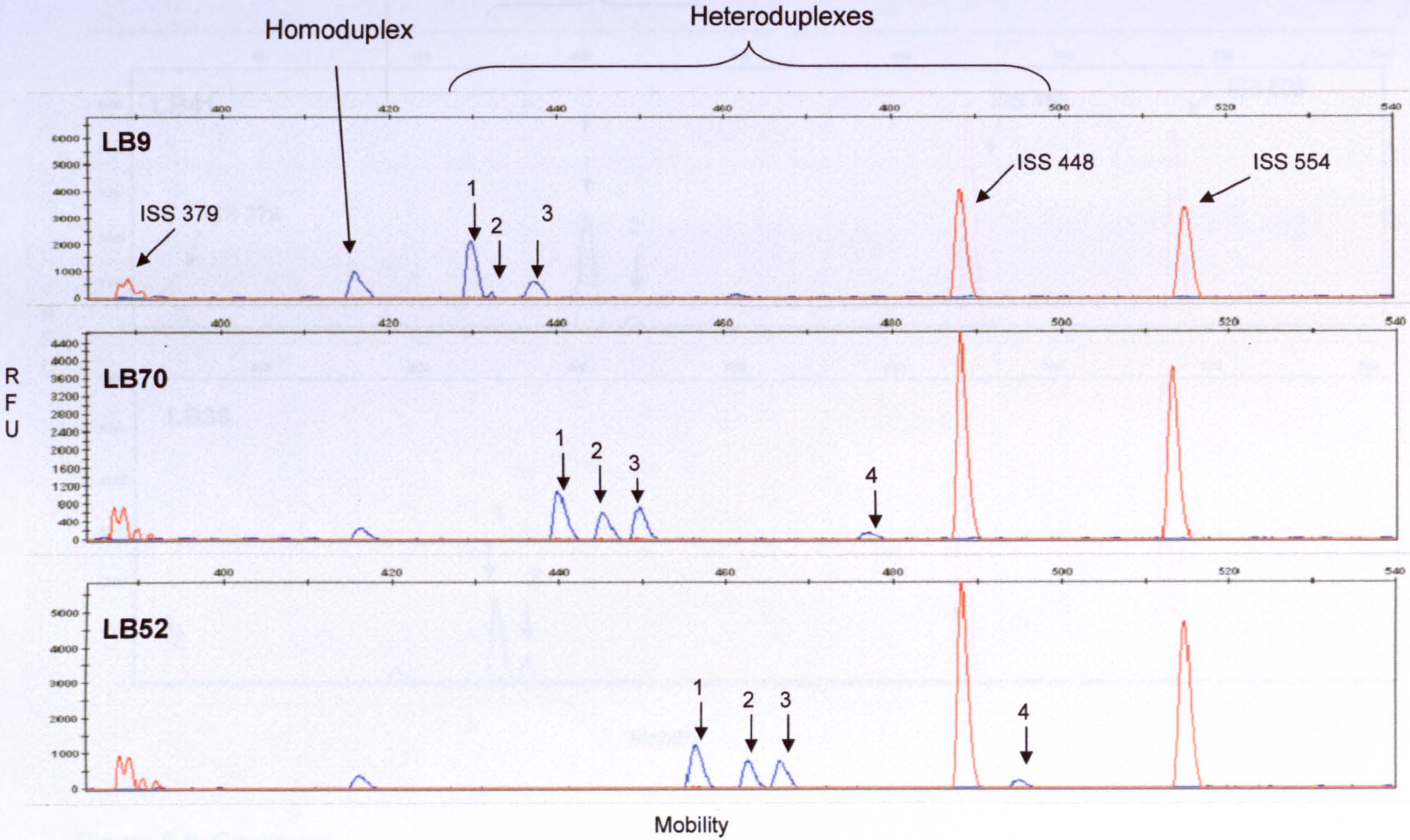

Figure 5.8 (continued overleaf): RSCA profiles for a selection of liver biopsies (LB) displaying multiple heteroduplexes. ISS = internal size standard, with mobility value given. The heteroduplex species are numbered. See Table 5.4 for clinical characteristics for each biopsy specimen.

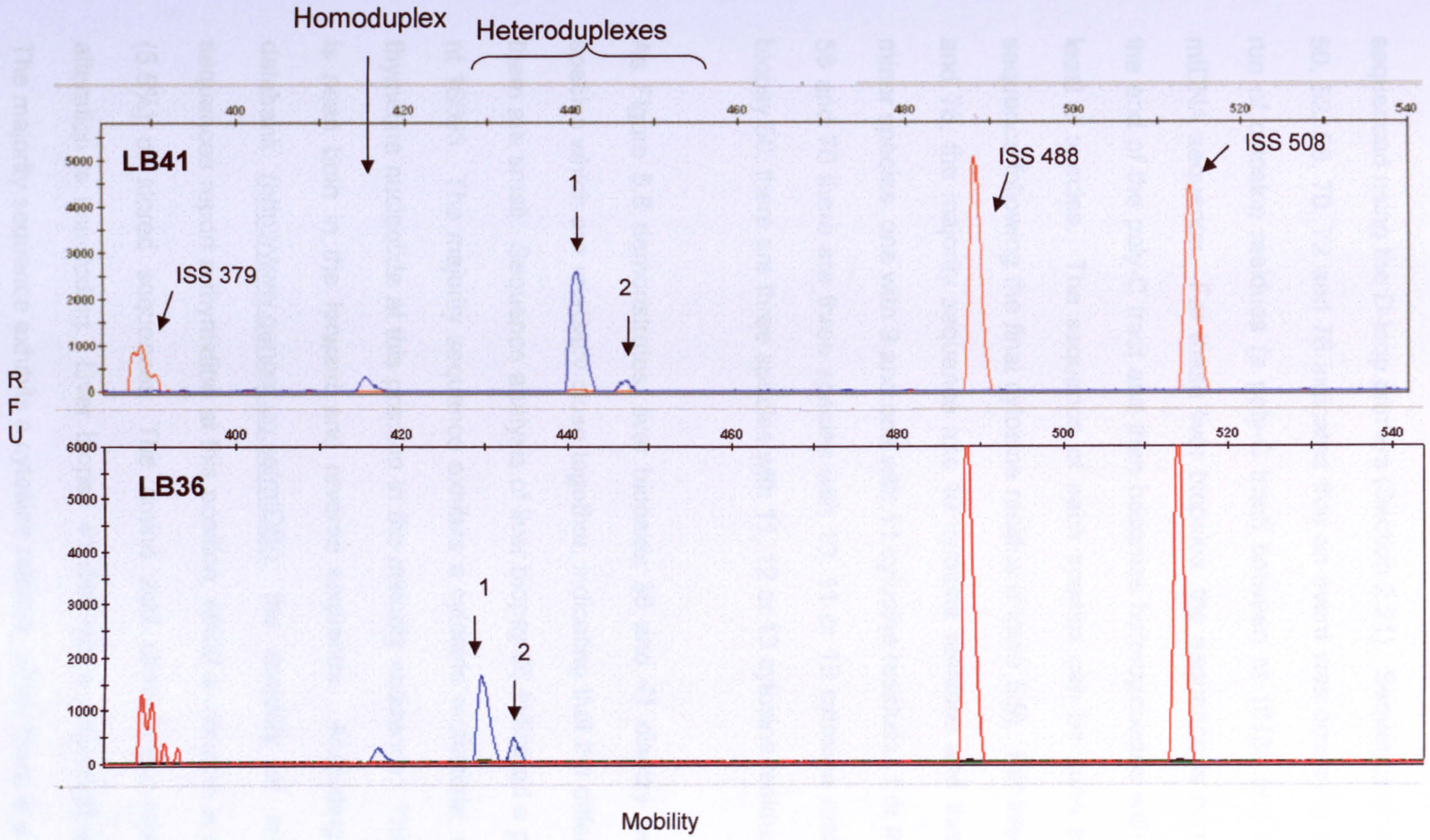

Figure 5.8: Continued.

In order to characterise the observed RSCA profiles in individuals with multiple heteroduplexes, the purified D-loop amplicons from these liver biopsies were sequenced using the D-loop primers (Section 2.21). Sequence analysis of livers 9, 50, 52, 58, 70, 72 and 76 indicated that an event was occurring around a repeat run of cytosine residues (a poly-C tract) between nt 16184 and nt 16193 of the mtDNA sequence. For these liver biopsies, the sequence is homogeneous until the end of the poly-C tract and then becomes heterogeneous with a mixture of at least 3 species. The sequence of each species can be seen as a 'staggered' sequence following the final cytosine residue (Figure 5.9). For liver biopsies 9, 72 and 76, the majority sequence has 10 cytosine residues and there are also two minor species, one with 9 and one with 11 cytosine residues. For liver biopsies 52, 58 and 70 there are three species with 10, 11 or 12 cytosine residues. For liver biopsy 50, there are three species with 11, 12 or 13 cytosine residues.

As Figure 5.8 demonstrates, liver biopsies 36 and 41 display two heteroduplex species which are relatively close together, indicating that the differences between them are small. Sequence analysis of liver biopsy 36 indicated a polymorphism at nt 16093. The majority sequence exhibits a cytosine nucleotide, whilst there is a thymidine nucleotide at this position in the minority sequence. This polymorphism is seen both in the forward and reverse sequence. According to the mtDNA databank (http://www.genpat.uu.se/mtDB/), the majority of recorded mtDNA sequences report a thymidine at this position, whilst a cytosine is seen in 98/1768 (5.5%) of stored sequences. The amino acid change encoded by the T→C alteration is non-coding. Liver biopsy 41 displays a polymorphism at nt 16234. The majority sequence exhibits a cytosine residue, whilst there is a thymidine

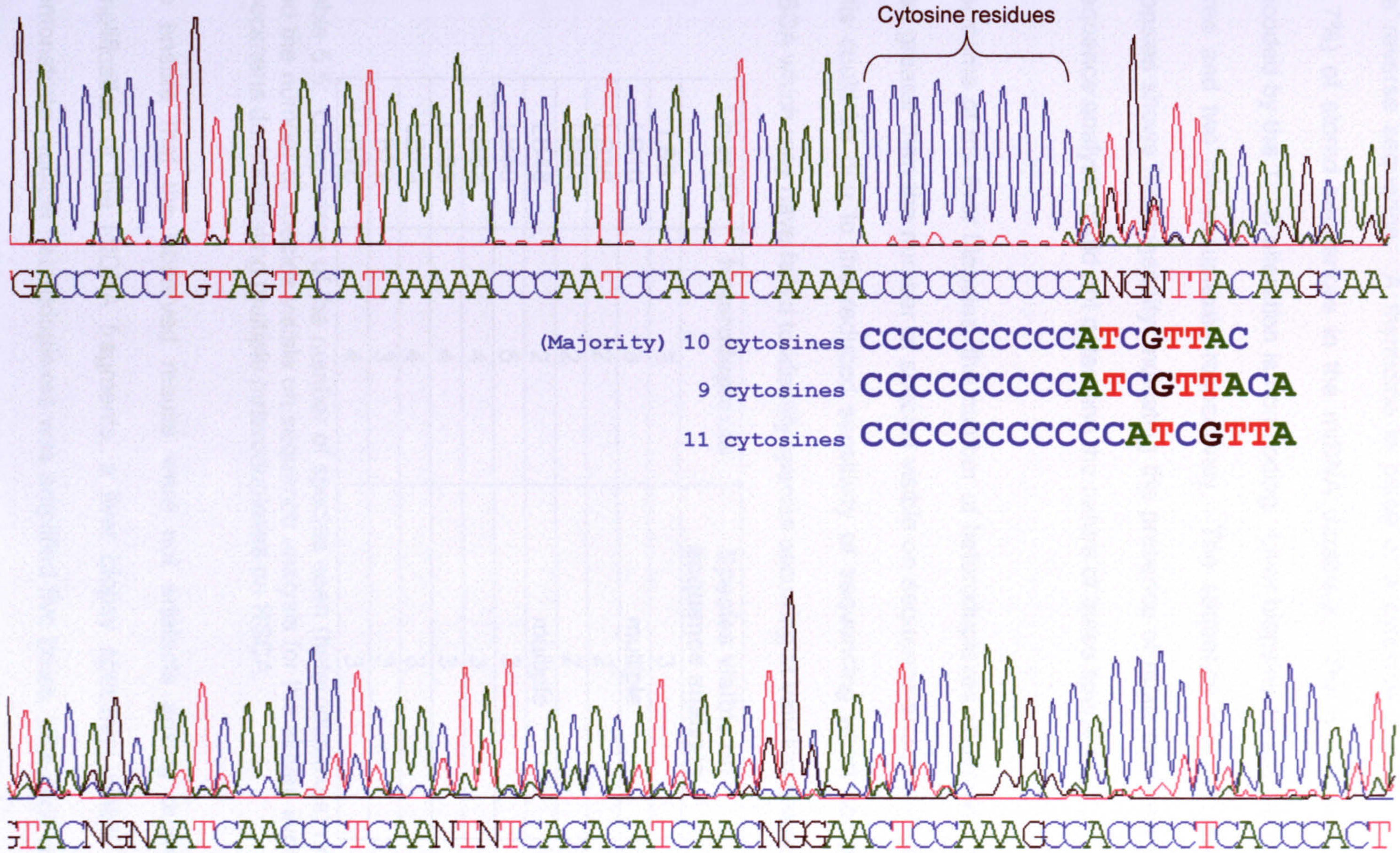

Figure 5.9: Sequence around the poly-C tract at nucleotide position 16184-16193 demonstrating the staggering of the sequence after the poly-C tract due to heteroplasmy in the number of cytosine (C) residues. The sequence illustrated has a majority species which has a poly-C tract of 10 cytosines and two minority species with 9 and 11 cytosine residues respectively.

residue in the minority sequence. This polymorphism is, however, not confirmed in the reverse sequence. A thymidine in place of a cytosine is seen in 67/1800 (3.7%) of stored sequences in the mtDNA databank. The amino acid change encoded by the T→C alteration is non-coding. Liver biopsies 10 and 48 displayed three and two heteroduplexes respectively. The sequence data for these liver biopsies shows heterogeneity, indicating the presence of more than one species. Sequence analysis could not determine the nature of these species.

For some of the liver biopsies, the number of heteroduplexes observed on RSCA was greater than the number of species visible on sequence analysis (Table 5.5). This could be due to the reduced sensitivity of sequencing when compared to RSCA which may have failed to identify species occurring at very low levels.

Liver ID	Heteroduplexes	Species visible on sequence analysis
LB9	3	3
LB10	3	multiple
LB36	2	2
LB41	2	2
LB48	2	multiple
LB50	5	3
LB52	4	3
LB58	4	3
LB70	4	3
LB72	3	3
LB76	4	3

Table 5.5: Comparison of the number of species seen (heteroduplexes) on RSCA and the number of species visible on sequence analysis for the eleven liver biopsy specimens demonstrating multiple heteroduplexes on RSCA.

To ensure that the observed results were not artefacts arising during PCR amplification of the mtDNA fragments, a liver biopsy specimen which did not demonstrate multiple heteroduplexes was amplified five times, with each amplicon subjected to both RSCA and sequence analysis. RSCA demonstrated no

additional heteroduplexes and sequence analysis confirmed only a single species with no evidence of poly-C tract alterations (data not shown).

5.5 Discussion

5.5.1 D-loop region as a target for mtDNA damage detection

This study was undertaken to examine mtDNA damage resulting from attack by reactive oxygen species (ROS) during oxidative stress. mtDNA is well recognised as being more susceptible to ROS than nuclear DNA (Richter *et al*, 1988; Yakes and Van Houten, 1997). Numerous factors account for this increased susceptibility, including lack of protective histones (Celeste *et al*, 2003) and the generation of substantial amounts of ROS by mitochondria. As mtDNA suffers a greater level of damage than nuclear DNA, it is therefore easier to detect, providing an ideal marker to determine absolute cellular DNA damage.

mtDNA damage is region-dependent, with the D-loop being particularly susceptible. This is thought to be due to its unique three-strand 'loop' structure which is prone to attack (ter Schegget *et al*, 1997) and to the reduced level of mtDNA repair which occurs in this region (Mambo *et al*, 2003). Even within the D-loop itself, there are certain 'hot-spots' of mutation (Stoneking *et al*, 2000) known as hypervariable segments (HVS1 and HVS2). The heightened level of mutation seen within these regions is thought to be due to the presence of micro-satellites - stretches of DNA with high base pair repetition (Sia *et al*, 1997). There are several accounts of mtDNA mutations within a poly-cytidine stretch in HVS2 which has been observed in human cancers (Sanchez-Cespedes *et al*, 2001; Wang *et al*, 2005).

Although the D-loop region is 'non-coding', its integrity is vital to mitochondrial survival as it contains the signals that control both its DNA and RNA synthesis. Small alterations within the region could, therefore, have an extremely detrimental effect, disrupting mitochondrial function and therefore reducing the oxidative phosphorylation capacity of cells. These functional impairments could also enhance the generation of ROS, which in turn would accelerate DNA mutation. Accordingly, the D-loop was chosen as the target region to examine oxidative-stress related mtDNA damage. To maximise the possibility of detecting damage within this region, attention was focused on the hot-spots of mutation. Mutations in HVS2 are well documented, primarily in association with human cancer (Sanchez-Cespedes, 2001; Nomoto *et al*, 2002; Okochi *et al*, 2002). Therefore it was decided to focus on the other hot-spot of mutation - HVS1 as the target for this research.

As described extensively in Section 1.18, HCV is strongly associated with increased levels of oxidative stress within infected individuals. Attack by ROS leads to different types of DNA damage, including strand breaks and base/ nucleotide modifications. As cells contain 10^3-10^4 mtDNA molecules, the attack by ROS would likely lead to a variety of D-loop species each with different amounts and types of damage. With this in mind, it was decided to develop a method which could be utilised, not to detect specific mutations within the D-loop, but to screen a section of the region which is known to be a particular hot-spot of mutation to detect and quantify the number of D-loop 'species' within an individual, with each species harbouring different types of damage.

5.5.2 D-loop mutations/damage and liver disease

The vast majority of studies examining D-loop mutation in liver disease have focused on hepatocellular carcinoma (HCC). This interest in liver cancer stems from the accumulating body of evidence that somatic mtDNA mutations occur in a variety of human cancers. Somatic mtDNA mutations have been identified in bladder, head and neck and lung cancers (Fliss *et al*, 2000), ovarian (Liu *et al*, 2001), prostate (Petros *et al*, 2005) and colorectal cancers (Lievre *et al*, 2005) and gastric tumours (Alonso *et al*, 1997; Wu *et al*, 2005; Zhao *et al*, 2005). In contrast to inherited mitochondrial diseases, in which mtDNA mutations are mainly observed in the tRNA and coding regions, somatic mutations in human cancers are commonly located within the D-loop region.

Approximately 20% of people infected with HCV will develop cirrhosis of the liver, and a proportion of these will go on to develop HCC (Figure 1.2, Chapter One). Studies on patients with HCC mirror the findings of other human cancers in that somatic mtDNA mutations appear to play an integral role in tumorigenesis, with mtDNA mutations associated with HCC occurring mainly within the D-loop region. HCC is unique in that the cancer is usually preceded by chronic infection or disease for many years before the cancer, although the development of carcinoma itself is rapid. The presence of HCV within liver cells prior to progression to HCC results in a high level of oxidative stress, further increasing the likelihood of D-loop mutations. Direct sequencing of the D-loop of mtDNA has demonstrated somatic mutations in the tumour mtDNA of 34% (n=50) (Okochi *et al*, 2002) and 68% (n=19) (Nomoto *et al*, 2002) of human HCC cases. The matching of mutations in paired serum samples from these patients led Okochi and colleagues (2002) to

suggest the screening of patients at high risk for HCC for the presence of tumour cells in the serum by detection of mtDNA mutations.

The frequency of mtDNA mutations was found to be markedly increased in both the cancerous and non-cancerous liver tissue from individuals with HCC, compared to healthy controls. The vast majority of mutations were found to occur within the D-loop region (Nishikawa *et al,* 2001; Lee *et al*, 2004; Tamori *et al*, 2004; Yoneyama *et al*, 2005). The frequency of D-loop mutations was found to be greater than described previously for other tumours, suggesting accumulation of mtDNA mutations as a useful predictor of hepatocarcinogenesis. Many of these mutations were located in a poly-cytidine stretch in HVS2. The observation of high numbers of mutations in the non-cancerous tissue suggests that the hepatocytes in such tissue may already have undergone the initial stage of malignant transformation during chronic inflammation. These studies all describe D-loop mutation in individuals who have already progressed to HCC. The only published study on D-loop damage in chronic HCV infection, in the absence of HCC has found the frequency of mtDNA mutations to be increased in liver tissue from patients with chronic HCV infection compared to normal controls (Nishikawa *et al*, 2005). The greatest number of mutations was apparent in the D-loop, particularly within HVS2. Interferon therapy resulted in a significant decrease in the number of mutations within the D-loop. This study suggested that the hepatocytes in these patients were continuously undergoing malignant transformation during inflammation induced by HCV infection, which was reduced by interferon therapy.

The studies described above all utilised direct sequencing for mutation detection. This is relatively insensitive at detecting DNA mutations and will not easily identify low-frequency differences below 20% (Hancock *et al*, 2005). It is also a labour-intensive process which requires time-consuming sequence data analysis. Very few studies have used methods other than sequencing for D-loop mutation detection in liver disease. Temporal temperature gradient gel electrophoresis (TTGE) involves separation of PCR amplicons on a gel immersed in buffer which warms up through the melting temperature range of the fragment of interest. This allows the separation of DNA fragments based on minute differences. In the presence of homoplasmy, a single band is observed. If heteroplasmy occurs, melting and annealing after the last PCR cycle results in two homoduplex and two heteroduplex bands with different mobilities. This technique has been used in a study by Wong *et al* (2004) in which the entire mitochondrial genome was amplified and then subjected to TTGE. This enabled the detection of somatic mutations in 10/20 (50%) liver tumour biopsies from patients with HCC, with 24 different mutations found. Unlike other studies, which focused only on the D-loop region, this assay enabled comprehensive mutational analysis of the entire mitochondrial genome. All of the identified mutations except one (96%) were in the D-loop region, a rate much higher than other tumours and the poly-cytidine stretch in HVS2 was seen to be a mutation hot-spot. Onishi *et al* (2007) have developed a PCR-single strand conformation polymorphism (SSCP) assay to study D-loop mutations in the liver tissue of rats with HCC induced through diet modifications. This method involves PCR amplification, followed by agarose gel electrophoresis. Presence of mutations is detected by abnormally shifted bands on the gel which are extracted, re-amplified and directly sequenced. In this study, mutations were

detected in the liver tissue of 50% (n=10) of rats with HCC induced by an n-nitrosodiethylamine diet. TTGE and PCR-SSCP are methods which are similar to RSCA. However, both are gel-based and therefore suffer from poor gel-to-gel reproducibility. TGGE is also a time-consuming process, with gel run times of 4-6 hours.

These studies have all demonstrated that D-loop mutations are commonly seen in association with HCC, at a frequency much higher than observed in other tumours. Several of the studies noted alterations in the amount of mtDNA in tumour tissues with D-loop mutations (Lee *et al*, 2004; Wong *et al*, 2004). This suggests that the alterations in the D-loop region are displaying an effect on mtDNA replication, which could repress mitochondrial gene expression, resulting in a detrimental effect on the bioenergetic function of cells in affected liver tissue. These studies have all centred on HCC, often in association with HCV infection, yet there is only one report on D-loop mutation/damage in the liver tissue of individuals chronically infected with HCV in the absence of HCC (Nishikawa *et al*, 2005). The methods used to detect these mutations have been restricted to sequencing, with its lack of sensitivity and gel-based duplex assays (PCR-SSCP and TTGE) which suffer gel-variability and poor reproducibility. Thus, the design of a study to examine D-loop mutations in individuals chronically infected with HCV, with a new assay which has improved sensitivity and reproducibility was thought to be a useful addition to the existing literature.

5.5.3 Development of RSCA

The transfer of RSCA from gel-based to capillary electrophoresis has improved its resolution and sensitivity and increased throughput. This allowed the further development of this method for HLA typing (Turner *et al*, 1999; 2001). Furthermore, it enabled the technique to be used in a number of new applications, particularly within the field of genetics in screening for unknown mutations in disease-related genes, including those implicated in cancer (Davies *et al*, 2002; Esteban-Cardenosa *et al*, 2004). The method utilises simple DNA manipulations and short run times for capillary electrophoresis, promoting it as a useful tool in the diagnostic environment (Kozlowski *et al*, 2005). The high reproducibility of migration profiles has also lead RSCA to be developed as a powerful typing tool which has been applied for identification of pathogenic fungi (McIlhatton *et al*, 2002) and HCV genotyping (White *et al*, 2000).

Several studies have indicated that RSCA could be used as a screening method to identify multiple species within an individual. RSCA (using gel electrophoresis for duplex separation) was able to identify mixed viral infections (HCV and TT virus), even when the co-infecting virus represented only 1% of the viral population in the serum or 2% of the amplified product (White *et al*, 2000a). Multiple HCV quasispecies could be identified within HCV-infected individuals (Rossi *et al* 2003), with each heteroduplex peak representing an HCV quasispecies. The heteroduplex profile within individuals altered considerably during interferon treatment and post-liver transplant, demonstrating evolution of quasispecies. RSCA has also recently been applied in the detection of dual-subtype HIV infections which could be identified by the observation of multiple heteroduplexes

following gel electrophoresis (Powell *et al*, 2008). Ross *et al* (2002) used gel-based RSCA to look at the damage in the D-loop region associated with increasing age. The technique was able to detect a level of polyplasmy, with the maximum number of mtDNA species in any one sample totalling four. However, these species were not sequenced to show the nature of the damage. These studies have all demonstrated that RSCA could be a useful tool to screen for different D-loop species within an individual.

In the design of RSCA for this study, several factors had to be carefully considered to enable to the creation of an assay which had good sensitivity and reproducibility and also produced data which was easy to analyse. The generation of a good FLR was paramount as this would provide the reference against which all unknowns were compared. If the FLR is not significantly different from the unknown samples then the migration of heteroduplexes would be restricted and would make differentiation between duplexes very difficult. Fortunately, an FLR could be created from a laboratory worker who clearly demonstrated a number of differences from the rCRS. The alternative would have been to create an FLR through site-directed mutagenesis of the target sequence which would have produced a unique sequence to be employed as a reference.

The dilution protocol for the products of duplex formation needed to be carefully optimised. Over-dilution of products would have lessened the sensitivity of the assay, which may then have failed to detect D-loop species occurring at low-levels. Conversely, under-dilution of products would lead to 'pull-up' peaks from bleed through of dyes and extremely high fluorescent signals which would produce peaks

that were flattened and impossible to accurately size. The two-step dilution protocol described in section 5.3.5 resulted from a long series of optimisation experiments. The capillary electrophoresis protocol was adapted from that used by others (e.g. Mattocks *et al*, 2007) and was carefully fine-tuned to produce quality data and high-throughput. The injection time of capillary electrophoresis also plays a role in the quality of peaks and the sensitivity of the assay, and so this needed to be carefully optimised in association with the dilution protocol.

As a result of the optimisation assays, the fully developed RSCA assay was found to produce migration profiles with good resolution of homo- and heteroduplexes. Experiments simulating mixed D-loop species demonstrated that the assay was highly sensitive, with the ability to detect minority species when it represented only 2% of the product (Section 5.3.8). The developed assay would only be useful in the clinical setting if it produced results which were reproducible; its low intra- and inter-run variability demonstrated that this was indeed the case. The RSCA assay benefits from its ease of use, with straight-forward duplex-formation and capillary electrophoresis steps which require minimal hands-on time. The short run time of capillary electrophoresis (1 h) enables run through of the entire assay from DNA extraction to data analysis to be achievable within a working day.

5.5.4 Clinical study

The clinical study described in this chapter examines a cohort of individuals with a variety of liver aetiologies including HCV, HBV, excessive alcohol intake and NAFLD/NASH (Appendix G). The overall aim was to determine whether mtDNA damage was occurring to a greater extent in individuals infected with HCV

compared to other liver aetiologies. The optimised RSCA assay was clearly demonstrated to be extremely sensitive, with the capacity to detect minority species occurring at the 2% level. It was, therefore unexpected that the majority (68/79, 86.1%) of livers analysed displayed only a single heteroduplex species. This indicated that, in these individuals, there was no detectable damage occurring in the HVS1 region of the D-loop, or that any damage was below the level of detection of the RSCA assay. For the specimens exhibiting a single heteroduplex, thirty-one different heteroduplex mobility profiles were observed. This is not surprising, as HVS1 is highly polymorphic and therefore used as a tool in human identity forensic testing (Budowle *et al*, 1999) and in the understanding of human evolution (Salas *et al*, 2000).

Eleven of the liver biopsy specimens (13.9%) exhibited two or more heteroduplexes (Table 5.6), indicating that several HVS1 species existed within the liver tissue of these individuals. Sequence analysis of the specimens displaying two or more heteroduplexes demonstrated that in seven of these, an event was occurring at the same location – an uninterrupted run of cytosine residues (a poly-cytidine or poly-C tract) between nucleotides 16184 and 16193, close to the origin of heavy strand replication (Anderson *et al*, 1981). Interrogation of the Mitomap database indicated that genetic variation of the 16184-16193 poly-C tract had been previously reported (Horai and Hayasaka, 1990). In the wild-type mitochondrial genome, a thymidine residue at nt 16189 interrupts the poly-C tract (CCCCCTCCCC). Several other variants exist in which the tract is interrupted by a thymidine at a position other than nt 16189. In approximately 10% of Europeans, there is a T→C substitution at nt 16189, creating a tract of ten uninterrupted

cytosine residues (known as the 16184-16193 poly-C tract). This sequence is unstable and potentially undergoes expansion/contraction, most likely through replication slippage (Hauswirth *et al*, 1984). This generates a heteroplasmic mixture of poly-C tract variants, usually between 9 and 11 cytosine residues in length, but ranging from 8 to 14 within a single individual during their lifetime (Bendall and Sykes, 1995; Lee *et al*, 2004a).

The significance of the 16184-16193 poly-C tract identified in this study is difficult to determine. The clinical characteristics of the individuals demonstrating this occurrence did not identify a common link (Table 5.4) and the small number (n=7) makes it impossible to assign statistical significance. The majority (57%) had viral hepatitis (with viral hepatitis accounting for 63.3% in the study cohort). The average age (45.6 years) did not differ substantially from the study cohort (46.1 years). The male to female ratio (6:1) was higher than in the study cohort (2.3:1) and the reason for this cannot be ascertained.

The D-loop region of mtDNA is non-coding and therefore the 16184-16193 poly-C tract would not have a direct affect on the transcription of particular mitochondrial proteins. However the poly-C tract lies in close proximity to the heavy strand origin of mtDNA replication and both heavy and light strand promoters, so any variations could exert some effect on mtDNA. Any variations in the poly-C tract could alter mtDNA bending thus affecting interaction at these protein-binding sites, resulting in decreased mtDNA transcription/replication. Furthermore, the presence of an uninterrupted poly-C tract could result in decreased replication of mtDNA as DNA

polymerase-γ, the enzyme responsible for mtDNA replication, has a reduced fidelity for homopolymeric sequences (Longley *et al*, 2001).

The 16184-16193 poly-C tract has been linked to several types of cancer. It has been observed in a significantly higher number of women with breast and endometrial cancers than in normal individuals (Liu *et al*, 2003; Wang *et al*, 2005, 2006). It has also recently been detected in 50/100 D-loop clones from both the cancerous and non-cancerous parts of liver tumour tissues (Yoneyama *et al*, 2005). This would indicate that the oxidative stress resulting from chronic infection/disease in the liver induces instability in the mtDNA D-loop regions in both non-cancerous and cancerous parts of the tumour. Alterations in the D-loop poly-C tracts have been seen in premalignant lesions and demonstrate a rising incidence that parallels histological severity (Ha *et al*, 2002). As the D-loop region is the start site of replication of the mitochondrial genome, alterations here may play an important role for growth advantage in tumour cells.

The presence of 10 or more cytosine residues has also been associated with a variety of multifactorial disorders including susceptibility to idiopathic dilated cardiomyopathy (Khogali *et al*, 2001), iron-loading in haemochromatosis (Livesey *et al*, 2004), susceptibility to type 2 diabetes (Casteels *et al*, 1999) and insulin resistance (Poulton *et al*, 2002), although the latter association has been put into question by a further, larger study (Chinnery *et al*, 2005). There is a body of evidence that HCV is linked to and indeed causes type II diabetes (Mason *et al*, 1999; Mehta *et al*, 2003; Noto and Raskin, 2006). One of the individuals demonstrating the 16184-16193 poly-C tract did have diabetes in addition to HCV

infection (LB52). Follow-up analysis of the HCV-infected patients with the 16184-16193 poly-C tract in our study would be informative to examine whether these individuals go on to develop type II diabetes, although further ethical approval would need to be sought for this to be possible.

Four other liver biopsies exhibited multiple heteroduplexes. Two of these specimens demonstrated, on sequence analysis, single nucleotide transitions (T→C in both cases) which results in a non-coding amino acid change. The significance of these observations is difficult to determine. The other livers displaying multiple heteroduplexes demonstrated a mixture of species on sequence analysis, but these could not be characterised. Cloning prior to sequencing may have allowed the isolation and characterisation of each species, if the minority species was present at a sufficient level to be successfully cloned.

The overall aim of this study was to determine whether D-loop damage was occurring to a greater extent in individuals with HCV compared to other liver aetiologies. It was thought that some biochemical or physiologic changes within infected cells might induce instability in the mtDNA D-loop region. Five (45.5%, n=11) of the liver biopsies exhibiting multiple heteroduplexes were from individuals infected with HCV (Table 5.4). As the percentage of HCV-infected individuals in the entire cohort was 53% (n=79), this is not a statistically significant finding and does not indicate that mtDNA damage in the D-loop region was occurring more frequently in HCV-infected individuals. The cohort size for this study was relatively small and would need to be increased to examine further the relationship between HCV and mtDNA damage. The level of D-loop mutations reported in this study

was less than that observed in previously described studies of individuals with HCC in which D-loop mutations were reported in between 34-68% of individuals (Okochi *et al*, 2002; Nomoto *et al*, 2002; Lee *et al*, 2004; Wong *et al*, 2004). As the RSCA assay demonstrated increased sensitivity than that reported of sequencing (Hancock *et al*, 2005), it would not seem that the lower level was due to non-detection of mutations. It may be that D-loop damage is not apparent until chronic infection has proceeded to HCC.

A disadvantage of this study was the lack of matching serum samples for each liver biopsy specimen, which could not be obtained for logistical reasons. A comparison between the blood and liver specimens would have been useful to determine whether the identified mutations/damage were seen solely in the liver or were apparent in the blood. If the latter were the case, this could indicate that the observed D-loop mutations were in the germ line and were not occurring as a result of oxidative damage. It is also impossible to tell from this analysis if the observed alterations in the D-loop were due to the DNA-damaging effects of oxidative stress or whether they resulted from some other occurrence such as replication slippage (Hauswirth *et al*, 1984). Detection of markers of oxidative stress in the liver biopsies could have identified whether the liver tissues demonstrating multiple D-loop species were exhibiting increased levels of oxidative stress compared to livers with single D-loop species.

5.6 Conclusion and future work

The clinical study outlined in this chapter demonstrated detectable D-loop mtDNA damage in only a small percentage of individuals with liver disease. Furthermore, there was no association between HCV infection and D-loop damage. This could be due to the absence of damage occurring within this region, damage occurring at levels below the sensitivity of detection of the assay or the presence of efficient mtDNA repair pathways. As the RSCA assay was able to detect minority D-loop species representing just 2% of the total product, it is likely that damage was either occurring at extremely low levels (<2%) or was not present in the individuals studied. Repair of mtDNA damage, especially within the D-loop, was thought to be less efficient than nuclear DNA repair (Pinz *et al*, 1995; Yakes and Van Houten, 1997; Graziewicz *et al*, 2002). However, as the D-loop damage seen in this study was so low, it may be that mtDNA repair mechanisms are more efficient than originally thought, with mitochondrially-targeted repair enzymes such as OGG1 functioning proficiently (Takao *et al*, 1998; de Souza-Pinto *et al*, 2001).

Although the RSCA assay could not detect mtDNA damage in this clinical cohort, it is none-the-less a very powerful tool which could be utilised for a variety of applications. It could, for example, be used to assess the DNA-damaging potential of certain drug therapies or to look at *in vitro* damage in cell lines. The association of D-loop mutations, especially those occurring around poly-C tracts in both the D-loop hypervariable segments, with human cancers (Lièvre *et al*, 2006; Wang *et al*, 2006) indicates that the developed assay could provide a useful tool to further study D-loop damage as a potential biomarker for cancer detection. The ease with which the assay can be carried out, with its simple DNA manipulations and short

run times for capillary electrophoresis, promotes the developed RSCA assay as a high-throughput diagnostic method for pathogen identification and genotyping. Progress on this has already been made with the development of RSCA for the identification of pathogenic fungi (McIlhatton *et al*, 2002) and as a method for HCV genotyping (White *et al*, 2000) and will be an extremely useful tool for further development within our diagnostic microbiology laboratory.

REFERENCES

Abacioglu, YH, Bacaksiz, F, Bahar, IH and Simmonds, P (2000). "Molecular evidence of nosocomial transmission of hepatitis C virus in a haemodialysis unit." Eur J Clin Microbiol Infect Dis **19**(3): 182-6.

Abdalla, MY, Ahmad, IM, Spitz, DR, Schmidt, WN and Britigan, BE (2005). "Hepatitis C virus-core and non structural proteins lead to different effects on cellular antioxidant defenses." J Med Virol **76**(4): 489-97.

Agnello, V, Abel, G, Elfahal, M, Knight, GB and Zhang, QX (1999). "Hepatitis C virus and other flaviviridae viruses enter cells via low density lipoprotein receptor." Proc Natl Acad Sci U S A **96**(22): 12766-71.

Alberts B, Johnson A, Lewis J, Raff M, Roberts K and Walter (eds). (2002). Chapter 14: Energy conversion: mitochondria and chloroplasts. Molecular Biology of the Cell. Fourth Edition. New York. Garland Science.

Allander, T, Gruber, A, Naghavi, M, Beyene, A, Soderstrom, T, Bjorkholm, M, Grillner, L and Persson, MA (1995). "Frequent patient-to-patient transmission of hepatitis C virus in a haematology ward." Lancet **345**(8950): 603-7.

Alonso, A, Martin, P, Albarran, C, Aquilera, B, Garcia, O, Guzman, A, Oliva, H and Sancho, M (1997). "Detection of somatic mutations in the mitochondrial DNA control region of colorectal and gastric tumors by heteroduplex and single-strand conformation analysis." Electrophoresis **18**(5): 682-5.

Alric, L, Fort, M, Izopet, J, Vinel, JP, Bureau, C, Sandre, K, Charlet, JP, Beraud, M, Abbal, M and Duffaut, M (2000). "Study of host- and virus-related factors associated with spontaneous hepatitis C virus clearance." Tissue Antigens **56**(2): 154-8.

Alter, MJ (1993). "The detection, transmission, and outcome of hepatitis C virus infection." Infect Agents Dis **2**(3): 155-66.

Alter, MJ, Margolis, HS, Krawczynski, K, Judson, FN, Mares, A, Alexander, WJ, Hu, PY, Miller, JK, Gerber, MA, Sampliner, RE and et al. (1992). "The natural history of community-acquired hepatitis C in the United States. The Sentinel Counties Chronic non-A, non-B Hepatitis Study Team." N Engl J Med **327**(27): 1899-905.

Amoroso, P, Rapicetta, M, Tosti, ME, Mele, A, Spada, E, Buonocore, S, Lettieri, G, Pierri, P, Chionne, P, Ciccaglione, AR and Sagliocca, L (1998). "Correlation between virus genotype and chronicity rate in acute hepatitis C." J Hepatol **28**(6): 939-44.

Anderson, S, Bankier, AT, Barrell, BG, de Bruijn, MH, Coulson, AR, Drouin, J, Eperon, IC, Nierlich, DP, Roe, BA, Sanger, F, Schreier, PH, Smith, AJ, Staden, R and Young, IG (1981). "Sequence and organization of the human mitochondrial genome." Nature **290**(5806): 457-65.

Andonov, A and Chaudhary, RK (1995). "Subtyping of hepatitis C virus isolates by a line probe assay using hybridization." J Clin Microbiol **33**(1): 254-6.

Andrews, RM, Kubacka, I, Chinnery, PF, Lightowlers, RN, Turnbull, DM and Howell, N (1999). "Reanalysis and revision of the Cambridge reference sequence for human mitochondrial DNA." Nat Genet **23**(2): 147.

Ansaldi, F, Torre, F, Bruzzone, BM, Picciotto, A, Crovari, P and Icardi, G (2001). "Evaluation of a new hepatitis C virus sequencing assay as a routine method for genotyping." J Med Virol **63**(1): 17-21.

Applied Biosystems. (2000). GeneScan® Reference Guide. Available at www.appliedbiosystems.com.

Argüello, JR, Little, AM, Bohan, E, Goldman, JM, Marsh, SG and Madrigal, JA (1998). "High resolution HLA class I typing by reference strand mediated conformation analysis (RSCA)." Tissue Antigens **52**(1): 57-66.

Argüello, JR, Little, AM, Pay, AL, Gallardo, D, Rojas, I, Marsh, SG, Goldman, JM and Madrigal, JA (1998a). "Mutation detection and typing of polymorphic loci through double-strand conformation analysis." Nat Genet **18**(2): 192-4.

Bai, RK and Wong, LJ (2005). "Simultaneous detection and quantification of mitochondrial DNA deletion(s), depletion, and over-replication in patients with mitochondrial disease." J Mol Diagn **7**(5): 613-22.

Bai, RK, Perng, CL, Hsu, CH and Wong, LJ (2004). "Quantitative PCR analysis of mitochondrial DNA content in patients with mitochondrial disease." Ann N Y Acad Sci **1011**: 304-9.

Bailey, SM and Cunningham, CC (1999). "Effect of dietary fat on chronic ethanol-induced oxidative stress in hepatocytes." Alcohol Clin Exp Res **23**(7): 1210-8.

Balogun, MA, Ramsay, ME, Parry, JV, Donovan, L, Andrews, NJ, Newham, JA, McGarrigle, C, Harris, KA and Teo, CG (2003). "A national survey of genitourinary medicine clinic attenders provides little evidence of sexual transmission of hepatitis C virus infection." Sex Transm Infect **79**(4): 301-6.

Balogun, MA, Ramsay, ME, Hesketh, LM, Andrews, N, Osborne, KP, Gay, NJ and Morgan-Capner, P (2002). "The prevalence of hepatitis C in England and Wales." J Infect **45**(4): 219-26.

Balogun, MA, Ramsay, ME, Parry, JV, Donovan, L, Andrews, NJ, Newham, JA, Cliffe, S, Harris, KA and Teo, CG (2000). "The prevalence and genetic diversity of hepatitis C infection in antenatal clinic attenders in two regions of England." Epidemiol Infect **125**(3): 705-12.

Bandy, B and Davison, AJ (1990). "Mitochondrial mutations may increase oxidative stress: implications for carcinogenesis and aging?" Free Radic Biol Med **8**(6): 523-39.

Bandyopadhyay, SK and Dutta, A (2005). "Mitochondrial hepatopathies." J Assoc Physicians India **53**: 973-8.

Barbaro, G, Di Lorenzo, G, Asti, A, Ribersani, M, Belloni, G, Grisorio, B, Filice, G and Barbarini, G (1999). "Hepatocellular mitochondrial alterations in patients with chronic hepatitis C: ultrastructural and biochemical findings." Am J Gastroenterol **94**(8): 2198-205.

Bartenschlager, R and Lohmann, V (2000). "Replication of hepatitis C virus." J Gen Virol **81**(Pt 7): 1631-48.

Bartley, PB, Westacott, L, Boots, RJ, Lawson, M, Potter, JM, Hyland, VJ and Woods, ML, 2nd (2001). "Large hepatic mitochondrial DNA deletions associated with L-lactic acidosis and highly active antiretroviral therapy." Aids **15**(3): 419-20.

Bartolome, J, Lopez-Alcorocho, JM, Castillo, I, Rodriguez-Inigo, E, Quiroga, JA, Palacios, R and Carreno, V (2007). "Ultracentrifugation of serum samples allows detection of hepatitis C virus RNA in patients with occult hepatitis C." J Virol **81**(14): 7710-5.

Bartosch, B, Vitelli, A, Granier, C, Goujon, C, Dubuisson, J, Pascale, S, Scarselli, E, Cortese, R, Nicosia, A and Cosset, FL (2003). "Cell entry of hepatitis C virus requires a set of co-receptors that include the CD81 tetraspanin and the SR-B1 scavenger receptor." J Biol Chem **278**(43): 41624-30.

Beckman, KB and Ames, BN (1998). "The free radical theory of aging matures." Physiol Rev **78**(2): 547-81.

Beckman, JS, Beckman, TW, Chen, J, Marshall, PA and Freeman, BA (1990). "Apparent hydroxyl radical production by peroxynitrite: implications for endothelial injury from nitric oxide and superoxide." Proc Natl Acad Sci U S A **87**(4): 1620-4.

Beld, M, Minnaar, R, Weel, J, Sol, C, Damen, M, van der Avoort, H, Wertheim-van Dillen, P, van Breda, A and Boom, R (2004). "Highly sensitive assay for detection of enterovirus in clinical specimens by reverse transcription-PCR with an armored RNA internal control." J Clin Microbiol **42**(7): 3059-64.

Beld, M, Sentjens, R, Rebers, S, Weegink, C, Weel, J, Sol, C and Boom, R (2002). "Performance of the New Bayer VERSANT HCV RNA 3.0 assay for quantitation of hepatitis C virus RNA in plasma and serum: conversion to international units and comparison with the Roche COBAS Amplicor HCV Monitor, Version 2.0, assay." J Clin Microbiol **40**(3): 788-93.

Beld, M, Penning, M, van Putten, M, van den Hoek, A, Lukashov, V, McMorrow, M and Goudsmit, J (1998). "Hepatitis C virus serotype-specific core and NS4 antibodies in injecting drug users participating in the Amsterdam cohort studies." J Clin Microbiol **36**(10): 3002-6.

Bendall, KE and Sykes, BC (1995). "Length heteroplasmy in the first hypervariable segment of the human mtDNA control region." Am J Hum Genet **57**(2): 248-56.

Benvegnu, L, Pontisso, P, Cavalletto, D, Noventa, F, Chemello, L and Alberti, A (1997). "Lack of correlation between hepatitis C virus genotypes and clinical course of hepatitis C virus-related cirrhosis." Hepatology **25**(1): 211-5.

Blanchard, E, Belouzard, S, Goueslain, L, Wakita, T, Dubuisson, J, Wychowski, C and Rouille, Y (2006). "Hepatitis C virus entry depends on clathrin-mediated endocytosis." J Virol **80**(14): 6964-72.

Bogenhagen, DF, Pinz, KG and Perez-Jannotti, RM (2001). "Enzymology of mitochondrial base excision repair." Prog Nucleic Acid Res Mol Biol **68**: 257-71.

Bogenhagen, D and Clayton, DA (1974). "The number of mitochondrial deoxyribonucleic acid genomes in mouse L and human HeLa cells. Quantitative isolation of mitochondrial deoxyribonucleic acid." J Biol Chem **249**(24): 7991-5.

Bonkovsky, HL, Banner, BF and Rothman, AL (1997). "Iron and chronic viral hepatitis." Hepatology **25**(3): 759-68.

Bouchardeau, F, Cantaloube, JF, Chevaliez, S, Portal, C, Razer, A, Lefrere, JJ, Pawlotsky, JM, De Micco, P and Laperche, S (2007). "Improvement of hepatitis C virus (HCV) genotype determination with the new version of the INNO-LiPA HCV assay." J Clin Microbiol **45**(4): 1140-5.

Boulet, L, Karpati, G and Shoubridge, EA (1992). "Distribution and threshold expression of the tRNA(Lys) mutation in skeletal muscle of patients with myoclonic epilepsy and ragged-red fibers (MERRF)." Am J Hum Genet **51**(6): 1187-200.

Bourgeron, T, Chretien, D, Rotig, A, Munnich, A and Rustin, P (1993). "Fate and expression of the deleted mitochondrial DNA differ between human heteroplasmic skin fibroblast and Epstein-Barr virus-transformed lymphocyte cultures." J Biol Chem **268**(26): 19369-76.

Boveris, A and Chance, B (1973). "The mitochondrial generation of hydrogen peroxide. General properties and effect of hyperbaric oxygen." Biochem J **134**(3): 707-16.

Bracho, MA, Gosalbes, MJ, Blasco, D, Moya, A and Gonzalez-Candelas, F (2005). "Molecular epidemiology of a hepatitis C virus outbreak in a hemodialysis unit." J Clin Microbiol **43**(6): 2750-5.

Brant, LJ, Hurrelle, M, Balogun, MA, Klapper, P, Ahmad, F, Boxall, E, Hale, A, Hollyoak, V, Ibrahim, IB, Irving, W, Meigh, R, Mutton, KJ, Patel, BC, Paver, WK, Pugh, S, Taylor, C, Turner, AJ and Ramsay, ME (2007). "Sentinel laboratory surveillance of hepatitis C antibody testing in England: understanding the epidemiology of HCV infection." Epidemiol Infect **135**(3): 417-26.

Bromberg, JF, Wrzeszczynska, MH, Devgan, G, Zhao, Y, Pestell, RG, Albanese, C and Darnell, JE, Jr. (1999). "Stat3 as an oncogene." Cell **98**(3): 295-303.

Brown, TA, Cecconi, C, Tkachuk, AN, Bustamante, C and Clayton, DA (2005). "Replication of mitochondrial DNA occurs by strand displacement with alternative light-strand origins, not via a strand-coupled mechanism." Genes Dev **19**(20): 2466-76.

Browne, R, Asboe, D, Gilleece, Y, Atkins, M, Mandalia, S, Gazzard, B and Nelson, M (2004). "Increased numbers of acute hepatitis C infections in HIV positive homosexual men; is sexual transmission feeding the increase?" Sex Transm Infect **80**(4): 326-7.

Bruno, S, Silini, E, Crosignani, A, Borzio, F, Leandro, G, Bono, F, Asti, M, Rossi, S, Larghi, A, Cerino, A, Podda, M and Mondelli, MU (1997). "Hepatitis C virus genotypes and risk of hepatocellular carcinoma in cirrhosis: a prospective study." Hepatology **25**(3): 754-8.

Buckton, AJ, Ngui, SL, Arnold, C, Boast, K, Kovacs, J, Klapper, PE, Patel, B, Ibrahim, I, Rangarajan, S, Ramsay, ME and Teo, CG (2006). "Multitypic hepatitis C virus infection identified by real-time nucleotide sequencing of minority genotypes." J Clin Microbiol **44**(8): 2779-84.

Budowle, B, Wilson, MR, DiZinno, JA, Stauffer, C, Fasano, MA, Holland, MM and Monson, KL (1999). "Mitochondrial DNA regions HVI and HVII population data." Forensic Sci Int **103**(1): 23-35.

Bullock, GC, Bruns, DE and Haverstick, DM (2002). "Hepatitis C genotype determination by melting curve analysis with a single set of fluorescence resonance energy transfer probes." Clin Chem **48**(12): 2147-54.

Cahill, A, Wang, X and Hoek, JB (1997). "Increased oxidative damage to mitochondrial DNA following chronic ethanol consumption." Biochem Biophys Res Commun **235**(2): 286-90.

Caldwell, SH, Swerdlow, RH, Khan, EM, Iezzoni, JC, Hespenheide, EE, Parks, JK and Parker, WD, Jr. (1999). "Mitochondrial abnormalities in non-alcoholic steatohepatitis." J Hepatol **31**(3): 430-4.

Caliendo, AM, Valsamakis, A, Zhou, Y, Yen-Lieberman, B, Andersen, J, Young, S, Ferreira-Gonzalez, A, Tsongalis, GJ, Pyles, R, Bremer, JW and Lurain, NS (2006). "Multilaboratory comparison of hepatitis C virus viral load assays." J Clin Microbiol **44**(5): 1726-32.

Cardin, R, Saccoccio, G, Masutti, F, Bellentani, S, Farinati, F and Tiribelli, C (2001). "DNA oxidative damage in leukocytes correlates with the severity of HCV-related liver disease: validation in an open population study." J Hepatol **34**(4): 587-92.

Carithers, RL, Jr. and Emerson, SS (1997). "Therapy of hepatitis C: meta-analysis of interferon alfa-2b trials." Hepatology **26**(3 Suppl 1): 83S-88S.

Carreno, V, Bartolome, J, Castillo, I and Quiroga, JA (2008). "Occult hepatitis B virus and hepatitis C virus infections." Rev Med Virol **18**(3): 139-57.

Carreno, V (2006). "Occult hepatitis C virus infection: a new form of hepatitis C." World J Gastroenterol **12**(43): 6922-5.

Carreno, V, Pardo, M, Lopez-Alcorocho, JM, Rodriguez-Inigo, E, Bartolome, J and Castillo, I (2006). "Detection of hepatitis C virus (HCV) RNA in the liver of healthy, anti-HCV antibody-positive, serum HCV RNA-negative patients with normal alanine aminotransferase levels." J Infect Dis **194**(1): 53-60.

Casteels, K, Ong, K, Phillips, D, Bendall, H and Pembrey, M (1999). "Mitochondrial 16189 variant, thinness at birth, and type-2 diabetes. ALSPAC study team. Avon Longitudinal Study of Pregnancy and Childhood." Lancet **353**(9163): 1499-500.

Castelain, S, Descamps, V, Thibault, V, Francois, C, Bonte, D, Morel, V, Izopet, J, Capron, D, Zawadzki, P and Duverlie, G (2004). "TaqMan amplification system with an internal positive control for HCV RNA quantitation." J Clin Virol **31**(3): 227-34.

Castillo, I, Pardo, M, Bartolome, J, Ortiz-Movilla, N, Rodriguez-Inigo, E, de Lucas, S, Salas, C, Jimenez-Heffernan, JA, Perez-Mota, A, Graus, J, Lopez-Alcorocho, JM and Carreno, V (2004). "Occult hepatitis C virus infection in patients in whom the etiology of persistently abnormal results of liver-function tests is unknown." J Infect Dis **189**(1): 7-14.

Celeste, A, Difilippantonio, S, Difilippantonio, MJ, Fernandez-Capetillo, O, Pilch, DR, Sedelnikova, OA, Eckhaus, M, Ried, T, Bonner, WM and Nussenzweig, A (2003). "H2AX haploinsufficiency modifies genomic stability and tumor susceptibility." Cell **114**(3): 371-83.

Chabi, B, Mousson de Camaret, B, Duborjal, H, Issartel, JP and Stepien, G (2003). "Quantification of mitochondrial DNA deletion, depletion, and overreplication: application to diagnosis." Clin Chem **49**(8): 1309-17.

Chamberlain, RW, Adams, N, Saeed, AA, Simmonds, P and Elliott, RM (1997). "Complete nucleotide sequence of a type 4 hepatitis C virus variant, the predominant genotype in the Middle East." J Gen Virol **78 (Pt 6)**: 1341-7.

Chance, B, Sies, H and Boveris, A (1979). "Hydroperoxide metabolism in mammalian organs." Physiol Rev **59**(3): 527-605.

Chang, DD and Clayton, DA (1984). "Precise identification of individual promoters for transcription of each strand of human mitochondrial DNA." Cell **36**(3): 635-43.

Chen, Z and Weck, KE (2002). "Hepatitis C virus genotyping: interrogation of the 5' untranslated region cannot accurately distinguish genotypes 1a and 1b." J Clin Microbiol **40**(9): 3127-34.

Cheng, S, Higuchi, R and Stoneking, M (1994). "Complete mitochondrial genome amplification." Nat Genet **7**(3): 350-1.

Chinnery, PF, Elliott, HR, Patel, S, Lambert, C, Keers, SM, Durham, SE, McCarthy, MI, Hitman, GA, Hattersley, AT and Walker, M (2005). "Role of the mitochondrial DNA 16184-16193 poly-C tract in type 2 diabetes." Lancet **366**(9497): 1650-1.

Choi, J and Ou, JH (2006). "Mechanisms of liver injury. III. Oxidative stress in the pathogenesis of hepatitis C virus." Am J Physiol Gastrointest Liver Physiol **290**(5): G847-51.

Choi, J, Lee, KJ, Zheng, Y, Yamaga, AK, Lai, MM and Ou, JH (2004). "Reactive oxygen species suppress hepatitis C virus RNA replication in human hepatoma cells." Hepatology **39**(1): 81-9.

Choo, QL, Richman, KH, Han, JH, Berger, K, Lee, C, Dong, C, Gallegos, C, Coit, D, Medina-Selby, R, Barr, PJ and et al. (1991). "Genetic organization and diversity of the hepatitis C virus." Proc Natl Acad Sci U S A **88**(6): 2451-5.

Choo, QL, Kuo, G, Weiner, AJ, Overby, LR, Bradley, DW and Houghton, M (1989). "Isolation of a cDNA clone derived from a blood-borne non-A, non-B viral hepatitis genome." Science **244**(4902): 359-62.
Clayton, DA (1982). "Replication of animal mitochondrial DNA." Cell **28**(4): 693-705.

Colson, P, Motte, A and Tamalet, C (2006). "Broad differences between the COBAS ampliprep total nucleic acid isolation-COBAS TaqMan 48 hepatitis C virus (HCV) and COBAS HCV monitor v2.0 assays for quantification of serum HCV RNA of non-1 genotypes." J Clin Microbiol **44**(4): 1602-3.

Corcoran, GD, Brink, NS, Millar, CG, Garson, JA, Waite, J, Deaville, R, Thompson, FD and Tedder, RS (1994). "Hepatitis C virus infection in haemodialysis patients: a clinical and virological study." J Infect **28**(3): 279-85.

Corral-Debrinski, M, Shoffner, JM, Lott, MT and Wallace, DC (1992). "Association of mitochondrial DNA damage with aging and coronary atherosclerotic heart disease." Mutat Res **275**(3-6): 169-80.

Cortopassi, GA and Arnheim, N (1990). "Detection of a specific mitochondrial DNA deletion in tissues of older humans." Nucleic Acids Res **18**(23): 6927-33.

Cortopassi, GA, Shibata, D, Soong, NW and Arnheim, N (1992). "A pattern of accumulation of a somatic deletion of mitochondrial DNA in aging human tissues." Proc Natl Acad Sci U S A **89**(16): 7370-4.

Cote, HC, Brumme, ZL, Craib, KJ, Alexander, CS, Wynhoven, B, Ting, L, Wong, H, Harris, M, Harrigan, PR, O'Shaughnessy, MV and Montaner, JS (2002). "Changes in mitochondrial DNA as a marker of nucleoside toxicity in HIV-infected patients." N Engl J Med **346**(11): 811-20.

Cree, LM, Samuels, DC, de Sousa Lopes, SC, Rajasimha, HK, Wonnapinij, P, Mann, JR, Dahl, HH and Chinnery, PF (2008). "A reduction of mitochondrial DNA molecules during embryogenesis explains the rapid segregation of genotypes." Nat Genet **40**(2): 249-54.

Damen, M, Sillekens, P, Sjerps, M, Melsert, R, Frantzen, I, Reesink, HW, Lelie, PN and Cuypers, HT (1998). "Stability of hepatitis C virus RNA during specimen handling and storage prior to NASBA amplification." J Virol Methods **72**(2): 175-84.

Darley-Usmar V, RI, Smith P and Wilson M. (1994). The proteins of the mitochondrial inner membrane and their role in oxidative phosphorylation. Mitochondria: DNA, Proteins and Disease. Darley-Usmar V and Schapira AHV, Portland Press: 1-26.

Davies, H, Bignell, GR, Cox, C, Stephens, P, Edkins, S, Clegg, S, Teague, J, Woffendin, H, Garnett, MJ, Bottomley, W, Davis, N, Dicks, E, Ewing, R, Floyd, Y, Gray, K, Hall, S, Hawes, R, Hughes, J, Kosmidou, V, Menzies, A, Mould, C, Parker, A, Stevens, C, Watt, S, Hooper, S, Wilson, R, Jayatilake, H, Gusterson, BA, Cooper, C, Shipley, J, Hargrave, D, Pritchard-Jones, K, Maitland, N, Chenevix-Trench, G, Riggins, GJ, Bigner, DD, Palmieri, G, Cossu, A, Flanagan, A, Nicholson, A, Ho, JW, Leung, SY, Yuen, ST, Weber, BL, Seigler, HF, Darrow, TL, Paterson, H, Marais, R, Marshall, CJ, Wooster, R, Stratton, MR and Futreal, PA (2002). "Mutations of the BRAF gene in human cancer." Nature **417**(6892): 949-54.

Davis, GL, Wong, JB, McHutchison, JG, Manns, MP, Harvey, J and Albrecht, J (2003). "Early virologic response to treatment with peginterferon alfa-2b plus ribavirin in patients with chronic hepatitis C." Hepatology **38**(3): 645-52.

De Francesco, R (1999). "Molecular virology of the hepatitis C virus." J Hepatol **31 Suppl 1**: 47-53.

De Francesco, R and Carfi, A (2007) "Advances in the development of new therapeutic agents targeting the NS3-4A serine protease or the NS5B RNA-dependent RNA polymerase of the hepatitis C virus" Adv Drug Deliv Rev, **59**(12): 1242-62.

de Grey, AD (1997). "A proposed refinement of the mitochondrial free radical theory of aging." Bioessays **19**(2): 161-6.

De Maria, N, Colantoni, A, Fagiuoli, S, Liu, GJ, Rogers, BK, Farinati, F, Van Thiel, DH and Floyd, RA (1996). "Association between reactive oxygen species and disease activity in chronic hepatitis C." Free Radic Biol Med **21**(3): 291-5.

de Mendoza, C, de Ronde, A, Smolders, K, Blanco, F, Garcia-Benayas, T, de Baar, M, Fernandez-Casas, P, Gonzalez-Lahoz, J and Soriano, V (2004). "Changes in mitochondrial DNA copy number in blood cells from HIV-infected patients undergoing antiretroviral therapy." AIDS Res Hum Retroviruses **20**(3): 271-3.

de Souza-Pinto, NC, Eide, L, Hogue, BA, Thybo, T, Stevnsner, T, Seeberg, E, Klungland, A and Bohr, VA (2001). "Repair of 8-oxodeoxyguanosine lesions in mitochondrial DNA depends on the oxoguanine DNA glycosylase (OGG1) gene and 8-oxoguanine accumulates in the mitochondrial DNA of OGG1-defective mice." Cancer Res **61**(14): 5378-81.

Deleersnyder, V, Pillez, A, Wychowski, C, Blight, K, Xu, J, Hahn, YS, Rice, CM and Dubuisson, J (1997). "Formation of native hepatitis C virus glycoprotein complexes." J Virol **71**(1): 697-704.

Department of Health. (2002) Hepatitis C Strategy for England. Department of Health, London.

Diaz, F, Bayona-Bafaluy, MP, Rana, M, Mora, M, Hao, H and Moraes, CT (2002). "Human mitochondrial DNA with large deletions repopulates organelles faster than full-length genomes under relaxed copy number control." Nucleic Acids Res **30**(21): 4626-33.

Dreier, J, Stormer, M, Made, D, Burkhardt, S and Kleesiek, K (2006). "Enhanced reverse transcription-PCR assay for detection of norovirus genogroup I." J Clin Microbiol **44**(8): 2714-20.

Dreier, J, Stormer, M and Kleesiek, K (2005). "Use of bacteriophage MS2 as an internal control in viral reverse transcription-PCR assays." J Clin Microbiol **43**(9): 4551-7.

Drummer, HE and Poumbourios, P (2004). "Hepatitis C virus glycoprotein E2 contains a membrane-proximal heptad repeat sequence that is essential for E1E2 glycoprotein heterodimerization and viral entry." J Biol Chem **279**(29): 30066-72.

Duchen, MR (2000). "Mitochondria and Ca(2+)in cell physiology and pathophysiology." Cell Calcium **28**(5-6): 339-48.

Dusheiko, GM. Hezode C, Pol S, Goeser T, Bronowicki J-P, Bourliere M, Buggish P, Serfaty L, Berg T, Couzige P, Benhamou Y, Forestier N, Bengtsoon L, Gharakhanian S, Kauffman R, Alam J, Ferenci P, Pawlotsky J-M, Zeuzem S. (2008). "Treatment of chronic hepatitis C with Telaprevir (TVR) in combination with peginterferon-alfa02A with or without ribavirin. Further interim analysis results of the PROVE2 study". J Hepatol **48**(S2): S26

Egger, D, Wolk, B, Gosert, R, Bianchi, L, Blum, HE, Moradpour, D and Bienz, K (2002). "Expression of hepatitis C virus proteins induces distinct membrane alterations including a candidate viral replication complex." J Virol **76**(12): 5974-84.

Elahi, E, Pourmand, N, Chaung, R, Rofoogaran, A, Boisver, J, Samimi-Rad, K, Davis, RW and Ronaghi, M (2003). "Determination of hepatitis C virus genotype by Pyrosequencing." J Virol Methods **109**(2): 171-6.

Elbeik, T, Surtihadi, J, Destree, M, Gorlin, J, Holodniy, M, Jortani, SA, Kuramoto, K, Ng, V, Valdes, R, Jr., Valsamakis, A and Terrault, NA (2004). "Multicenter evaluation of the performance characteristics of the bayer VERSANT HCV RNA 3.0 assay (bDNA)." J Clin Microbiol **42**(2): 563-9.

Enomoto, N, Sakuma, I, Asahina, Y, Kurosaki, M, Murakami, T, Yamamoto, C, Ogura, Y, Izumi, N, Marumo, F and Sato, C (1996). "Mutations in the nonstructural protein 5A gene and response to interferon in patients with chronic hepatitis C virus 1b infection." N Engl J Med **334**(2): 77-81.

Escobar-Herrera, J, Cancio, C, Guzman, GI, Villegas-Sepulveda, N, Estrada-Garcia, T, Garcia-Lozano, H, Gomez-Santiago, F and Gutierrez-Escolano, AL (2006). "Construction of an internal RT-PCR standard control for the detection of human caliciviruses in stool." J Virol Methods **137**(2): 334-8.

Esteban-Cardenosa, E, Duran, M, Infante, M, Velasco, E and Miner, C (2004). "High-throughput mutation detection method to scan BRCA1 and BRCA2 based on heteroduplex analysis by capillary array electrophoresis." Clin Chem **50**(2): 313-20.

Evans, MJ, Rice, CM and Goff, SP (2004). "Phosphorylation of hepatitis C virus nonstructural protein 5A modulates its protein interactions and viral RNA replication." Proc Natl Acad Sci U S A **101**(35): 13038-43.

Ezzikouri, S, El Feydi, AE, Chafik, A, Afifi, R, El Kihal, L, Benazzouz, M, Hassar, M, Pineau, P and Benjelloun, S (2008). "Genetic polymorphism in the manganese superoxide dismutase gene is associated with an increased risk for hepatocellular carcinoma in HCV-infected Moroccan patients." Mutat Res **649**(1-2): 1-6.

Farci, P, Shimoda, A, Wong, D, Cabezon, T, De Gioannis, D, Strazzera, A, Shimizu, Y, Shapiro, M, Alter, HJ and Purcell, RH (1996). "Prevention of hepatitis C virus infection in chimpanzees by hyperimmune serum against the hypervariable region 1 of the envelope 2 protein." Proc Natl Acad Sci U S A **93**(26): 15394-9.

Farinati, F, Cardin, R, Degan, P, De Maria, N, Floyd, RA, Van Thiel, DH and Naccarato, R (1999). "Oxidative DNA damage in circulating leukocytes occurs as an early event in chronic HCV infection." Free Radic Biol Med **27**(11-12): 1284-91.

Farinati, F, Cardin, R, De Maria, N, Della Libera, G, Marafin, C, Lecis, E, Burra, P, Floreani, A, Cecchetto, A and Naccarato, R (1995). "Iron storage, lipid peroxidation and glutathione turnover in chronic anti-HCV positive hepatitis." J Hepatol **22**(4): 449-56.

Ferenci, P, Fried, MW, Shiffman, ML, Smith, CI, Marinos, G, Goncales, FL, Jr., Haussinger, D, Diago, M, Carosi, G, Dhumeaux, D, Craxi, A, Chaneac, M and Reddy, KR (2005). "Predicting sustained virological responses in chronic hepatitis C patients treated with peginterferon alfa-2a (40 KD)/ribavirin." J Hepatol **43**(3): 425-33.

Flemington, EK (2001). "Herpesvirus lytic replication and the cell cycle: arresting new developments." J Virol **75**(10): 4475-81.

Fliss, MS, Usadel, H, Caballero, OL, Wu, L, Buta, MR, Eleff, SM, Jen, J and Sidransky, D (2000). "Facile detection of mitochondrial DNA mutations in tumors and bodily fluids." Science **287**(5460): 2017-9.

Forman, MS and Valsamakis, A (2004). "Increased sensitivity of the Roche COBAS AMPLICOR HCV test, version 2.0, using modified extraction techniques." J Mol Diagn **6**(3): 225-30.

Fortini, P, Pascucci, B, Parlanti, E, D'Errico, M, Simonelli, V and Dogliotti, E (2003). "8-Oxoguanine DNA damage: at the crossroad of alternative repair pathways." Mutat Res **531**(1-2): 127-39.

Franco, R, Schoneveld, O, Georgakilas, AG and Panayiotidis, MI (2008). "Oxidative stress, DNA methylation and carcinogenesis." Cancer Lett **266**(1): 6-11.

Frank, C, Mohamed, MK, Strickland, GT, Lavanchy, D, Arthur, RR, Magder, LS, El Khoby, T, Abdel-Wahab, Y, Aly Ohn, ES, Anwar, W and Sallam, I (2000). "The role of parenteral antischistosomal therapy in the spread of hepatitis C virus in Egypt." Lancet **355**(9207): 887-91.

Freeman, AJ, Dore, GJ, Law, MG, Thorpe, M, Von Overbeck, J, Lloyd, AR, Marinos, G and Kaldor, JM (2001). "Estimating progression to cirrhosis in chronic hepatitis C virus infection." Hepatology **34**(4 Pt 1): 809-16.

Fried, MW, Shiffman, ML, Reddy, KR, Smith, C, Marinos, G, Goncales, FL, Jr., Haussinger, D, Diago, M, Carosi, G, Dhumeaux, D, Craxi, A, Lin, A, Hoffman, J and Yu, J (2002). "Peginterferon alfa-2a plus ribavirin for chronic hepatitis C virus infection." N Engl J Med **347**(13): 975-82.

Fromenty, B, Grimbert, S, Mansouri, A, Beaugrand, M, Erlinger, S, Rotig, A and Pessayre, D (1995). "Hepatic mitochondrial DNA deletion in alcoholics: association with microvesicular steatosis." Gastroenterology **108**(1): 193-200.

Fu, B, Tom, BD, Delahooke, T, Alexander, GJ and Bird, SM (2007). "Event-biased referral can distort estimation of hepatitis C virus progression rate to cirrhosis, and of prognostic influences." J Clin Epidemiol **60**(11): 1140-8.

Fujita, N, Horiike, S, Sugimoto, R, Tanaka, H, Iwasa, M, Kobayashi, Y, Hasegawa, K, Ma, N, Kawanishi, S, Adachi, Y and Kaito, M (2007). "Hepatic oxidative DNA damage correlates with iron overload in chronic hepatitis C patients." Free Radic Biol Med **42**(3): 353-62.

Fukushima, S, Honda, K, Awane, M, Yamamoto, E, Takeda, R, Kaneko, I, Tanaka, A, Morimoto, T, Tanaka, K and Yamaoka, Y (1995). "The frequency of 4977 base pair deletion of mitochondrial DNA in various types of liver disease and in normal liver." Hepatology **21**(6): 1547-51.

Furione, M, Simoncini, L, Gatti, M, Baldanti, F, Grazia Revello, M and Gerna, G (1999). "HCV genotyping by three methods: analysis of discordant results based on sequencing." J Clin Virol **13**(3): 121-30.

Gao, D, Wei, C, Chen, L, Huang, J, Yang, S and Diehl, AM (2004). "Oxidative DNA damage and DNA repair enzyme expression are inversely related in murine models of fatty liver disease." Am J Physiol Gastrointest Liver Physiol **287**(5): G1070-7.

Garcia-Mediavilla, MV, Sanchez-Campos, S, Gonzalez-Perez, P, Gomez-Gonzalo, M, Majano, PL, Lopez-Cabrera, M, Clemente, G, Garcia-Monzon, C and Gonzalez-Gallego, J (2005). "Differential contribution of hepatitis C virus NS5A and core proteins to the induction of oxidative and nitrosative stress in human hepatocyte-derived cells." J Hepatol **43**(4): 606-13.

Garson, JA, Ring, C, Tuke, P and Tedder, RS (1990). "Enhanced detection by PCR of hepatitis C virus RNA." Lancet **336**(8719): 878-9.

Gelderblom, HC and Beld, MG (2007). "Hepatitis C virus RNA quantification by the COBAS AmpliPrep/COBAS TaqMan System: averages do not tell the whole story." J Clin Virol **39**(4): 326-7.

Gerlach, JT, Diepolder, HM, Zachoval, R, Gruener, NH, Jung, MC, Ulsenheimer, A, Schraut, WW, Schirren, CA, Waechtler, M, Backmund, M and Pape, GR (2003). "Acute hepatitis C: high rate of both spontaneous and treatment-induced viral clearance." Gastroenterology **125**(1): 80-8.

Germer, JJ, Harmsen, WS, Mandrekar, JN, Mitchell, PS and Yao, JD (2005). "Evaluation of the COBAS TaqMan HCV test with automated sample processing using the MagNA pure LC instrument." J Clin Microbiol **43**(1): 293-8.

Germer, JJ, Majewski, DW, Rosser, M, Thompson, A, Mitchell, PS, Smith, TF, Elagin, S and Yao, JD (2003). "Evaluation of the TRUGENE HCV 5'NC genotyping kit with the new GeneLibrarian module 3.1.2 for genotyping of hepatitis C virus from clinical specimens." J Clin Microbiol **41**(10): 4855-7.

Germer, JJ, Rys, PN, Thorvilson, JN and Persing, DH (1999). "Determination of hepatitis C virus genotype by direct sequence analysis of products generated with the Amplicor HCV test." J Clin Microbiol **37**(8): 2625-30.

Giulivi, C, Poderoso, JJ and Boveris, A (1998). "Production of nitric oxide by mitochondria." J Biol Chem **273**(18): 11038-43.

Gong, G, Waris, G, Tanveer, R and Siddiqui, A (2001). "Human hepatitis C virus NS5A protein alters intracellular calcium levels, induces oxidative stress, and activates STAT-3 and NF-kappa B." Proc Natl Acad Sci U S A **98**(17): 9599-604.

Goto, Y, Nonaka, I and Horai, S (1990). "A mutation in the tRNA(Leu)(UUR) gene associated with the MELAS subgroup of mitochondrial encephalomyopathies." Nature **348**(6302): 651-3.

Graziewicz, MA, Day, BJ and Copeland, WC (2002). "The mitochondrial DNA polymerase as a target of oxidative damage." Nucleic Acids Res **30**(13): 2817-24.

Griffin, SD, Harvey, R, Clarke, DS, Barclay, WS, Harris, M and Rowlands, DJ (2004). "A conserved basic loop in hepatitis C virus p7 protein is required for amantadine-sensitive ion channel activity in mammalian cells but is dispensable for localization to mitochondria." J Gen Virol **85**(Pt 2): 451-61.

Griffin, SD, Beales, LP, Clarke, DS, Worsfold, O, Evans, SD, Jaeger, J, Harris, MP and Rowlands, DJ (2003). "The p7 protein of hepatitis C virus forms an ion channel that is blocked by the antiviral drug, Amantadine." FEBS Lett **535**(1-3): 34-8.

Ha, PK, Tong, BC, Westra, WH, Sanchez-Cespedes, M, Parrella, P, Zahurak, M, Sidransky, D and Califano, JA (2002). "Mitochondrial C-tract alteration in premalignant lesions of the head and neck: a marker for progression and clonal proliferation." Clin Cancer Res **8**(7): 2260-5.

Hadziyannis, SJ, Sette, H, Jr., Morgan, TR, Balan, V, Diago, M, Marcellin, P, Ramadori, G, Bodenheimer, H, Jr., Bernstein, D, Rizzetto, M, Zeuzem, S, Pockros, PJ, Lin, A and Ackrill, AM (2004). "Peginterferon-alpha2a and ribavirin combination therapy in chronic hepatitis C: a randomized study of treatment duration and ribavirin dose." Ann Intern Med **140**(5): 346-55.

Halfon, P, Bourliere, M, Penaranda, G, Khiri, H and Ouzan, D (2006). "Real-time PCR assays for hepatitis C virus (HCV) RNA quantitation are adequate for clinical management of patients with chronic HCV infection." J Clin Microbiol **44**(7): 2507-11.

Halfon, P, Trimoulet, P, Bourliere, M, Khiri, H, de Ledinghen, V, Couzigou, P, Feryn, JM, Alcaraz, P, Renou, C, Fleury, HJ and Ouzan, D (2001). "Hepatitis C virus genotyping based on 5' noncoding sequence analysis (Trugene)." J Clin Microbiol **39**(5): 1771-3.

Hancock, DK, Tully, LA and Levin, BC (2005). "A Standard Reference Material to determine the sensitivity of techniques for detecting low-frequency mutations, SNPs, and heteroplasmies in mitochondrial DNA." Genomics **86**(4): 446-61.

Hanes, JW, Thal, DM and Johnson, KA (2006). "Incorporation and replication of 8-oxo-deoxyguanosine by the human mitochondrial DNA polymerase." J Biol Chem **281**(47): 36241-8.

Hanna, MG, Nelson, IP, Morgan-Hughes, JA and Harding, AE (1995). "Impaired mitochondrial translation in human myoblasts harbouring the mitochondrial DNA tRNA lysine 8344 A-->G (MERRF) mutation: relationship to proportion of mutant mitochondrial DNA." J Neurol Sci **130**(2): 154-60.

Harman D. (1981). "The aging process". Proc Natl Acad Sci USA. **78**: 7124-7128.

Harman D. (1972). "The biological clock: the mitochondria?" J Amer Ger Soc. **20**: 145-147.

Harman D. (1956). "Aging: theory based on free radical and radiation chemistry". J Gerontol. **11**: 298-300.

Harris, HE, Eldridge, KP, Harbour, S, Alexander, G, Teo, CG and Ramsay, ME (2007). "Does the clinical outcome of hepatitis C infection vary with the infecting hepatitis C virus type?" J Viral Hepat **14**(3): 213-20.

Harris, HE, Ramsay, ME, Heptonstall, J, Soldan, K and Eldridge, KP (2000). "The HCV National Register: towards informing the natural history of hepatitis C infection in the UK." J Viral Hepat **7**(6): 420-7.

Harris, KA, Gilham, C, Mortimer, PP and Teo, CG (1999). "The most prevalent hepatitis C virus genotypes in England and Wales are 3a and 1a." J Med Virol **58**(2): 127-31.

Hatefi, Y (1985). "The mitochondrial electron transport and oxidative phosphorylation system." Annu Rev Biochem **54**: 1015-69.

Hattori, K, Tanaka, M, Sugiyama, S, Obayashi, T, Ito, T, Satake, T, Hanaki, Y, Asai, J, Nagano, M and Ozawa, T (1991). "Age-dependent increase in deleted mitochondrial DNA in the human heart: possible contributory factor to presbycardia." Am Heart J **121**(6 Pt 1): 1735-42.

Haushofer, AC, Berg, J, Hauer, R, Trubert-Exinger, D, Stekel, HG and Kessler, HH (2003). "Genotyping of hepatitis C virus-comparison of three assays." J Clin Virol **27**(3): 276-85.

Hauswirth, WW, Van de Walle, MJ, Laipis, PJ and Olivo, PD (1984). "Heterogeneous mitochondrial DNA D-loop sequences in bovine tissue." Cell **37**(3): 1001-7.

Haverstick, DM, Bullock, GC and Bruns, DE (2004). "Genotyping of hepatitis C virus by melting curve analysis: analytical characteristics and performance." Clin Chem **50**(12): 2405-7.

Hayakawa, M, Hattori, K, Sugiyama, S and Ozawa, T (1992). "Age-associated oxygen damage and mutations in mitochondrial DNA in human hearts." Biochem Biophys Res Commun **189**(2): 979-85.

Hayashi, J, Ohta, S, Kikuchi, A, Takemitsu, M, Goto, Y and Nonaka, I (1991). "Introduction of disease-related mitochondrial DNA deletions into HeLa cells lacking mitochondrial DNA results in mitochondrial dysfunction." Proc Natl Acad Sci U S A **88**(23): 10614-8.

He, L, Chinnery, PF, Durham, SE, Blakely, EL, Wardell, TM, Borthwick, GM, Taylor, RW and Turnbull, DM (2002). "Detection and quantification of mitochondrial DNA deletions in individual cells by real-time PCR." Nucleic Acids Res **30**(14): e68.

Health Protection Agency. (2007). Hepatitis C in England: The Health Protection Agency Annual Report 2007. Health Protection Agency, Centre for Infections.

Health Protection Agency. (2006). Hepatitis C in England: An update 2006. The Health Protection Agency Annual Report 2006. Harris HE and Ramsay M. Health Protection Agency, Centre for Infections.

Health Protection Agency. (2006a). Eye of the Needle. United Kingdom surveillance of significant occupational exposures to bloodborne viruses in healthcare workers. Health Protection Agency Centre for Infections.

Helbock, HJ, Beckman, KB, Shigenaga, MK, Walter, PB, Woodall, AA, Yeo, HC and Ames, BN (1998). "DNA oxidation matters: the HPLC-electrochemical detection assay of 8-oxo-deoxyguanosine and 8-oxo-guanine." Proc Natl Acad Sci U S A **95**(1): 288-93.

Holmes, EC, Worobey, M and Rambaut, A (1999). "Phylogenetic evidence for recombination in dengue virus." Mol Biol Evol **16**(3): 405-9.

Holt, IJ, Harding, AE, Cooper, JM, Schapira, AH, Toscano, A, Clark, JB and Morgan-Hughes, JA (1989). "Mitochondrial myopathies: clinical and biochemical features of 30 patients with major deletions of muscle mitochondrial DNA." Ann Neurol **26**(6): 699-708.

Holt, IJ, Harding, AE and Morgan-Hughes, JA (1988). "Deletions of muscle mitochondrial DNA in patients with mitochondrial myopathies." Nature **331**(6158): 717-9.

Hoorfar, J, Malorny, B, Abdulmawjood, A, Cook, N, Wagner, M and Fach, P (2004). "Practical considerations in design of internal amplification controls for diagnostic PCR assays." J Clin Microbiol **42**(5): 1863-8.

Horai, S and Hayasaka, K (1990). "Intraspecific nucleotide sequence differences in the major noncoding region of human mitochondrial DNA." Am J Hum Genet **46**(4): 828-42.

Houglum, K, Venkataramani, A, Lyche, K and Chojkier, M (1997). "A pilot study of the effects of d-alpha-tocopherol on hepatic stellate cell activation in chronic hepatitis C." Gastroenterology **113**(4): 1069-73.

Hruszkewycz, AM (1988). "Evidence for mitochondrial DNA damage by lipid peroxidation." Biochem Biophys Res Commun **153**(1): 191-7.

Hübscher SG. (2007). Histological assessment of the liver. The Foundation Years. **3**(3): 139-133

Hwang, SJ, Lee, SD, Lu, RH, Chu, CW, Wu, JC, Lai, ST and Chang, FY (2001). "Hepatitis C viral genotype influences the clinical outcome of patients with acute posttransfusion hepatitis C." J Med Virol **65**(3): 505-9.

Ingman, M and Gyllensten, U (2006). "mtDB: Human Mitochondrial Genome Database, a resource for population genetics and medical sciences." Nucleic Acids Res **34**(Database issue): D749-51.

Innis, MA and Gelfand, DH (1990). Optimization of PCRs. PCR Protocols. M. A. Innis, G. H. Gelfand, J. J. Sninsky and T. J. White. New York, Academic Press: 3-12.

Jain, SK, Pemberton, PW, Smith, A, McMahon, RF, Burrows, PC, Aboutwerat, A and Warnes, TW (2002). "Oxidative stress in chronic hepatitis C: not just a feature of late stage disease." J Hepatol **36**(6): 805-11.

Jensen, DM, Morgan, TR, Marcellin, P, Pockros, PJ, Reddy, KR, Hadziyannis, SJ, Ferenci, P, Ackrill, AM and Willems, B (2006) "Early identification of HCV genotype 1 patients responding to 24 weeks peginterferon alpha-2a (40 kd)/ribavirin therapy" Hepatology, **43**(5): 954-60.

Johns, DR, Rutledge, SL, Stine, OC and Hurko, O (1989). "Directly repeated sequences associated with pathogenic mitochondrial DNA deletions." Proc Natl Acad Sci U S A **86**(20): 8059-62.

Joint Formulary Committee. (2008). British National Formulary. (58) ed. London: British Medical Association and Royal Pharmaceutical Society of Great Britain.

Kageyama, F, Kobayashi, Y, Kawasaki, T, Toyokuni, S, Uchida, K and Nakamura, H (2000). "Successful interferon therapy reverses enhanced hepatic iron accumulation and lipid peroxidation in chronic hepatitis C." Am J Gastroenterol **95**(4): 1041-50.

Kajander, OA, Kunnas, TA, Perola, M, Lehtinen, SK, Karhunen, PJ and Jacobs, HT (1999). "Long-extension PCR to detect deleted mitochondrial DNA molecules is compromized by technical artefacts." Biochem Biophys Res Commun **254**(2): 507-14.

Kalinina, O, Norder, H and Magnius, LO (2004). "Full-length open reading frame of a recombinant hepatitis C virus strain from St Petersburg: proposed mechanism for its formation." J Gen Virol **85**(Pt 7): 1853-7.

Kalinina, O, Norder, H, Mukomolov, S and Magnius, LO (2002). "A natural intergenotypic recombinant of hepatitis C virus identified in St. Petersburg." J Virol **76**(8): 4034-43.

Kasamatsu, H and Vinograd, J (1974). "Replication of circular DNA in eukaryotic cells." Annu Rev Biochem **43**(0): 695-719.

Kasamatsu, H, Robberson, DL and Vinograd, J (1971). "A novel closed-circular mitochondrial DNA with properties of a replicating intermediate." Proc Natl Acad Sci U S A **68**(9): 2252-7.

Kato, J, Kobune, M, Nakamura, T, Kuroiwa, G, Takada, K, Takimoto, R, Sato, Y, Fujikawa, K, Takahashi, M, Takayama, T, Ikeda, T and Niitsu, Y (2001). "Normalization of elevated hepatic 8-hydroxy-2'-deoxyguanosine levels in chronic hepatitis C patients by phlebotomy and low iron diet." Cancer Res **61**(24): 8697-702.

Kenny-Walsh, E (1999). "Clinical outcomes after hepatitis C infection from contaminated anti-D immune globulin. Irish Hepatology Research Group." N Engl J Med **340**(16): 1228-33.

Kessler, HH, Stelzl, E, Raggam, RB, Haas, J, Kirchmeir, F, Hegenbarth, K, Daghofer, E, Santner, BI, Marth, E and Stauber, RE (2001). "Effects of storage and type of blood collection tubes on hepatitis C virus level in whole blood samples." J Clin Microbiol **39**(5): 1788-90.

Khan, RU, Tong, CY, Bloom, S, Gilmore, IT, Toh, CH, Bolton-Maggs, PH, Beeching, NJ and Hart, CA (1997). "Evaluation of two simplified methods for genotyping hepatitis C virus." J Med Virol **52**(1): 35-41.

Khogali, SS, Mayosi, BM, Beattie, JM, McKenna, WJ, Watkins, H and Poulton, J (2001). "A common mitochondrial DNA variant associated with susceptibility to dilated cardiomyopathy in two different populations." Lancet **357**(9264): 1265-7.

Kim, K, Park, J, Chung, Y, Cheon, D, Lee, IB, Lee, S, Yoon, J, Cho, H, Song, C and Lee, KH (2002). "Use of internal standard RNA molecules for the RT-PCR amplification of the faeces-borne RNA viruses." J Virol Methods **104**(2): 107-15.

Kitada, T, Seki, S, Iwai, S, Yamada, T, Sakaguchi, H and Wakasa, K (2001). "In situ detection of oxidative DNA damage, 8-hydroxydeoxyguanosine, in chronic human liver disease." J Hepatol **35**(5): 613-8.

Kleiber, J, Walter, T, Haberhausen, G, Tsang, S, Babiel, R and Rosenstraus, M (2000). "Performance characteristics of a quantitative, homogeneous TaqMan RT-PCR test for HCV RNA." J Mol Diagn **2**(3): 158-66.

Knapp, S, Yee, LJ, Frodsham, AJ, Hennig, BJ, Hellier, S, Zhang, L, Wright, M, Chiaramonte, M, Graves, M, Thomas, HC, Hill, AV and Thursz, MR (2003). "Polymorphisms in interferon-induced genes and the outcome of hepatitis C virus infection: roles of MxA, OAS-1 and PKR." Genes Immun **4**(6): 411-9.

Ko, YC, Ho, MS, Chiang, TA, Chang, SJ and Chang, PY (1992). "Tattooing as a risk of hepatitis C virus infection." J Med Virol **38**(4): 288-91.

Komurian-Pradel, F, Paranhos-Baccala, G, Sodoyer, M, Chevallier, P, Mandrand, B, Lotteau, V and Andre, P (2001). "Quantitation of HCV RNA using real-time PCR and fluorimetry." J Virol Methods **95**(1-2): 111-9.

Kondili, LA, Genovese, D, Argentini, C, Chionne, P, Toscani, P, Fabro, R, Cocconi, R and Rapicetta, M (2006). "Nosocomial transmission in simultaneous outbreaks of hepatitis C and B virus infections in a hemodialysis center." Eur J Clin Microbiol Infect Dis **25**(8): 527-31.

Kopsidas, G, Kovalenko, SA, Heffernan, DR, Yarovaya, N, Kramarova, L, Stojanovski, D, Borg, J, Islam, MM, Caragounis, A and Linnane, AW (2000). "Tissue mitochondrial DNA changes. A stochastic system." Ann N Y Acad Sci **908**: 226-43.

Korenaga, M, Wang, T, Li, Y, Showalter, LA, Chan, T, Sun, J and Weinman, SA (2005). "Hepatitis C virus core protein inhibits mitochondrial electron transport and increases reactive oxygen species (ROS) production." J Biol Chem **280**(45): 37481-8.

Kotake, K, Nonami, T, Kurokawa, T, Nakao, A, Murakami, T and Shimomura, Y (1999). "Human livers with cirrhosis and hepatocellular carcinoma have less mitochondrial DNA deletion than normal human livers." Life Sci **64**(19): 1785-91.

Kovalenko, SA, Kopsidas, G, Kelso, J, Rosenfeldt, F and Linnane, AW (1998). "Tissue-specific distribution of multiple mitochondrial DNA rearrangements during human aging." Ann N Y Acad Sci **854**: 171-81.

Kozlowski, P, Olejniczak, M and Krzyzosiak, WJ (2005). "Rapid heteroduplex analysis by capillary electrophoresis." Clin Chim Acta **353**(1-2): 209-14.

Krajden, M, Minor, JM, Rifkin, O and Comanor, L (1999). "Effect of multiple freeze-thaw cycles on hepatitis B virus DNA and hepatitis C virus RNA quantification as measured with branched-DNA technology." J Clin Microbiol **37**(6): 1683-6.

Kuo, G, Choo, QL, Alter, HJ, Gitnick, GL, Redeker, AG, Purcell, RH, Miyamura, T, Dienstag, JL, Alter, MJ, Stevens, CE and et al. (1989). "An assay for circulating antibodies to a major etiologic virus of human non-A, non-B hepatitis." Science **244**(4902): 362-4.

Kusumoto, K, Uto, H, Hayashi, K, Takahama, Y, Nakao, H, Suruki, R, Stuver, SO, Ido, A and Tsubouchi, H (2006). "Interleukin-10 or tumor necrosis factor-alpha polymorphisms and the natural course of hepatitis C virus infection in a hyperendemic area of Japan." Cytokine **34**(1-2): 24-31.

Lai, CK, Jeng, KS, Machida, K, Cheng, YS and Lai, MM (2008). "Hepatitis C virus NS3/4A protein interacts with ATM, impairs DNA repair and enhances sensitivity to ionizing radiation." Virology **370**(2): 295-309.

Lanford, RE, Chavez, D, Chisari, FV and Sureau, C (1995). "Lack of detection of negative-strand hepatitis C virus RNA in peripheral blood mononuclear cells and other extrahepatic tissues by the highly strand-specific rTth reverse transcriptase PCR." J Virol **69**(12): 8079-83.

Laperche, S, Lunel, F, Izopet, J, Alain, S, Deny, P, Duverlie, G, Gaudy, C, Pawlotsky, JM, Plantier, JC, Pozzetto, B, Thibault, V, Tosetti, F and Lefrere, JJ (2005). "Comparison of hepatitis C virus NS5b and 5' noncoding gene sequencing methods in a multicenter study." J Clin Microbiol **43**(2): 733-9.

Laperche, S, Saune, K, Deny, P, Duverlie, G, Alain, S, Chaix, ML, Gaudy, C, Lunel, F, Pawlotsky, JM, Payan, C, Pozzetto, B, Tamalet, C, Thibault, V, Vallet, S, Bouchardeau, F, Izopet, J and Lefrere, JJ (2006). "Unique NS5b hepatitis C virus gene sequence consensus database is essential for standardization of genotype determinations in multicenter epidemiological studies." J Clin Microbiol **44**(2): 614-6.

Larrea, E, Beloqui, O, Munoz-Navas, MA, Civeira, MP and Prieto, J (1998). "Superoxide dismutase in patients with chronic hepatitis C virus infection." Free Radic Biol Med **24**(7-8): 1235-41.

Larrea, E, Garcia, N, Qian, C, Civeira, MP and Prieto, J (1996). "Tumor necrosis factor alpha gene expression and the response to interferon in chronic hepatitis C." Hepatology **23**(2): 210-7.

Larsen, NB, Rasmussen, M and Rasmussen, LJ (2005). "Nuclear and mitochondrial DNA repair: similar pathways?" Mitochondrion **5**(2): 89-108.

Laskus, T, Operskalski, EA, Radkowski, M, Wilkinson, J, Mack, WJ, deGiacomo, M, Al-Harthi, L, Chen, Z, Xu, J and Kovacs, A (2007). "Negative-strand hepatitis C virus (HCV) RNA in peripheral blood mononuclear cells from anti-HCV-positive/HIV-infected women." J Infect Dis **195**(1): 124-33.

Laskus, T, Radkowski, M, Wang, LF, Vargas, H and Rakela, J (1998). "Search for hepatitis C virus extrahepatic replication sites in patients with acquired immunodeficiency syndrome: specific detection of negative-strand viral RNA in various tissues." Hepatology **28**(5): 1398-401.

Laskus, T, Radkowski, M, Wang, LF, Cianciara, J, Vargas, H and Rakela, J (1997). "Hepatitis C virus negative strand RNA is not detected in peripheral blood mononuclear cells and viral sequences are identical to those in serum: a case against extrahepatic replication." J Gen Virol **78 (Pt 11)**: 2747-50.

LeDoux, SP, Wilson, GL, Beecham, EJ, Stevnsner, T, Wassermann, K and Bohr, VA (1992). "Repair of mitochondrial DNA after various types of DNA damage in Chinese hamster ovary cells." Carcinogenesis **13**(11): 1967-73.

Lee, HC, Li, SH, Lin, JC, Wu, CC, Yeh, DC and Wei, YH (2004). "Somatic mutations in the D-loop and decrease in the copy number of mitochondrial DNA in human hepatocellular carcinoma." Mutat Res **547**(1-2): 71-8.

Lee, HC, Pang, CY, Hsu, HS and Wei, YH (1994). "Differential accumulations of 4,977 bp deletion in mitochondrial DNA of various tissues in human ageing." Biochim Biophys Acta **1226**(1): 37-43.

Lee, HY, Chung, U, Yoo, JE, Park, MJ and Shin, KJ (2004a). "Quantitative and qualitative profiling of mitochondrial DNA length heteroplasmy." Electrophoresis **25**(1): 28-34.

Lee, SC, Antony, A, Lee, N, Leibow, J, Yang, JQ, Soviero, S, Gutekunst, K and Rosenstraus, M (2000). "Improved version 2.0 qualitative and quantitative AMPLICOR reverse transcription-PCR tests for hepatitis C virus RNA: calibration to international units, enhanced genotype reactivity, and performance characteristics." J Clin Microbiol **38**(11): 4171-9.

Lee, SS, Heathcote, EJ, Reddy, KR, Zeuzem, S, Fried, MW, Wright, TL, Pockros, PJ, Haussinger, D, Smith, CI, Lin, A and Pappas, SC (2002). "Prognostic factors and early predictability of sustained viral response with peginterferon alfa-2a (40KD)." J Hepatol **37**(4): 500-6.

Legrand-Abravanel, F, Claudinon, J, Nicot, F, Dubois, M, Chapuy-Regaud, S, Sandres-Saune, K, Pasquier, C and Izopet, J (2007). "New natural intergenotypic (2/5) recombinant of hepatitis C virus." J Virol **81**(8): 4357-62.

Lehmann, M, Meyer, MF, Monazahian, M, Tillmann, HL, Manns, MP and Wedemeyer, H (2004). "High rate of spontaneous clearance of acute hepatitis C virus genotype 3 infection." J Med Virol **73**(3): 387-91.

Lemon SM, Walker C, Alter MJ and Yi M. (2007). Chapter 35: Hepatitis C virus. Fields Virology. Fifth Edition. Volume One. Eds in Chief: Knipe DM, and Howley PM. Philadelphia. Lippincott Williams & Wilkins.

Lewis, JG and Adams, DO (1987). "Inflammation, oxidative DNA damage, and carcinogenesis." Environ Health Perspect **76**: 19-27.

Li, Y, Boehning, DF, Qian, T, Popov, VL and Weinman, SA (2007). "Hepatitis C virus core protein increases mitochondrial ROS production by stimulation of Ca2+ uniporter activity." Faseb J **21**(10): 2474-85.

Lievre, A, Blons, H, Houllier, AM, Laccourreye, O, Brasnu, D, Beaune, P and Laurent-Puig, P (2006). "Clinicopathological significance of mitochondrial D-Loop mutations in head and neck carcinoma." Br J Cancer **94**(5): 692-7.

Lievre, A, Chapusot, C, Bouvier, AM, Zinzindohoue, F, Piard, F, Roignot, P, Arnould, L, Beaune, P, Faivre, J and Laurent-Puig, P (2005). "Clinical value of mitochondrial mutations in colorectal cancer." J Clin Oncol **23**(15): 3517-25.

Lightowlers, RN, Chinnery, PF, Turnbull, DM and Howell, N (1997). "Mammalian mitochondrial genetics: heredity, heteroplasmy and disease." Trends Genet **13**(11): 450-5.

Lindh, M and Hannoun, C (2005). "Genotyping of hepatitis C virus by Taqman real-time PCR." J Clin Virol **34**(2): 108-14.

Linnane, AW, Marzuki, S, Ozawa, T and Tanaka, M (1989). "Mitochondrial DNA mutations as an important contributor to ageing and degenerative diseases." Lancet 1(8639): 642-5.

Lio, D, Caruso, C, Di Stefano, R, Colonna Romano, G, Ferraro, D, Scola, L, Crivello, A, Licata, A, Valenza, LM, Candore, G, Craxi, A and Almasio, PL (2003). "IL-10 and TNF-alpha polymorphisms and the recovery from HCV infection." Hum Immunol **64**(7): 674-80.

Liu, CY, Lee, CF and Wei, YH (2007). "Quantitative effect of 4977 bp deletion of mitochondrial DNA on the susceptibility of human cells to UV-induced apoptosis." Mitochondrion **7**(1-2): 89-95.

Liu, CY, Lee, CF, Hong, CH and Wei, YH (2004). "Mitochondrial DNA mutation and depletion increase the susceptibility of human cells to apoptosis." Ann N Y Acad Sci **1011**: 133-45.

Liu, VW, Wang, Y, Yang, HJ, Tsang, PC, Ng, TY, Wong, LC, Nagley, P and Ngan, HY (2003). "Mitochondrial DNA variant 16189T>C is associated with susceptibility to endometrial cancer." Hum Mutat **22**(2): 173-4.

Liu, VW, Shi, HH, Cheung, AN, Chiu, PM, Leung, TW, Nagley, P, Wong, LC and Ngan, HY (2001). "High incidence of somatic mitochondrial DNA mutations in human ovarian carcinomas." Cancer Res **61**(16): 5998-6001.

Liu, VW, Zhang, C and Nagley, P (1998). "Mutations in mitochondrial DNA accumulate differentially in three different human tissues during ageing." Nucleic Acids Res **26**(5): 1268-75.

Livesey, KJ, Wimhurst, VL, Carter, K, Worwood, M, Cadet, E, Rochette, J, Roberts, AG, Pointon, JJ, Merryweather-Clarke, AT, Bassett, ML, Jouanolle, AM, Mosser, A, David, V, Poulton, J and Robson, KJ (2004). "The 16189 variant of mitochondrial DNA occurs more frequently in C282Y homozygotes with haemochromatosis than those without iron loading." J Med Genet **41**(1): 6-10.

Lodish H, Berk A, Matsudaira P, Kaiser CA, Krieger M, Scott MP, Zipursky SL and Darnell J (eds). (2004). Chapter 8: Cellular energetics. Molecular Cell Biology. Fifth Edition. New York . W. H. Freeman and Company.

Lohmann, V, Korner, F, Koch, J, Herian, U, Theilmann, L and Bartenschlager, R (1999). "Replication of subgenomic hepatitis C virus RNAs in a hepatoma cell line." Science **285**(5424): 110-3.

Longley, MJ, Nguyen, D, Kunkel, TA and Copeland, WC (2001). "The fidelity of human DNA polymerase gamma with and without exonucleolytic proofreading and the p55 accessory subunit." J Biol Chem **276**(42): 38555-62.

Lopez-Labrador, FX, Ampurdanes, S, Forns, X, Castells, A, Saiz, JC, Costa, J, Bruix, J, Sanchez Tapias, JM, Jimenez de Anta, MT and Rodes, J (1997). "Hepatitis C virus (HCV) genotypes in Spanish patients with HCV infection: relationship between HCV genotype 1b, cirrhosis and hepatocellular carcinoma." J Hepatol **27**(6): 959-65.

Machida, K, Cheng, KT, Lai, CK, Jeng, KS, Sung, VM and Lai, MM (2006). "Hepatitis C virus triggers mitochondrial permeability transition with production of reactive oxygen species, leading to DNA damage and STAT3 activation." J Virol **80**(14): 7199-207.

Machida, K, Cheng, KT, Sung, VM, Lee, KJ, Levine, AM and Lai, MM (2004). "Hepatitis C virus infection activates the immunologic (type II) isoform of nitric oxide synthase and thereby enhances DNA damage and mutations of cellular genes." J Virol **78**(16): 8835-43.

Maertens G and Stuyver L. (1997). Genotypes and genetic variation of hepatitis C virus. The Molecular Medicine of Viral Hepatitis. Harrison TJ and Zuckerman AJ. Chichester. John Wiley & Sons Ltd. 183-233.

Mahmood, S, Kawanaka, M, Kamei, A, Izumi, A, Nakata, K, Niiyama, G, Ikeda, H, Hanano, S, Suehiro, M, Togawa, K and Yamada, G (2004). "Immunohistochemical evaluation of oxidative stress markers in chronic hepatitis C." Antioxid Redox Signal **6**(1): 19-24.

Major, ME and Feinstone, SM (1997). "The molecular virology of hepatitis C." Hepatology **25**(6): 1527-38.

Mambo, E, Gao, X, Cohen, Y, Guo, Z, Talalay, P and Sidransky, D (2003). "Electrophile and oxidant damage of mitochondrial DNA leading to rapid evolution of homoplasmic mutations." Proc Natl Acad Sci U S A **100**(4): 1838-43.

Manesis, EK, Papaioannou, C, Gioustozi, A, Kafiri, G, Koskinas, J and Hadziyannis, SJ (1997). "Biochemical and virological outcome of patients with chronic hepatitis C treated with interferon alfa-2b for 6 or 12 months: a 4-year follow-up of 211 patients." Hepatology **26**(3): 734-9.

Mangia, A, Santoro, R, Piattelli, M, Pazienza, V, Grifa, G, Iacobellis, A and Andriulli, A (2004). "IL-10 haplotypes as possible predictors of spontaneous clearance of HCV infection." Cytokine **25**(3): 103-9.

Manns, MP, McHutchison, JG, Gordon, SC, Rustgi, VK, Shiffman, M, Reindollar, R, Goodman, ZD, Koury, K, Ling, M and Albrecht, JK (2001). "Peginterferon alfa-2b plus ribavirin compared with interferon alfa-2b plus ribavirin for initial treatment of chronic hepatitis C: a randomised trial." Lancet **358**(9286): 958-65.

Mansouri, A, Fromenty, B, Berson, A, Robin, MA, Grimbert, S, Beaugrand, M, Erlinger, S and Pessayre, D (1997). "Multiple hepatic mitochondrial DNA deletions suggest premature oxidative aging in alcoholic patients." J Hepatol **27**(1): 96-102.

Marchington, DR, Poulton, J, Sellar, A and Holt, IJ (1996). "Do sequence variants in the major non-coding region of the mitochondrial genome influence mitochondrial mutations associated with disease?" Hum Mol Genet **5**(4): 473-9.

Marshall, A, Rushbrook, S, Davies, SE, Morris, LS, Scott, IS, Vowler, SL, Coleman, N and Alexander, G (2005). "Relation between hepatocyte G1 arrest, impaired hepatic regeneration, and fibrosis in chronic hepatitis C virus infection." Gastroenterology **128**(1): 33-42.

Martell, M, Gomez, J, Esteban, JI, Sauleda, S, Quer, J, Cabot, B, Esteban, R and Guardia, J (1999). "High-throughput real-time reverse transcription-PCR quantitation of hepatitis C virus RNA." J Clin Microbiol **37**(2): 327-32.

Martell, M, Esteban, JI, Quer, J, Genesca, J, Weiner, A, Esteban, R, Guardia, J and Gomez, J (1992). "Hepatitis C virus (HCV) circulates as a population of different but closely related genomes: quasispecies nature of HCV genome distribution." J Virol **66**(5): 3225-9.

Martinot-Peignoux, M, Marcellin, P, Pouteau, M, Castelnau, C, Boyer, N, Poliquin, M, Degott, C, Descombes, I, Le Breton, V, Milotova, V and et al. (1995). "Pretreatment serum hepatitis C virus RNA levels and hepatitis C virus genotype are the main and independent prognostic factors of sustained response to interferon alfa therapy in chronic hepatitis C." Hepatology **22**(4 Pt 1): 1050-6.

Martro, E, Gonzalez, V, Buckton, AJ, Saludes, V, Fernandez, G, Matas, L, Planas, R and Ausina, V (2008). "Evaluation of a new assay in comparison with reverse hybridization and sequencing methods for hepatitis C virus genotyping targeting both 5' noncoding and nonstructural 5b genomic regions." J Clin Microbiol **46**(1): 192-7.

Mason, AL, Lau, JY, Hoang, N, Qian, K, Alexander, GJ, Xu, L, Guo, L, Jacob, S, Regenstein, FG, Zimmerman, R, Everhart, JE, Wasserfall, C, Maclaren, NK and Perrillo, RP (1999). "Association of diabetes mellitus and chronic hepatitis C virus infection." Hepatology **29**(2): 328-33.

Mason, PA, Matheson, EC, Hall, AG and Lightowlers, RN (2003a). "Mismatch repair activity in mammalian mitochondria." Nucleic Acids Res **31**(3): 1052-8.

Mattocks C, White H, Owen N and Ward D. (2007). Conformation sensitive capillary electrophoresis. NHS Application Note. National Genetics Reference Laboratory (Wessex). Available at www.ngrl.org.uk/Wessex/downloads/pdf/NGRLW_CSCE_3.1.pdf.

McHutchison JG, Everson GT, Gordon SC, Jacobson I, Kauffman R, McNair L, Muir A (2008). "PROVE1: Results from a phase 2 study of telaprevir with peginterferon alfa-2A and ribavirin in treatment-naïve subjects with hepatitis C". J Hepatol **48**(S2): S4

McHutchison, JG, Bacon, BR, Gordon, SC, Lawitz, E, Shiffman, M, Afdhal, NH, Jacobson, IM, Muir, A, Al-Adhami, M, Morris, ML, Lekstrom-Himes, JA, Efler, SM and Davis, HL (2007) "Phase 1B, randomized, double-blind, dose-escalation trial of CPG 10101 in patients with chronic hepatitis C virus" Hepatology, **46**(5): 1341-9.

McHutchison, JG and Fried, MW (2003). "Current therapy for hepatitis C: pegylated interferon and ribavirin." Clin Liver Dis **7**(1): 149-61.

McHutchison, JG, Blatt, LM, Ponnudurai, R, Goodarzi, K, Russell, J and Conrad, A (1999). "Ultracentrifugation and concentration of a large volume of serum for HCV RNA during treatment may predict sustained and relapse response in chronic HCV infection." J Med Virol **57**(4): 351-5.

McHutchison, JG and Poynard, T (1999). "Combination therapy with interferon plus ribavirin for the initial treatment of chronic hepatitis C." Semin Liver Dis **19 Suppl 1**: 57-65.

McHutchison, JG, Gordon, SC, Schiff, ER, Shiffman, ML, Lee, WM, Rustgi, VK, Goodman, ZD, Ling, MH, Cort, S and Albrecht, JK (1998). "Interferon alfa-2b alone or in combination with ribavirin as initial treatment for chronic hepatitis C. Hepatitis Interventional Therapy Group." N Engl J Med **339**(21): 1485-92.

McIlhatton, BP, Keating, C, Curran, MD, McMullin, MF, Barr, JG, Madrigal, JA and Middleton, D (2002). "Identification of medically important pathogenic fungi by reference strand-mediated conformational analysis (RSCA)." J Med Microbiol **51**(6): 468-78.

McOmish, F, Yap, PL, Dow, BC, Follett, EA, Seed, C, Keller, AJ, Cobain, TJ, Krusius, T, Kolho, E, Naukkarinen, R and et al. (1994). "Geographical distribution of hepatitis C virus genotypes in blood donors: an international collaborative survey." J Clin Microbiol **32**(4): 884-92.

Mehta, SH, Brancati, FL, Strathdee, SA, Pankow, JS, Netski, D, Coresh, J, Szklo, M and Thomas, DL (2003). "Hepatitis C virus infection and incident type 2 diabetes." Hepatology **38**(1): 50-6.

Mellor, J, Hawkins, A and Simmonds, P (1999). "Genotype dependence of hepatitis C virus load measurement in commercially available quantitative assays." J Clin Microbiol **37**(8): 2525-32.

Mercurio, F and Manning, AM (1999). "NF-kappaB as a primary regulator of the stress response." Oncogene **18**(45): 6163-71.

Micallef, JM, Kaldor, JM and Dore, GJ (2006). "Spontaneous viral clearance following acute hepatitis C infection: a systematic review of longitudinal studies." J Viral Hepat **13**(1): 34-41.

Michelin, BD, Muller, Z, Stelzl, E, Marth, E and Kessler, HH (2007). "Evaluation of the Abbott RealTime HCV assay for quantitative detection of hepatitis C virus RNA." J Clin Virol **38**(2): 96-100.

Miller, FJ, Rosenfeldt, FL, Zhang, C, Linnane, AW and Nagley, P (2003). "Precise determination of mitochondrial DNA copy number in human skeletal and cardiac muscle by a PCR-based assay: lack of change of copy number with age." Nucleic Acids Res **31**(11): e61.

Miller, SA, Dykes, DD and Polesky, HF (1988). "A simple salting out procedure for extracting DNA from human nucleated cells." Nucleic Acids Res **16**(3): 1215.

Minola, E, Prati, D, Suter, F, Maggiolo, F, Caprioli, F, Sonzogni, A, Fraquelli, M, Paggi, S and Conte, D (2002). "Age at infection affects the long-term outcome of transfusion-associated chronic hepatitis C." Blood **99**(12): 4588-91.

Minton, EJ, Smillie, D, Smith, P, Shipley, S, McKendrick, MW, Gleeson, DC, Underwood, JC, Cannings, C and Wilson, AG (2005). "Clearance of hepatitis C virus is not associated with single nucleotide polymorphisms in the IL-1, -6, or -10 genes." Hum Immunol **66**(2): 127-32.

Miro, O, Gomez, M, Pedrol, E, Cardellach, F, Nunes, V and Casademont, J (2000). "Respiratory chain dysfunction associated with multiple mitochondrial DNA deletions in antiretroviral therapy-related lipodystrophy." Aids **14**(12): 1855-7.

Mita, S, Rizzuto, R, Moraes, CT, Shanske, S, Arnaudo, E, Fabrizi, GM, Koga, Y, DiMauro, S and Schon, EA (1990). "Recombination via flanking direct repeats is a major cause of large-scale deletions of human mitochondrial DNA." Nucleic Acids Res **18**(3): 561-7.

Mohamed, SA, Hanke, T, Erasmi, AW, Bechtel, MJ, Scharfschwerdt, M, Meissner, C, Sievers, HH and Gosslau, A (2006). "Mitochondrial DNA deletions and the aging heart." Exp Gerontol **41**(5): 508-17.

Mohsen, AH (2001). "The epidemiology of hepatitis C in a UK health regional population of 5.12 million." Gut **48**(5): 707-13.

Moradpour, D, Wakita, T, Wands, JR and Blum, HE (1998). "Tightly regulated expression of the entire hepatitis C virus structural region in continuous human cell lines." Biochem Biophys Res Commun **246**(3): 920-4.

Moraes, CT, Shanske, S, Tritschler, HJ, Aprille, JR, Andreetta, F, Bonilla, E, Schon, EA and DiMauro, S (1991). "mtDNA depletion with variable tissue expression: a novel genetic abnormality in mitochondrial diseases." Am J Hum Genet **48**(3): 492-501.

Moraes, CT, DiMauro, S, Zeviani, M, Lombes, A, Shanske, S, Miranda, AF, Nakase, H, Bonilla, E, Werneck, LC, Servidei, S and et al. (1989). "Mitochondrial DNA deletions in progressive external ophthalmoplegia and Kearns-Sayre syndrome." N Engl J Med **320**(20): 1293-9.

Morandi, L, Ferrari, D, Lombardo, C, Pession, A and Tallini, G (2007). "Monitoring HCV RNA viral load by locked nucleic acid molecular beacons real time PCR." J Virol Methods **140**(1-2): 148-54.

Moriya, K, Nakagawa, K, Santa, T, Shintani, Y, Fujie, H, Miyoshi, H, Tsutsumi, T, Miyazawa, T, Ishibashi, K, Horie, T, Imai, K, Todoroki, T, Kimura, S and Koike, K (2001). "Oxidative stress in the absence of inflammation in a mouse model for hepatitis C virus-associated hepatocarcinogenesis." Cancer Res **61**(11): 4365-70.

Moriya, K, Fujie, H, Shintani, Y, Yotsuyanagi, H, Tsutsumi, T, Ishibashi, K, Matsuura, Y, Kimura, S, Miyamura, T and Koike, K (1998). "The core protein of hepatitis C virus induces hepatocellular carcinoma in transgenic mice." Nat Med **4**(9): 1065-7.

Mottola, G, Cardinali, G, Ceccacci, A, Trozzi, C, Bartholomew, L, Torrisi, MR, Pedrazzini, E, Bonatti, S and Migliaccio, G (2002). "Hepatitis C virus nonstructural proteins are localized in a modified endoplasmic reticulum of cells expressing viral subgenomic replicons." Virology **293**(1): 31-43.

Muller, HM, Pfaff, E, Goeser, T, Kallinowski, B, Solbach, C and Theilmann, L (1993). "Peripheral blood leukocytes serve as a possible extrahepatic site for hepatitis C virus replication." J Gen Virol **74 (Pt 4)**: 669-76.

Muller-Hocker, J, Aust, D, Rohrbach, H, Napiwotzky, J, Reith, A, Link, TA, Seibel, P, Holzel, D and Kadenbach, B (1997). "Defects of the respiratory chain in the normal human liver and in cirrhosis during aging." Hepatology **26**(3): 709-19.

Nakano, I, Fukuda, Y, Katano, Y, Toyoda, H, Hayashi, K, Hayakawa, T, Kumada, T and Nakano, S (2001). "Interferon responsiveness in patients infected with hepatitis C virus 1b differs depending on viral subtype." Gut **49**(2): 263-7.

Nakano, I, Fukuda, Y, Katano, Y, Toyoda, H, Hayashi, K, Kumada, T and Nakano, S (2001a). "Japan-specific subtype of hepatitis C virus genotype 1b, J subtype, has relatively low pathogenicity." J Med Virol **65**(1): 45-51.

Nakao, T, Enomoto, N, Takada, N, Takada, A and Date, T (1991). "Typing of hepatitis C virus genomes by restriction fragment length polymorphism." J Gen Virol **72 (Pt 9)**: 2105-12.

Nelson D, Pockros P, Godofsky E, *et al.* (2008). "84% end-of-treatment response (EOTR, week 48) achieved with R1626, peginterferon alfa 2a (40KD) and ribavirin for 4 weeks followed by the standard of care: Results of a phase 2a study in treatment-naive HCV genotype 1 patients". In: 43rd Annual Meeting of the European Association for the Study of the Liver (EASL); 2008 April 26, 2008; Milan, Italy; 2008.

Nishikawa, M, Nishiguchi, S, Kioka, K, Tamori, A and Inoue, M (2005). "Interferon reduces somatic mutation of mitochondrial DNA in liver tissues from chronic viral hepatitis patients." J Viral Hepat **12**(5): 494-8.

Nishikawa, M, Nishiguchi, S, Shiomi, S, Tamori, A, Koh, N, Takeda, T, Kubo, S, Hirohashi, K, Kinoshita, H, Sato, E and Inoue, M (2001). "Somatic mutation of mitochondrial DNA in cancerous and noncancerous liver tissue in individuals with hepatocellular carcinoma." Cancer Res **61**(5): 1843-5.

Nolte, FS, Green, AM, Fiebelkorn, KR, Caliendo, AM, Sturchio, C, Grunwald, A and Healy, M (2003). "Clinical evaluation of two methods for genotyping hepatitis C virus based on analysis of the 5' noncoding region." J Clin Microbiol **41**(4): 1558-64.

Nomoto, S, Yamashita, K, Koshikawa, K, Nakao, A and Sidransky, D (2002). "Mitochondrial D-loop mutations as clonal markers in multicentric hepatocellular carcinoma and plasma." Clin Cancer Res **8**(2): 481-7.

Noppornpanth, S, Lien, TX, Poovorawan, Y, Smits, SL, Osterhaus, AD and Haagmans, BL (2006). "Identification of a naturally occurring recombinant genotype 2/6 hepatitis C virus." J Virol **80**(15): 7569-77.

Noto, H and Raskin, P (2006). "Hepatitis C infection and diabetes." J Diabetes Complications **20**(2): 113-20.

Nousbaum, JB, Pol, S, Nalpas, B, Landais, P, Berthelot, P and Brechot, C (1995). "Hepatitis C virus type 1b (II) infection in France and Italy. Collaborative Study Group." Ann Intern Med **122**(3): 161-8.

Oh, JW, Ito, T and Lai, MM (1999). "A recombinant hepatitis C virus RNA-dependent RNA polymerase capable of copying the full-length viral RNA." J Virol **73**(9): 7694-702.

Ohno, O, Mizokami, M, Wu, RR, Saleh, MG, Ohba, K, Orito, E, Mukaide, M, Williams, R and Lau, JY (1997). "New hepatitis C virus (HCV) genotyping system that allows for identification of HCV genotypes 1a, 1b, 2a, 2b, 3a, 3b, 4, 5a, and 6a." J Clin Microbiol **35**(1): 201-7.

Ohto, H, Terazawa, S, Sasaki, N, Hino, K, Ishiwata, C, Kako, M, Ujiie, N, Endo, C, Matsui, A and et al. (1994). "Transmission of hepatitis C virus from mothers to infants. The Vertical Transmission of Hepatitis C Virus Collaborative Study Group." N Engl J Med **330**(11): 744-50.

Ohtsubo, T, Nishioka, K, Imaiso, Y, Iwai, S, Shimokawa, H, Oda, H, Fujiwara, T and Nakabeppu, Y (2000). "Identification of human MutY homolog (hMYH) as a repair enzyme for 2-hydroxyadenine in DNA and detection of multiple forms of hMYH located in nuclei and mitochondria." Nucleic Acids Res **28**(6): 1355-64.

Okamoto, H, Kobata, S, Tokita, H, Inoue, T, Woodfield, GD, Holland, PV, Al-Knawy, BA, Uzunalimoglu, O, Miyakawa, Y and Mayumi, M (1996). "A second-generation method of genotyping hepatitis C virus by the polymerase chain reaction with sense and antisense primers deduced from the core gene." J Virol Methods **57**(1): 31-45.

Okamoto, H, Tokita, H, Sakamoto, M, Horikita, M, Kojima, M, Iizuka, H and Mishiro, S (1993). "Characterization of the genomic sequence of type V (or 3a) hepatitis C virus isolates and PCR primers for specific detection." J Gen Virol **74 (Pt 11)**: 2385-90.

Okamoto, H, Sugiyama, Y, Okada, S, Kurai, K, Akahane, Y, Sugai, Y, Tanaka, T, Sato, K, Tsuda, F, Miyakawa, Y and et al. (1992). "Typing hepatitis C virus by polymerase chain reaction with type-specific primers: application to clinical surveys and tracing infectious sources." J Gen Virol **73 (Pt 3)**: 673-9.

Okamoto, H, Okada, S, Sugiyama, Y, Tanaka, T, Sugai, Y, Akahane, Y, Machida, A, Mishiro, S, Yoshizawa, H, Miyakawa, Y and et al. (1990) "Detection of hepatitis C virus RNA by a two-stage polymerase chain reaction with two pairs of primers deduced from the 5'-noncoding region" Jpn J Exp Med, **60**(4): 215-22.

Okochi, O, Hibi, K, Uemura, T, Inoue, S, Takeda, S, Kaneko, T and Nakao, A (2002). "Detection of mitochondrial DNA alterations in the serum of hepatocellular carcinoma patients." Clin Cancer Res **8**(9): 2875-8.

Okuda, M, Li, K, Beard, MR, Showalter, LA, Scholle, F, Lemon, SM and Weinman, SA (2002). "Mitochondrial injury, oxidative stress, and antioxidant gene expression are induced by hepatitis C virus core protein." Gastroenterology **122**(2): 366-75.

Onishi, M, Sokuza, Y, Nishikawa, T, Mori, C, Uwataki, K, Honoki, K and Tsujiuchi, T (2007). "Different mutation patterns of mitochondrial DNA displacement-loop in hepatocellular carcinomas induced by N-nitrosodiethylamine and a choline-deficient l-amino acid-defined diet in rats." Biochem Biophys Res Commun **362**(1): 183-7.

Otani, K, Korenaga, M, Beard, MR, Li, K, Qian, T, Showalter, LA, Singh, AK, Wang, T and Weinman, SA (2005). "Hepatitis C virus core protein, cytochrome P450 2E1, and alcohol produce combined mitochondrial injury and cytotoxicity in hepatoma cells." Gastroenterology **128**(1): 96-107.

Othman, SB, Trabelsi, A, Monnet, A, Bouzgarrou, N, Grattard, F, Beyou, A, Bourlet, T and Pozzetto, B (2004). "Evaluation of a prototype HCV NS5b assay for typing strains of hepatitis C virus isolated from Tunisian haemodialysis patients." J Virol Methods **119**(2): 177-81.

Palade, GE (1952). "The fine structure of mitochondria." Anat Rec **114**(3): 427-51.

Pasloske, BL, Walkerpeach, CR, Obermoeller, RD, Winkler, M and DuBois, DB (1998). "Armored RNA technology for production of ribonuclease-resistant viral RNA controls and standards." J Clin Microbiol **36**(12): 3590-4.

Pawlotsky, JM, Bouvier-Alias, M, Hezode, C, Darthuy, F, Remire, J and Dhumeaux, D (2000). "Standardization of hepatitis C virus RNA quantification." Hepatology **32**(3): 654-9.

Pawlotsky, JM, Prescott, L, Simmonds, P, Pellet, C, Laurent-Puig, P, Labonne, C, Darthuy, F, Remire, J, Duval, J, Buffet, C, Etienne, JP, Dhumeaux, D and Dussaix, E (1997). "Serological determination of hepatitis C virus genotype: comparison with a standardized genotyping assay." J Clin Microbiol **35**(7): 1734-9.

Pawlotsky, JM, Tsakiris, L, Roudot-Thoraval, F, Pellet, C, Stuyver, L, Duval, J and Dhumeaux, D (1995). "Relationship between hepatitis C virus genotypes and sources of infection in patients with chronic hepatitis C." J Infect Dis **171**(6): 1607-10.

Pejovic, T, Ladner, D, Intengan, M, Zheng, K, Fairchild, T, Dillon, D, Easley, S, Marchetti, D, Schwartz, P, Lele, S, Costa, J and Odunsi, K (2004). "Somatic D-loop mitochondrial DNA mutations are frequent in uterine serous carcinoma." Eur J Cancer **40**(16): 2519-24.

Peng, TI, Yu, PR, Chen, JY, Wang, HL, Wu, HY, Wei, YH and Jou, MJ (2006). "Visualizing common deletion of mitochondrial DNA-augmented mitochondrial reactive oxygen species generation and apoptosis upon oxidative stress." Biochim Biophys Acta **1762**(2): 241-55.

Pessayre, D and Fromenty, B (2005). "NASH: a mitochondrial disease." J Hepatol **42**(6): 928-40.

Petros, JA, Baumann, AK, Ruiz-Pesini, E, Amin, MB, Sun, CQ, Hall, J, Lim, S, Issa, MM, Flanders, WD, Hosseini, SH, Marshall, FF and Wallace, DC (2005). "mtDNA mutations increase tumorigenicity in prostate cancer." Proc Natl Acad Sci U S A **102**(3): 719-24.

Pfaffl, MW and Hageleit, M (2001). "Validities of mRNA quantification using recombinant RNA and recombinant DNA external calibration curves in real-time RT-PCR." Biotechnology Letters **23**: 275-282.

Pham, TN, MacParland, SA, Mulrooney, PM, Cooksley, H, Naoumov, NV and Michalak, TI (2004). "Hepatitis C virus persistence after spontaneous or treatment-induced resolution of hepatitis C." J Virol **78**(11): 5867-74.

Piasecki, BA, Lewis, JD, Reddy, KR, Bellamy, SL, Porter, SB, Weinrieb, RM, Stieritz, DD and Chang, KM (2004). "Influence of alcohol use, race, and viral coinfections on spontaneous HCV clearance in a US veteran population." Hepatology **40**(4): 892-9.

Piccoli, C, Scrima, R, D'Aprile, A, Ripoli, M, Lecce, L, Boffoli, D and Capitanio, N (2006). "Mitochondrial dysfunction in hepatitis C virus infection." Biochim Biophys Acta **1757**(9-10): 1429-37.

Pileri, P, Uematsu, Y, Campagnoli, S, Galli, G, Falugi, F, Petracca, R, Weiner, AJ, Houghton, M, Rosa, D, Grandi, G and Abrignani, S (1998). "Binding of hepatitis C virus to CD81." Science **282**(5390): 938-41.

Pinz, KG, Shibutani, S and Bogenhagen, DF (1995). "Action of mitochondrial DNA polymerase gamma at sites of base loss or oxidative damage." J Biol Chem **270**(16): 9202-6.

Poe, BG, Navratil, M and Arriaga, EA (2007). "Absolute quantitation of a heteroplasmic mitochondrial DNA deletion using a multiplex three-primer real-time PCR assay." Anal Biochem **362**(2): 193-200.

Pogozelski, WK, Hamel, CJ, Woeller, CF, Jackson, WE, Zullo, SJ, Fischel-Ghodsian, N and Blakely, WF (2003). "Quantification of total mitochondrial DNA and the 4977-bp common deletion in Pearson's syndrome lymphoblasts using a fluorogenic 5'-nuclease (TaqMan) real-time polymerase chain reaction assay and plasmid external calibration standards." Mitochondrion **2**(6): 415-27.

Polyak, SJ, McArdle, S, Liu, SL, Sullivan, DG, Chung, M, Hofgartner, WT, Carithers, RL, Jr., McMahon, BJ, Mullins, JI, Corey, L and Gretch, DR (1998). "Evolution of hepatitis C virus quasispecies in hypervariable region 1 and the putative interferon sensitivity-determining region during interferon therapy and natural infection." J Virol **72**(5): 4288-96.

Poordad, F, Reddy, KR and Martin, P (2008) "Rapid virologic response: a new milestone in the management of chronic hepatitis C" Clin Infect Dis, **46**(1): 78-84.

Porteous, WK, James, AM, Sheard, PW, Porteous, CM, Packer, MA, Hyslop, SJ, Melton, JV, Pang, CY, Wei, YH and Murphy, MP (1998). "Bioenergetic consequences of accumulating the common 4977-bp mitochondrial DNA deletion." Eur J Biochem **257**(1): 192-201.

Poulton, J, Luan, J, Macaulay, V, Hennings, S, Mitchell, J and Wareham, NJ (2002). "Type 2 diabetes is associated with a common mitochondrial variant: evidence from a population-based case-control study." Hum Mol Genet **11**(13): 1581-3.

Powell, RL, Urbanski, MM and Nyambi, PN (2008). "A heteroduplex assay for the rapid detection of dual Human Immunodeficiency Virus Type 1 infections." J Virol Methods **149**(1): 20-7.

Poynard, T, Ratziu, V, Charlotte, F, Goodman, Z, McHutchison, J and Albrecht, J (2001). "Rates and risk factors of liver fibrosis progression in patients with chronic hepatitis c." J Hepatol **34**(5): 730-9.

Poynard, T, Marcellin, P, Lee, SS, Niederau, C, Minuk, GS, Ideo, G, Bain, V, Heathcote, J, Zeuzem, S, Trepo, C and Albrecht, J (1998). "Randomised trial of interferon alpha2b plus ribavirin for 48 weeks or for 24 weeks versus interferon alpha2b plus placebo for 48 weeks for treatment of chronic infection with hepatitis C virus. International Hepatitis Interventional Therapy Group (IHIT)." Lancet **352**(9138): 1426-32.

Poynard, T, Bedossa, P and Opolon, P (1997). "Natural history of liver fibrosis progression in patients with chronic hepatitis C. The OBSVIRC, METAVIR, CLINIVIR, and DOSVIRC groups." Lancet **349**(9055): 825-32.

Pozzato, G, Kaneko, S, Moretti, M, Croce, LS, Franzin, F, Unoura, M, Bercich, L, Tiribelli, C, Crovatto, M, Santini, G and et al. (1994). "Different genotypes of hepatitis C virus are associated with different severity of chronic liver disease." J Med Virol **43**(3): 291-6.

Radkowski, M, Horban, A, Gallegos-Orozco, JF, Pawelczyk, A, Jablonska, J, Wilkinson, J, Adair, D and Laskus, T (2005). "Evidence for viral persistence in patients who test positive for anti-hepatitis C virus antibodies and have normal alanine aminotransferase levels." J Infect Dis **191**(10): 1730-3.

Radkowski, M, Wang, LF, Vargas, HE, Rakela, J and Laskus, T (1998). "Detection of hepatitis C virus replication in peripheral blood mononuclear cells after orthotopic liver transplantation." Transplantation **66**(5): 664-6.

Ramon, DS, Arguello, JR, Cox, ST, McWhinnie, A, Little, AM, Marsh, SG and Madrigal, JA (1998). "Application of RSCA for the typing of HLA-DPB1." Hum Immunol **59**(11): 734-47.

Ratge, D, Scheiblhuber, B, Landt, O, Berg, J and Knabbe, C (2002). "Two-round rapid-cycle RT-PCR in single closed capillaries increases the sensitivity of HCV RNA detection and avoids amplicon carry-over." J Clin Virol **24**(3): 161-72.

Reinke, LA (2002). "Spin trapping evidence for alcohol-associated oxidative stress." Free Radic Biol Med **32**(10): 953-7.

Richter, C, Park, JW and Ames, BN (1988). "Normal oxidative damage to mitochondrial and nuclear DNA is extensive." Proc Natl Acad Sci U S A **85**(17): 6465-7.

Robertson, B, Myers, G, Howard, C, Brettin, T, Bukh, J, Gaschen, B, Gojobori, T, Maertens, G, Mizokami, M, Nainan, O, Netesov, S, Nishioka, K, Shin i, T, Simmonds, P, Smith, D, Stuyver, L and Weiner, A (1998). "Classification, nomenclature, and database development for hepatitis C virus (HCV) and related viruses: proposals for standardization. International Committee on Virus Taxonomy." Arch Virol **143**(12): 2493-503.

Robinson, LC and Marchant, JS (2008). "Enhanced Ca2+ leak from ER Ca2+ stores induced by hepatitis C NS5A protein." Biochem Biophys Res Commun **368**(3): 593-9.

Rolfe KJ, Wreghitt TG, Alexander GJM and Curran MD. *In press.* Chapter 5: A real-time Taqman method for hepatitis C virus genotyping and methods for further subtyping of isolates. Hepatitis C Second Edition. Methods in Molecular Medicine series. Series editor John Walker, book editor Hengli Tang. New Jersey. Humana Press.

Rolfe, KJ, Parmar, S, Mururi, D, Wreghitt, TG, Jalal, H, Zhang, H and Curran, MD (2007). "An internally controlled, one-step, real-time RT-PCR assay for norovirus detection and genogrouping." J Clin Virol **39**(4): 318-21.

Rolfe, KJ, Alexander, GJ, Wreghitt, TG, Parmar, S, Jalal, H and Curran, MD (2005). "A real-time Taqman method for hepatitis C virus genotyping." J Clin Virol **34**(2): 115-21.

Ronaghi, M, Uhlen, M and Nyren, P (1998). "A sequencing method based on real-time pyrophosphate." Science **281**(5375): 363, 365.

Ross, OA, Hyland, P, Curran, MD, McIlhatton, BP, Wikby, A, Johansson, B, Tompa, A, Pawelec, G, Barnett, CR, Middleton, D and Barnett, YA (2002). "Mitochondrial DNA damage in lymphocytes: a role in immunosenescence?" Exp Gerontol **37**(2-3): 329-40.

Ross, RS, Viazov, S, Wolters, B and Roggendorf, M (2008). "Towards a better resolution of hepatitis C virus variants: CLIP sequencing of an HCV core fragment and automated assignment of genotypes and subtypes." J Virol Methods **148**(1-2): 25-33.

Ross, RS, Viazov, S and Roggendorf, M (2007). "Genotyping of hepatitis C virus isolates by a new line probe assay using sequence information from both the 5'untranslated and the core regions." J Virol Methods **143**(2): 153-60.

Ross, RS, Viazov, SO, Holtzer, CD, Beyou, A, Monnet, A, Mazure, C and Roggendorf, M (2000). "Genotyping of hepatitis C virus isolates using CLIP sequencing." J Clin Microbiol **38**(10): 3581-4.

Rossi, L, Leveri, M, Marinelli, D, Belli, L, Civardi, E and Silini, EM (2003). "An heteroduplex mobility analysis assay based on capillary electrophoresis for the study of HCV quasispecies." J Virol Methods **110**(1): 37-49.

Rossman, TG and Goncharova, EI (1998). "Spontaneous mutagenesis in mammalian cells is caused mainly by oxidative events and can be blocked by antioxidants and metallothionein." Mutat Res **402**(1-2): 103-10.

Salas, A, Lareu, V, Calafell, F, Bertranpetit, J and Carracedo, A (2000). "mtDNA hypervariable region II (HVII) sequences in human evolution studies." Eur J Hum Genet **8**(12): 964-74.

Saldanha, J, Heath, A, Aberham, C, Albrecht, J, Gentili, G, Gessner, M and Pisani, G (2005). "World Health Organization collaborative study to establish a replacement WHO international standard for hepatitis C virus RNA nucleic acid amplification technology assays." Vox Sang **88**(3): 202-4.

Saldanha, J, Lelie, N and Heath, A (1999). "Establishment of the first international standard for nucleic acid amplification technology (NAT) assays for HCV RNA. WHO Collaborative Study Group." Vox Sang **76**(3): 149-58.

Sambrook J and Russell DW. (2001). Molecular Cloning: A Laboratory Manual. Third Edition. New York. Cold Spring Harbor Laboratory Press.

Samuels, DC, Schon, EA and Chinnery, PF (2004). "Two direct repeats cause most human mtDNA deletions." Trends Genet **20**(9): 393-8.

Sanchez-Cespedes, M, Parrella, P, Nomoto, S, Cohen, D, Xiao, Y, Esteller, M, Jeronimo, C, Jordan, RC, Nicol, T, Koch, WM, Schoenberg, M, Mazzarelli, P, Fazio, VM and Sidransky, D (2001). "Identification of a mononucleotide repeat as a major target for mitochondrial DNA alterations in human tumors." Cancer Res **61**(19): 7015-9.

Sandres-Saune, K, Deny, P, Pasquier, C, Thibaut, V, Duverlie, G and Izopet, J (2003). "Determining hepatitis C genotype by analyzing the sequence of the NS5b region." J Virol Methods **109**(2): 187-93.

Santantonio, T, Sinisi, E, Guastadisegni, A, Casalino, C, Mazzola, M, Gentile, A, Leandro, G and Pastore, G (2003). "Natural course of acute hepatitis C: a long-term prospective study." Dig Liver Dis **35**(2): 104-13.

Sarrazin, C, Gartner, BC, Sizmann, D, Babiel, R, Mihm, U, Hofmann, WP, von Wagner, M and Zeuzem, S (2006). "Comparison of conventional PCR with real-time PCR and branched DNA-based assays for hepatitis C virus RNA quantification and clinical significance for genotypes 1 to 5." J Clin Microbiol **44**(3): 729-37.

Scheltinga, SA, Templeton, KE, Beersma, MF and Claas, EC (2005). "Diagnosis of human metapneumovirus and rhinovirus in patients with respiratory tract infections by an internally controlled multiplex real-time RNA PCR." J Clin Virol **33**(4): 306-11.

Schild, L, Reinheckel, T, Reiser, M, Horn, TF, Wolf, G and Augustin, W (2003). "Nitric oxide produced in rat liver mitochondria causes oxidative stress and impairment of respiration after transient hypoxia." Faseb J **17**(15): 2194-201.

Schneeberger, PM, Keur, I, van der Vliet, W, van Hoek, K, Boswijk, H, van Loon, AM, van Dijk, WC, Kauffmann, RH, Quint, W and van Doorn, LJ (1998). "Hepatitis C virus infections in dialysis centers in The Netherlands: a national survey by serological and molecular methods." J Clin Microbiol **36**(6): 1711-5.

Schoeler, S, Szibor, R, Gellerich, FN, Wartmann, T, Mawrin, C, Dietzmann, K and Kirches, E (2005). "Mitochondrial DNA deletions sensitize cells to apoptosis at low heteroplasmy levels." Biochem Biophys Res Commun **332**(1): 43-9.

Schon, EA, Rizzuto, R, Moraes, CT, Nakase, H, Zeviani, M and DiMauro, S (1989). "A direct repeat is a hotspot for large-scale deletion of human mitochondrial DNA." Science **244**(4902): 346-9.

Schroter, M, Zollner, B, Schafer, P, Landt, O, Lass, U, Laufs, R and Feucht, HH (2002). "Genotyping of hepatitis C virus types 1, 2, 3, and 4 by a one-step LightCycler method using three different pairs of hybridization probes." J Clin Microbiol **40**(6): 2046-50.

Sciacco, M, Bonilla, E, Schon, EA, DiMauro, S and Moraes, CT (1994). "Distribution of wild-type and common deletion forms of mtDNA in normal and respiration-deficient muscle fibers from patients with mitochondrial myopathy." Hum Mol Genet **3**(1): 13-9.

Sen, GC (2001). "Viruses and interferons." Annu Rev Microbiol **55**: 255-81.

Shanske, S, Moraes, CT, Lombes, A, Miranda, AF, Bonilla, E, Lewis, P, Whelan, MA, Ellsworth, CA and DiMauro, S (1990). "Widespread tissue distribution of mitochondrial DNA deletions in Kearns-Sayre syndrome." Neurology **40**(1): 24-8.

Shao, JY, Gao, HY, Li, YH, Zhang, Y, Lu, YY and Zeng, YX (2004). "Quantitative detection of common deletion of mitochondrial DNA in hepatocellular carcinoma and hepatocellular nodular hyperplasia." World J Gastroenterol **10**(11): 1560-4.

Shay, JW and Ishii, S (1990). "Unexpected nonrandom mitochondrial DNA segregation in human cell hybrids." Anticancer Res **10**(2A): 279-84.

Shay, JW and Werbin, H (1987). "Are mitochondrial DNA mutations involved in the carcinogenic process?" Mutat Res **186**(2): 149-60.

Shibutani, S, Takeshita, M and Grollman, AP (1991). "Insertion of specific bases during DNA synthesis past the oxidation-damaged base 8-oxodG." Nature **349**(6308): 431-4.

Shieh, DB, Chou, WP, Wei, YH, Wong, TY and Jin, YT (2004). "Mitochondrial DNA 4,977-bp deletion in paired oral cancer and precancerous lesions revealed by laser microdissection and real-time quantitative PCR." Ann N Y Acad Sci **1011**: 154-67.

Shigenaga, MK, Hagen, TM and Ames, BN (1994). "Oxidative damage and mitochondrial decay in aging." Proc Natl Acad Sci U S A **91**(23): 10771-8.

Shimizu, YK, Hijikata, M, Iwamoto, A, Alter, HJ, Purcell, RH and Yoshikura, H (1994). "Neutralizing antibodies against hepatitis C virus and the emergence of neutralization escape mutant viruses." J Virol **68**(3): 1494-500.

Shimoda, R, Nagashima, M, Sakamoto, M, Yamaguchi, N, Hirohashi, S, Yokota, J and Kasai, H (1994). "Increased formation of oxidative DNA damage, 8-hydroxydeoxyguanosine, in human livers with chronic hepatitis." Cancer Res **54**(12): 3171-2.

Shoffner, JM, Lott, MT, Voljavec, AS, Soueidan, SA, Costigan, DA and Wallace, DC (1989). "Spontaneous Kearns-Sayre/chronic external ophthalmoplegia plus syndrome associated with a mitochondrial DNA deletion: a slip-replication model and metabolic therapy." Proc Natl Acad Sci U S A **86**(20): 7952-6.

Sia, EA, Kokoska, RJ, Dominska, M, Greenwell, P and Petes, TD (1997). "Microsatellite instability in yeast: dependence on repeat unit size and DNA mismatch repair genes." Mol Cell Biol **17**(5): 2851-8.

Silini, E, Bottelli, R, Asti, M, Bruno, S, Candusso, ME, Brambilla, S, Bono, F, Iamoni, G, Tinelli, C, Mondelli, MU and Ideo, G (1996). "Hepatitis C virus genotypes and risk of hepatocellular carcinoma in cirrhosis: a case-control study." Gastroenterology **111**(1): 199-205.

Simmonds, P (2001). "The origin and evolution of hepatitis viruses in humans." J Gen Virol **82**(Pt 4): 693-712.

Simmonds, P (1995). "Variability of hepatitis C virus." Hepatology **21**(2): 570-83.

Simmonds, P, Bukh, J, Combet, C, Deleage, G, Enomoto, N, Feinstone, S, Halfon, P, Inchauspe, G, Kuiken, C, Maertens, G, Mizokami, M, Murphy, DG, Okamoto, H, Pawlotsky, JM, Penin, F, Sablon, E, Shin, IT, Stuyver, LJ, Thiel, HJ, Viazov, S, Weiner, AJ and Widell, A (2005). "Consensus proposals for a unified system of nomenclature of hepatitis C virus genotypes." Hepatology **42**(4): 962-73.

Simmonds, P, Mellor, J, Sakuldamrongpanich, T, Nuchaprayoon, C, Tanprasert, S, Holmes, EC and Smith, DB (1996). "Evolutionary analysis of variants of hepatitis C virus found in South-East Asia: comparison with classifications based upon sequence similarity." J Gen Virol **77 (Pt 12)**: 3013-24.

Simmonds, P, Alberti, A, Alter, HJ, Bonino, F, Bradley, DW, Brechot, C, Brouwer, JT, Chan, SW, Chayama, K, Chen, DS and et al. (1994). "A proposed system for the nomenclature of hepatitis C viral genotypes." Hepatology **19**(5): 1321-4.

Simmonds, P, Holmes, EC, Cha, TA, Chan, SW, McOmish, F, Irvine, B, Beall, E, Yap, PL, Kolberg, J and Urdea, MS (1993). "Classification of hepatitis C virus into six major genotypes and a series of subtypes by phylogenetic analysis of the NS-5 region." J Gen Virol **74 (Pt 11)**: 2391-9.

Sizmann, D, Boeck, C, Boelter, J, Fischer, D, Miethke, M, Nicolaus, S, Zadak, M and Babiel, R (2007). "Fully automated quantification of hepatitis C virus (HCV) RNA in human plasma and human serum by the COBAS AmpliPrep/COBAS TaqMan system." J Clin Virol **38**(4): 326-33.

Sokol, RJ and Treem, WR (2001). Mitochondrial hepatopathies. Liver Diseases in Children. F. Suchy, R. J. Sokol and W. Balistreri. Philadelphia, Lippincott, Williams & Wilkins: 787-810.

Soldan, K, Davison, K and Dow, B (2005). "Estimates of the frequency of HBV, HCV, and HIV infectious donations entering the blood supply in the United Kingdom, 1996 to 2003." Euro Surveill **10**(2): 17-9.

Soldan, K, Barbara, JA, Ramsay, ME and Hall, AJ (2003). "Estimation of the risk of hepatitis B virus, hepatitis C virus and human immunodeficiency virus infectious donations entering the blood supply in England, 1993-2001." Vox Sang **84**(4): 274-86.

Soldan, K, Ramsay, M, Robinson, A, Harris, H, Anderson, N, Caffrey, E, Chapman, C, Dike, A, Gabra, G, Gorman, A, Herborn, A, Hewitt, P, Hewson, N, Jones, DA, Llewelyn, C, Love, E, Muddu, V, Martlew, V and Townley, A (2002). "The contribution of transfusion to HCV infection in England." Epidemiol Infect **129**(3): 587-91.

Sterling, RK and Bralow, S (2006). "Extrahepatic manifestations of hepatitis C virus." Curr Gastroenterol Rep **8**(1): 53-9.

Stoneking, M (2000). "Hypervariable sites in the mtDNA control region are mutational hotspots." Am J Hum Genet **67**(4): 1029-32.

Stuyver, L, Wyseur, A, van Arnhem, W, Hernandez, F and Maertens, G (1996). "Second-generation line probe assay for hepatitis C virus genotyping." J Clin Microbiol **34**(9): 2259-66.

Stuyver, L, Rossau, R, Wyseur, A, Duhamel, M, Vanderborght, B, Van Heuverswyn, H and Maertens, G (1993). "Typing of hepatitis C virus isolates and characterization of new subtypes using a line probe assay." J Gen Virol **74 (Pt 6)**: 1093-102.

Suzuki, R, Sakamoto, S, Tsutsumi, T, Rikimaru, A, Tanaka, K, Shimoike, T, Moriishi, K, Iwasaki, T, Mizumoto, K, Matsuura, Y, Miyamura, T and Suzuki, T (2005). "Molecular determinants for subcellular localization of hepatitis C virus core protein." J Virol **79**(2): 1271-81.

Sweeting, MJ, De Angelis, D, Brant, LJ, Harris, HE, Mann, AG and Ramsay, ME (2007). "The burden of hepatitis C in England." J Viral Hepat **14**(8): 570-6.

Sweeting, MJ, De Angelis, D, Neal, KR, Ramsay, ME, Irving, WL, Wright, M, Brant, L and Harris, HE (2006). "Estimated progression rates in three United Kingdom hepatitis C cohorts differed according to method of recruitment." J Clin Epidemiol **59**(2): 144-52.

Takada, N, Takase, S, Takada, A and Date, T (1993). "Differences in the hepatitis C virus genotypes in different countries." J Hepatol **17**(3): 277-83.

Takao, M, Aburatani, H, Kobayashi, K and Yasui, A (1998). "Mitochondrial targeting of human DNA glycosylases for repair of oxidative DNA damage." Nucleic Acids Res **26**(12): 2917-22.

Takeuchi, T, Katsume, A, Tanaka, T, Abe, A, Inoue, K, Tsukiyama-Kohara, K, Kawaguchi, R, Tanaka, S and Kohara, M (1999). "Real-time detection system for quantification of hepatitis C virus genome." Gastroenterology **116**(3): 636-42.

Tamori, A, Nishiguchi, S, Nishikawa, M, Kubo, S, Koh, N, Hirohashi, K, Shiomi, S and Inoue, M (2004). "Correlation between clinical characteristics and mitochondrial D-loop DNA mutations in hepatocellular carcinoma." J Gastroenterol **39**(11): 1063-8.

Tan, DJ, Chang, J, Liu, LL, Bai, RK, Wang, YF, Yeh, KT and Wong, LJ (2006). "Significance of somatic mutations and content alteration of mitochondrial DNA in esophageal cancer." BMC Cancer **6**: 93.

Tanaka, H, Fujita, N, Sugimoto, R, Urawa, N, Horiike, S, Kobayashi, Y, Iwasa, M, Ma, N, Kawanishi, S, Watanabe, S, Kaito, M and Takei, Y (2008). "Hepatic oxidative DNA damage is associated with increased risk for hepatocellular carcinoma in chronic hepatitis C." Br J Cancer **98**(3): 580-6.

Tanaka, H, Tsukuma, H, Yamano, H, Okubo, Y, Inoue, A, Kasahara, A and Hayashi, N (1998). "Hepatitis C virus 1b(II) infection and development of chronic hepatitis, liver cirrhosis and hepatocellular carcinoma: a case-control study in Japan." J Epidemiol **8**(4): 244-9.

Tardif, KD, Mori, K and Siddiqui, A (2002). "Hepatitis C virus subgenomic replicons induce endoplasmic reticulum stress activating an intracellular signaling pathway." J Virol **76**(15): 7453-9.

ter Schegget, J, Flavell, RA and Borst, P (1971). "DNA synthesis by isolated mitochondria. 3. Characterization of D-loop DNA, a novel intermediate in mtDNA synthesis." Biochim Biophys Acta **254**(1): 1-14.

Thomas, DL, Astemborski, J, Rai, RM, Anania, FA, Schaeffer, M, Galai, N, Nolt, K, Nelson, KE, Strathdee, SA, Johnson, L, Laeyendecker, O, Boitnott, J, Wilson, LE and Vlahov, D (2000). "The natural history of hepatitis C virus infection: host, viral, and environmental factors." Jama **284**(4): 450-6.

Thomas, SL, Newell, ML, Peckham, CS, Ades, AE and Hall, AJ (1998). "A review of hepatitis C virus (HCV) vertical transmission: risks of transmission to infants born to mothers with and without HCV viraemia or human immunodeficiency virus infection." Int J Epidemiol **27**(1): 108-17.

Tilg, H (1997). "New insights into the mechanisms of interferon alfa: an immunoregulatory and anti-inflammatory cytokine." Gastroenterology **112**(3): 1017-21.

Tokita, H, Okamoto, H, Iizuka, H, Kishimoto, J, Tsuda, F, Lesmana, LA, Miyakawa, Y and Mayumi, M (1996). "Hepatitis C virus variants from Jakarta, Indonesia classifiable into novel genotypes in the second (2e and 2f), tenth (10a) and eleventh (11a) genetic groups." J Gen Virol **77 (Pt 2)**: 293-301.

Tolou, HJ, Couissinier-Paris, P, Durand, JP, Mercier, V, de Pina, JJ, de Micco, P, Billoir, F, Charrel, RN and de Lamballerie, X (2001). "Evidence for recombination in natural populations of dengue virus type 1 based on the analysis of complete genome sequences." J Gen Virol **82**(Pt 6): 1283-90.

Touzet, S, Kraemer, L, Colin, C, Pradat, P, Lanoir, D, Bailly, F, Coppola, RC, Sauleda, S, Thursz, MR, Tillmann, H, Alberti, A, Braconier, JH, Esteban, JI, Hadziyannis, SJ, Manns, MP, Saracco, G, Thomas, HC and Trepo, C (2000). "Epidemiology of hepatitis C virus infection in seven European Union countries: a critical analysis of the literature. HENCORE Group. (Hepatitis C European Network for Co-operative Research." Eur J Gastroenterol Hepatol **12**(6): 667-78.

Turner, D, Akpe, S, Brown, J, Brown, C, McWhinnie, A, Madrigal, A and Navarrete, C (2001). "HLA-B typing by reference strand mediated conformation analysis using a capillary-based semiautomated genetic analyzer." Hum Immunol **62**(4): 414-8.

Turner, DM, Poles, A, Brown, J, Arguello, JR, Madrigal, JA and Navarrete, CV (1999). "HLA-A typing by reference strand-mediated conformation analysis (RSCA) using a capillary-based semi-automated genetic analyser." Tissue Antigens **54**(4): 400-4.

van der Poel, CL (1999). "Hepatitis C virus and blood transfusion: past and present risks." J Hepatol **31 Suppl 1**: 101-6.

Van Houten, B, Woshner, V and Santos, JH (2006). "Role of mitochondrial DNA in toxic responses to oxidative stress." DNA Repair (Amst) **5**(2): 145-52.

Vidali, M, Tripodi, MF, Ivaldi, A, Zampino, R, Occhino, G, Restivo, L, Sutti, S, Marrone, A, Ruggiero, G, Albano, E and Adinolfi, LE (2008). "Interplay between oxidative stress and hepatic steatosis in the progression of chronic hepatitis C." J Hepatol **48**(3): 399-406.

von Wagner, M, Huber, M, Berg, T, Hinrichsen, H, Rasenack, J, Heintges, T, Bergk, A, Bernsmeier, C, Haussinger, D, Herrmann, E and Zeuzem, S (2005). "Peginterferon-alpha-2a (40KD) and ribavirin for 16 or 24 weeks in patients with genotype 2 or 3 chronic hepatitis C." Gastroenterology **129**(2): 522-7.

Walberg, MW and Clayton, DA (1981). "Sequence and properties of the human KB cell and mouse L cell D-loop regions of mitochondrial DNA." Nucleic Acids Res **9**(20): 5411-21.

Wallace, DC (1994). "Mitochondrial DNA sequence variation in human evolution and disease." Proc Natl Acad Sci U S A **91**(19): 8739-46.

Wallace, DC (1992). "Diseases of the mitochondrial DNA." Annu Rev Biochem **61**: 1175-212.

Wang, C, Sarnow, P and Siddiqui, A (1993). "Translation of human hepatitis C virus RNA in cultured cells is mediated by an internal ribosome-binding mechanism." J Virol **67**(6): 3338-44.

Wang, CC, Krantz, E, Klarquist, J, Krows, M, McBride, L, Scott, EP, Shaw-Stiffel, T, Weston, SJ, Thiede, H, Wald, A and Rosen, HR (2007). "Acute hepatitis C in a contemporary US cohort: modes of acquisition and factors influencing viral clearance." J Infect Dis **196**(10): 1474-82.

Wang, JT, Sheu, JC, Lin, JT, Wang, TH and Chen, DS (1992). "Detection of replicative form of hepatitis C virus RNA in peripheral blood mononuclear cells." J Infect Dis **166**(5): 1167-9.

Wang, Y, Liu, VW, Tsang, PC, Chiu, PM, Cheung, AN, Khoo, US, Nagley, P and Ngan, HY (2006). "Microsatellite instability in mitochondrial genome of common female cancers." Int J Gynecol Cancer **16 Suppl 1**: 259-66.

Wang, Y, Liu, VW, Ngan, HY and Nagley, P (2005). "Frequent occurrence of mitochondrial microsatellite instability in the D-loop region of human cancers." Ann N Y Acad Sci **1042**: 123-9.

Waris, G, Turkson, J, Hassanein, T and Siddiqui, A (2005). "Hepatitis C virus (HCV) constitutively activates STAT-3 via oxidative stress: role of STAT-3 in HCV replication." J Virol **79**(3): 1569-80.

Waris, G, Tardif, KD and Siddiqui, A (2002). "Endoplasmic reticulum (ER) stress: hepatitis C virus induces an ER-nucleus signal transduction pathway and activates NF-kappaB and STAT-3." Biochem Pharmacol **64**(10): 1425-30.

Wasley, A and Alter, MJ (2000). "Epidemiology of hepatitis C: geographic differences and temporal trends." Semin Liver Dis **20**(1): 1-16.

Watson, JP, Brind, AM, Chapman, CE, Bates, CL, Gould, FK, Johnson, SJ, Burt, AD, Ferguson, J, Simmonds, P and Bassendine, MF (1996). "Hepatitis C virus: epidemiology and genotypes in the north east of England." Gut **38**(2): 269-76.

Wei, YH (1998). "Oxidative stress and mitochondrial DNA mutations in human aging." Proc Soc Exp Biol Med **217**(1): 53-63.

Wei, YH, Kao, SH and Lee, HC (1996). "Simultaneous increase of mitochondrial DNA deletions and lipid peroxidation in human aging." Ann N Y Acad Sci **786**: 24-43.

Weiner, AJ, Geysen, HM, Christopherson, C, Hall, JE, Mason, TJ, Saracco, G, Bonino, F, Crawford, K, Marion, CD, Crawford, KA and et al. (1992). "Evidence for immune selection of hepatitis C virus (HCV) putative envelope glycoprotein variants: potential role in chronic HCV infections." Proc Natl Acad Sci U S A **89**(8): 3468-72.

Weiner, AJ, Brauer, MJ, Rosenblatt, J, Richman, KH, Tung, J, Crawford, K, Bonino, F, Saracco, G, Choo, QL, Houghton, M and et al. (1991). "Variable and hypervariable domains are found in the regions of HCV corresponding to the flavivirus envelope and NS1 proteins and the pestivirus envelope glycoproteins." Virology **180**(2): 842-8.

Wheelhouse, NM, Lai, PB, Wigmore, SJ, Ross, JA and Harrison, DJ (2005). "Mitochondrial D-loop mutations and deletion profiles of cancerous and noncancerous liver tissue in hepatitis B virus-infected liver." Br J Cancer **92**(7): 1268-72.

White, PA, Pan, Y, Freeman, AJ, Marinos, G, Ffrench, RA, Lloyd, AR and Rawlinson, WD (2002). "Quantification of hepatitis C virus in human liver and serum samples by using LightCycler reverse transcriptase PCR." J Clin Microbiol **40**(11): 4346-8.

White, PA, Zhai, X, Carter, I, Zhao, Y and Rawlinson, WD (2000). "Simplified hepatitis C virus genotyping by heteroduplex mobility analysis." J Clin Microbiol **38**(2): 477-82.

White, PA, Li, Z, Zhai, X, Marinos, G and Rawlinson, WD (2000a). "Mixed viral infection identified using heteroduplex mobility analysis (HMA)." Virology **271**(2): 382-9.

Willems, M, Moshage, H, Nevens, F, Fevery, J and Yap, SH (1993). "Plasma collected from heparinized blood is not suitable for HCV-RNA detection by conventional RT-PCR assay." J Virol Methods **42**(1): 127-30.

Wink, DA, Kasprzak, KS, Maragos, CM, Elespuru, RK, Misra, M, Dunams, TM, Cebula, TA, Koch, WH, Andrews, AW, Allen, JS and et al. (1991). "DNA deaminating ability and genotoxicity of nitric oxide and its progenitors." Science **254**(5034): 1001-3.

Wispe, JR, Clark, JC, Burhans, MS, Kropp, KE, Korfhagen, TR and Whitsett, JA (1989). "Synthesis and processing of the precursor for human mangano-superoxide dismutase." Biochim Biophys Acta **994**(1): 30-6.

Wolff, D and Gerritzen, A (2007). "Comparison of the Roche COBAS Amplicor Monitor, Roche COBAS Ampliprep/COBAS Taqman and Abbott RealTime Test assays for quantification of hepatitis C virus and HIV RNA." Clin Chem Lab Med **45**(7): 917-22.

Wong, LJ, Tan, DJ, Bai, RK, Yeh, KT and Chang, J (2004). "Molecular alterations in mitochondrial DNA of hepatocellular carcinomas: is there a correlation with clinicopathological profile?" J Med Genet **41**(5): e65.

Wong, LJ, Perng, CL, Hsu, CH, Bai, RK, Schelley, S, Vladutiu, GD, Vogel, H and Enns, GM (2003). "Compensatory amplification of mtDNA in a patient with a novel deletion/duplication and high mutant load." J Med Genet **40**(11): e125.

Wong, LJ, Liang, MH, Kwon, H, Park, J, Bai, RK and Tan, DJ (2002). "Comprehensive scanning of the entire mitochondrial genome for mutations." Clin Chem **48**(11): 1901-12.

World Health Organization. (10 December 1999). Hepatitis C – global prevalence (update). Weekly Epidemiological Record. **49**.

World Health Organization. (8 February 2002). Global distribution of hepatitis A, B and C, 2001. Weekly Epidemiological Record. **6**.

Wreghitt, TG (2004). "Bloodborne virus infections in dialysis units: a mini-review." Commun Dis Public Health **7**(2): 92-3.

Wreghitt, TG (1999). "Blood-borne virus infections in dialysis units--a review." Rev Med Virol **9**(2): 101-9.

Wu, CW, Yin, PH, Hung, WY, Li, AF, Li, SH, Chi, CW, Wei, YH and Lee, HC (2005). "Mitochondrial DNA mutations and mitochondrial DNA depletion in gastric cancer." Genes Chromosomes Cancer **44**(1): 19-28.

Xu, LZ, Larzul, D, Delaporte, E, Brechot, C and Kremsdorf, D (1994). "Hepatitis C virus genotype 4 is highly prevalent in central Africa (Gabon)." J Gen Virol **75 (Pt 9)**: 2393-8.

Yakes, FM and Van Houten, B (1997). "Mitochondrial DNA damage is more extensive and persists longer than nuclear DNA damage in human cells following oxidative stress." Proc Natl Acad Sci U S A **94**(2): 514-9.

Yamamoto, H, Tanaka, M, Katayama, M, Obayashi, T, Nimura, Y and Ozawa, T (1992). "Significant existence of deleted mitochondrial DNA in cirrhotic liver surrounding hepatic tumor." Biochem Biophys Res Commun **182**(2): 913-20.

Yang, JH, Lai, JP, Douglas, SD, Metzger, D, Zhu, XH and Ho, WZ (2002). "Real-time RT-PCR for quantitation of hepatitis C virus RNA." J Virol Methods **102**(1-2): 119-28.

Yasui, K, Okanoue, T, Murakami, Y, Itoh, Y, Minami, M, Sakamoto, S, Sakamoto, M and Nishioji, K (1998). "Dynamics of hepatitis C viremia following interferon-alpha administration." J Infect Dis **177**(6): 1475-9.

Ye, C, Shu, XO, Wen, W, Pierce, L, Courtney, R, Gao, YT, Zheng, W and Cai, Q (2008). "Quantitative analysis of mitochondrial DNA 4977-bp deletion in sporadic breast cancer and benign breast diseases." Breast Cancer Res Treat **108**(3): 427-34.

Yee, LJ (2004). "Host genetic determinants in hepatitis C virus infection." Genes Immun **5**(4): 237-45.

Yeung, LT, To, T, King, SM and Roberts, EA (2007). "Spontaneous clearance of childhood hepatitis C virus infection." J Viral Hepat **14**(11): 797-805.

Yoneyama, H, Hara, T, Kato, Y, Yamori, T, Matsuura, ET and Koike, K (2005). "Nucleotide sequence variation is frequent in the mitochondrial DNA displacement loop region of individual human tumor cells." Mol Cancer Res **3**(1): 14-20.

Yu, JW, Wang, GQ, Sun, LJ, Li, XG and Li, SC (2007) "Predictive value of rapid virological response and early virological response on sustained virological response in HCV patients treated with pegylated interferon alpha-2a and ribavirin" J Gastroenterol Hepatol, **22**(6): 832-6.

Yu, TW and Anderson, D (1997). "Reactive oxygen species-induced DNA damage and its modification: a chemical investigation." Mutat Res **379**(2): 201-10.

Zaera, MG, Miro, O, Pedrol, E, Soler, A, Picon, M, Cardellach, F, Casademont, J and Nunes, V (2001). "Mitochondrial involvement in antiretroviral therapy-related lipodystrophy." Aids **15**(13): 1643-51.

Zein, NN (2000). "Clinical significance of hepatitis C virus genotypes." Clin Microbiol Rev **13**(2): 223-35.

Zein, NN, Poterucha, JJ, Gross, JB, Jr., Wiesner, RH, Therneau, TM, Gossard, AA, Wendt, NK, Mitchell, PS, Germer, JJ and Persing, DH (1996). "Increased risk of hepatocellular carcinoma in patients infected with hepatitis C genotype 1b." Am J Gastroenterol **91**(12): 2560-2.

Zeuzem, S, Buti, M, Ferenci, P, Sperl, J, Horsmans, Y, Cianciara, J, Ibranyi, E, Weiland, O, Noviello, S, Brass, C and Albrecht, J (2006). "Efficacy of 24 weeks treatment with peginterferon alfa-2b plus ribavirin in patients with chronic hepatitis C infected with genotype 1 and low pretreatment viremia." J Hepatol **44**(1): 97-103.

Zeuzem, S, Hultcrantz, R, Bourliere, M, Goeser, T, Marcellin, P, Sanchez-Tapias, J, Sarrazin, C, Harvey, J, Brass, C and Albrecht, J (2004). "Peginterferon alfa-2b plus ribavirin for treatment of chronic hepatitis C in previously untreated patients infected with HCV genotypes 2 or 3." J Hepatol **40**(6): 993-9.

Zeuzem, S, Diago, M, Gane, E, Reddy, KR, Pockros, P, Prati, D, Shiffman, M, Farci, P, Gitlin, N, O'Brien, CB, Lamour, F and Lardelli, P (2004a). "Peginterferon alfa-2a (40 kilodaltons) and ribavirin in patients with chronic hepatitis C and normal aminotransferase levels." Gastroenterology **127**(6): 1724-32.

Zeuzem, S, Herrmann, E, Lee, JH, Fricke, J, Neumann, AU, Modi, M, Colucci, G and Roth, WK (2001). "Viral kinetics in patients with chronic hepatitis C treated with standard or peginterferon alpha2a." Gastroenterology **120**(6): 1438-47.

Zeuzem, S, Feinman, SV, Rasenack, J, Heathcote, EJ, Lai, MY, Gane, E, O'Grady, J, Reichen, J, Diago, M, Lin, A, Hoffman, J and Brunda, MJ (2000). "Peginterferon alfa-2a in patients with chronic hepatitis C." N Engl J Med **343**(23): 1666-72.

Zeuzem, S, Lee, JH, Franke, A, Ruster, B, Prummer, O, Herrmann, G and Roth, WK (1998). "Quantification of the initial decline of serum hepatitis C virus RNA and response to interferon alfa." Hepatology **27**(4): 1149-56.

Zeviani, M, Moraes, CT, DiMauro, S, Nakase, H, Bonilla, E, Schon, EA and Rowland, LP (1988). "Deletions of mitochondrial DNA in Kearns-Sayre syndrome." Neurology **38**(9): 1339-46.

Zhang, C, Liu, VW, Addessi, CL, Sheffield, DA, Linnane, AW and Nagley, P (1998). "Differential occurrence of mutations in mitochondrial DNA of human skeletal muscle during aging." Hum Mutat **11**(5): 360-71.

Zhao, YB, Yang, HY, Zhang, XW and Chen, GY (2005). "Mutation in D-loop region of mitochondrial DNA in gastric cancer and its significance." World J Gastroenterol **11**(21): 3304-6.

Zheng, X, Pang, M, Chan, A, Roberto, A, Warner, D and Yen-Lieberman, B (2003). "Direct comparison of hepatitis C virus genotypes tested by INNO-LiPA HCV II and TRUGENE HCV genotyping methods." J Clin Virol **28**(2): 214-6.

Zylberberg, H, Rimaniol, AC, Pol, S, Masson, A, De Groote, D, Berthelot, P, Bach, JF, Brechot, C and Zavala, F (1999). "Soluble tumor necrosis factor receptors in chronic hepatitis C: a correlation with histological fibrosis and activity." J Hepatol **30**(2): 185-91.

APPENDICES

Appendix A - Working Solutions

70% Ethanol

Fifty millitres of 70% ethanol was prepared by combining 35 ml of absolute ethanol (Sigma-Aldrich, Dorset UK, cat. no. 32221) with 15 ml of ddH_20. The solution was mixed by inversion.

75% Ethanol

Fifty millitres of 75% ethanol was prepared by combining 37.5 ml of absolute ethanol with 12.5 ml of ddH_20. The solution was mixed by inversion.

Proteinase K (10 mg/ml)

A 10 mg/ml working solution of proteinase K was made by reconstituting the lipophilised powder (Promega, Madison USA, cat. no. V302B) in 10 ml ddH_20. This was distributed into 1 ml aliquots and stored at -20°C until required.

Saturated Sodium Chloride (~6 M NaCl)

Saturated sodium chloride was prepared by adding 350.64 g of sodium chloride to 600 ml of ddH_20 and mixing. The solution was then made up to 1 litre with ddH_20, before being autoclaved to maintain sterility.

4 M sodium chloride (NaCl)

4 M NaCl was made by dissolving 233.75 g of NaCl (VWR International Ltd, Poole, UK cat. no. 301235Q) in 800 ml ddH_20 and making up the solution to 1 litre with ddH_20. The solution was then autoclaved to maintain sterility.

Tris-EDTA (TE) buffer (10mm Tris, 1mm EDTA [pH 8.0])

A 1 litre volume of TE buffer was prepared by adding 10 ml of 100x Tris-EDTA buffer (Sigma-Aldrich, Dorset UK, cat. no. T-9285) to 990 ml of ddH_20.

1x Tris Borate EDTA Buffer (TBE) (0.1 M Tris, 0.09 M Boric acid, 0.001 M EDTA)

To prepare 1500 ml of 1x TBE buffer, 150 ml of UltraPure™ 10x TBE buffer (Invitrogen, Paisley UK, cat. no. 15581-044) was combined with 1350 ml of ddH_2O and mixed by inversion.

Ethidium bromide

A stock solution of ethidium bromide (Sigma-Aldrich, Dorset UK, cat. no. E-8751) (10 mg/ml) was diluted 1 in 20 in TE buffer to give a 500 µg/ml working solution. Twenty microlitres of this were added to molten agarose to give a final concentration of 2 µg/ml.

Orange G loading buffer

Orange G loading buffer was prepared by adding 1 g of Ficoll® 70 (Fluka Biochemika, cat. no. 46326) to 10 ml TBE in a sterile universal and vortexing until the solution became clear. A small amount (0.025 g) of orange G powder (Sigma-Aldrich, Dorset UK, cat. no. 03756) was added to the solution and mixed. The loading buffer was stored at 4°C until use.

10% Glucose

A 10 ml solution of 10% glucose was prepared by combining 1 g of anhydrous D-glucose (BDH Laboratory Supplies Poole, UK, cat. no. 1011747) with 9 ml of ddH_20 in a sterile universal tube. This was mixed until the powder had dissolved. The solution was then made up to 10 ml with ddH_2O and sterilised by filtration through a 0.22 µm Millex-GP sterilising filter unit (Millipore Ireland BV, Cork, cat. no. SLGP 033 RS).

1 M Calcium chloride

A 10 ml volume of $CaCl_2$ (1 M) was prepared by combining 1.47 g of $CaCl_2$ (Sigma-Aldrich, Dorset UK, cat. no. C5080) with 9 ml of ddH_20 in a sterile universal tube. This was mixed until the powder had dissolved. The solution was then made up to 10 ml with ddH_2O and sterilised by filtration as above.

Thiamine (10 mg/ml)

A 10 ml volume of thiamine (10 mg/ml) was prepared by combining 100 mg of thiamine hydrochloride (Sigma-Aldrich, Dorset UK, cat. no. T4625) with 9 ml ddH_2O in a sterile universal tube and mixing until the powder had dissolved. The solution was then made up to 10 ml with ddH_2O and sterilised by filtration as above.

10mM dNTP

A stock dNTP mix was prepared by adding 250 µl of dATP, dTTP, dCTP and dGTP together (100 mM each) (Invitrogen, Paisley UK, cat. no. 18427-013). These were aliquoted into 100 µl volumes. To prepare a working solution of dNTPs (10 mM of each dNTP), 150 µl of UltraPURE™ DNase/RNase-free distilled water (Invitrogen, Paisley UK, cat. no. 10977035) were added to an aliquot.

125mM EDTA

Two millitres of 125 mM EDTA was prepared by combining 0.5 ml of 0.5 M EDTA (Sigma Aldrich, Dorset, UK, cat. no. E-7889) with 1.5 ml of ddH_20. The solution was mixed by inversion.

4 M Sodium hydroxide (NaOH)

One litre of NaOH was prepared by adding 160 g NaOH in parts to 700 ml ddH_20. The solution was mixed by inversion and then made up to 1 litre with ddH_20.

Ampicillin solution (10 mg/ml)

Ampicillin solution was prepared by adding 0.1 g of ampicillin sodium salt (Sigma-Aldrich, Dorset UK cat. no. A9518-5G) to 10 ml of ddH_20. One to two drops of 4 M NaOH were added and the solution was vortexed. The solution was filtered through a 0.22 µm Millex-GP sterilising filter unit (Millipore Ireland BV, Cork, cat. no. SLGP 033 RS) and stored at -20°C until use.

50% glycerol

A 200 ml solution of 50% glycerol was prepared by adding 100 ml of ddH_20 to 100 ml of glycerol (Sigma Aldrich, Dorset, UK, cat. no. G5516) and mixing.

Red Cell Lysis Buffer (RCLB) (0.144 M NH_4Cl, 1mM $NaHCO_3$)

RCLB was prepared by adding 15.41 g of ammonium chloride (VWR International Ltd, Poole, UK, cat. no. 100173D) and 0.168 g of sodium hydrogen carbonate (International Ltd, Poole UK, cat. no. 102475W) to 500 ml of ddH_20 in a fume cupboard. The solution was mixed gently and made up to 2 litres with ddH_20, before being autoclaved to maintain sterility.

Nuclei Lysis Buffer (NLB) (0.01 M Tris-HCl pH 8.0, 0.4 M NaCl, 2 mM EDTA)

NLB was prepared by combining 20 ml of 1 M Trizma®-HCl (pH 7.5) (Sigma-Aldrich, Dorset UK, cat. no. T-2319), 200 ml of 4 M sodium chloride and 8 ml 0.5 M EDTA. The solution was adjusted to a final volume of 2 litre with ddH_20, before being autoclaved to maintain sterility.

#271 broth

#271 broth medium was prepared using the same ingredients and quantities as for the #271 solid agar with the exception that agar was omitted. The broth was autoclaved at 121°C for 30 min at a pressure of 1.1 bar, cooled and stored at 4°C until use. Ten millilitres of 10% glucose, 2.0 ml of 1M $CaCl_2$ and 1.0 ml of thiamine (10 mg/ml) were added to 1 litre of broth medium prior to use.

#271 solid agar plates

Solid agar (#271) was prepared by mixing 10 g tryptone powder, 1 g yeast extract powder, 8 g sodium chloride, 15 g Difco™ Agar Noble in 1 litre of ddH_20. The solution was autoclaved at 121°C for 30 min at a pressure of 1.1 bar and cooled to ~ 55°C. Ten millilitres of 10% glucose, 2 ml of 1M $CaCl_2$ and 1 ml of thiamine (10 mg/ml) were added and the molten agar was distributed evenly between sterile petri dishes. Once set, the plates were inverted and placed in a 37°C incubator to evaporate residual condensation.

#271 soft (0.5%) agar

Soft agar (#271) was prepared by mixing 1 g tryptone powder, 0.1 g yeast extract, 0.8 g sodium chloride and 0.5 g Difco™ Agar Noble in 100 ml ddH_20. The solution was autoclaved at 121°C for 30 min at a pressure of 1.1 bar. Soft agar was used

as an overlay for the #271 solid agar plates. Prior to use, it was placed in a microwave to melt, and subsequently cooled to 4 -50°C in a water bath. One millilitre of 10% glucose, 0.2 ml of 1M $CaCl_2$ and 0.1 ml of thiamine (10 mg/ml) were added prior to use and the soft agar was distributed evenly as a layer over each of the #271 solid agar plates (after addition of MS2 phage and host).

LB/ampicillin agar plates (1.5% agar, 1.0% tryptone, 0.5% yeast extract, 0.5% NaCl, 0.01 mg/ml ampicillin)

A batch of 10 plates was made by combining 10 g of tryptone (Oxoid, Basingstoke UK, LP0043), 15 g of Difco™ Agar Noble (Becton, Dickinson and Company, Pont de Claix France, cat. no. 214230), 5 g of sodium chloride (VWR International Ltd, Poole, UK cat. no. 301235Q) and 5 g of yeast extract (Oxoid, Basingstoke UK, cat. no. LP0021) and dissolving in 800 ml of ddH_20. The volume was adjusted to 1 litre with ddH_20 and autoclaved at 121°C for 30 min at a pressure of 1.1 bar and cooled to ~ 55°C. Ten millitres of ampicillin solution (10 mg/ml) were added to give a final concentration of 100 μg/ml. The molten agar solution was poured evenly between 10 sterile petri dishes. Once set, the plates were inverted and placed in a 37°C incubator to evaporate residual condensation.

LB/Ampicillin nutrient broth medium

LB nutrient broth medium was made by dissolving 2 g of tryptone, 1 g of sodium chloride and 1 g of yeast extract in 200 ml of ddH_2O. The solution was autoclaved at 121°C for 30 min at a pressure of 1.1 bar and when cooled, the broth medium was then stored at room temperature until required. Two millitres of ampicillin solution were added to the broth medium to give a final concentration of 50 μg/ml.

Appendix B - Primer and Probe Sequences

HCV genotyping and subtyping

Primers

Primer	Sequence	Position[a]
HCV 4	TTCACGCAGAAAGCGTCTAG	63-82
HCV 3	CACTCG[1]CA[1]AGCACCCTATCAGGCAGT	313-288
NS5bF2	TATGAYACCCGCTGYTTYGACTC	8256-8278
NS5bR	TACCTNGTCATRGCYTCCGTGAA	8638-8616

Probes

Genotyping Probe	Sequence	Position[a]	Reporter/ Quencher
Panel One			
T1	CGGAATTGCCAGGACGACCGGGTCCT	169-194	FAM/Tamra
T2	ATTRCCGGRAAGACTGGGTCCTTTC	173-197	JOE/Tamra
T3	CCCCGCRAGATCACTAGCCGAGT	237-259	ROX/BHQ-2
T11	ACCCGCTCAATGCCTGGAGATTTGG	206-230	Cy5/BHQ-2
Panel Two (Original)			
T22 (MGB)	ATAAACCCACTCTATGYCCG	202-221	FAM/NFQ
T33 (MGB)	CTCAATACCCAGAAATTTGG	211-230	JOE/NFQ
T4 (MGB)	AGGCTGTACAACACTCATA	113-95	FAM/NFQ
Panel Two (New)			
T22 (LNA)	ATA+AACCC+ACTC+TATGYCCG	202-221	Cy5/BHQ-2
T33 (MGB)	CTCAATACCCAGAAATTTGG	211-230	JOE/NFQ
NCT333	CCCGGTCACCCCAGCGATTC	190-171	ROX/BHQ-2
T4 (MGB)	AGGCTGTACAACACTCATA	113-95	FAM/NFQ
Additional Probe			
NS53	TGTRTTGCCRAAGCTGGTAGGCA	8477-8454	ROX/BHQ2
Subtyping Probe			
Non-1b	GAYATCCGTACGGAGGAGGCAATCTA	8295-8320	FAM/BHQ
1b (MGB)	CCGAAGCCAGRCAG	8342-8355	JOE/NFQ

Primers used for HCV genotyping and subtyping. [a] Position relative to HCV type 1a sequence (GenBank accession number M62321).
[1] Modifications to original (NCR4) primer, to improve its generic nature, a T→G and a G→A change, respectively.

For all primers/probes: R=A or G, Y= C or T, N=A,C,T or G. A '+' in front of the nucleotide indicates an LNA addition.

HCV quantitation with MS2 internal control

Primers

Primer	Sequence	Position [a,b]
Taq1	GTCTAGCCATGGCGTTAGTA	77-96
Taq2	GTACTCACCGGTTCCGC	166-150
MS2F	TGGCACTACCCCTCTCCGTATTCACG	289-314
MS2R	GTACGGGCGACCCCACGATGAC	387-366

Probes

Probe	Sequence	Position	Reporter/ Quencher
HCVTaq	CCCTCCCGGGAGAGCCATAGTG	124-145	FAM/Tamra
MS2Taq	CACATCGATAGATCAAGGTGCCTACAAGC	330-359	JOE/Tamra

[a] Position of the HCV primers/probe is of the 5' base relative to HCV genomic sequence with reference to HCV type 1 sequence (acc. no. M62321).
[b] Position of the MS2 primers/probe is of the 5' base relative to the MS2 genomic sequence (acc. no. NC_001417)

M13 PCR (primers included with the pCR® 4-TOPO cloning vector)

Primer	Sequence	Position
M13F	CGCCAGGGTTTTCCCAGTCACGAC	397-374
M13R	TCACACAGGAAACAGCTATGAC	200-221

Position is according to pCR® 4-TOPO cloning vector (http://www.invitrogen.com)

For all primers/probes: R=A or G, Y= C or T, N=A,C,T or G. A '+' in front of the nucleotide indicates an LNA addition.

mtDNA deletion detection/quantitation

Primers

Primer	Sequence	Position
CD1	AAGAGAACCAACACCTCTTTACAGTGA	8323-8349
CD1LNA	G+AGA+ACCAAC+ACCTCT+TTACAGTGA	8325-8349
CD2	TATTCGAGTGCTATAGGCGCTTGTCAG	13599-13573
SCD	AAGGATACTAGTATAAGAGATCAGGTTCGTC	8735-8705
7436LNA	CTAC+AGG+TGGTCAAG+TAT+TTA+TGGTAC	16156-16130

Probes

Probe	Sequence	Position	Reporter/Quencher
UD(MGB)	CGCCRCAGTACTGATC	8565-8580	FAM/NFQ
DEL(MGB)	ATACACAAACGCCTGAGC	13527-13544	JOE/NFQ
7436(MGB)	CATTACTGCCAGCCAC	16099-16114	FAM/NFQ
7420(MGB)	AACCTCAAGCCACCATGA	8682-8689/ 16110-16119	FAM/NFQ

Primers and probe for mtDNA deletion detection/quantitation. Position is according to the revised Cambridge Reference Sequence (acc. no. AC000021).

β-Globin gene detection/quantitation

Primer	Sequence	Position	Reporter/ Quencher
β-globin-FP	CTCTTTCTTTCAGGGCAATA	1268-1287	
β-globin-RP	TTGCCTTAACCCAGAAATTA	1386-1367	
β-globin Probe	TATCATGCCTCTTTGCACCA	1309-1328	JOE/BHQ-1

Position is according to the β-globin gene sequence (acc. no. AY260740)

RSCA

Primer	Reporter	Sequence	Position
DLoopFLab*	FAM	AACTCCACCATTAGCACCCAAAGC	15973-15996
DLoopR		TGCGGGATATTGATTTCACGGAGGATGG	16430-16403

Position is according to the revised Cambridge Reference Sequence (acc. no. AC000021). *The unlabelled D-loop forward (DLoopF) primer is identical in sequence to DLoopFLab, without the 5' FAM attachment.

For all primers/probes: R=A or G, Y= C or T, N=A,C,T or G. A '+' in front of the nucleotide indicates an LNA addition.

Appendix C - PCR master mixes and cycling conditions

Unless stated, all PCR reactions were carried out on the Rotor-Gene 3000 using the LightCycler® FastStart DNA Master HybProbe kit.

Reverse transcription (cDNA preparation)

Reagents	µl/14µl	Stock concentration	Final concentration (per reaction)
PCR buffer-II	3.5	10x	1x
$MgCl_2$	3.5	50 mM	5 mM
dNTPs	1	10 mM each	100 µM each
M-MLV RT [a]	1	200 U/µl	0.2 U/µl
RNAse-free water	5		

+21 µl extracted RNA/random hexamer mix
Carried out on a PTC-200 Peltier thermal cycler (MJ Research, Waltham, USA) using the *Taq* DNA polymerase recombinant kit (Invitrogen, Paisley, UK)
Total reaction volume is 35 µl
[a] M-MLV Reverse Transcriptase (RT) (Invitrogen, Paisley, UK)

M13 PCR (used in PCR product cloning)

Reagents	µl/1000 µl	Stock concentration	Final Concentration (per µl)
PCR buffer-II	100	10x	1x
$MgCl_2$	30	50 mM	1.5 mM
M13F primer	2	100 pmol/µl	0.2 pmol
M13R primer	2	100 pmol/µl	0.2 pmol
dNTPs	20	10 mM each	200µM each
Taq Polymerase	6	5 U/µl	3U/100µl
RNAse-free water	840		

+1 µl *E. coli* lysate
Carried out on a PTC-200 Peltier thermal cycler using the *Taq* DNA polymerase recombinant kit

Cycling conditions: 5 min 96°C, 30 s 96°C, 30 s 50°C, 1 min 72°C for 25 cycles then 10 min 72°C.

The Master HybProbe of the LightCycler® FastStart DNA Master HybProbe kit and the 2x reaction mix of the SuperScript™ III Platinum® One-Step Quantitative RT-PCR System contain $MgCl_2$. Therefore the final concentration of $MgCl_2$ may differ from that expected.

HCV Genotyping

HCV 5' UTR qualititative assay (LightCycler)

Reagents	µl/20µl	Stock concentration	Final concentration (per reaction)
Mastermix (vial 1)	2	10x	1x
$MgCl_2$	1.6	25 mM	2 mM
HCV3 primer	0.75	20 pmol/µl	15 pmol
HCV4 primer	0.75	20 pmol/µl	15 pmol
RNAse-free water	12.9		

+2 µl cDNA
Carried out using FastStart DNA Master SYBR green kit (Roche Diagnostics)

Cycling conditions: Quantitation: Hold 10 min at 95°C. 50 cycles of raising temperature up to 95°C (20°C/s) then 2 s at 55°C (20°C/s) and 10 s at 72°C (20°C/s). Melt Curve: Hold 1 s at 95°C then cool/hold for 30 s at 65°C, then ramp from 65-95°C at 0.1°C/s with continuous fluorescence acquisition then cool for 10 s to 40°C.

HCV genotyping panel one

Reagents	µl/20µl	Stock concentration	Final concentration (per reaction)
Master HybProbe	2	10x	1x
$MgCl_2$	0.4	25 mM	1.5 mM
HCV3 primer	0.75	20 pmol/µl	15 pmol
HCV4 primer	0.75	20 pmol/µl	15 pmol
T1 probe	0.5	10 pmol/µl	5 pmol
T11 probe	0.5	10 pmol/µl	5 pmol
T2 probe	0.5	10 pmol/µl	5 pmol
T3 probe	0.5	10 pmol/µl	5 pmol
RNAse-free water	11.1		

+3 µl cDNA

Cycling conditions: Hold 10 min at 95°C, then 45 cycles of 8 s at 95°C (not acquiring) and 45 s at 65°C (acquiring on FAM, Cy5, JOE and ROX).

The Master HybProbe of the LightCycler® FastStart DNA Master HybProbe kit and the 2x reaction mix of the SuperScript™ III Platinum® One-Step Quantitative RT-PCR System contain $MgCl_2$. Therefore the final concentration of $MgCl_2$ may differ from that expected.

HCV genotyping panel two (original)

Reagents	µl/20µl	Stock concentration	Final Concentration (per reaction)
Master HybProbe	2	10x	1x
$MgCl_2$	0.8	25 mM	2 mM
HCV3 primer	0.75	20 pmol/µl	15 pmol
HCV4 primer	0.75	20 pmol/µl	15 pmol
T22[a] probe	0.5	10 pmol/µl	5 pmol
T33 probe	0.5	10 pmol/µl	5 pmol
RNAse-free water	11.7		

+3 µl cDNA
[a] or T4

Cycling conditions: Hold 10 min at 95°C, then 45 cycles of 8 s at 95°C (not acquiring) and 45 s at 60°C (acquiring on FAM and JOE)

HCV genotyping panel two (new)

Reagents	µl/20µl	Stock concentration	Final concentration (per reaction)
Master HybProbe	2	10x	1x
$MgCl_2$	0.8	25 mM	2 mM
HCV3 primer	0.75	20 pmol/µl	15 pmol
HCV4 primer	0.75	20 pmol/µl	15 pmol
T22 probe	0.5	10 pmol/µl	5 pmol
T33 probe	0.5	10 pmol/µl	5 pmol
NCT333 probe	0.5	10 pmol/µl	5 pmol
T4 probe	0.5	10 pmol/µl	5 pmol
RNAse-free water	10.7		

+3 µl cDNA

Cycling conditions: Hold 10 min at 95°C, then 45 cycles of 8 s at 95°C (not acquiring) and 45 s at 60°C (acquiring on FAM, Cy5, JOE and ROX).

The Master HybProbe of the LightCycler® FastStart DNA Master HybProbe kit and the 2x reaction mix of the SuperScript™ III Platinum® One-Step Quantitative RT-PCR System contain $MgCl_2$. Therefore the final concentration of $MgCl_2$ may differ from that expected.

HCV additional genotype 3 probe

Reagents	µl/20µl	Stock concentration	Final concentration (per reaction)
Master HybProbe (vial 1)	2	10x	1x
$MgCl_2$	1.2	25 mM	2.5 mM
NS5bF2 primer	0.75	20 pmol/µl	15 pmol
NS5bR primer	0.75	20 pmol/µl	15 pmol
NS53 probe	0.35	10 pmol/µl	3.5 pmol
RNAse-free water	11.95		

+3 µl cDNA

Cycling conditions: Hold 10 min at 95°C, then 45 cycles of 8 s at 95°C (not acquiring) and 45 s at 60°C (acquiring on ROX)

HCV subtyping

HCV generic subtyping assay (LightCycler)

Reagents	µl/20µl	Stock concentration	Final concentration (per reaction)
Mastermix (vial 1)	2	10x	1x
$MgCl_2$	0.8	25 mM	2 mM
NS5bF2 primer	0.3	20 pmol/µl	6 pmol
NS5bR primer	0.3	20 pmol/µl	6 pmol
1:1000 dilution SYBR green	1		
Water	12.6		

+3 µl cDNA

Cycling conditions: Quantitation: Pre-incubation 10 min at 95°C. Then 45 cycles of 10 s at 95°C then 30 s at 60°C, then 30 s at 72°C (acquiring on FAM). Melt Curve: Hold 30 s at 95°C then cool to 50°C. Ramp from 50-99°C rising by 1°C each step, holding the first step for 30 s and 5 s for each step afterwards, acquiring to MeltA on FAM.

The Master HybProbe of the LightCycler® FastStart DNA Master HybProbe kit and the 2x reaction mix of the SuperScript™ III Platinum® One-Step Quantitative RT-PCR System contain $MgCl_2$. Therefore the final concentration of $MgCl_2$ may differ from that expected.

HCV subtyping 1b/non-1b

Reagents	µl/20µl	Stock concentration	Final Concentration (per reaction)
Master HybProbe (vial 1)	2	10x	1x
$MgCl_2$	0.8	25 mM	2 mM
NS5bF2 primer	0.3	20 pmol/µl	6 pmol
NS5bR primer	0.6	20 pmol/µl	12 pmol
Non-1b probe	0.25	10 pmol/µl	2.5 pmol
1b probe	0.25	10 pmol/µl	2.5 pmol
RNAse-free water	12.8		

+3 µl cDNA

Cycling conditions: Hold 10 min at 95°C, then 40 cycles of 8 s at 95°C (not acquiring) and 45 s at 55°C (acquiring on FAM and JOE)

HCV Quantitation

RealArt™ HCV RG RT PCR Quantitation

Reagents	µl/20µl
HCV RG Master	15
HCV RG IC	0.5

5 µl extract

Cycling conditions: Hold 10 min at 50°C (reverse transcription), then 50 s at 95°C. 45 cycles of 8 s at 95°C (not acquiring), 20 s at 55°C (acquiring on FAM and JOE) and 20 s at 72°C (not acquiring).

The Master HybProbe of the LightCycler® FastStart DNA Master HybProbe kit and the 2x reaction mix of the SuperScript™ III Platinum® One-Step Quantitative RT-PCR System contain $MgCl_2$. Therefore the final concentration of $MgCl_2$ may differ from that expected.

MS2 detection

Reagents	µl/25µl	Stock concentration	Final concentration (per reaction)
Reaction mix	12.5	2x	1x
$MgSO_4$		50 mM	4 mM
MS2F primer	0.5	20 pmol/µl	10 pmol
MS2R primer	0.5	20 pmol/µl	10 pmol
MS2Taq probe	0.2	10 pmol/µl	2 pmol
RT/Platinum® *Taq* mix	0.8		
RNAse-free water	5.5		

+5 µl MS2 extract
SuperScript™ III Platinum® One-Step Quantitative RT-PCR System, Invitrogen, Paisley, UK)

Cycling conditions: Incubate 30 min at 50°C then hold 2 min at 95°C, then 50 cycles of 15 s at 95°C (not acquiring), and 1 min at 56°C (acquiring on JOE).

HCV quantitation with MS2 internal control

Reagents	µl/25µl	Stock concentration	Final Concentration (per reaction)
Reaction mix	12.5	2x	1x
$MgSO_4$	1	50 mM	5 mM
Taq1 primer	0.15	100 pmol/µl	15 pmol
Taq2 primer	0.15	100 pmol/µl	15 pmol
HCVTaq probe	0.25	20 pmol/µl	5 pmol
MS2F primer	0.1	20 pmol/µl	2 pmol
MS2R primer	0.1	20 pmol/µl	2 pmol
MS2Taq probe	0.2	10 pmol/µl	2 pmol
RT/Platinum® *Taq* mix	0.8µl		

+10 µl extract
SuperScript™ III Platinum® One-Step Quantitative RT-PCR System, (Invitrogen, Paisley, UK)

Cycling conditions: Incubate 30 min at 50°C, then hold 2 min at 95°C, then 50 cycles of 15 s at 95°C (not acquiring), and 1 min at 56°C (acquiring on FAM and JOE).

The Master HybProbe of the LightCycler® FastStart DNA Master HybProbe kit and the 2x reaction mix of the SuperScript™ III Platinum® One-Step Quantitative RT-PCR System contain $MgCl_2$. Therefore the final concentration of $MgCl_2$ may differ from that expected.

mtDNA deletion detection/quantitation

Block-based PCR

Reagents	µl/50µl	Stock concentration	Final Concentration (per reaction)
PCR buffer-II	5	10x	1x
$MgCl_2$	1.5	50 mM	1.5 mM
dNTPs	1	10 mM each	0.5µM
CD1 primer	1	20 pmol/µl	20 pmol
SCD primer	1	20 pmol/µl	20 pmol
Invitrogen Taq	0.2	5 U/µl	1U
RNAse-free water	35.3		

+5 µl extract
Carried out on a PTC-200 Peltier thermal cycler (MJ Research, Waltham, USA) using the *Taq* DNA polymerase recombinant kit.

Cycling conditions: 10 min 95°C, 1 min 95°C, 1 min 60°C, 1 min 72°C for 35 cycles then 10 min 72°C.

Increased stringency block-based PCR

Reagents	µl/50µl	Stock concentration	Final Concentration (per reaction)
PCR buffer-II	5	10x	1x
$MgCl_2$	1	50 mM	1 mM
dNTPs	1	10 mM each	0.5µM
CD1 primer	1	20 pmol/µl	20 pmol
CD2 primer	1	20 pmol/µl	20 pmol
Invitrogen Taq	0.2	5U/µl	1U
RNAse-free water	35.8		

+5 µl extract
Carried out on a PTC-200 Peltier thermal cycler (MJ Research, Waltham, USA) using the *Taq* DNA polymerase recombinant kit.

Cycling conditions: 10 min 95°C, 1 min 95°C, 1 min 65°C, 1 min 72°C for 35 cycles then 10 min 72°C.

The Master HybProbe of the LightCycler® FastStart DNA Master HybProbe kit and the 2x reaction mix of the SuperScript™ III Platinum® One-Step Quantitative RT-PCR System contain $MgCl_2$. Therefore the final concentration of $MgCl_2$ may differ from that expected.

wt mtDNA detection/quantitation

Reagents	µl/20µl	Stock concentration	Final concentration (per reaction)
Master HybProbe (vial 1)	2	10x	1x
$MgCl_2$	0.8	25 mM	2 mM
CD1 primer	0.5	20 pmol/µl	10 pmol
SCD primer	0.5	20 pmol/µl	10 pmol
Undel probe	0.2	10 pmol/µl	2 pmol
RNAse-free water	13		

+3 µl cDNA

Cycling conditions: Hold 10 min at 95°C, then 40 cycles of 8 s at 95°C (not acquiring) and 45 s at 65°C (acquiring on FAM).

mt^{4977} detection/quantitation

Reagents	µl/20µl	Stock concentration	Final concentration (per reaction)
Master HybProbe (vial 1)	2	10x	1x
$MgCl_2$	2.4	25 mM	4 mM
CD1 primer	0.75	20 pmol/µl	15 pmol
CD2 primer	0.75	20 pmol/µl	15 pmol
Del probe	0.5	10 pmol/µl	5 pmol
RNAse-free water	10.6		

+3 µl cDNA

Cycling conditions: Hold 10 min at 95°C, then 45 cycles of 8 s at 95°C (not acquiring) and 45 s at 65°C (acquiring on JOE).

The Master HybProbe of the LightCycler® FastStart DNA Master HybProbe kit and the 2x reaction mix of the SuperScript™ III Platinum® One-Step Quantitative RT-PCR System contain $MgCl_2$. Therefore the final concentration of $MgCl_2$ may differ from that expected.

mt^{7436} detection/quantitation

Reagents	µl/20µl	Stock concentration	Final concentration (per reaction)
Master HybProbe (vial 1)	2	10x	1x
$MgCl_2$	0.8	25 mM	2 mM
CD1LNA primer	0.75	20 pmol/µl	15 pmol
7436LNA primer	0.75	20 pmol/µl	15 pmol
7436 probe	0.35	10 pmol/µl	3.5 pmol
RNAse-free water	12.35		

+3 µl cDNA

Cycling conditions: Hold 10 min at 95°C, then 40 cycles of 8 s at 95°C (not acquiring) and 45 s at 62°C (acquiring on FAM).

mt^{7420} detection/quantitation

Reagents	µl/20µl	Stock concentration	Final concentration (per reaction)
Master HybProbe (vial 1)	2	10x	1x
$MgCl_2$	0.8	25 mM	2 mM
CD1LNA primer	0.5	20 pmol/µl	10 pmol
7436LNA primer	0.5	20 pmol/µl	10 pmol
7420 probe	0.5	10 pmol/µl	5 pmol
RNAse-free water	12.7		

+3 µl cDNA

Cycling conditions: Hold 10 min at 95°C, then 40 cycles of 8 s at 95°C (not acquiring) and 45 s at 60°C (acquiring on FAM).

The Master HybProbe of the LightCycler® FastStart DNA Master HybProbe kit and the 2x reaction mix of the SuperScript™ III Platinum® One-Step Quantitative RT-PCR System contain $MgCl_2$. Therefore the final concentration of $MgCl_2$ may differ from that expected.

β-Globin quantitation

Reagents	µl/25µl	Stock concentration	Final concentration (per reaction)
	12.5	2x	1x
$MgCl_2$	1	50 mM	5 mM
Primer G3	0.25	25 pmol	6.25
Primer G2	0.25	25 pmol	6.25
Globin probe	0.1	25 pmol	2.5

+10 µl DNA extract
Carried out using the Platinum® Quantitative PCR SuperMix-UDG kit (Invitrogen, Paisley, UK)

Cycling conditions: Hold 2 min at 50°C, then 2 min at 95°C. 45 cycles of 1 s at 95°C (not acquiring) and 1 min at 60°C (acquiring on JOE).

mtDNA D-loop amplification

Reagents	µl/50µl	Stock concentration	Final Concentration (per reaction)
PCR buffer-II	5	10x	1x
$MgCl_2$	1.5	50 mM	1.5 mM
DLoop F primer*	1	20 pmol/µl	20 pmol
DLoop R primer	1	20 pmol/µl	20 pmol
dNTPs	1	10 mM each	0.5µM each
Taq Polymerase	0.2	5 U/µl	1U
RNAse-free water	35.3		

+5 µl DNA extract
*or DLoopFLab in FLR production
Carried out on a PTC-200 Peltier thermal cycler using the *Taq* DNA polymerase recombinant kit.

Cycling conditions: 10 min 95°C, 1 min 95°C, 1 min 60°C, 1 min 72°C for 35 cycles then 10 min 72°C.

The Master HybProbe of the LightCycler® FastStart DNA Master HybProbe kit and the 2x reaction mix of the SuperScript™ III Platinum® One-Step Quantitative RT-PCR System contain $MgCl_2$. Therefore the final concentration of $MgCl_2$ may differ from that expected.

Appendix D Univariable analysis comparing cases included in multivariable analysis in the HCV clearance study (n=175) with those excluded (n=161)

	Included in multivariable analysis (n=175)	Excluded from multivariable analysis (n=161)	Statistic	P value
Male	118	96	$\chi^2 = 2.207$	0.137
Female	57	65		
UK	82	77	$\chi^2 = 11.996$	0.002
Non-UK	15	33		
Not-known	78	51		
White	143	108	$\chi^2 = 16.152$	<0.001
Non-white	4	21		
Not-known	28	32		
IDU	154	65	$\chi^2 = 106.302$	<0.001
Transfusion	21	26		
Not-known	0	70		
<21(M) or <14 (F) units alcohol	88	117	$\chi^2 = 34.743$	<0.001
>21(M) or >14 (F) units alcohol	87	35		
Not known	0	9		
Type 1	86	60	$\chi^2 = 55.156$	<0.001
Non-1 type	89	57		
Not known	0	44		
Mean age at infection (yrs)	21.70	22.16	t= 0.361	0.718
Mean duration of infection (yrs)	21.21	22.28	t= 0.627	0.532

Cambridge Research Ethics Committee
Victoria House
Capital Park
Fulbourn
Cambridge
CB1 5XB

Telephone: 01223 597657
Facsimile: 01223 597645
Email: karen.ignatian@nscstha.nhs.uk

14 JAN 2005

22 December 2004

Dr M E D Allison
Addenbrooke's Hospital
Consultant Hepatologist
Box 210
Hills Road, Cambridge
CB2 2QQ

Dear Dr Allison

Full title of study: *Investigation into the presence of nuclear and mitochondrial DNA damage and induction of DNA repair mechanisms in liver disease*
REC reference number: *04/Q0108/124*

Thank you for your letter of 17 November 2004, responding to the Committee's request for further information on the above research and submitting revised documentation.

The further information has been considered on behalf of the Committee by the Chairman, Dr Berrios.

Confirmation of ethical opinion

On behalf of the Committee, I am pleased to confirm a favourable ethical opinion for the above research on the basis described in the application form, protocol and supporting documentation as revised.

The favourable opinion applies to the research sites listed on the attached form. Confirmation of approval for other sites listed in the application will be issued as soon as local assessors have confirmed that they have no objection.

Conditions of approval

The favourable opinion is given provided that you comply with the conditions set out in the attached document. You are advised to study the conditions carefully.

Approved documents

The final list of documents reviewed and approved by the Committee is as follows:

Document Type:	Version:	Dated:	Date Received:
Application		30/06/2004	30/06/2004
Protocol	1	30/06/2004	30/06/2004
Summary/Synopsis	1	30/06/2004	30/06/2004
Participant Information Sheet	1	30/06/2004	30/06/2004

Participant Information Sheet	2	07/09/2004	17/11/2004
Participant Consent Form	2	07/09/2004	17/11/2004
Participant Consent Form		05/07/2004	30/06/2004
Response to Request for Further Information		17/11/2004	17/11/2004

Management approval

The study should not commence at any NHS site until the local Principal Investigator has obtained final management approval from the R&D Department for the relevant NHS care organisation.

Membership of the Committee

The members of the Ethics Committee who were present at the meeting are listed on the attached sheet.

Notification of other bodies

The Committee Administrator will notify the research sponsor that the study has a favourable ethical opinion.

Statement of compliance

The Committee is constituted in accordance with the Governance Arrangements for Research Ethics Committees (July 2001) and complies fully with the Standard Operating Procedures for Research Ethics Committees in the UK.

04/Q0108/124 **Please quote this number on all correspondence**

With the Committee's best wishes for the success of this project,

Yours sincerely,

Dr German Berrios
Chair

E-mail: karen.ignatian@nscstha.nhs.uk

Enclosures *List of names and professions of members who were present at the meeting and those who submitted written comments*

Standard approval conditions

Site approval form (SF1)

Appendix F Patient Information Sheet

Study Title: Investigation into the presence of nuclear and mitochondrial DNA damage and induction of DNA repair mechanisms in liver disease.

You are being invited to take part in a research study. Before you decide it is important for you to understand why the research is being done and what it will involve. Please take time to read the following information carefully and discuss it with others if you wish. Ask us if there is anything that is not clear or if you would like more information. Take time to decide whether or not you wish to take part.

Purpose of the study

We would like to you to participate in a research study being conducted in the Department looking at the ways in which liver damage is caused in different conditions. Although liver damage can be caused by a number of different illnesses, the exact way in which the liver is damaged is not fully understood. In addition, it is not at all clear why some people get liver damage and others do not. Some conditions that can cause liver disease may do so by damaging a person's DNA in the liver cells. The aim of this study is to see whether this does occur, and to get a better understanding of how the damage occurs. It is hoped that this may, in time, allow us to develop better treatment to protect the liver in various conditions.

Do I have to take part?

It is up to you to decide whether or not to take part. If you do decide to take part you will be given this information sheet to keep and be asked to sign a consent form. If you decide to take part you are still free to withdraw at any time and without giving a reason. A decision to withdraw at any time, or a decision not to take part, will not affect the standard of care you receive.

What will happen to me if I take part?

If you do agree to take part, when you come into hospital to have your liver biopsy, a blood sample will be taken and stored. At the time of the liver biopsy, some of the biopsy will be taken for research, once enough has been sent for routine clinical analysis. The study does not involve any tests beyond this, and no extra clinic visits are required.

Will my taking part in this study be kept confidential?
All information which is collected about you during the course of the research will be kept strictly confidential. Any information about you will have your name and details removed so that you cannot be recognised from it.

If you do have any questions, please do not hesitate to ask us, either at your clinic visit, or by contacting my secretary, Kaye Barr on 01223 586641 or by email at kaye.barr@addenbrookes.nhs.uk.

Thank-you for taking part in this study.

Yours sincerely.

Dr Michael Allison
Consultant Hepatologist

Version 2 Date 7th September 2004

Appendix F

CONSENT FORM

LREC Reference Number: 04/Q0108/124

Title of Project: Investigation into the presence of nuclear and mitochondrial DNA damage and induction of DNA repair mechanisms in liver disease.

Name of Lead Investigator: Dr Michael Allison

Please initial box

1. I confirm that I have read and understand the study Information Sheet dated 07.09.04 (version 2) for the above study and have had the opportunity to ask questions. ☐

2. I understand that my participation is voluntary and that I am free to withdraw at any time, without giving any reason, without my medical care or legal rights being affected. ☐

3. I understand that sections of any of my medical notes may be looked at by responsible individuals from regulatory authorities where it is relevant to my taking part in research. I give permission for these individuals to have access to my records. ☐

4. I agree to take part in the above study. ☐

Name of Research Subject *(Please print)*	Date	Signature
Name of Witness to Signature (Must **not** be member of research team) *(Please print)*	Date	Signature
Name of Research Team member *(Please print)*	Date	Signature

3 copies required: top copy for researcher; one copy for patient; one copy to be kept with research subject's notes.

Version No: 2 / Dated: 7th September 2004

Appendix G - Clinical study data (liver biopsies)

Biopsy	Age	Sex	Liver Pathology	mt4977:undeleted	mt7436:undeleted	He
1	39	M	HCV	6.58E-05	2.54E-06	1
2	65	F	alcoholic liver disease	2.14E-03	0	1
3	32	F	HCV	3.70E-05	1.03E-05	1
4	45	M	genetic haematochromatosis	0.00E+00	0	1
5	56	M	NAFLD	1.46E-04	1.24E-05	1
6	65	M	alcoholic liver disease	5.58E-04	0	1
7	57	F	HCV	5.03E-06	5.08E-07	1
8	32	F	Primary sclerosing cholangitis	2.41E-05	3.20E+06	1
9	35	M	no evidence of fibrosis	2.25E-05	1.12E-06	3
10	44	M	HCV	1.33E-05	9.06E-07	3
11	38	M	HCV	4.43E-05	0.00E+00	1
12	22	M	HBV	2.73E-05	0.00E+00	1
13	40	M	HCV	1.03E-04	5.41E-06	1
14	55	M	alcoholic liver disease	2.23E-05	4.75E-05	1
15	43	M	HCV	1.45E-04	2.59E-06	1
16	57	F	alpha-7 anti-tryspin	1.93E-04	1.10E-04	1
17	51	M	HCV and alcohol	4.76E-05	8.86E-06	1
18	55	M	biliary tract abnormality	1.31E-05	4.33E-05	1
19	33	M	chronic HBV	4.29E-05	0.00011	1
20	36	M	chronic HBV	5.53E-06	4.08E-05	1
21	36	M	HBV	1.31E-05	0.00019	1
22	51	F	Genetic haematochromatosis	4.30E-06	5.92E-05	1
23	32	M	borderline steatohepatitis	1.08E-05	9.44E-05	1
24	47	F	HCV	2.07E-05	5.41E-05	1
25	50	F	HCV	2.44E-04	9.04E-06	1
26	52	F	HCV	8.58E-06	0.00E+00	1
27	54	F	HCV	1.93E-04	0.00E+00	1
28	20	M	Autoimmune	4.68E-04	0.00E+00	1
29	54	F	HCV	2.81E-05	3.25E-06	1
30	58	M	NAFLD	7.03E-05	4.33E-05	1
31	50	M	HCV	2.46E-06	3.41E-06	1
32	49	F	HCV	2.28E-06	9.01E-07	1
33	44	M	HCV	1.42E-05	5.77E-07	1
34	49	M	HCV	9.26E-05	2.37E-05	1
35	52	F	minimal chronic hepatitis	5.68E-04	0.00E+00	1
36	53	M	HCV	1.03E-05	3.14E-07	2
37	26	M	HCV and HBV	6.94E-05	2.60E-06	1
38	47	M	HCV	3.63E-06	8.19E-05	1
39	70	M	HCV	3.23E-05	4.11E-06	1
40	36	M	genetic haematochromatosis	1.87E-04	5.78E-05	1
41	31	M	HBV	3.85E-05	0.0001	2
42	41	M	HCV	4.23E-05	3.09E-07	1
43	41	M	HCV + alcohol	2.23E-05	2.52E-05	1
44	51	M	alcoholic liver disease	2.53E-05	0	1
45	54	F	HCV	9.40E-05	3.19E-06	1
46	31	M	HCV	1.32E-04	2.96E-05	1
47	42	M	alcoholic liver disease	1.50E-04	2.67E-05	1
48	63	F	alcoholic liver disease	1.75E-04	2.60E-04	2
49	38	M	HCV + HIV	9.73E-05	2.62E-05	1
50	29	M	HBV	8.94E-05	7.86E-06	5
51	38	M	HCV	4.41E-05	7.56E-06	1
52	47	F	HCV	3.12E-04	1.27E-05	4
53	47	M	HCV	4.36E-05	8.55E-06	1
54	53	F	HCV	1.08E-04	6.54E-07	1
55	52	M	HCV	2.54E-05	2.39E-07	1

NAFLD; non-alcoholic fatty liver disease, NASH; non-alcoholic steatohepatitis, HBV; hepatitis B virus

Appendix G - Clinical study data (liver biopsies)

Biopsy	Age	Sex	Liver Pathology	mt4977:undeleted	mt7436:undeleted	He
56	37	F	HCV	6.83E-05	6.53E-06	1
57	21	F	HBV	6.74E-05	2.65E-06	4
58	33	M	HCV	1.51E-04	3.50E-06	1
59	41	F	Alcohol	1.49E-05	9.78E-07	1
60	40	M	NAFLD	1.50E-04	1.92E-06	1
61	30	M	HCV alcohol	1.84E-06	7.88E-07	1
62	40	M	NAFLD	2.06E-05	2.71E-06	1
63	66	F	Autoimmune	7.59E-05	5.79E-06	1
64	48	M	colitis + previous alcohol	1.08E-04	4.20E-05	1
65	68	F	non-specific reactive hepatitis	1.91E-05	2.78E-06	1
66	48	M	?NASH	1.98E-04	5.79E-06	1
67	30	M	HCV	1.23E-05	1.76E-05	1
68	55	F	HCV and alcohol	5.61E-06	1.33E-06	1
69	39	M	HCV and previous HBV	7.40E-05	2.53E-06	1
70	52	M	HCV	1.09E-05	1.49E-06	4
71	63	M	HCV + alcohol	2.05E-05	7.11E-06	1
72	60	M	Alcohol ?ASH/?NASH	1.73E-04	2.59E-05	3
73	51	M	Autoimmune	1.22E-04	7.81E-06	1
74	50	M	HCV + alcohol	8.94E-06	1.22E-06	1
75	62	F	HBV	3.75E-05	4.71E-06	1
76	57	M	?dysplasia	1.60E-04	6.68E-06	4
77	59	M	HCV	4.14E-04	3.24E-06	1
78	54	M	alcoholic liver disease	1.55E-04	8.86E-06	1
79	55	M	HCV + alcohol	2.11E-05	7.73E-07	1
			median	**4.36E-05**	**4.71E-06**	

NAFLD; non-alcoholic fatty liver disease, NASH; non-alcoholic steatohepatitis, HBV; hepatitis B virus

Appendix H - RSCA inter- and intra-assay variability

		Homoduplex mobility value	Heteroduplex mobility value
LB3	**Run 1**	416.19	446.1
		416.53	446.5
		416.11	446.24
	Mean	416.28	446.28
	SD	0.22	0.20
	Run 2	415.88	446.67
		416.13	446.81
		415.98	445.65
	Mean	416.00	446.38
	SD	0.13	0.63
	Run 3	415.45	446.2
		415.73	445.78
		416.17	446.04
	Mean	415.78	446.01
	SD	0.36	0.21
LB33	**Run 1**	416.44	438.31
		416.65	438.15
		416.43	438
	Mean	416.51	438.15
	SD	0.12	0.16
	Run 2	416.54	438.14
		416.4	438
		416.52	438.23
	Mean	416.49	438.12
	SD	0.08	0.12
	Run 3	415.94	438.34
		416.31	438.41
		416.31	438.55
	Mean	416.19	438.43
	SD	0.21	0.11
LB34	**Run 1**	416.89	422.26
		416.82	421.92
		416.83	421.78
	Mean	416.85	421.99
	SD	0.038	0.25
	Run 2	416.44	421.23
		416.73	421.55
		416.22	421.61
	Mean	416.46	421.46
	SD	0.26	0.204
	Run 3	416.71	421.95
		415.99	421.33
		416.14	421.38
	Mean	416.28	421.55
	SD	0.38	0.34

Appendix I - RSCA heteroduplex data

							Mobility	Values	
Biopsy	Age	Sex	Number of He	Ho mobility	He 1	He 2	He 3	He 4	He 5
1	39	M	1	416.89	422.26				
2	65	F	1	416.15	430.44				
3	32	F	1	417.57	457.53				
4	45	M	1	416.44	438.31				
5	56	M	1	415.5	437.06				
6	65	M	1	416.53	429.01				
7	57	F	1	415.39	425.45				
8	32	F	1	415.1	455.31				
9	35	M	3	416.06	429.69	432.21	436.1		
10	44	M	3	415.52	432.12	439.76	443.6		
11	38	M	1	416.37	444.01				
12	22	M	1	415.04	441.02				
13	40	M	1	416.01	454.58				
14	55	M	1	416.97	432.94				
15	43	M	1	416.54	431.91				
16	57	F	1	416.19	432.85				
17	51	M	1	416.85	447.7				
18	55	M	1	417.71	434.29				
19	33	M	1	417.18	431.45				
20	36	M	1	417.47	454.97				
21	36	M	1	415.5	474.01				
22	51	F	1	417.21	428.42				
23	32	M	1	417.15	432.69				
24	47	F	1	416.96	428.66				
25	50	F	1	416.46	432.2				
26	52	F	1	416.53	431.18				
27	54	F	1	416.45	427.72				
28	20	M	1	416.3	428.44				
29	54	F	1	417.09	427.71				
30	58	M	1	415.64	442.46				
31	50	M	1	416.01	440.17				
32	49	F	1	415.27	439.23				
33	44	M	1	415.23	463.31				
34	49	M	1	415.02	444.08				
35	52	F	1	417.63	427.18				
36	53	M	2	416.11	428.91	433.01			
37	26	M	1	416.63	459.5				
38	47	M	1	416.03	435.49				
39	70	M	1	416.42	428.56				
40	36	M	1	415.98	420.85				
41	31	M	2	416.25	441.74	448.08			
42	41	M	1	416.23	429.93				
43	41	M	1	416.37	440.66				
44	51	M	1	415.7	433.17				
45	54	F	1	417.58	421.72				
46	31	M	1	415.9	442.76				
47	42	M	1	416.34	440.86				
48	63	F	2	417.19	430.43	440.69			
49	38	M	1	417.06	440.37				
50	29	M	5	416.98	438.44	447.01	449.16	473.05	477.89
51	38	M	1	416.68	444.26				
52	47	F	4	416.42	455.54	461.99	465.53	493.23	
53	47	M	1	416.24	432.02				
54	53	F	1	416.25	431.87				

Ho; homoduplex, He; heteroduplex

Appendix I - RSCA heteroduplex data

							Mobility	Values	
Biopsy	Age	Sex	Number of He	Ho mobility	He 1	He 2	He 3	He 4	He 5
55	52	M	1	416.85	421.9				
56	37	F	1	415.94	437.67				
57	21	F	4	415.37	439.02				
58	33	M	1	416.87	437.62	444.28	447.12	453.6	
59	41	F	1	416.12	433.71				
60	40	M	1	415.13	426.61				
61	30	M	1	416.63	438.39				
62	40	M	1	415.28	432.27				
63	66	F	1	416.45	459.5				
64	48	M	1	417.38	421.14				
65	68	F	1	415.27	462				
66	48	M	1	416.32	427.22				
67	30	M	1	415.74	426.82				
68	55	F	1	416.53	428.81				
69	39	M	1	416.96	442.76				
70	52	M	4	416.46	439.95	445.41	449.85	476.96	
71	63	M	1	416.07	443.44				
72	60	M	3	416.38	432.31	438.75	461.93		
73	51	M	1	416.88	426.04				
74	50	M	1	416.07	461.45				
75	62	F	1	416.16	420.14				
76	57	M	4	416.25	429.63	432.47	473.03	461.44	
77	59	M	1	416.4	427.16				
78	54	M	1	416.35	430.41				
79	55	M	1	415.15	426.37				

Ho; homoduplex, He; heteroduplex